ТЕХНІКА ТА ЕНЕРГЕТИКА

Засновник:
Національний університет біоресурсів і природокористування України

Рік заснування: 2010

Рекомендовано до друку та поширення
через мережу Інтернет Вченою радою
Національного університету біоресурсів і природокористування України
(протокол № 5 від 22 листопада 2023 р.)

Свідоцтво про державну реєстрацію
друкованого засобу масової інформації
серії КВ № 25126-15066 ПР від 17 лютого 2022

Журнал входить до переліку наукових фахових видань України

Категорія «Б». Галузь наук – Технічні.
Спеціальність: 131 – «Прикладна механіка», 133 – «Галузеве машинобудування»,
141 – «Електроенергетика, електротехніка та електромеханіка»,
174 – «Автоматизація, комп'ютерно-інтегровані технології та робототехніка»
(Наказ Міністерства освіти і науки України від 23 грудня 2022 року № 1166)

Журнал представлено у міжнародних наукометричних базах даних,
репозитаріях та пошукових системах:
Index Copernicus International,
Google Scholar, Фахові видання України,
Національна бібліотека України імені В. І. Вернадського,
BASE, Academic Resource Index ResearchBib, DOAJ, J-Gate

Адреса редакції:
Національний університет біоресурсів і природокористування України
03041, вул. Героїв Оборони, 15, м. Київ, Україна
E-mail: info@technicalscience.com.ua
www: https://technicalscience.com.ua/uk

MACHINERY & ENERGETICS

Founders:
National University of Life and Environmental Sciences of Ukraine

Year of foundation: 2010

Recommended for printing and distribution
via the Internet by the Academic Council
of National University of Life and Environmental Sciences of Ukraine
(Minutes No. 5 of November 22, 2023)

Certificate of state registration
of the print media
Series KV No. 25126-15066 PR of February 17, 2022

The journal is included in the list of Professional Scientific Publications of Ukraine
Category “B”. Branch of sciences – Technical.
Specialty: 131 – “Applied Mechanics”, 133 – “Branch Mechanical Engineering”,
141 – “Electric Power Industry, Electrical Engineering and Electromechanics”,
174 – “Automation, Computer-integrated Technologies and Robotics”
(Order of the Ministry of Education and Science of Ukraine of December 23, 2022, No. 1166)

The journal is presented international scientometric databases, repositories
and scientific systems:
Index Copernicus International,
Google Scholar, Professional publications of Ukraine,
Vernadsky National Library of Ukraine, BASE,
Academic Resource Index ResearchBib, DOAJ, J-Gate

Editors office address:
National University of Life and Environmental Sciences of Ukraine
03041, 15 Heroiv Oborony, Kyiv, Ukraine
E-mail: info@technicalscience.com.ua
www: https://technicalscience.com.ua/en

Міжнародні члени редколегії:

Editorial Board

ЗМІСТ

CONTENTS

Machinery & Energetics
Vol. 14, No. 4. 2023

Journal homepage:
https://technicalscience.com.ua/en

UDC 658.562.2:635.11:633.63
DOI: 10.31548/machinery/4.2023.09

Myroslav Budzanivskyi*
Postgraduate Student
Institute of Mechanics and Automatics of Agroindustrial Production
of the National Academy of Agrarian Sciences of Ukraine
08631, 11/1 Vokzalna Str., Glevakha, Kyiv region, Ukraine
https://orcid.org/0000-0002-0508-3816

Development of the theory of root crop head cleaner movement in the longitudinal-vertical plane mounted behind a wheeled tractor

Abstract. The relevance of developing analytical methods for studying the stability of root crop cleaners on tractors is determined by the need to improve the efficiency and quality of root crop head cleaning, as this affects the quality of the final product and its marketable properties. The research aims to increase the stability of the cleaner movement by constructing a mathematical model of its oscillatory motion in the longitudinal-vertical plane and its numerical solution to determine the influence of parameters in response to external disturbances. To achieve this goal, a new theory of the movement of a root crop head cleaner in the longitudinal-vertical plane, mounted behind a wheeled tractor, under the influence of the disturbing effect of irregularities in the longitudinal profile of the soil surface on the amplitude and phase frequency characteristics of its angular oscillations was developed. Using numerical calculations carried out on a personal computer, the conditions were found under which the stability of the cleaner's movement in the specified plane will increase when the stiffness coefficient of the pneumatic tyres of the doubler wheels is 315 $kN \cdot m^{-1}$.· This result is achieved when the pressure in the pneumatic wheel tyres is 135 kPa. As for the damping characteristics of the doubler wheel tyres, which are determined by the coefficient μ, it was found that when it changes from 350 $N \cdot s \cdot m^{-1}$ to 1350 $N \cdot s \cdot m^{-1}$, there is an invariance of the delay in the reaction of the cleaner to the disturbing effect when its frequencies change from 0 to 24 s^{-1}. It was also found that the influence of the geometric dimensions of the cleaner is insignificant in the range of frequencies of oscillations of the ordinates of the longitudinal profile of soil surface irregularities from 0 to 24 s^{-1}. This follows from the nature of changes in the obtained amplitude-frequency and phase-frequency characteristics. The methodology for constructing a mathematical model of the plane-parallel oscillatory motion of the cleaner can be used in similar analytical studies of other agricultural machines mounted on a wheeled aggregating tractor

Keywords: ground irregularities; equivalent circuit; oscillations; differential equations; amplitude-frequency; phase-frequency characteristics

INTRODUCTION

In the cultivation of most root crops, the most common technology is separate harvesting, which involves cleaning the heads from the remains of the tops on the root. Most heads contain both short green and strong petioles (uncut parts of the green stalks of the tops), which are located on the top, and dry and lying residues in the form of threads of a certain length, which are firmly connected to the side parts of the heads and are located between the rows of crops or between the roots in the row itself, their high-quality removal is a difficult technical task. The conditions for a successful solution to this problem include not damaging the spherical surfaces of the heads and not knocking the root bodies out of the soil. It is possible to guarantee the separation of such residues by applying forces to the surface of each head to separate these types of residues.

The use of rubber cleaning pairs of blades, which cover the row of root crops on both sides, allows you to successfully perform this task. However, when the operating speeds of the cleaners increase, certain difficulties arise, one of the main ones being the oscillations that necessar-

Article's History: Received: 07.08.2023; Revised: 02.11.2023; Accepted: 22.11.2023.

Suggested Citation:
Budzanivskyi, M. (2023). Development of the theory of root crop head cleaner movement in the longitudinal-vertical plane mounted behind a wheeled tractor. *Machinery & Energetics,* 14(4), 9-22. doi: 10.31548/machinery/4.2023.09.

*Corresponding author

ily occur for the cleaning tines in the longitudinal-vertical plane. These oscillations cause the ends of the rubber blades to lose contact with the spherical surfaces of the root crop heads, which can lead to a deterioration in the quality of the cleaning process.

According to V. Bulgakov *et al.* (2023), these oscillations are caused by uneven soil surfaces, which in itself is an external disturbance for the cleaner if it is considered a complex dynamic system. Furthermore, the source of such oscillations can be the pneumatic doubler wheels that the cleaners are equipped with.

R. Hevko *et al.* (2014; 2018) and M. Budzanivskyi (2022) studied bunchers, cleaners, and root harvesters under modelling conditions that involve the use of significantly simplified equivalent circuits. This, in turn, leads to the use of initial equations based on the basic law of dynamics. This does not provide the appropriate accuracy of the built mathematical models. The issues of potato tops removal are discussed by H. Kainuma *et al.* (2013). Theoretical studies are given only conditionally and do not reflect the actual technological process of potato tops removal. Some results of solving this problem are presented by F. Wang (2021) and K.P. Titiwa *et al.* (2019). Attempts to solve this problem were made by Ye. Ihnatiev (2017). However, when building the computational mathematical model, an extra generalised coordinate was introduced here, which distorted the accuracy of the final result. These studies do not contain a modern representation of oscillatory processes carried out by complex dynamic systems. Namely, they do not contain either amplitude-frequency or phase-frequency characteristics, which in no way confirms the approximation of the modelled process to the real process.

Analytical studies of the oscillatory movements of agricultural machines rear-mounted on tractor units equipped with support wheels with pneumatic tyres were investigated by V. Nadykto *et al.* (2020). The theoretical models were based on a method that is based on the representation of support and doubler wheels that have elastic-damping properties characterised by stiffness and damping coefficients. In general, these studies do not consider the exact configuration of the oscillating system under study. Namely, the closest location to the tractor's rear hitch mechanism of the machine is aggregated doubler wheels, and behind them are the cleaning working bodies that form the working loads. In general, the point of contact of the doubler wheel with the soil can be the point around which this oscillatory system can rotate.

Although a detailed consideration of solving similar problems has been carried out in the study of car oscillations (Deng *et al.*, 2016; Friedl & Mangerig, 2017) and wheeled tractors (Zheng *et al.*, 2019; Yoo *et al.*, 2021), the study of oscillatory movements of root crop head cleaners requires new approaches related primarily to the specifics of the operating conditions associated with the application of combing forces directed downwards (to the row of root crops located on the soil surface) by external forces, that have different physical characteristics and directions, which will largely determine the nature of these oscillations, as well as the configuration of the location of the suspension points to the aggregating wheeled tractor, the installation of the doubler wheels, and the places where the working forces are formed. Therefore, the research aims to determine the conditions of stable movement of the cleaner based on the constructed mathematical model of its oscillatory movement in the longitudinal-vertical plane and the numerical solution of this model to determine the influence of parameters in response to an external disturbance.

MATERIALS AND METHODS

In 2021, at the National University of Life and Environmental Sciences of Ukraine, the Department of Mechanics of the Faculty of Construction and Design, under the leadership of Prof. V. Bulgakov, developed a new root crop head cleaner, in which each row of root crops was cleaned of the residues of tops on the heads at once using two cleaning shafts, on which pairs of rubber blades are hinged on hubs.

The design feature of the developed cleaner, which is shown in Figure 1, is that it is mounted on the rear hitch 2 of the wheeled aggregating tractor 1, has two drive cleaning shafts 6 mounted on the frame 3 and is located horizontally at an acute angle to each other in the transverse plane, covering the row with root crops from both sides. The rows of rubber cleaning blades 7 are fixed on them with the help of clips 8 with an appropriate spacing. Drive shafts 6 have counter-rotating movements provided by the drive 4 (Fig. 1).

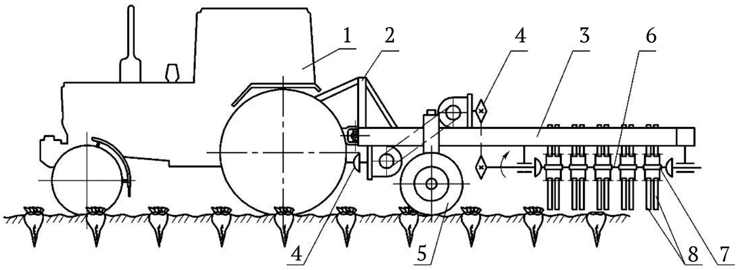

Figure 1. Design and technological scheme of a twin-shaft root crop head cleaner for removing tops from the root
Note: 1 – wheeled aggregating tractor; 2 – rear tractor hitch; 3 – frame; 4 – elements of the cleaning shaft drive; 5 – doubler wheels; 6 – cleaning shafts; 7 – rubber cleaning blades; 8 – blade clips
Source: compiled by the author

The installation of the drive cleaning shafts 6 in the horizontal plane at an angle creates a so-called capture zone for all root crop heads in case they deviate from the row axis. This ensures that they are guaranteed to fall into the cleaning channel formed by the drive cleaning shafts 6 and that they are in contact with the ends of the rubber blades 7.

At the same time, the efficiency of cleaning the heads of root crops from the remains of tops on the root depends on the height of the drive cleaning shafts 6 above the soil surface. For setting and adjusting this parameter, frame 3 of the root crop cleaner is equipped with two doubler wheels 5 located on both sides of frame 3, which have pneumatic tyres.

At the same time, the doubler wheels 5 can be installed in different places on the side parts of frame 3, thanks to the screw mechanisms for their movement and fixation on the specified side parts of frame 3. The doubler wheels 5 move in the rows of root crops, copying the unevenness of the soil surface. This causes oscillations of frame 3 and cleaning shafts 6 in the longitudinal-vertical plane, which can significantly reduce the quality of cleaning the heads of root crops, especially at a sufficiently high speed of the forward movement of the cleaner. In addition, the copying wheels 5 are made in the form of pneumatic tyres, which, with a significant mass of the cleaner, causes oscillatory movements of its frame 3 in the longitudinal-vertical plane. To develop the theory of the movement of the cleaner for cleaning root crop heads from the remains of tops on the root in the longitudinal-vertical plane, considering that it is hitched to the rear of a wheeled aggregating tractor, it is necessary to develop a mathematical model, the first stage of which was to draw up its equivalent scheme.

On this basis, it is necessary to consider the cleaner mounted behind the tractor as a dynamic system consisting of specific elements and moving under the influence of external forces. In this case, as a first approximation, it can be assumed that the aggregating wheeled tractor with which the cleaner is connected moves in a straight line and uniformly (i.e., moves forward at a constant speed $\bar{V}$) and its influence on the movement of the cleaner itself is minimal. It is also important that the movement of the cleaner as a dynamic system must be considered in one plane, i.e., in this case, it is the longitudinal-vertical plane.

The main assumptions in the development of this theory, and, accordingly, the equivalent diagram, are that, based on the specified conditions, the rear-mounted root crop header is an oscillating system that can be represented as independent of the aggregating tractor, which, in the course of its operation, oscillates in the specified plane relative to the elements of the tractor's rear hitch. In terms of construction, the cleaner consists of a frame, two doubler wheels and cleaning tines, and therefore all these elements should be shown in an equivalent diagram.

Given the above, the cleaner was presented in the form of a frame *BE*, which, with the help of the two lower *AB* and one upper *TD* joints is attached with its hitch *BD* to the rear hitch of the tractor. Points *A* and *T* belong to the tractor and as shown above, move in a straight line and uniformly in the direction shown by the arrow with a constant forward speed $\bar{V}$. Cleaner's frame *BE* relies on two copying pneumatic wheels, which, in the case of considering this dynamic system in the longitudinal-vertical plane, can be shown in the equivalent diagram as one common wheel with the centre marked by the point O_1. Point *U* Fixing the doubler wheel brackets to the frame *BE* can be located anywhere on the machine. The cleaning parts (horizontal cleaning shafts with rubber blades) can be mounted on the frame *BE*, are located mainly in the rear part of the machine and are represented in the equivalent diagram as one common working body. Point *E* may be closer to point *U*. These elements of the cleaner as a dynamic system are shown in Figure 2.

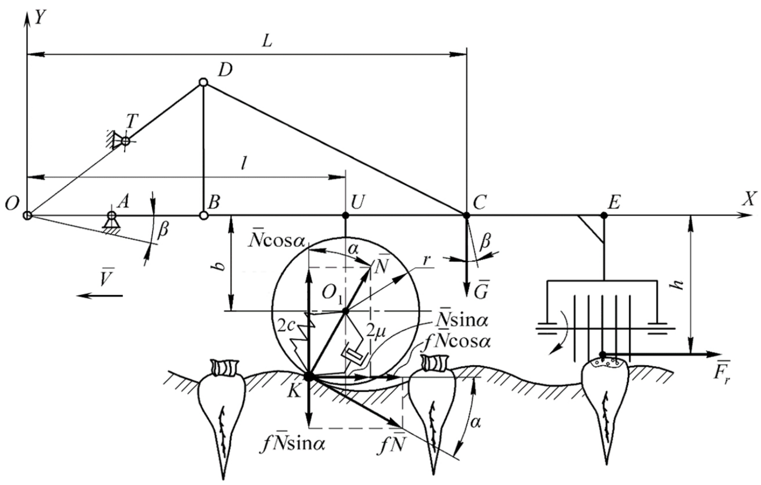

Figure 2. Equivalent scheme of the root crop head cleaner

Note: β – angle of rotation of the cleaner in the longitudinal-vertical plane (generalised coordinate); c – stiffness factor of the pneumatic tyres of the doubler wheels; μ – damping coefficient of the pneumatic tyres of the doubler wheels; N – normal reaction at the point of contact between the doubler wheel and the uneven ground surface; F_r – the force of resistance to the movement of the cleaning working body on the heads of root crops; f – rolling resistance coefficient of the doubler wheel; α – angle of inclination to the horizon of the unevenness of the soil surface passing through the contact point

Source: compiled by the author

All external forces acting on this dynamic system in the process of its movement were identified. If the centre of gravity of the cleaner is *C*, the force of gravity is applied to it $\bar{G}$, which is directed vertically downwards. The cleaning elements in the form of two horizontal shafts form the total force of the working resistance, which is determined by $\bar{F}_r$. In the first approximation, it was assumed that this force is parallel to the frame *BE* and is directed backwards. Furthermore, assuming that the two pneumatic doubler wheels move between the rows of root crops over uneven soil surfaces, the unevenness itself can be approximated by a harmonic function. An equivalent wheel relies on this inequality at the contact point *K* (the equivalent diagram shows that this is a point contact and occurs at any position on the harmonic curve itself). Then at this point of contact, *K* two forces will be applied, one of which is the normal reaction $\bar{N}$ the ground on the doubler wheel, which passes through the centre of the wheel, i.e., the point O_1 and tangent $f\bar{N}$ of soil reaction. Shown reactions $\bar{N}$ and $f\bar{N}$ are mutually perpendicular, and the tangential reaction $f\bar{N}$ is a frictional force equal to the product of the normal reaction $\bar{N}$ and friction coefficient *f*.

Furthermore, since the cleaner's doubler wheels (one equivalent wheel in Fig. 2) are pneumatic, they can be represented as elastic-damping models. Specifically, they should have the appropriate elasticity coefficients *c* and damping coefficients *μ*. Since Figure 2 shows a single equivalent wheel, the coefficients should be double.

The rear hitch of the implement, which has two lower *AB* and central *TD* rods in the operating (floating) position allows free angular rotation of the frame *BE* cleaner, but it occurs around point *O*, a conditional point, located at the intersection of the lines drawn through the specified lower and upper links of the tractor hitch (i.e. lines that are an extension of the specified links).

The next step in constructing an equivalent diagram was to select and designate a coordinate system. Considering that this theory considers the movement of the cleaner in only one plane (longitudinal-vertical), a flat Cartesian coordinate system was chosen. If using point *O* as a coordinate centre, the following coordinate plane will be true: *XOY*. Then, axis *OX* is horizontal and passes through the frame *BE* of the cleaner backwards, and the axis *OY* is directed vertically upwards.

The linear and angular dimensions were then marked on an equivalent diagram. First of all, if, as mentioned above, the cleaner can make free angular turns relative to the reference point *O*, then this point can be the axis of the instantaneous centre of rotation of the central *TD* and lower *AB* The linkage of the rear linkage of the implement. If the angle is presented as *β*, by which the frame *BE* deflects, then it will characterise the oscillatory movements of the cleaner as a dynamic system under consideration relative to the centre *O*. Next, the distance from the point *O* to centre *C* The weight of the cleaner is indicated by *L*. And the corresponding distance from the point *O* to the vertical axis of the doubler wheel (i.e., to the point *U*) is determined as *l*. The radius of the equivalent doubler wheel is denoted by *r*, The height of the centre of the doubler wheel relative to the frame *BE* (thus distance UO_1) to *b*, while the distance from frame *BE* to the ends of the rubber blades of the cleaner (where the total force of working resistance is applied) through *h*. Tangential reaction $f\bar{N}$ deviated from the horizontal by an angle *α*.

Given the accepted designations and dimensions of a normal $\bar{N}$ and tangential $f\bar{N}$ reactions of the soil to the doubler wheel applied at the point *K* can be immediately presented in the form of vertical and horizontal components. The next stage in the development of the theory of the cleaner's motion in the longitudinal-vertical plane was the selection of the dynamics law, which will be used to describe the motion. The most suitable for this purpose is the initial general equation in the form of Lagrange of the second kind of the following form:

$$\frac{d}{dt}\left(\frac{\partial T}{\partial \dot{\beta}}\right) - \frac{\partial T}{\partial \beta} = Q_\beta - \frac{\partial P}{\partial \beta} - \frac{\partial R}{\partial \dot{\beta}}, \quad (1)$$

where *T* – kinetic energy of the system; Q_β – generalised force; *P* – potential energy of the system; *R* – dissipative function; β – generalised coordinate; $\dot{\beta}$ – generalised velocity.

Using the original equation (1), it will be possible to compile a differential equation of motion of the root crop head cleaner in the longitudinal-vertical plane. Since, under the influence of external forces acting on the elements of this dynamic system, it can perform only angular oscillatory movements relative to the point *O*, one generalised coordinate, i.e., the angle of rotation *β*, is true. Thus, the theory of motion of the cleaner in the longitudinal-vertical plane will consist of a single differential equation of its motion in this plane.

The next step is to determine the conditions of the doubler wheel movement when considering the angular oscillatory movements of the cleaner. In general, each of the two tracing wheels of the cleaner moves in the row spacing of root crops, where, at the time of harvesting, the soil has sufficient density and hardness. However, due to the weight of the entire cleaner, its doubler wheels slightly deform the surface layers of the soil and move over uneven surfaces that can be identified by a harmonic function, such as a cosine function. Then the current ordinate *y* of this harmonic function can be an equation of the following form:

$$y = y_0\left(1 - \cos\frac{2\pi \cdot x}{l_1}\right) = y_0\left(1 - \cos\frac{2\pi \cdot V \cdot t}{l_1}\right), \quad (2)$$

where y_o – amplitude of inequality fluctuations; l_1 – period of fluctuations in soil surface roughness; *x* – current coordinate of the bump.

In this case, the current coordinate x unevenness of the soil surface is defined as:

$$x = V \cdot t, \quad (3)$$

where *V* – translational speed; *t* – current time. Subsequently, all the components included in the general initial equation (1) were determined for the considered dynamic system.

Following the equivalent scheme (Fig. 2) kinetic energy T of this dynamic system should be determined under the condition of rotational movement of the cleaner around the point O. Therefore, given that the angle of rotation of the cleaner is marked β, the expression for kinetic energy T was presented as follows:

$$T = \frac{I_{oz} \cdot \dot{\beta}^2}{2}, \tag{4}$$

where I_{oz} – moment of inertia of the cleaner relative to the axis passing through the point O, perpendicular to the longitudinal-vertical plane.

The potential energy P of the dynamic system under consideration is determined by the work of elastic forces of the doubler wheels, which in this case are pneumatic. As is well known, this elasticity force work is a function of the deflections of the pneumatic wheel tyres. These deflections can be analytically determined as follows. Considering the smallness of the angle α These deflections can be represented as the difference between the amplitudes of vertical vibrations y_1 the centres of the doubler wheels, i.e., the point O_1 and the longitudinal profile of the soil surface itself, which is determined by the current ordinate y. And the determined difference $(y_1 - y)$ identifies deflections of the pneumatic wheel.

Considering the above expression for determining the potential energy P of the oscillatory motions of this dynamic system was as follows:

$$P = \frac{2 \cdot c \cdot (y_1 - y)^2}{2} = c \cdot (y_1 - y)^2. \tag{5}$$

Next, the components of expression (5) were identified. As such, amplitude y_1 of vertical oscillations of the centre of the doubler wheel (point O_1) related to the rotation angle β as follows:

$$y_1 = l \cdot \beta, \tag{6}$$

where l – constructional dimensions are shown in the equivalent diagram.

Then, considering (6), expression (5) takes the following form:

$$P = c \cdot (l \cdot \beta - y)^2 = c \cdot (l^2 \cdot \beta^2 - 2 \cdot l \cdot \beta \cdot y + y^2). \tag{7}$$

To determine the dissipative function R the following expression was used:

$$R = \frac{2\mu \cdot (\dot{y}_1 - \dot{y})^2}{2} = \mu \cdot (\dot{y}_1 - \dot{y})^2. \tag{8}$$

Given that the first derivative of expression (6) is equal to $\dot{y}_1 = l \cdot \dot{\beta}$, then the dissipative function R will have the final form:

$$R = \mu \cdot (l^2 \cdot \dot{\beta}^2 - 2 \cdot l \cdot \dot{\beta} \cdot \dot{y}_1 + \dot{y}^2). \tag{9}$$

Thus, all the values on the left side of equation (1) and most of the values on the right side have been determined. Based on this, it was possible to transform them according to the requirements of the general equation (1). So partial derivatives, as well as derivatives from the results obtained in time t, that are related to kinetic energy T, were as follows:

$$\frac{\partial T}{\partial \beta} = 0, \tag{10}$$

and

$$\frac{d}{dt}\left(\frac{\partial T}{\partial \dot{\beta}}\right) = I_{oz} \cdot \ddot{\beta}. \tag{11}$$

Next, similar transformations were performed for the potential energy P by the requirements of expression (1). The partial derivative of the function (7) by the parameter β (i.e., the generalised coordinate) was as follows:

$$\frac{\partial P}{\partial \beta} = 2c \cdot l^2 \cdot \beta - 2c \cdot l \cdot \beta \cdot y. \tag{12}$$

Following the conditions stipulated by expression (1), the partial derivative of the dissipative function R by parameter $\dot{\beta}$ (i.e., the generalised speed) will be determined as follows:

$$\frac{\partial R}{\partial \dot{\beta}} = 2\mu \cdot l^2 \cdot \dot{\beta} - 2\mu \cdot l \cdot \dot{y}. \tag{13}$$

The next step was to find an expression that would define the generalised force Q_β at the generalised coordinate β. For this purpose, an expression was first drawn up, according to which the basic operation was defined δA_β of all active forces on the possible displacement of a given dynamic system. In this case, these possible displacements will be on the possible angular displacement $\delta\beta$. First, a basic operation δA_β of active forces on the possible movement $\delta\beta$. Using the equivalent scheme (Fig. 2), it is possible to calculate:

$$\begin{aligned} \delta A_\beta = {} & G \cdot L \cdot \delta\beta - N \cdot \cos\alpha \cdot (l - r \cdot \sin\alpha) \cdot \delta\beta - N \cdot \\ & \cdot \sin\alpha \cdot (b + r \cdot \cos\alpha) \cdot \delta\beta - f \cdot N \cdot \cos\alpha (b + r \cdot \cos\alpha) \cdot \delta\beta + f \cdot N \cdot \\ & \cdot \sin\alpha \cdot (l - r \cdot \sin\alpha) \cdot \delta\beta - F_r \cdot h \cdot \delta\beta. \end{aligned} \tag{14}$$

Since:

$$\delta A_\beta = Q_\beta \cdot \delta\beta, \tag{15}$$

where Q_β – generalised force by angular coordinate β, then based on (14), the expression of the generalised force Q_β is as follows:

$$\begin{aligned} Q_\beta = \frac{\delta A_\beta}{\delta\beta} = {} & G \cdot L - N \cdot \cos\alpha \cdot (l - r \cdot \sin\alpha) - N \cdot \sin\alpha \cdot \\ & \cdot (b + r \cdot \cos\alpha) - f \cdot N \cdot \cos\alpha (b + r \cdot \cos\alpha) + \\ & + f \cdot N \cdot \sin\alpha \cdot (l - r \cdot \sin\alpha) - F_r \cdot h, \end{aligned} \tag{16}$$

where L, r, b, h and α – the corresponding linear and angular dimensions, which are indicated on the equivalent diagram (Fig. 2). Expression (16) shows that the generalised force Q_β is the algebraic sum of the moments of all active forces acting on a given dynamic system. Assuming that the angle α is small enough, the following is true: $\cos\alpha \approx 1$, and $\sin\alpha \approx \alpha$. The expression (16) may be presented in a simplified form:

$$\begin{aligned} Q_\beta = {} & G \cdot L - N \cdot (l - r \cdot \alpha) - N \cdot \alpha \cdot (b + r) - f \cdot N \cdot (b + r) + \\ & + f \cdot N \cdot \alpha (l - r \cdot \alpha) - F_r \cdot h. \end{aligned} \tag{17}$$

After several transformations, the following was obtained:

$$Q_\beta = G \cdot L - N \cdot [-f \cdot r \cdot \alpha^2 - (b - f \cdot l) \cdot \\ \cdot \alpha - f \cdot b - f \cdot r - l] - F_r \cdot h. \quad (18)$$

Assuming that the doubler wheel is close enough to the frame, and therefore $b \approx r$, the final generalised power of the Q_β will be as follows:

$$Q_\beta = G \cdot L - N \cdot [-f \cdot r \cdot \alpha^2 - (b - f \cdot l) \cdot \\ \cdot \alpha - 2f \cdot r - l] - F_r \cdot h. \quad (19)$$

Next, it was necessary to determine the angle α, which is included in expressions (14)-(19). The angle α is related to the function y, i.e., with the function of vertical ordinates of a cosine function that reflects the longitudinal profile of the soil surface roughness given by expression (2). After differentiating expression (2) by the coordinate x the following expression is obtained, the value of which is equal to tan α:

$$\frac{dy}{dx} = \frac{2\pi \cdot h_0}{l_1} \cdot \sin\frac{2\pi \cdot V \cdot t}{l_1} = \tan\alpha. \quad (20)$$

From expression (20), the value of the desired angle α is found:

$$\alpha = \arctan\left(\frac{2\pi \cdot h_0}{l_1} \cdot \sin\frac{2\pi \cdot V \cdot t}{l_1}\right). \quad (21)$$

Finally, based on the use of the obtained expressions (10)-(13) and (21), their substitution in the original equation (1) and the necessary general transformations, the following differential equation of movement of the root crop head cleaner in the longitudinal-vertical plane was obtained:

$$a_2 \cdot \ddot{\beta} + a_1 \cdot \dot{\beta} + a_o \cdot \beta = \\ = b_1 \cdot \dot{y} + b_o \cdot y + C, \quad (22)$$

where $a_2 = I_{oz}$; $a_1 = 2\mu \cdot l^2$; $a_o = 2c \cdot l^2$; $b_1 = 2\mu \cdot l$; $b_o = 2c \cdot l$; $C = G \cdot L + N \cdot [f \cdot r \cdot a^2 - (b + f \cdot l) \cdot \alpha + 2r \cdot f - l] - F_r \cdot h$.

Equation (22) is a second-degree linear differential equation and is a mathematical model of the movement of a root crop head cleaner in the longitudinal-vertical plane mounted behind a wheeled aggregating tractor. The output parameter of this dynamic system is the angle , i.e., the angle of rotation of the cleaner in the longitudinal-vertical plane.

The next step was to solve the differential equation (22). For this purpose, the most suitable method is the transformation of the differential equation (22) into an algebraic equation. In this case, the method of operational calculus, in particular the Laplace transform method, was applied. According to this method, an operator of the following form was introduced (Bulgakov, 2023):

$$s = \frac{d}{dt}. \quad (23)$$

Using the operator (23) and transforming the differential equation (22), an algebraic equation is obtained, which has the following form:

$$(a_2 \cdot s^2 + a_1 \cdot s + a_o) \cdot \beta(s) = (b_1 \cdot s + b_o) \cdot y(s) + C \cdot 1(s). \quad (24)$$

Analysing expression (24), its components reflect the input external disturbances $y(s)$, in the form of oscillations of the ordinates y profile of soil surface irregularities, which are transferred to the output parameter $\beta(s)$, and also reflect discrete changes in the values of the parameters included in the coefficient C on the same output parameter $\beta(s)$.

This circumstance allowed us to create two transfer functions $W_1(s)$ and $W_2(s)$, which reflect the nature of the oscillatory movements of the cleaner in the longitudinal-vertical plane. The values of these transfer functions are respectively equal:

$$W_1(s) = \frac{b_1 \cdot s + b_o}{a_2 \cdot s^2 + a_1 \cdot s + a_o}, \quad (25)$$

and

$$W_2(s) = \frac{C}{a_2 \cdot s^2 + a_1 \cdot s + a_o}. \quad (26)$$

It should be noted that, due to the linearity of the algebraic equation (24), any parameter determined by the coefficient C can be chosen in the numerator of the transfer function (26) using the principle of superposition. The next stage was the numerical solution of the obtained mathematical model of the oscillatory movements of the cleaner according to the developed theory.

To carry out numerical modelling, first of all, it was determined what the values of the parameters and quantities included in equations (21) and (22) could be. It concerns the force $\bar{N}$, the effect of which is transmitted to the wheel from the ground and drag forces $\bar{F}_r$ movement of the cleaning working body along the head of the root crop during the technological process of cleaning it from the remains of tops.

In general, the unknown normal reaction of the soil $\bar{N}$ can be determined by directly measuring it in the field. In this study, its value was determined by the calculation method at the static equilibrium of the root crop head cleaner. For this purpose, equation (19) was considered since $Q_\beta = 0$.

Resistance force $\bar{F}_r$ of the movement of the cleaning operating element along the head of the root crop was determined under the condition of its equality in size to the combing force Q of tops remains from the head of the root crop (Pogorely & Tatyanko, 2004). For the analytical expression of this combing force Q, the following steps were followed. For example, it is well known that the taproot stems of many root crops (e.g., sugar beet), located close to the head, have a cross-sectional shape close to a triangular shape. At the same time, it has a similarly triangular depression on one side. A conditional graphical model of the cross-section of a sugar beet tops petiole was developed (Fig. 3). The geometric dimensions of the section are shown on the graphical model itself. They were used to calculate the cross-sectional area of the petiole stalk.

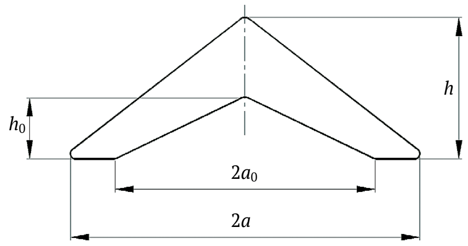

Figure 3. Graphical model of the cross-section of the petiole of a root crop
Source: compiled by the author

Further, it was assumed that the process of combing off the residual tops is carried out directly on the root crop head itself, in the place of conditional fixation of the petiole due to deformation of the mechanical shear (combing) of the petiole. Then the process of combing the tops from the head of the root crop will be possible if the following ratio is met (Pogorely & Tatyanko, 2004):

$$\frac{Q}{n \cdot F} \geq [t], \tag{27}$$

where Q – the force required to comb the tops off, N; $[t]$ – permissible tangential shear stresses for the stalk, $N{\cdot}mm^{-2}$; F – cross-sectional area of one petiole, mm^2; n – number of cuttings to be combed at the same time.

Using expression (27), the force Q, The number of tops necessary for combing the petioles from the root crop head was determined as follows:

$$Q = n \cdot F \cdot [t]. \tag{28}$$

Next, the necessary values included in expression (28) were determined. Thus, using the graphical model of the petiole (Fig. 3), the area of its cross-section was equal to:

$$F = \frac{1}{2} \cdot 2a \cdot h - \frac{1}{2} \cdot 2a_o \cdot h_o, \tag{29}$$

or

$$F = a \cdot h - a_o \cdot h_o. \tag{30}$$

Using expressions (28) and (30), the final force found is $\bar{Q}$ combing the petiole of the tops. It is equal to:

$$Q = (a \cdot h - a_o \cdot h_o) \cdot n \cdot [t]. \tag{31}$$

Considering the aforesaid, a specific numerical value of the force was determined as Q, which is required to comb one stalk of sugar beet tops. The values that can be used in the calculations were suggested by L. Pogorely and N. Tatyanko (2004). Specifically, the following linear dimensions of the cuttings were used: $a = 5$ mm; $a_o = 2$ mm; $h = 5$ mm; $h_o = 2$ mm. Permissible tangential stress values $[t]$ for this plant material were also used according to L. Pogorely & N. Tatyanko (2004) and were deemed equal: $[t] = 1.14 \cdot 10^6$ Pa.

Applying the expression (31) and the specified dimensions of the force Q of combing for 1 petiole stalk was:

$$Q = (5 \cdot 5 - 2 \cdot 2) \cdot 10^{-6} \cdot 1.14 \cdot 10^6 = 23.9, \text{N}. \tag{32}$$

Considering that the combing of green and strong petioles in this cleaner occurs on both sides and that each head of the root crop will contain on average 4 petioles that need to be separated (combed), then, based on the value obtained in (32), it was assumed that $F_r = Q \approx 100$ N.

The prototype of the root crop head cleaner was equipped with tracing wheels with pneumatic tyres 7.50R16, which are widely used in various agricultural machines. For them, the values of the stiffness coefficients c and damping μ were selected from the reference literature.

Radius r of a doubler wheel with a pneumatic tyre of this brand in an undeformed state was also selected from the reference literature. The force of gravity G of the cleaner was determined by weighing the improved design of the cleaner, considering some of the adhering soil. The moment of inertia I_{oz} of the root crop head cleaner was determined analytically. Parameters of the soil surface unevenness profile (h_o, l_1 and f), as well as the design parameters of this device (l, L, b and h), were set and changed during numerical calculations on a personal computer (PC). The speed of translational movement V of the cleaner was adopted according to its field tests.

The PTC Mathcad 15 software was used to perform numerical calculations. Using the obtained analytical dependencies, as well as design and kinematic parameters, the amplitude-frequency, and phase-frequency characteristics of the oscillatory movements of the cleaner, which was modelled as an oscillatory dynamic system, were calculated on a PC and plotted in the form of graphical dependencies.

RESULTS AND DISCUSSION

The nature of the curves reflected in the constructed dependencies precisely indicates the response of the specified dynamic system to external perturbations provided to it and changes in specific structural, kinematic, and operational parameters of the cleaner when it performs the technological cleaning process.

Numerical calculations of the obtained mathematical model are impossible without the use of constant values included in the final expression. The values of structural and force parameters (with an indication of their ranges of variation) used in the calculations are given in Table 1.

The graphical dependences obtained in the calculations make it possible to evaluate the behaviour of the cleaner as an oscillatory system under the action of a disturbing influence at the appropriate frequency, i.e. when the ordinates y change, due to the unevenness of the soil surface and the elastic-damping properties of the doubler wheels (stiffness coefficients c and damping μ), as well as some design parameters of the cleaner (e.g. length l and L).

It should be emphasised at once that the external disturbance, determined by the fluctuations of the ordinates y, given by expression (2), provides the frequency of oscillations of the main range, which varies from 0 to 24 s^{-1}. This is determined by the fact that the main tillage in the fields where root crops are grown forms zones of greater and lesser compaction, which alternate periodically. This is caused by the formation of soil layers that are laid down during ploughing. And although the high-frequency components of the bumps are levelled out later, their low-frequency components remain. Therefore, the representation of soil surface irregularities identified by harmonic functions is quite natural. Based on repeated measurements, it was found that in many cases, soil surface irregularities provide fluctuations in the longitudinal profile ordinates that reach 12 m^{-1}. If we assume that the translational movement of the cleaner will be carried out with a translational speed not exceeding 2.0 ms^{-1}, then the maximum frequency of oscillations of soil surface irregularities, based on which, in this theory, an external disturbance is formed, will be in the range of up to 24 s^{-1}. At the same time, if the behaviour of the dynamic system under consideration is not fully determined by the specified basic frequency range, it will be increased.

Table 1. Structural and kinematic parameters of the root crop head cleaner of improved design

Parameter	Determinant	Unit of measurement	Value
Distance from the suspension axis to the centre of mass	L	m	3.0...4.0
Distance from the suspension axis to the vertical axis of the doubler wheel	l	m	2.8...3.8
Distance from the ends of the rubber blades to the frame	h	m	0.685
Stiffness coefficient of pneumatic tyres for doubler wheels	c	kN·m^{-1}	115...515
Damping coefficient of pneumatic tyres for doubler wheels	μ	N·s·m^{-1}	350...1350
Half the height of uneven ground	h_o	m	0.01...0.03
Step unevenness of the soil surface	l_1	m	0.70
Gravitation force	G	N	9100
Moment of inertia relative to the axis of rotation	I_{oz}	N·m·s^2	3000...3500
Rolling resistance coefficient of the doubler wheel	f	–	0.12...0.16
Resistance force for moving the cleaning implement on root crop heads	F_r	N	100
Normal reaction at the point of contact between the doubler wheel and uneven ground surface	N	N	4100
The radius of the doubler wheel in the undeformed state	r	m	0.370
Distance from frame to centre of doubler wheel	b	m	0.420
Translational speed	V	m·s^{-1}	1.5...2.5

Source: compiled by the author

The amplitude-frequency characteristics of the dynamic system's working out of the oscillations of the soil surface unevenness profile at different values of the stiffness coefficient c of the pneumatic tyres of the doubler wheels were considered. As follows from the curves shown in Figure 4, the amplitude-frequency characteristics tend to increase. At the same time, the increase in the ratio c, for example, from 115 kN·m^{-1} to 315 kN·m^{-1}, and then to 515 kN·m^{-1} makes this increase slower. In all cases, this increase is a negative development. Using pneumatic tyres for doubler wheels with the lowest values c, in our case $c = 115$ kN·m^{-1}, the increase in the amplitude-frequency response occurs at a disturbance frequency from 0 to 28 s^{-1}. At a frequency of 28 s^{-1}, the peak value of this increase occurs, after which there is a sharp decrease in the amplitude-frequency response. It is known from the theory of automatic control that this is the so-called resonant peak, which corresponds to 1.54 rad·m^{-1}, which is characterised by changes in the height of soil surface irregularities not exceeding 0.03 m. However, to match the resonance peak, the cleaner has to be rotated by an angle β no more than 3°. Then, when the frequency of oscillations of the disturbing effect on this dynamic system is increased by more than 28 s^{-1} and to values of 40 s^{-1} doubler wheels with the following coefficient values c, have a sharply decreasing amplitude-frequency response that is close to its desired value.

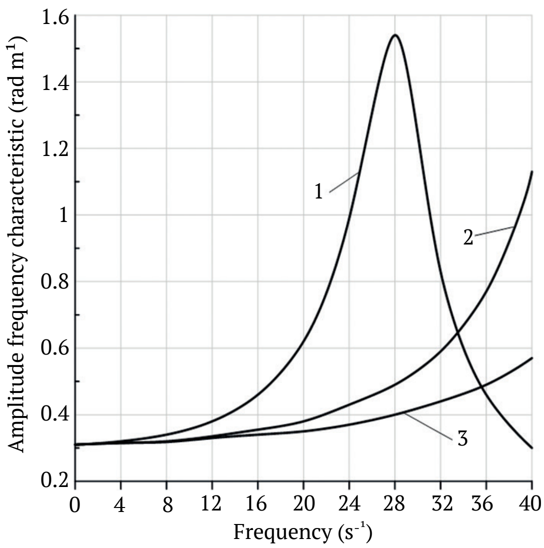

Figure 4. Dependence of the amplitude-frequency response of the cleaner's processing of oscillations of the soil surface unevenness profile on different values of the stiffness coefficient c pneumatic tyres of the doubler wheels

Note: 1 – 115 kN·m^{-1}; 2 – 315 kN·m^{-1}; 3 – 515 kN·m^{-1}

Source: compiled by the author

Analysis of the amplitude-frequency characteristics of the dynamic system's working out of the soil surface irregularities profile at different values of the stiffness coefficient *c* at higher values, namely 315 kN·m^{-1} and 515 kN·m^{-1} shows that there are no longer any peak values, but only a corresponding slow increase, which makes it possible to recommend them as preferred. In addition, based on the graphs in Figure 4, even with a disturbance frequency of 24 s^{-1} an increase of coefficient *c* from 115 kN·m^{-1} to 515 kN·m^{-1} provides the required reduction of the amplitude-frequency characteristics, starting from 1.00 rad·m^{-1} (curve 1), then 0.42 rad·m^{-1} (curve 2) and 0.38 rad·m^{-1} (curve 3) respectively, a 42% reduction in the first case and a 10% reduction in the second case.

The phase-frequency characteristics were also plotted, which indicate a delay in the reaction of the dynamic system under consideration to the action of a disturbing influence (Fig. 5). As shown by the above phase-frequency characteristics at different values of the stiffness coefficient *c* of the pneumatic doubler wheels of the cleaner, an increase in this indicator leads to an improvement in the actual phase-frequency characteristics. At the same time, it is at the disturbance frequencies at the level of up to 12 s^{-1} that various coefficient values *c* do not significantly affect the delayed reaction time of the cleaner.

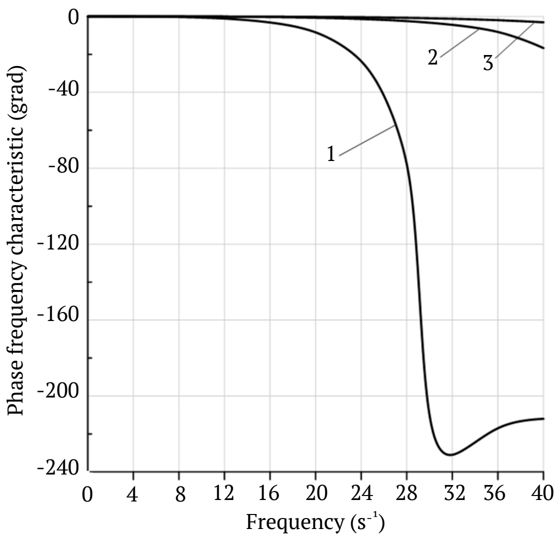

Figure 5. Dependence of the phase-frequency response of the cleaner's processing of oscillations of the soil surface unevenness profile on different values of the stiffness coefficient *c* pneumatic tyres of the doubler wheels

Note: 1 – 115 kN·m^{-1}; 2 – 315 kN·m^{-1}; 3 – 515 kN·m^{-1}

Source: compiled by the author

As can be seen from the changes in the phase-frequency characteristics shown in Figure 5, with an increase in the frequency of the disturbing effect from 12 s^{-1} to 32 s$_{-1}$ at *c*, which equals 315 kN·m^{-1} (curve 2) and *c*, which equals 515 kN·m^{-1} (curve 3) The values of these indicators in both cases are close to zero. From the theory of automatic control, it is known that this indicates that the reaction of the cleaner, as a dynamic system under consideration, is too late. This is the case that should not be considered desirable. At the value of the coefficient *c*, which equals 115 kN·m^{-1} at frequency y 32 s^{-1} the phase-frequency response increases, up to the value of 230o (4 rad), that, on the contrary, there is a possibility to consider this phenomenon positive.

Thus, the phase-frequency characteristics that characterize the delay in the response of the root crop head cleaner to the disturbing effect as shown by the calculations, are almost independent of the coefficient *c* of the stiffness of the tyres of its doubler wheels. As a result, if we assess the impact of the *c* cleare's functionality as a dynamic system under consideration, based on the obtained amplitude-frequency and phase-frequency characteristics, the optimal value *c* is an indicator whose value equals 315 kN·m^{-1}, provided that the fluctuations of the ordinates of the longitudinal profile of soil surface irregularities do not exceed the mark in 12 s^{-1}. To implement this numerical value of the coefficient *c*. The stiffness of the pneumatic tyres of its doubler wheels requires the calculation of specific indicators that will ensure it, provided that the doubler wheels of the previously mentioned brand are used. Coefficient *c* for a doubler wheel is almost entirely determined by air pressure ρ_a in its pneumatic tyre.

To perform this calculation, the normal strain h_{pt} of the pneumatic tyre was first determined following the known formula:

$$h_{pt} = \frac{G_k}{2\pi \cdot \rho_t \cdot \sqrt{r_0 \cdot r_c}}, \tag{33}$$

where G_k – normal load of doubler wheel, N; ρ_t – pneumatic tyre air pressure, Pa; r_o – wheel radius in the unloaded state, m; r_c – radius of curvature of the pneumatic tyre tread, m.

Using Hooke's linear law for elastic deformations, the elasticity coefficient was found to be c for the pneumatic tyre of the doubler wheel using the following expression:

$$c = \frac{G_k}{h_{pt}} = 2\pi \cdot \rho_t \cdot \sqrt{r_0 \cdot r_c}. \tag{34}$$

Finally, the air pressure ρ_t was determined in a pneumatic tyre, depending on the elasticity coefficient *c* and design parameters of the doubler wheel:

$$\rho_t = \frac{c}{2\pi \cdot \sqrt{r_0 \cdot r_c}}. \tag{35}$$

Since for the root crop head cleaner under consideration, the main parameter has the value $r_o \approx rc = r = 0.37$ m, of doubler wheels, the calculation showed that the air pressure inside its pneumatic tyres ρ_a should be approximately 135 kPa. It is quite possible to achieve this parameter for the specified pneumatic tyre. Also, the corresponding calculations were carried out on a PC and the amplitude-frequency and phase-frequency characteristics were obtained, showing their influence on the oscillations of the rear-mounted cleaner depending on another indicator of the pneumatic tyres of its doubler wheels, i.e., the damping coefficient μ. Thus, the amplitude-frequency and phase-frequency characteristics shown in Figure 6 and Figure 7 show that an increase in the external disturbance, i.e.,

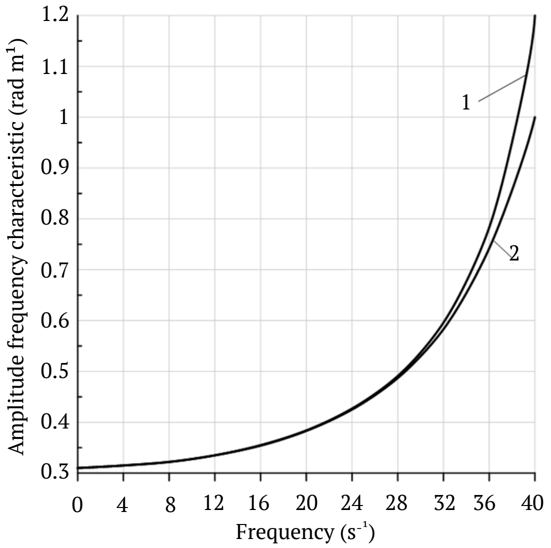

Figure 6. Dependence of the amplitude-frequency characteristics of the cleaner's response to vibrations of the soil surface unevenness profile on different values of the damping coefficient μ

Note: 1 – 350 $N{\cdot}s{\cdot}m^{-1}$; 2 – 1350 $N{\cdot}s{\cdot}m^{-1}$

Source: compiled by the author

fluctuations in the ordinates y longitudinal profile of soil surface irregularities, depending on the values of the coefficient μ have an upward trend.

However, the form of the obtained dependences shown in Figure 6 indicates that the nature of the change in these amplitude-frequency characteristics has little dependence on the value of the damping coefficient μ of of the pneumatic tyres of the cleaner's doubler wheels. At oscillation frequencies of the disturbing influence, which are in the range from 0 to 24 s^{-1}, this dependence is negligible, despite a significant increase in the coefficient μ.

Although outside this frequency range (higher than 24 s^{-1}) there is a difference between the obtained amplitude-frequency characteristics, but it is also insignificant. As follows from the curves shown in Figure 6, at the frequency of the disturbing effect from 30 s^{-1} to 40 s^{-1} of lower coefficient values μ, the higher value of the amplitude-frequency response corresponds to (curve 1). That is the lower the scattering (dissipative) potential of the purifier as a dynamic system, the more sensitive it is to the action of external disturbing influences and vice versa.

In the selected frequency range of the external disturbance from 0 to 24 s^{-1} the difference between the obtained phase-frequency characteristics shown in Figure 7 (curves 1 and 2) is insignificant since it does not exceed 1.5°. In general, the analysis of these indicators shows that the higher the value of the coefficient μ damping of a given dynamic system, which is shown by curve 2, the later this dynamic system reacts to the action of an external disturbance. If the frequency of the latter is only at the level of 40 s^{-1}. The difference in this delay is approximately 17° (meaning 0.3 rad) or 0.0075 s by time.

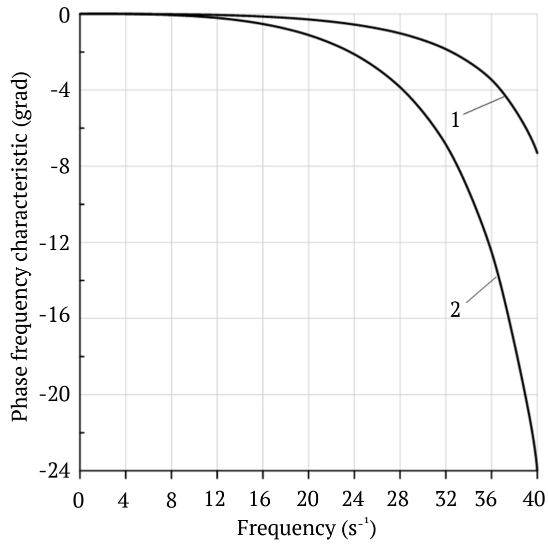

Figure 7. Dependence of the phase-frequency characteristics of the cleaner's response to vibrations of the soil surface unevenness profile on different values of the damping coefficient μ

Note: 1 – 350 $N{\cdot}s{\cdot}m^{-1}$; 2 – 1350 $N{\cdot}s{\cdot}m^{-1}$

Source: compiled by the author

Based on the assessment of the impact of the damping characteristics of the wiper's doubler wheels, there are two important cases:

- the invariance of the response of the cleaner to the disturbing effect when the coefficient is changed was established μ in the range 350 $N{\cdot}s{\cdot}m^{-1}$ to 1350 $N{\cdot}s{\cdot}m^{-1}$;
- the qualitative regularity of the growth of the phase-frequency characteristic of a given dynamic system is observed, provided that the value of its damping coefficient μ increases.

Next, amplitude and frequency characteristics of the cleaner, as a dynamic system, working out the disturbing effect associated with fluctuations in the profile of soil surface irregularities at different values l of the length were considered, i.e., the distance from the suspension axis of the cleaner to the vertical axis of its doubler wheel. As can be seen from the curves in Figure 8, the amplitude-frequency characteristics tend to increase at given lengths l. However, with a shorter length l, which equals 2.8 m the growth is the most intensive.

A significant improvement in the amplitude-frequency characteristics of the disturbance working out by the cleaner can be achieved by increasing the length of the l. That is, an increase in length l from 2.8 to 3.8 m ensures a decrease in the amplitude-frequency characteristics of the cleaner as a dynamic system. Analysis of the change in the amplitude-frequency characteristics of the cleaner's processing of oscillations of the soil surface roughness profile from different values of the length l, shown in Figure 9, shows that at oscillations in frequencies from 0 to 24 s^{-1} the difference in these characteristics can reach 0.22 rad·m^{-1}. At the same time, since the height of soil surface irregularities varies from 0.01 m to 0.03 m, this difference is from 0.13 to 0.39°.

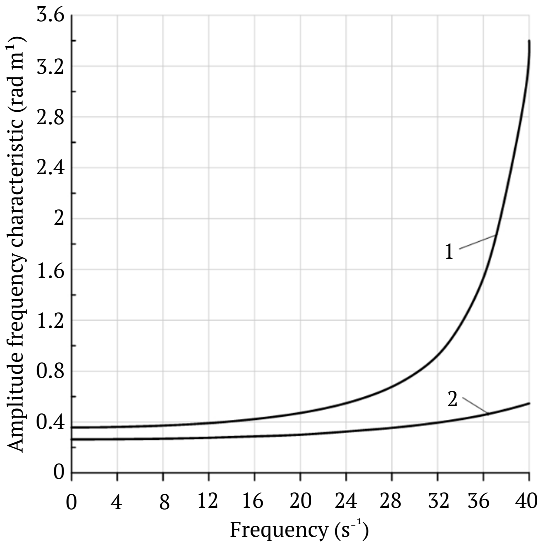

Figure 8. Dependence of the amplitude-frequency characteristics of the cleaner's response to vibrations of the soil surface unevenness profile on different values of the length l

Note: 1 – 2.8 m; 2 – 3.8 m

Source: compiled by the author

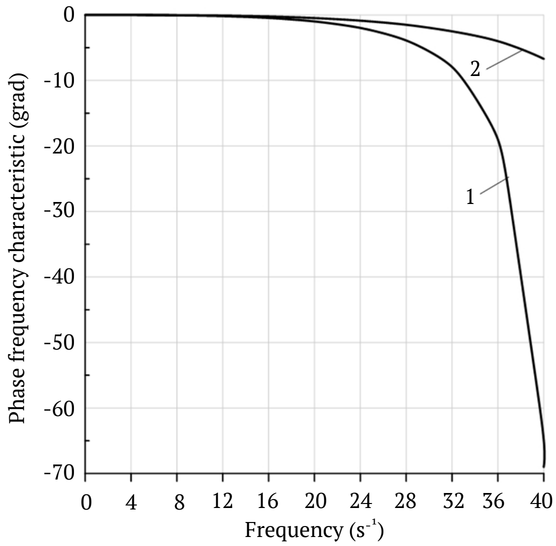

Figure 9. Dependence of the phase-frequency characteristics of the cleaner's response to vibrations of the soil surface unevenness profile on different length values l

Note: 1 – 2.8 m; 2 – 3.8 m

Source: compiled by the author

The graphical dependences of the phase-frequency characteristics of the cleaner's processing of oscillations of the soil surface roughness profile at different values of the length l were constructed, which show that increasing the length of the l leads to a decrease in the phase-frequency response. This is undesirable for the cleaner as an oscillating system. This shows that at the oscillation frequency of the disturbing influence, which is equal to 40 s^{-1} The decrease is 1 rad. Considering the time over which this decrease occurs, it is only 0.025 s, which indicates the high sensitivity of the cleaner to this disturbance. Considering the frequency changes from 0 to 24 s^{-1}, length l changes do not cause corresponding changes in phase-frequency characteristics.

It can be argued that the oscillation of the cleaner is not affected by changes in length l. The installation location of the doubler wheels on the cleaner frame should be considered close to the cleaning working bodies, which will certainly create conditions for accurate copying of root crop heads from the remains of tops on the root. Amplitude and frequency characteristics of the cleaner, as a dynamic system, working out the disturbing effect associated with fluctuations in the profile of soil surface irregularities at different length values L, thus distance from point O of the cleaner suspension to the centre of mass of the cleaner, i.e., the point C. These changes in the amplitude-frequency characteristics are shown in Figure 10.

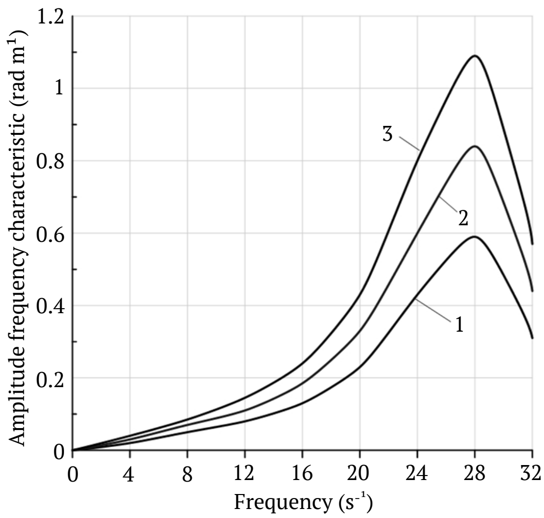

Figure 10. Dependence of the amplitude-frequency characteristics of the cleaner's processing of oscillations of the soil surface unevenness profile from different length values L

Note: 1 – 2.5 m; 2 – 3.0 m; 3 – 3.5 m

Source: compiled by the author

As the view of the above amplitude-frequency characteristics shows, it is necessary to strive to ensure that the centre of mass of the cleaner (point C, Fig. 2) was as close as possible to the pole of the instantaneous centre of rotation of the rear linkage of the implement (point *O*). In this case, the amplitude-frequency characteristics of the cleaner in terms of its working out of vibrations of the ordinates of the longitudinal profile of soil surface irregularities are reduced.

It should be noted that the maximum values of these amplitude-frequency characteristics occur at the frequency of the disturbance, which is 28 s^{-1}. Two significant cases follow from this. First, the frequency value is outside the accepted range of 0 to 24 s^{-1}. Secondly, the resonance peaks occurring at this frequency (however, as in Fig. 4) are far from those that may be undesirable for the design of a root crop head cleaner from the remains of tops on the root. Moreover, the lower the frequency of oscillations of the disturbing influence, the closer the obtained amplitude-frequency characteristics are to the zero mark, which is certainly desirable. A lower frequency corresponds to a longer period of oscillations of the ordinates of the profile of soil surface irregularities. This indicates the need to improve the quality of basic tillage in the process of growing both root crops and any other crops, which are known to form a harmonious appearance of surface irregularities.

Dependence of the phase-frequency characteristics of the cleaner's processing of oscillations of the soil surface unevenness profile on different values of the length *L*, which was established by computer calculations, showed the complete invariance of changes in this constructive index concerning the phase shift. Therefore, these graphical dependencies are not presented here. Analysing the results of the study and comparing them with previously published works, it should be noted that the closest earlier cited studies of M. Khelemendyk (2011); V. Bulgakov *et al.* (2017; 2023), while aimed to obtain qualitative indicators of oscillatory movements of the cleaner attached to the aggregating tractor, do not cover studies of all possible options for the influence of the design, kinematic and operational characteristics of the cleaners themselves on the stability of their movements in the longitudinal-vertical plane. In addition, the study by V. Bulgakov *et al.* (2017) does not perform a qualitative analysis of the oscillatory movement of the cleaner itself, but only provides a detailed mathematical formalisation of the cleaner's movement over uneven soil surfaces.

In addition, although the influence of the elastic-damping properties of the caster wheels on the stability of the wiper as a dynamic system, in particular, the elasticity coefficient c and the damping coefficient μ is certainly important, considering several other design parameters of the wiper as a whole can cause even better conditions for stable movement. In addition, increasing the stability of the cleaner frame in the longitudinal-vertical plane by changing only the elastic-damping properties of the doubler wheels and finding a place for their placement on the mainframe can cause controversial situations related not only to the accuracy of doubler soil surface irregularities in the row spacing but also directly in the row itself. For example, for a certain set of parameters, their influence, i.e., even greater sensitivity to external disturbances, can be so intense that other indicators that ensure the accuracy of copying each head of the root crop will deteriorate. In this case, the most suitable conditions are compromise solutions that will allow the prevailing factors to be the main ones. These factors take place only in the case of movement of root crop head cleaners from the remains of tops on the root when both the stability of movement and the accuracy of copying each root crop head are extremely important.

The search for the accuracy of copying the rows of sugar beet root crops during the harvesting of tops, and, accordingly, the quality indicators of this technological process were considered by I. Storozhuk & V. Pankiv, (2015) and E. Berezhenko (2020). However, theoretical studies in this particular formulation are not considered here and the amplitude-frequency and phase-frequency characteristics were not provided. Some results of solving a similar problem were considered in the works of V. Nadykto *et al.* (2020), but they consider agricultural machines hitched to the rear of the aggregating tractor or frontally mounted ploughing and chopping machines. Moreover, all these works consider the stability of the movement of the aggregated agricultural machines in the longitudinal-vertical plane. However, the specifics of the functioning of tractor-mounted machines and the studies in the known works differ significantly from the operation of the cleaner, where the conditions of stable movement under the influence of external disturbances, such as uneven soil surface in the rows of crops, must be combined with external disturbances in the row itself.

Fundamental studies of the stability of agricultural machines mounted on tractor-mounted aggregates were presented by H. Beloev *et al.* (2021). However, the study considered various effects of external disturbances on the forced oscillations of ploughs in the longitudinal-vertical plane, which, although generally important, are not required to be sensitive to the copying of soil surface irregularities, as is the case when considering the oscillations of cleaners. The main focus is on the vertical oscillations of the front and rear axles of the power vehicle itself, i.e., the wheeled tractor. In this study, the amplitude-frequency and phase-frequency characteristics of the tractor are also plotted following the oscillations of the unevenness of the soil surface. However, the energy vehicle is essentially a symmetric dynamic system, and the vibrations of its front and rear axles are interconnected. Consideration of the oscillatory movements of the rear-mounted implement as a dynamic system that represents a "physical pendulum" is not presented here.

Thus, using the constructed new mathematical model, which is the theory of oscillatory movements in the process of plane-parallel oscillatory motion in the longitudinal-vertical plane, it was possible to determine the design, kinematic and operational parameters of the rear-mounted peeler that ensures the stability of its movement using a computer. This, in turn, will contribute to a significant improvement in the quality of the technological process performed by the root crop head cleaner to remove the remains of tops on the roots. A comparative analysis of the numerical values of the obtained parameters with the results of similar studies by other authors indicates the reliability of the developed theory.

CONCLUSIONS

The basic principles of the theory of oscillatory motion of the root crop head cleaner in the longitudinal-vertical plane, mounted behind a wheeled aggregating tractor, have been developed, which allow numerical modelling on a PC to determine its dynamic properties depending on the action of the disturbing influence caused by changes in the ordinates of soil surface irregularities at the appropriate frequency.

The influence of the stiffness of pneumatic doubler wheels, characterised by the coefficient c on the functioning of the cleaner as a dynamic system under consideration, based on the obtained amplitude-frequency and phase-frequency characteristics, and it is established that the optimal value of this indicator is 315 $kN \cdot m^{-1}$, provided that the oscillations of the ordinates y of the longitudinal profile of soil surface irregularities will not exceed 12 s^{-1}. The implementation of this condition can be ensured by the formation of air pressure in the pneumatic tyres of the wiper's doubler wheels, which should be 135 kPa.

Based on the evaluation of the influence of the damping characteristics of the pneumatic doubler wheels of the cleaner, it was found that when the coefficient μ changes from 350 $N \cdot s \cdot m^{-1}$ to 1350 $N \cdot s \cdot m^{-1}$ an invariance of the delay in the response of the cleaner to the disturbance in the frequency range from 0 to 24 s^{-1} is present. At the same time, there is a regularity of growth of the phase-frequency characteristic of this dynamic system under the condition of increasing the value of its damping coefficient μ.

The influence of such a design parameter as the distance from the suspension axis of the rear-mounted cleaner to the vertical axis of its doubler wheel in the considered frequency range from 0 to 24 s^{-1} of oscillations of the ordinates of the longitudinal profile of soil surface irregularities is insignificant. This follows from the nature of changes in the obtained amplitude-frequency and phase-frequency characteristics. However, to ensure more accurate copying of root crop heads, which will generally improve the quality of this technological process, the place of installation of the doubler wheels on the cleaner frame should be considered their close location to the cleaning working bodies. To improve the dynamics of oscillatory movements of the rear-mounted cleaner in the longitudinal-vertical plane, its centre of mass should be located as close as possible to the pole of the instantaneous centre of rotation of the rear hitch of the aggregating tractor.

The subject of the next theoretical study should be the construction of a mathematical model in which the irregularities of the soil surface are approximated by a non-harmonic curve, and the external disturbance is formed by a random function. The next stage of the research should include comprehensive experimental studies to determine the effect of angular oscillatory movements of the rear-mounted cleaner on the quality of separation of the residual tops from the heads of root crops on the root. In conducting these field studies, a wide range of changes in the design, kinematic and operational parameters of the cleaner should be used when performing this technological process. It is also necessary to find an opportunity to determine the qualitative indicators of cleaning by a variable input parameter, namely different frequencies of oscillations of the disturbing effect created by different types of soil surface irregularities.

ACKNOWLEDGEMENTS

None.

CONFLICT OF INTEREST

None.

REFERENCES

[1] Beloev, H., Adamchuk, V., Kaletnik, G., & Bulgakova, O. (2021). *The basis of scientific research in the field of agricultural engineering*. Ruse: Academic Publishing House Ruse University.
[2] Beloev, H., Kaletnik, H., Adamchuk, V., & Delikostov, T. (2022). *Theoretical basis aggregation of plows*. Sofia: Prof. Marin Drinov Publishing House of Bulgarian Academy of Sciences.
[3] Berezhenko, E. (2020). Analysis of methods for harvesting haulm root crops and designs of harvest modules. *Innovative Solutions in Modern Science*, 38(2), 46-54. doi: 10.26886/2414-634X.2(38)2020.4.
[4] Budzanivskyi, M. (2022). Mathematical modelling of oscillations of a machine for cutting tops of root crops. *Machinery & Energetics*, 13(4), 16-27. doi: 10.31548/machenergy.13(4).2022.16-27.
[5] Bulgakov, V., Adamchuk, V., Holovach, I., & Ihnatiev, Ye. (2017). Mathematical model of the movement of a towed machine for cleaning beet tops residues from root crop heads. *Agricultural Science and Practice*, 4(1), 3-10. doi: 10.15407/agrisp4.01.003.
[6] Bulgakov, V., Adamchuk, V., Nadykto, V., & Budzanivskyi, M. (2023). Fluctuations dynamics of the root crops cleaner heads from the remnants of tops on the root. *Bulletin of Agricultural Science*, 101(2), 43-52. doi: 10.31073/agrovisnyk202302-06.
[7] Deng, L., Yan, W., & Zhu, Q. (2016). Vehicle impact on the deck slab of concrete box-girder bridges due to damaged expansion. *Journal of Bridge Engineering*, 21(2). doi: 10.1061/(ASCE)BE.1943-5592.0000796.
[8] Friedl, R., & Mangerig, I. (2017). Dynamic amplification of bridge-expansion-joints considering roughness induced vehicle vibrations. *Procedia Engineering*, 199, 2651-2656. doi: 10.1016/j.proeng.2017.09.515.
[9] Hevko, R., Brukhanskyi, R., Flonts, I., Synii, S., & Klendii, O. (2018). Advances in methods of cleaning root crops. *Bulletin of the Transilvania University of Braşov*, 11(60)(1), 127-138.

[10] Hevko, R.B., Synii, S.V., Pankiv, M.P., & Varholiak, M.A. (2014). Development and analysis of machine operation for energy saving technologies of root crop harvesting. *Bulletin of Engineering Academy of Ukraine*, 3-4, 46-52.
[11] Ihnatiev, Ye. (2017) Theoretical modelling of oscillating motion of root crops heads cleaning unit which is rear-mounted on integral arable and row-crop tractor. *Mechanization and Electrification of Agriculture*, 103(4), 47-56.
[12] Kainuma, H., Aoki, J., Suzuki, T., Oonami, M., & Kamata, M. (2013). Development of potato haulm remover (Part 1) – state of potatoes at harvest and the effects of different haulm removal methods on potato quality. *Journal of the Japanese Society of Agricultural Machinery*, 75(6), 434-439. doi: 10.11357/jsam.75.434.
[13] Khelemendyk, M.M. (2011). *Directions and methods of development of working bodies of agricultural machines*. Kyiv: Agrarian Science.
[14] Nadykto, V.T., Kyurchev, V.M., & Kuvachev, V.P. (2020). *Use of equipment in the agro-industrial complex*. Kherson: OLDI-PLUS, 2020.
[15] Pogorely, L.V., & Tatyanko, N.V. (2004). *Beet harvesters: History, design, theory, forecast*. Kyiv: Phenix.
[16] Storozhuk, I.M., & Pankiv, V.R. (2015). Research results of harvesting haulm remnants of root crops. *INMATEH – Agricultural Engineering*, 46(2), 101-108.
[17] Titiwa K.P., Gavino, H.F., Gavino, R.B., & Malamug, V.U. (2019). Development of potato (*Solanum Tuberosum* L.) haulm cutter. *IOP Conference Series: Earth and Environmental Science*, 301, article number 012009. doi: 10.1088/1755-1315/301/1/012009.
[18] Wang, F. (2021). Optimization and field experiment of an adjustable device for sugar beet digger. *International Journal of Agricultural and Biological Engineering*, 14(6), 68-74. doi 10.25165/J.IJABE.20211406.6667.
[19] Yoo, H., Oh, J., Chung, W.-J., Han, H.-W., Kim, J.-T., Park, Y.-J., & Park, Y. (2021). Measurement of stiffness and damping coefficient of rubber tractor tires using dynamic cleat test based on point contact model. *International Journal of Agricultural and Biological Engineering*, 14(1), 157-164. doi: 10.25165/j.ijabe.20211401.5799.
[20] Zheng, E., Zhong, X., Zhu, R., Xue, J., Cui, S., Gao, H., & Lin, X. (2019). Investigation into the vibration characteristics of agricultural wheeled tractor-implement system with hydro-pneumatic suspension on the front axle. *Journal of Terramechanics*, 186, 14-33. doi: 10.1016/j.biosystemseng.2019.05.004.

Мирослав Ігорович Будзанівський

Аспірант

Інститут механіки та автоматики агропромислового виробництва
Національної академії аграрних наук України
08631, вул. Вокзальна, 11/1, смт. Глеваха, Київська обл., Україна
https://orcid.org/0000-0002-0508-3816

Розробка теорії руху очисника головок коренеплодів у повздовжньо-вертикальній площині, навішеного позаду колісного трактора

Анотація. Актуальність розробки аналітичних методів для вивчення стійкості руху очисників коренеплідних культур на тракторах виникає з необхідності покращення ефективності і якості очищення головок коренеплодів, оскільки від цього залежить якість кінцевого продукту та його товарні властивості. Метою даного дослідження є підвищення стійкості руху очисника, шляхом побудови математичної моделі його коливального руху у повздовжньо-вертикальній площині, та її числового розв'язування для визначення впливу параметрів у відповідь на зовнішній збурювальний вплив. Для виконання поставленої мети була розроблена нова теорія руху очисника головок коренеплодів у повздовжньо-вертикальній площині, навішеного позаду колісного трактора, під дією збурювального впливу нерівностей повздовжнього профілю поверхні ґрунту на амплітудні та фазові частотні характеристики його кутових коливань. Шляхом проведених на персональному комп'ютері числових розрахунків знайдені умови, за якими підвищення стійкості руху очисника у зазначеній площині буде в разі, коли коефіцієнт c жорсткості пневматичних шин копіювальних коліс буде мати значення 315 $kN \cdot m^{-1}$. Такий результат забезпечується тоді, коли тиск у шинах пневматичних коліс буде 135 kPa. Що стосується демпфувальних характеристик шин пневматичних копіювальних коліс, які визначаються коефіцієнтом μ, то встановлено, що при його зміні від 350 $N \cdot s \cdot m^{-1}$ до 1350 $N \cdot s \cdot m^{-1}$ має місце інваріантність запізнення реакції очисника на збурювальний вплив при зміні його частот від 0 до 24 s^{-1}. Також встановлено, що вплив геометричних розмірів очисника, є несуттєвим у діапазоні частот коливань ординат повздовжнього профілю нерівностей поверхні ґрунту від 0 до 24 s^{-1}. Це випливає з характерів змін отриманих амплітудно-частотних та фазово-частотних характеристик. Методика побудови математичної моделі плоскопаралельного коливального руху очисника може бути використаною при аналогічних аналітичних дослідженнях інших задньонавішених на колісний агрегатуючий трактор сільськогосподарських машин

Ключові слова: нерівності ґрунту; еквівалентна схема; коливання; диференціальні рівняння; амплітудно-частотні; фазово-частотні характеристики

Machinery & Energetics
Vol. 14, No. 4. 2023

Journal homepage:
https://technicalscience.com.ua/en

UDC 355.358.4:624.01
DOI: 10.31548/machinery/4.2023.23

Andrii Volkov*

Head of the Department
Ivan Kozhedub Kharkiv National Air Force University
61045, 228 Klochkivska Str., Kharkiv, Ukraine
https://orcid.org/0000-0003-1566-9893

Mykhailo Brechka

PhD in Technical Sciences, Senior Lecturer
Ivan Kozhedub Kharkiv National Air Force University
61045, 228 Klochkivska Str., Kharkiv, Ukraine
https://orcid.org/0000-0003-1566-9893

Volodymyr Stadnichenko

Deputy Head of the Department
Ivan Kozhedub Kharkiv National Air Force University
61045, 228 Klochkivska Str., Kharkiv, Ukraine
https://orcid.org/0000-0002-1780-9215

Vitalii Yaroshchuk

Lecturer
Ivan Kozhedub Kharkiv National Air Force University
61045, 228 Klochkivska Str., Kharkiv, Ukraine
https://orcid.org/0000-0001-5318-5692

Serhii Cherkashyn

Lecturer
Ivan Kozhedub Kharkiv National Air Force University
61045, 228 Klochkivska Str., Kharkiv, Ukraine
https://orcid.org/0009-0002-6940-3863

The protection of critical infrastructure facilities from air strikes due to compatible use of various forces and means

Abstract. The relevance of the study is emphasised by the need to investigate and develop effective strategies for protecting critical state infrastructure in the context of the Russian-Ukrainian war of 2022. The purpose of this study is to evaluate the effectiveness of interaction between the means of physical and electronic influence in the context of protecting critical infrastructure facilities of the energy sector from air strikes. The object of research is the system of protection of critical facilities of the state's energy sector. Research methods included the use of system analysis, the development of strategies for determining the optimal locations of the means of physical influence, and the use of mathematical modelling. Research in the field of interaction and simultaneous use of physical and radio-electronic means included a theoretical analysis of abstract objects and their relationships. These objects were designed to create an idealised description and investigate possible scenarios, as well as to determine optimal actions in specific situations. This study examined in detail

Article's History: Received: 04.07.2023; Revised: 17.10.2023; Accepted: 22.11.2023.

Suggested Citation:
Volkov, A., Brechka, M., Stadnichenko, V., Yaroshchuk, V., & Cherkashyn, S. (2023). The protection of critical infrastructure facilities from air strikes due to compatible use of various forces and means. *Machinery & Energetics,* 14(4), 23-32. doi: 10.31548/machinery/4.2023.23.

*Corresponding author

the possibilities of improving the effectiveness of protecting important energy facilities from air strikes through the use of combined strategies such as anti-aircraft fire and fire protection. Methods for determining the optimal locations of the means of physical influence were analysed, which allowed predicting expected results when using them together. It was developed evidence-based recommendations for the effective integration of these methods, which is an innovative approach to the problem. The means of physical influence included small arms, which were part of the armament of the Armed Forces, and interceptor drones. Electronic means of influence included technical means of radio frequency warfare and electromagnetic guns. The practical significance of this study lies in the fact that it presents specific strategies and technological solutions for comprehensive protection of critical infrastructure facilities from air strikes. This paper can serve as a basis for developing effective security and protection policies in countries and regions, helping to improve overall sustainability and security

Keywords: energy sector of the state; the Russian-Ukrainian war; means of physical influence; radio waves; air attack

INTRODUCTION

The need to investigate this topic is conditioned by modern geopolitical realities and the evolution of security threats. The results of terrorist attacks and examples of the use of drones to attack critical energy facilities indicate an increase in the vulnerability of states to new forms of aggression. The use of air strikes, in particular, through the use of unmanned aircraft, is becoming an effective tool for terrorist organisations and countries, and therefore, the study and development of strategies for the protection of critical facilities is an extremely urgent task for ensuring national and international security, and protecting the economic interests of states. A significant number of dangerous critical facilities in the world are located in most countries. The level of danger of a facility is set considering the percentage of the civilian population and the area of the territory that may become part of the zone of possible impact in the event of an accident at a facility. The results of terrorist attacks during 2019-2022 in the world and the course of the Russian-Ukrainian war show that the most dangerous objects today are facilities of the energy sector. In just nine months of 2022, more than 184 cruise missiles and more than 95 unmanned aerial vehicles were fired at Ukrainian cities where critical facilities of the state's energy sector are located, including more than 70 Iranian Shahed-136 kamikaze drones (Chronicle of the war..., 2022). According to estimates of the world's leading economists, the economic damage caused by these blows to the state amounts to more than 300 billion USD.

The problem of the study is that modern technologies, in particular the use of drones, open up new opportunities for attacks on critical facilities of the energy sector. The global experience of terrorist attacks and examples of air strikes during armed conflicts confirm that the energy sector is particularly vulnerable to such threats. However, providing comprehensive protection of critical facilities from air strikes is a complex task, as it requires a combination of means of physical and electronic influence, including new technologies in the field of unmanned aviation, and developing effective security management strategies.

According to H. Dementiiuk *et al.* (2023a), modern technologies allow effectively using methods of radio-electronic influence on energy sector facilities. The study does not detail the consideration of possible defence options during air strikes. I.Yu. Chaika & Ye.G. Tsokur (2022) emphasise the high vulnerability of critical facilities to air strikes. The effectiveness of possible protection measures against such threats is not investigated. According to V. Hurkovskyi *et al.* (2023), terrorist acts and examples of the use of drones in armed conflicts emphasise the need for a combination of means of physical and electronic influence to provide comprehensive protection. The analysis did not address specific aspects of the development or use of specific strategies for combining means of physical and electronic influence.

S. Korsunov *et al.* (2021) note that new opportunities for the use of unmanned aerial vehicles, in particular kamikaze unmanned aerial vehicles (UAVs), are highlighted. This paper does not address new security challenges. Research conducted by V. Berezutskyi & N. Berezutska (2022) emphasises the importance of developing security management strategies and determining optimal methods for protecting critical facilities from air strikes. The study does not analyse specific aspects of developing security management strategies and determining optimal methods for protecting critical facilities from air strikes. The paper by V. Dykha & V. Lukianova (2023) raises the question of possible economic losses as a result of attacks on energy facilities. This study does not provide a specific detailed analysis of possible measures to reduce economic losses as a result of attacks on energy facilities.

The purpose of this study is to determine the effectiveness of interaction between physical and radio-electronic means in the context of protecting critical infrastructure facilities of the energy sector from air strikes. Objectives of the study:

1. onduct an analysis of the interaction of means of physical and electronic influence to determine their compatibility.
2. Develop a methodology for determining the optimal location of means of physical influence when protecting critical facilities of the energy sector from air strikes.
3. Develop scientifically based recommendations for the effective use and interaction of physical and electronic means of influence.

MATERIALS AND METHODS

The object of this study is a comprehensive system for protecting facilities of critical importance that are part of the state's energy complex. After evaluation, it was found that this system includes various tools and technologies aimed at protecting these facilities from potential air strikes and other threats. The subject of this study is a detailed review and optimisation of the combined use of physical and electronic means of influence in the protection system. This included investigating the interaction of these tools, evaluating their effectiveness, and developing strategies for optimal use in the context of protecting critical energy facilities.

The use of the system analysis method identified key elements of the system and assessed their importance and relationships, which contributed to a deeper understanding of the problem and the development of effective protection strategies. The system analysis also allowed identifying possible risks and predicted their consequences, which is a key stage in the development of comprehensive strategies for protecting critical facilities. This method has created a theoretical and practical basis for further steps in implementing innovative solutions and developing practical protection strategies in the face of modern threats and challenges.

The method of mathematical modelling allowed considering various factors, such as geographical conditions, characteristics of means of influence, possible attack paths, and risk dynamics. By creating mathematical models, possible scenarios were evaluated and optimal parameters for the location of means of physical influence were determined to maximise the effectiveness of facility protection. The use of mathematical modelling contributed to a deep understanding of the impact of various factors on security and helped improve security strategies, making them more accurate and adapted to specific conditions. This is a key step in creating comprehensive protection strategies for critical facilities that take into account all possible scenarios and risks to ensure full protection.

The development of a methodology for choosing the location of means of physical influence included a detailed study of the topography and geographical features of the facility. This process took into account various factors, such as population density, environmental conditions, and possible attack routes. Special attention was paid to aerodynamic characteristics and altitude parameters in order to ensure the optimal location of means of physical influence to maximise their effectiveness in protecting facilities. In the course of the study, an algorithm for determining the optimal location of an anti-aircraft missile system when protecting a facility from an air strike was developed and improved, and key aspects of their optimal use in real-world protection conditions were identified.

RESULTS

Development of a methodology for determining the optimal location of physical protection for energy sector facilities against air strikes

To develop a methodology for determining the optimal location of means of physical influence (MPI) in the protection of critical facilities of the energy complex (CFEC) from air strikes, it is proposed to use an algorithm (Fig. 1), which provides for the sequential execution of a number of procedures and tasks. The initial data for calculating the distance between MPI (Block 1) are the types of air-to-air missiles (AAM) that can be applied to the protected facility, the geographical coordinates and spatial dimensions of the protected facility, the composition of MPI allocated for the protected facility, the highest level of efficiency in the use of MPI, and characteristics describing the effectiveness of the use of MPI. Source data is selected from pre-created data or generated during database preparation (Block 1).

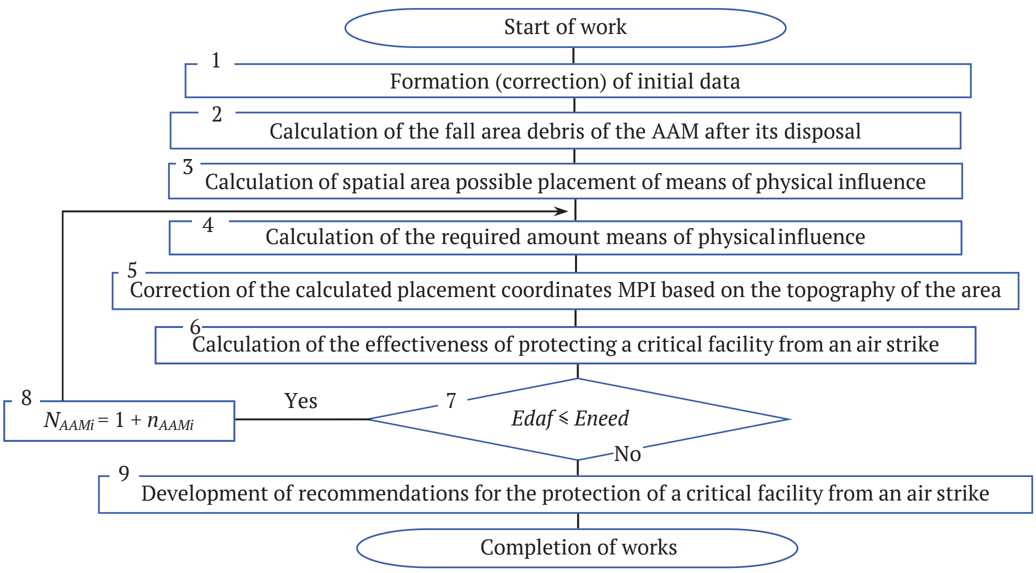

Figure 1. Algorithm for selecting the location of an anti-aircraft missile system when protecting a facility from an air strike
Source: compiled by the authors based on P. Hou *et al.* (2023)

In Block 2, the area of falling of fragments of an AAM after their neutralisation is calculated using the existing model (Park *et al.*, 2021). This calculation is key to determining the required distance by which locations should be removed from the perimeter of the protected facility. Analysis of the results of modelling the process of air defence system neutralisation during flight at different speeds and altitudes showed that the distance to the detection point should be within 1-2 km from the protected facility. Among the criteria that determine the effectiveness of MPI, the range of destruction of AAM from the protected facility, on which the task of their neutralisation is set, is of great importance. This range is determined by the specific means of physical influence, the flight altitude of the missile defence system, the time of detection and neutralisation, and the distance to which the defence zone extends from the facility. Setting the horizontal distance from the protected facility to its border, where tasks for the disposal of AAM are set, is carried out using the following equations:

$$d_{d.s.t} = d_{d.MPI} + V_{AAM}(t_{d.p.MPI} + t_{t.n}), \quad (1)$$

where: $d_{d.s.t}$ – horizontal distance from the protected facility to the task setting line, $d_{d.MPI}$ – distance of the MPI location from the protected facility, V_{AAM} – speed of air attack vehicle, $t_{d.p.MPI}$ – time of direct preparation of MPI for neutralisation of air attack vehicles, $t_{t.n}$ – time of neutralisation of air attack vehicles at the borders of the neutralisation zone.

Block 3 defines the area where the device can be placed for physical influence. Given the requirements for avoiding debris entering the protected facility, it is recommended to dispose of debris at an average distance of 2 km or more from the protected facility (depending on the type of debris). To do this, the location of anti-aircraft installations should be removed from the territory of the protected facility at a distance of 1 km or more. Increasing the distance of the MPI location increases the probability of saving the protected facility. On the other hand, the more remote the MPI is from the protected facility, the more tools need to be used for effective protection. It is noted that in practice there is a limited number of available tools (Kumar *et al.*, 2022). Therefore, it is recommended to determine the location of means of physical influence as close to the protected facility as possible, considering their characteristics and the number of MPI intended to protect this facility.

After determining the distance required for the location of the anti-aircraft system outside the protected facility, the required number of protection equipment is calculated in Block 4. The next step is to use the algorithm for correcting the calculated coordinates of the MPI location, based on the analysis of digital maps of the area (Block 5). If the terrain or natural obstacles affect the location of the MPI, its position can be adjusted. A programme is activated that reproduces the MPI on an electronic map in accordance with the proposed provision (Kasraei *et al.*, 2021). For a more detailed and high-quality assessment of the MPI location, Block 6 implements an algorithm for assessing the degree of protection of facility from physical influence. The assessment of the degree of security of the facility is presented in the form of a table with calculations, which reflects the coefficients of neutralisation zones and the load coefficients MPI. Based on this information (blocks 7-9), MPI location issues are resolved. Regarding the placement of electronic means of influence, it is advisable to note the definition of such places where they can operate without interfering with the operation of MPI. This is, for example, considering the norms of frequency-territorial propagation, the corresponding distance between MPI and radio-electronic influence (REI) when they work together.

Determination of the effectiveness of protection of critical energy facilities from air strikes due to the combined use of means of physical and electronic influence

To assess the impact of interaction between the means of physical and radio-electronic influence on the effectiveness of their joint action, it is important to analyse the essence of the term "compatibility" and logically establish the relationship of this concept with the terms related to "interaction of physical and radio-electronic influence" (Dementiiuk *et al.*, 2023b).

The terminological system and its elements should have interdependence, unambiguity in military-scientific and general scientific disciplines, context-independent clarity, correlation with only one concept, brevity and lexicographic approach to term formation, flexibility for expansion, clarification and changes, and the possibility that the term becomes a designation of a broader concept. Considering these requirements for terminology and analysing the existing basic terms, the "zone of joint action of means of physical influence and means of electronic influence" refers to the area of their location and the airspace where the neutralisation and suppression of means of air attack is carried out.

Scientific challenges in the study of the combined effects of means physical and radio-electronic influence in the protected areas of critical energy facilities are diverse, and their solution may vary depending on the specific case. Number of possible options (n_{var}) depends on the quantity and type, and can be determined using coefficients that take these parameters into account:

$$n_{var} = (\mathrm{N}_{\mathrm{MPI}_i} + 1)(\mathrm{N}_{\mathrm{MPI}_j} + 1)(\mathrm{N}_{\mathrm{n.r.s}} + 1)(\mathrm{N}_{\mathrm{r.r.s}} + 1)\ldots, \quad (2)$$

where: $\mathrm{N}_{\mathrm{MPI}_i}$ – number of means related to i-th type of physical influence, $\mathrm{N}_{\mathrm{MPI}_j}$ – number of physical means of influence of the j-th type, $\mathrm{N}_{\mathrm{n.r.s}}$ – number of radio interference stations that are in the noise state, $\mathrm{N}_{\mathrm{r.r.s}}$ – number of pulse response radio interference stations.

The composition and location of means of physical and electronic influence are closely related and interdependent. This interdependence is conditioned by methodological approaches to justifying the optimal number and order of placement of funds. This is conditioned by the fact that the effectiveness of a joint action depends both on its composition and on the order in which it is implemented ($d_{l.MPI}$) and means of electronic influence ($d_{l.REI}$) from the boundaries of the protected facility and mutual distances between the means of protection ($D_{MPI\text{-}REI}$). Consequently, there is a complex interdependence of the efficiency of interaction between MPI and REI, which can be expressed in the form of a functional dependence:

$$E = f\{N_{MPI}\}|_{N_{REI},\, d_{l.MPI},\, d_{l.REI},\, D_{MPIi},\, D_{REIi},\, D_{MPI-REI}} = \text{const}, \quad (3)$$

$$E = f\{N_{REI}\}|_{N_{REI},\, d_{l.MPI},\, d_{l.REI},\, D_{MPIi},\, D_{REIi},\, D_{MPI-REI}} = \text{const}. \quad (4)$$

The locations of systems are regulated by the requirements of the task, which means that the location of means of physical influence must correspond to the distance from the boundaries of the security facility, which guarantees the removal of the disposal zone abroad, from which the AAM task can be performed. To assess the impact of the maximum efficiency of using MPI and REI on the effectiveness of their joint operation, let us return to the essence of the term "compatibility". The result of the effectiveness of measures in the protection of critical facilities of the energy complex is an m-dimensional vector, including three main groups of components: the achieved (expected) effect (g), time expenditure (t), and resource expenditure (c). The result of the effectiveness of measures to protect critical energy facilities is (m) a measurable vector that includes three main components: the result obtained (g), time (t), and the cost of material or financial resources (c):

$$Y^m = [g^m, c^m, t^m], \quad (5)$$

where: Y^m – effectiveness of actions, m – factors and conditions that affect the effectiveness of events; g^m – received (or expected) useful result, c^m – resource costs, t^m – time spent.

The most appropriate target task for means of physical influence when protecting facilities from air strikes is a measured indicator – the number of saved air defence equipment compared to their total number that were used during the strike. As for the choice of indicators of the ratio of opposing forces, the most complete confrontation between MPI and AAM can reflect the ratio:

$$\sigma_i = \frac{K_{MPI_i neutmax}\left[1-\left(1-P_{prob.MPI_i neut}\right)^n\right] K_{e.inf.prov} N_{MPI_i}}{D_{lim.par.MPI_i zone}\, N_{AAM}} = \frac{K_{MPI_i c.p.} K_{e.inf.prov}}{N_{AAM}}, \quad (6)$$

where: $K_{MPI_i neutmax}$ – maximum number of MPI of *i*-th types that are simultaneously neutralised, $P_{prob.MPI_i neut}$ – probability of neutralisation of MPI of *i*-th type, n – amount of resources spent, $K_{e.inf.prov}$ – efficiency coefficient of information support, N_{MPI_i} – number of MPI of *i*-th type, $D_{lim.par.MPI_i zone}$ – limit parameter of the neutralisation zone of MPI of *i*-th type, N_{AAM} – number of military personnel involved in the attack on the security facility, $K_{MPI_i c.p}$ – combat potential ratio of MPI of *i*-th type.

$$K_{e.inf.prov} = \frac{K_{coef.f.p} K_{mask} \left(1+N_{\Sigma_{t.p}}\right) N_{\Sigma_{i.m}}}{t_{s.MPI}\ (1-t_{i.c})}, \quad (7)$$

where: $K_{coef.f.p}$ – coefficient of similarity of false placements with true ones, K_{mask} – facility masking coefficient, $N_{\Sigma_{t.p}}$ – total number of forces and means of protecting the facility of air strikes that carry out disinformation measures, $N_{\Sigma_{i.m}}$ – total number of intelligence tools that are part of the forces and means of protecting facilities from air strikes includes information flows that are involved in the process of collecting information, $t_{s.MPI}$ – time of MPI stay at the location, $t_{i.c.}$ – time to collect information.

Therefore, the process of neutralisation of air defence systems during CFEC protection from air strikes is considered probabilistic, and its main characteristics are the relationship of the forces of the parties (Dementiiuk *et al.*, 2023b). To assess the effectiveness of the use of electronic warfare equipment to protect critical facilities, the mathematical expectation of the number of airs attacking systems exposed to REI $M_{AAM\ sup.REI}$ is used:

$$M_{AAM\ sup.REI} = N_{AAM.sup} \Delta P_{i.p}, \quad (8)$$

where: $M_{AAM\ sup.REI}$ – number of air defence systems that have been subjected to electronic influence (suppression), $\Delta P_{i.p}$ – increase in the probability of preserving a facility equal to the probability of a conditionally neutralised automated control system, which is determined depending on the number of conditionally neutralised automated control systems and is calculated using the equation:

$$\Delta P_{i.p} = P^p_{p.rei} - P^o_{p.a.rei}, \quad (9)$$

where: $P^p_{p.rei}$ – probability of preserving protected facility in case of resistance to electronic means of influence (obstruction of them), $P^o_{p.a.rei}$ – probability of preserving the protected facility without taking measures to counteract the means of electronic influence.

For a situation where facility protection is performed, equation (9) can be rewritten as follows:

$$P_{REI} = 1 - e^{-N_{REI} \Delta P_{p.s.REI} / N_{AAM}}, \quad (10)$$

where: $P_{p.s.REI}$ – probability of preserving a critical facility only REI, N_{REI} – number of REI, N_{AAM} – number of AAM.

The analysis indicates that when evaluating the effectiveness of actions, only the ability of physical or radio/electronic exposure to a certain amount of air defence equipment to destroy the protected facility is considered (Sowers *et al.*, 2017). Thus, considering the above-mentioned disadvantage, it is proposed to formalise the dependence in such a way as to determine the effectiveness of interaction:

$$P_i = 1 - e^{-\left(\frac{M_{m.e.dest.MPI}}{N_{AAM}} + K_{comp.}\frac{M_{m.e.dest.REI}}{N_{AAM}} + K_{o.r.}\frac{M_{m.e.dest.low.alt}}{N_{AAM}}\right)}, \quad (11)$$

where: $M_{m.e.dest.MPI}$ – mathematical expectation of the number of destroyed AAM MPI, K_{comp} – MPI and REI compatibility ratio, $M_{m.e.dest.REI}$ – mathematical expectation of the number of AAM destroyed by REI, $K_{o.r}$ – opportunity realisation coefficient, $M_{m.e.dest.low.alt}$ – mathematical expectation of the number of destroyed air defence systems at low altitudes.

Therefore, it can be determined that to evaluate the effectiveness of joint actions of MPI and REI locations, generalised indicators are used in the form of mathematical expectations of the number of AAM air attack vehicles that are not able to perform their assigned tasks (P_i), and calculated by equation (11). Based on the value of this indicator, it is possible to estimate the expected results of MPI and REI actions, the level of AAM losses, and the degree to which they perform their task of hitting a critical energy facility. For the location of means of physical influence on the site, the method of directed selection of possible options for the composition of means within the existing structure was used, while MPI was placed at fixed distances from each other relative to the security facility. To apply this methodology, coefficients were used:

$$D_{MPI\text{-}REI\ min} = a \cdot J, \quad (12)$$

where: $D_{MPI\text{-}REI\ min}$ – minimum range of MPI and REI from the centre of the protected facility, at which their specified number is evenly distributed at J intervals, a – uniformity coefficient.

For the relative location of MPI and REI, their relationship and their location relative to the protected facility are taken into account using the appropriate ratios:

$$D_{MPI-REImin} = D_{det} \leqslant 0{,}65 D_{r.a}, \quad (13)$$

where: D_{det} – detection range, $D_{r.a}$ – minimum supply of ammunition.

$$D_{r.a} = V_{AAM} T_{am.d.AAM\ min} - \Delta + V_{AAM} T_{AAM\ dest}, \quad (14)$$

where: V_{AAM}VVV – AAM speed, km/min, $T_{am.d.AAMmin}$ – time of dropping ammunition from the air defence system, min, Δ – lag of weapons (ammunition) using air defence systems, km, $T_{AAM\ dest}$ – time of destruction of AAM.

For effective protection of the facility by means of electronic influence, it is important to place the REI at a certain distance , which should have less value , and at best be zero. However, limiting the reduction in the distance of the REI location is associated with the risk of hitting the defence facility when using homing weapons with REI radiation. The condition that sets the minimum and optimal values has the following form:

$$D_{REI} \geqslant D_{r.d.am} + d_{r.prot} + 3\sigma_{a.s.error}, \quad (15)$$

where: $D_{r.d.am}$ – radius of destruction of protected facility by ammunition, $d_{r.prot}$ – radius of protected facility, $\sigma_{a.s.error}$ – average square error of a homing weapon.

The problem of calculating the distance between the locations of anti-aircraft missiles when protecting a facility from air strikes is solved by selecting the locations of anti-aircraft missiles (Ivanets *et al.*, 2023). The results show that it is strategically important to pre-place physical and electronic warfare equipment throughout the protected area or in key areas. The simulation performed in this study allowed estimating the probability of holding a protected target in the event of an air attack by a standard anti-aircraft missile, such as cruise missiles or unmanned aerial vehicles, at different altitudes (Fig. 2).

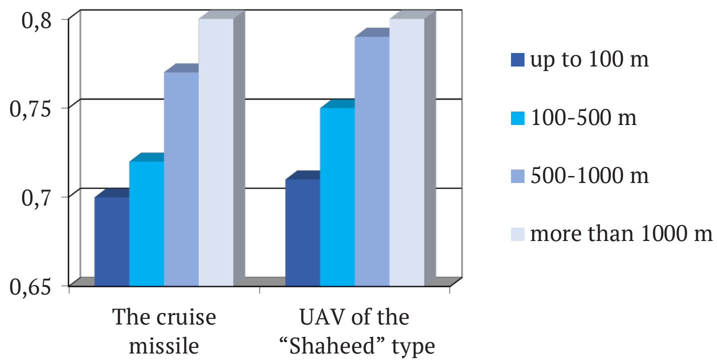

Figure 2. Diagram of the probability of preservation of critical facilities of the energy complex
Source: compiled by the authors

Analysis of the obtained data allows for the conclusion that the implementation of the proposed solutions can guarantee the safety of the protected facility during air strikes with a probability from 0.7 to 0.8 (Kopczewski *et al.*, 2023). Thus, the use of these recommendations will significantly increase the effectiveness of protecting both critical facilities and the civilian population, and territories from possible consequences of damage to energy facilities.

DISCUSSION

Protecting critical infrastructure facilities from air strikes is an extremely important task in the face of modern threats and conflicts. The ability to ensure effective protection of such facilities becomes strategically important not only for ensuring national security, but also for maintaining the stability and functioning of society. In the context of aviation threats, the modern development of unmanned aerial vehicles and cruise missiles creates new challenges for the protection of critical facilities. The combined use of various forces and means becomes a key aspect of the defence strategy. On the one hand, it is important to have effective means of physical influence, such as anti-aircraft systems, anti-aircraft missiles, and air defence systems that can provide active protection against aircraft and missiles. On the other hand, electronic means, such as early detection and prevention systems, can make important contributions to the prevention, detection, and neutralisation of threats. The effectiveness of the joint use of these forces and means is determined by their interaction and coordination. Research in the field of protecting critical infrastructure from air strikes can identify optimal strategies and technological solutions for this joint use. Solving these problems can serve as a basis for developing effective security and protection policies aimed at ensuring the stability and security of critical facilities in modern conditions of threats. This research can also contribute to the development of integrated protection strategies, taking into account the challenges of the modern military environment, and help improve security policies to ensure the sustainability of critical facilities.

Based on the results of recent study by M. Piekarski & K. Wojtasik (2022), protecting critical infrastructure from air threats in Poland is a high priority task in the context of modern security challenges. Poland, as a member of North Atlantic Treaty Organization (NATO) and the European Union (EU), faces a variety of potential threats, among which air attacks can be particularly serious. Given the country's geopolitical position, the importance of its economic infrastructure and energy facilities, effective protection becomes a key component of national security. Poland can use state-of-the-art technologies and strategies to ensure the protection of critical facilities. The development and improvement of early detection systems, air defences, and modern technical solutions for neutralising air threats can contribute to the creation of a reliable security system. The ability to integrate various means of physical and electronic influence, optimise their use and ensure coordination in activities is of great importance. Ukraine may also consider cooperation with other countries and international organisations to share experience and develop joint strategies in the field of critical infrastructure protection. This approach will ensure not only national, but also collective security in the face of increasing threats in the modern world.

Referring to the definition of T. Loveček *et al.* (2021), modelling and simulation are important tools for improving the protection of critical infrastructure and ensuring the sustainability of the basic needs of citizens. These approaches provide an opportunity to address complex challenges and identify optimal strategies for responding to possible threats. By creating mathematical models of vulnerabilities and scenarios of possible attacks, it is possible to effectively analyse the system and develop preventive measures. Simulations, in turn, allow virtually reproducing different situations and test the effectiveness of different protection strategies. These tools can be used to train personnel, analyse the reality of the security system, and improve infrastructure. Further development of simulation and simulation technologies can significantly improve preparedness and response to new threats, providing reliable protection for both critical infrastructure and the basic needs of citizens in today's unpredictable environment.

A.B. Daricili & S. Çelik (2022) determined that cybersecurity of critical infrastructure is a top priority in ensuring the sustainability of society in the face of an increasing number of cyber threats. Critical infrastructure, such as energy facilities, transportation systems, and communications, is being targeted by attempted cyber-attacks that can have serious consequences for national security. It is important to identify and implement measures to prevent cyber threats using advanced technologies and strategies. The development of effective systems for detecting and responding to cyber-attacks, and training personnel in the field of cybersecurity plays a key role in ensuring the integrity and operability of critical infrastructure. The analysis of the results and conclusions shows the relevance of using artificial intelligence and machine learning to predict and prevent cyber threats in the field of cybersecurity of critical infrastructure. Strengthening cooperation between government agencies, the private sector, and cybersecurity experts is becoming an important prerequisite for successfully countering cyber threats in critical infrastructure.

Researcher M. Böröcz (2021) determined that the policy of protecting critical infrastructure in the European Union is a key element of the strategy for ensuring national security and sustainability. This policy is developed and implemented to prevent and counter threats that may affect important sectors such as energy, transport, and telecommunications. One of the key initiatives is the creation of the European Union Agency for Cybersecurity (ENISA), which acts as a cybersecurity coordinator and consultant for EU member states. The centre promotes the exchange of information, provides recommendations and develops strategies to improve the protection of critical infrastructures in Europe. It can be agreed that considerable attention is also paid to the development of cyber defence standards and regulations that take into account the specifics of different critical infrastructure sectors. The introduction of innovative technologies such as artificial intelligence and blockchain into security systems is also becoming an important stage in the EU's critical infrastructure protection strategy.

As noted by Ł. Roman & K. Cygańczuk (2022), the legal dimension of protecting critical infrastructure is an important component of a national and international security strategy. Many countries are actively developing and improving legal frameworks for the effective protection of facilities of strategic importance for national security and sustainability. In most cases, these laws and regulations define the list of critical facilities, establish requirements for their protection, and also provide for liability for violation of these requirements. They can also define incident response procedures and interactions between public and private actors in protecting critical infrastructure. The findings of researchers confirm the results obtained. It is important to keep in mind that such a legal framework should be flexible and consider the rapid development of technologies and changing threats. Ensuring the effectiveness of these legal mechanisms requires constant updating and adaptation to new challenges, in particular, in the field of cybersecurity.

R. Cantelmi *et al.* (2021) showed by their work that in the context of the sustainability of critical infrastructure, the key element is the use of qualitative research approaches for comprehensive analysis and the development of effective protection strategies. One of these approaches – a system analysis method that allows considering a critical infrastructure as a complex system, considering the relationships and dependencies between its components. Researchers also actively use mathematical modelling to analyse the vulnerability and effectiveness of sustainability measures. This allows conducting scenario and strategic analyses, identifying weaknesses, and developing optimal protection methods. Modelling is also used to simulate a variety of scenarios, including natural disasters and cyber-attacks, which helps improve response and recovery strategies. However, it is important to note that the application of qualitative research methods also includes the analysis of modern technologies, considering socio-economic aspects and interaction between security actors. This approach allows viewing critical infrastructure in its full context, providing more effective sustainability and security management.

CONCLUSIONS

The list of critical energy sector targets for air strikes can be diverse and include important government facilities that require reliable protection from air strikes. Such facilities may include power plants, substations, gas pipelines, and infrastructure that is important for the normal functioning of the country and its economy. According to the above method, the means of physical and electronic influence are located at a certain distance from security facilities in order to prevent unmanned aerial vehicles and cruise missiles from entering the zone of critical energy facilities.

It is proposed to use physical means to protect critical energy facilities from air attacks, included in the integrated model for evaluating the effectiveness of using these means, provide an opportunity to confidently assert that their use in protecting critical energy facilities from air strikes will ensure its safety with a probability from 0.7 to 0.8. To assess the effectiveness of interaction between physical and electronic means, it is a generalised indicator in the form of mathematical expectation of the number of missiles that have not completed their mission, and is determined in relative terms. By the value of this indicator, it is possible to estimate the expected results of interaction between physical and electronic means of influence, the level of losses from air attack means and the degree of their performance of tasks.

The research shows the expediency of taking measures to improve the effectiveness of protecting critical facilities of the state's energy complex from air strikes due to the joint use of various forces and means, which is conditioned by the need to ensure the survival of the state, preserve th e environmental situation in the region of the location of a particular critical facility due to catastrophic consequences in case of damage.

It is advisable to further investigate the mechanisms of interaction and integration of innovative technologies in critical infrastructure protection systems to ensure the sustainability and effectiveness of countering modern aviation threats.

ACKNOWLEDGEMENTS

None.

CONFLICT OF INTEREST

None.

REFERENCES

[1] Berezutskyi, V., & Berezutska, N. (2022). Analysis of life protection of the population of cities and settlements during the war. *Science and Technology Today. Technics Series*, 8(8), 51-64. doi: 10.52058/2786-6025-2022-8(8)-51-64.

[2] Böröcz, M. (2021). Critical infrastructure protection policy in the EU. *Strategic Impact*, 3(80), 46-61. doi: 10.53477/1841-5784-21-15.

[3] Cantelmi, R., Di Gravio, G., & Patriarca, R. (2021). Reviewing qualitative research approaches in the context of critical infrastructure resilience. *Environment Systems and Decisions*, 41(3), 341-376. doi: 10.1007/s10669-020-09795-8.

[4] Chaika, I.Yu., & Tsokur, Ye.G. (2022). The phenomenon of hybrid genocide in the conditions of the Russian-Ukrainian war of 2014-2022. *Political Life*, 4, 45-54. doi: 10.31558/2519-2949.2022.4.6.

[5] Chronicle of the war: A full-scale invasion of Ukraine. (2022). *Intent*. Retrieved from: https://intent.press/publications/politics/2022/hronika-vtorgnennya-rosiya-zatverdila-vvedennya-vijsk-na-shid-ukrayini/.

[6] Daricili, A.B., & Çelik, S. (2022). National Security 2.0: The cyber security of critical infrastructure. *PERCEPTIONS: Journal of International Affairs*, 26(2), 259-276.

[7] Dementiiuk, H., Basarab, O., Horbachov, K., Yanenko, O., Volkov, A., Tokar, O., & Iasechko, M. (2023a). Development of the principles of protecting critical infrastructure facilities against the destructive impact of cruise missiles with radio-location correlation extreme guiding algorithms based on the application of an electromagnetic screen. *Scandinavian Journal of Information Systems*, 35(1), 185-193.

[8] Dementiiuk, H., Iasechko, M., Kolesnichenko, S., Polianskyi, K., Basarab, O., Horbachov, K., Yanenko, O., & Zaitsev, I. (2023b). Princes and requirements for the protection of civilian infrastructure from the devastating effects of air attack. *Revista De Gestão Social E Ambiental*, 17(4), article number e03421. doi: 10.24857/rgsa.v17n4-028.

[9] Dykha, V., & Lukianova, V. (2023). Energy market risks: Essence of definition and characteristics. *Modeling the Development of the Economic Systems*, 1, 28-36. doi: 10.31891/mdes/2023-7-4.

[10] Hou, P., Pei, Y., Ge, Y., & Zhu, M. (2023). Terminal attitude selection method of missile attack aircraft. *Chinese Journal of Aeronautics*. doi: 10.1016/j.cja.2023.09.019.

[11] Hurkovskyi, V., Kozak, I., & Dmitruk, S. (2023). Technological and communication challenges of SBU and AFU interaction during armed aggression: Seeking innovative solutions. *Scientific Perspectives*, 38(8), 112-121. doi: 10.52058/2708-7530-2023-8(38)-112-121.

[12] Ivanets, M., Kutsenko, V., Artikula, A., Shinkarenko, O., & Yachna, I. (2023). Management algorithm for the comprehensive system of testing samples of anti-aircraft missile systems. *Testing and Certification*, 1(1), 17-24. doi: 10.37701/ts.01.2023.02.

[13] Kasraei, B., Heung, B., Saurette, D.D., Schmidt, M.G., Bulmer, C.E., & Bethel, W. (2021). Quantile regression as a generic approach for estimating uncertainty of digital soil maps produced from machine-learning. *Environmental Modelling & Software*, 144, article number 105139. doi: 10.1016/j.envsoft.2021.105139.

[14] Kopczewski, M., Grobelny, Z., & Świętochowski, N. (2023). Defense and deterrence as the foundation of the a2/ad system in smart city air defense. *Safety & Defense*, 9(1), 14-23. doi: 10.37105/sd.198.

[15] Korsunov, S., Volkov, A., Oboronov, M., Oriekhov, S., Gurtovenko, V., & Fedchenko, S. (2021). Transformation of unmanned aviation tasks from its creation to application in modern military conflicts. *Science and Technology of the Air Force of Ukraine*, 3(44), 66-81. doi: 10.30748/nitps.2021.44.08.

[16] Kumar, A., Yadav, A.S., Gill, S.S., Pervaiz, H., Ni, Q., & Buyya, R. (2022). A secure drone-to-drone communication and software defined drone network-enabled traffic monitoring system. *Simulation Modelling Practice and Theory*, 120, article number 102621. doi: 10.1016/j.simpat.2022.102621.

[17] Loveček, T., Straková, L., & Kampová, K. (2021). Modeling and simulation as tools to increase the protection of critical infrastructure and the sustainability of the provision of essential needs of citizens. *Sustainability*, 13(11), article number 5898. doi: 10.3390/su13115898.

[18] Park, S., Kim, H.T., Lee, S., Joo, H., & Kim, H. (2021). Survey on anti-drone systems: Components, designs, and challenges. *IEEE Access*, 9, 42635-42659. doi: 10.1109/ACCESS.2021.3065926.

[19] Piekarski, M., & Wojtasik, K. (2022). Protection of Polish critical infrastructure (CI) against air threats. *Security and Defence Quarterly*, 39(3), 76-87. doi: 10.35467/sdq/147676.

[20] Roman, Ł., & Cygańczuk, K. (2022). Legal dimension of the protection of critical infrastructure – Selected aspects. *Safety & Fire Technology*, 59(1), 166-181.

[21] Sowers, J.L., Weinthal, E., & Zawahri, N. (2017). Targeting environmental infrastructures, international law, and civilians in the new Middle Eastern wars. *Security Dialogue*, 48(5), 410-430.

Андрій Федорович Волков
Завідувач кафедри
Харківський національний університет Повітряних Сил імені І. Кожедуба
61045, вул. Клочківська, 228, м. Харків, Україна
https://orcid.org/0000-0003-1566-9893

Михайло Михайлович Бречка
Кандидат технічних наук, старший викладач
Харківський національний університет Повітряних Сил імені І. Кожедуба
61045, вул. Клочківська, 228, м. Харків, Україна
https://orcid.org/0000-0002-0291-9665

Володимир Григорович Стадніченко
Заступник завідувача кафедри
Харківський національний університет Повітряних Сил імені І. Кожедуба
61045, вул. Клочківська, 228, м. Харків, Україна
https://orcid.org/0000-0002-1780-9215

Віталій Володимирович Ярощук
Викладач
Харківський національний університет Повітряних Сил імені І. Кожедуба
61045, вул. Клочківська, 228, м. Харків, Україна
https://orcid.org/0000-0001-5318-5692

Сергій Володимирович Черкашин
Викладач
Харківський національний університет Повітряних Сил імені І. Кожедуба
61045, вул. Клочківська, 228, м. Харків, Україна
https://orcid.org/0009-0002-6940-3863

Захист об’єктів критичної інфраструктури від повітряних ударів завдяки сумісному застосуванню різних сил і засобів

Анотація. Актуальність дослідження підкреслюється необхідністю вивчення та розробки ефективних стратегій захисту критично важливих об’єктів інфраструктури держави, в контексті російсько-української війни 2022 року. Метою даного дослідження є оцінка ефективності взаємодії між фізичними та радіоелектронними засобами впливу у контексті захисту об’єктів критичної інфраструктури енергетичного комплексу від атак повітряних ударів. Об’єктом дослідження є система захисту критично важливих об’єктів енергетичного комплексу держави. Дослідницькі методи включали в себе використання системного аналізу, розробку стратегій для визначення оптимальних місць розташування засобів фізичного впливу та використання математичного моделювання. Дослідження в області взаємодії та одночасного використання фізичних та радіоелектронних засобів включало теоретичний аналіз абстрактних об’єктів та їх взаємозв’язків. Ці об’єкти конструювалися для створення ідеалізованого опису та вивчення можливих сценаріїв, а також для визначення оптимальних дій у конкретних ситуаціях. У цьому дослідженні детально розглядалися можливості підвищення ефективності захисту важливих об’єктів енергетичного комплексу від авіаударів за допомогою використання комбінованих стратегій, таких як зенітний вогонь та протипожежний захист. Аналізувалися методи визначення оптимальних місць розташування засобів фізичного впливу, що дозволяли передбачати очікувані результати при їхньому спільному використанні. Розроблено науково-обґрунтовані рекомендації з ефективного інтегрування цих методів, що є новаторським підходом до проблеми. Засоби фізичного впливу включали стрілецьку зброю, яка становила частину озброєння Збройних Сил та інших правоохоронних органів, а також безпілотники-перехоплювачі. Засоби радіоелектронного впливу включали в себе технічні засоби радіочастотної боротьби та електромагнітні гармати. Практичне значення цієї роботи полягає в тому, що вона представляє конкретні стратегії та технологічні рішення для комплексного захисту об’єктів критичної інфраструктури від авіаударів. Це дослідження може служити основою для розробки ефективних політик безпеки та захисту в країнах та регіонах, сприяючи підвищенню загального рівня стійкості та безпеки

Ключові слова: енергетичний комплекс держави; російсько-українська війна; засоби фізичного впливу; радіохвилі; повітряний напад

Machinery & Energetics
Vol. 14, No. 4. 2023

Journal homepage:
https://technicalscience.com.ua/en

UDC 622.276
DOI: 10.31548/machinery/4.2023.33

Annaguly Deryaev*
Doctor of Technical Sciences, Principal Researcher
Scientific Research Institute of Natural Gas of the State Concern "Turkmengas"
744036, 58 Archabil Ave., Ashgabat, Turkmenistan
https://orcid.org/0009-0004-8569-6277

Dual completion operation technology for two gas condensate reservoirs with production lifting by one column of pumping and compressor pipes

Abstract. In the context of the active development of gas condensate fields with several reservoirs in the Gogrendag-Ekerem Upland (Korpedje, South Gamyshlja), the study of its technologies is an important area of work. The study aims to optimise the technology of simultaneously separating two gas condensate reservoirs by lifting products with one tubing string to increase hydrocarbon production efficiency. The methods used include the analytical method, functional method, statistical method, synthesis method, and others. In the course of the study, an innovative methodology was developed for the dual completion operation (DCO) of two gas condensate reservoirs, which involves lifting products with a single tubing string. The key element is the refinement of the calculations made. A detailed analysis of the equipment used in the Gogrendag-Ekerem area showed that it can also be effectively used in other regional fields, ensuring the proper functioning of each element above the packer level. At the same time, it is necessary to pay attention to the various individual characteristics of the field to achieve a truly effective configuration of this technology. The new technology incorporates optimised pressure, flow, and control parameters for each reservoir, resulting in increased production efficiency and reduced energy costs. A significant reduction in the negative impact on the environment and an increase in the overall sustainability of the production process have been identified. These features make the proposed technology an important contribution to the development of the oil and gas industry, contributing to more efficient and environmentally sustainable hydrocarbon production and highlighting its potential for application in modern field development. The practical significance of the research lies in the creation of a more efficient and sustainable hydrocarbon production technology, which not only helps to optimise production processes and reduce environmental impact but also provides the industry with a valuable tool to improve overall energy efficiency and sustainability in the face of ever-changing energy requirements and challenges

Keywords: hydrocarbon production; resource efficiency; environmental impact; improved methodology; sustainability of the production process

INTRODUCTION

The study of the technology of dual completion operation (DCO) of two gas condensate reservoirs using a single tubing string is undeniably important in today's energy industry. This technology promises significant benefits, including optimisation of hydrocarbon production processes, improved resource efficiency and reduced environmental impact. The development of an improved methodology incorporating optimised pressure, flow and control parameters not only improves production performance but also helps to reduce energy costs and enhance process sustainability. This research provides a valuable contribution to the oil and gas industry and its practical implications emphasise the relevance of these improved technologies in the pursuit of a more efficient and environmentally sustainable energy future.

The research problem is the need to develop and optimise a technology for the DCO of two gas condensate reservoirs using a single tubing string. Current hydrocarbon

Article's History: Received: 15.06.2023; Revised: 25.09.2023; Accepted: 22.11.2023.

Suggested Citation:
Deryaev, A. (2023). Dual completion operation technology for two gas condensate reservoirs with production lifting by one column of pumping and compressor pipes. *Machinery & Energetics,* 14(4), 33-41. doi: 10.31548/machinery/4.2023.33.

*Corresponding author

production methods face the challenges of effective management of multilayer reservoirs, which emphasises the need for a better understanding of the processes involved in lifting production. Developing optimal pressure, flow and control parameters for each reservoir is a key aspect, and successfully addressing this issue can significantly improve field stability and performance in today's energy resource recovery environment.

According to D.S. Akyev & T.B. Arazov (2022), the problem in hydrocarbon production is the inefficient use of existing technologies, which requires a new approach to DCO of gas condensate reservoirs. The study did not address the issue of implementing modern monitoring and data management systems. S.K. Veysov & G.O. Hamrayev (2023) stressed the importance of considering the geological features of the fields when developing improved extraction techniques to ensure optimal efficiency and sustainability of the processes. However, the impact of efficiency and sustainability of hydrocarbon extraction processes on the environment and environmental sustainability has not been assessed. According to the study by N. Ozbekov *et al.* (2023), DCO analysis is necessary for reducing the environmental impact of the oil and gas industry and ensuring the sustainability of the natural environment. The study is limited to assessing technological aspects and does not pay sufficient attention to social responsibility and interaction with local communities.

O.K. Abramovich & H.B. Hadzhigeldyev (2022) note that optimised pressure and flow parameters introduced in the new technology can lead to a significant reduction in energy consumption during hydrocarbon production. However, the impact of this technology on the quality of production and chemical composition of produced hydrocarbons was not considered. According to F.E. Safarov *et al.* (2022), the developed methodology of exploitation of two gas condensate reservoirs represents a significant step in the field of oil and gas technologies. However, the paper does not discuss in detail the issues of optimising the economic efficiency of this technique and its applicability to different geological and climatic conditions. E.A. Grinkova & G.I. Abaeva (2023) discuss the importance of optimised technologies for increasing resource efficiency in the context of hydrocarbon production. However, the interaction between different industry participants and oil and gas companies in the implementation of such technologies is not addressed.

The study aims to improve hydrocarbon recovery technology by optimising the DCO of two gas condensate reservoirs using a single tubing string to increase efficiency.

MATERIALS AND METHODS

The analytical method was used to identify the key parameters and factors that determine the effectiveness of the technology and to conduct a systematic analysis of the data, which helped in pinpointing the optimal conditions for implementing the improved technique. By applying a synthesis method, various aspects of DCO technology were combined to create an integrated approach to optimising hydrocarbon production processes. This method enabled the diverse elements of the system to be combined, providing synergy and overall efficiency in achieving the objectives of the study.

The abstraction method was used in the study to identify the main general principles and concepts underlying DCO technology. The abstraction simplified complex technical details by highlighting key aspects, which provided a deeper understanding of the basic principles of system operation and facilitated the development of generalised models for more effective optimisation.

The concretisation method was used to elaborate in detail the abstract ideas and concepts highlighted by the abstraction method. This method was used to move from generalised ideas to concrete technical solutions, defining the exact parameters and characteristics of the DCO technology. Thus, the concretisation method ensured the practical applicability of the identified principles, which became the basis for further successful implementation of the improved methodology in hydrocarbon production conditions.

The deduction method was substantially used to support the formation of valid conclusions and logical implications from the data collected. By applying this method, the general principles and laws underlying the effectiveness of DCOs were deduced. The deductive approach was used to clarify assumptions, conduct logical reasoning, and formulate precise conclusions, contributing to a deeper understanding of the mechanisms of system operation and optimisation of hydrocarbon production processes.

The induction method in this study was used to summarise specific results and experiences from practical experiments and observations of DCO. By investigating specific cases and data, the induction method was able to identify general trends, patterns, and effective approaches to improve hydrocarbon production processes. Thus, based on inductive findings, generalised principles were formulated that can be applied to optimise the technology in the broad context of the oil and gas industry.

The statistical method was used to systematically examine large volumes of data from experiments and observations of DCOs. This method allowed the identification of significant correlations, trends, and likely variations in hydrocarbon production processes. The statistical study provided an objective basis for decision-making and optimisation of the technology parameters, considering various conditions and factors, which helped to improve its efficiency and adapt it to a variety of application scenarios.

By applying the functional method, key functions and interrelationships within DCO were identified. This method provided a structured examination of the role of each element in the system, highlighting the essential components and their impact on overall performance. The functional approach provided an understanding of the internal dynamics of the system, which played a key role in optimising and improving each stage of the hydrocarbon production process while reflecting the overall objective of the study to improve the performance of this technology. The formulae used in this study were (1-8):

$$P_{l1} = P_{lf}(\bar{Q}_{g1}), \tag{1}$$

$$P_{c1} = \sqrt{P_1^2 P - (A_1 q_1 + B_1 q_1^2)}, \tag{2}$$

$$P_2 = e^{-Son}\sqrt{P_1^2 - 1.377\lambda_n \frac{Z^2T^2}{p_n d^5} Q_{m1}^2 (e^{2Son} - 1)}, \tag{3}$$

$$P_{c2} = P_3 + 3, \tag{4}$$

$$P_{l2} = f(Q_2), \tag{5}$$

$$q_1 = -\frac{A_2}{B_2} + \sqrt{\left(\frac{A_2}{B_2}\right)^2 + \frac{P_{l2}^2 + P_{c2}^2}{B_2}}, \tag{6}$$

$$q = q_1 + q_2, \tag{7}$$

$$P_y = e^{-Son}\sqrt{P_3^2 - 1.377\lambda_m \frac{Z^2T^2}{p_m d^5} Q_l^2 (e^{2Son} - 1)}, \tag{8}$$

where: P_{l1} – lower reservoir pressure; P_{l2} – upper reservoir pressure; P_{c1} – lower reservoir wellbore pressure; P_{c2} – upper reservoir wellbore pressure; P_2 – pre-packer pressure; P_2 – after-packer pressure, P_3 – upper reservoir tubing pressure: P_w – wellhead pressure. Q_m, Q_l, Q_g – volume flow rate of the gas-liquid mixture, liquid flow rate and gas flow rate, thousand m^3/day.

This multidisciplinary approach has contributed to an integrated methodology that considers technical, environmental and energy aspects and has been the basis for the development of improved methodology in hydrocarbon production in the oil and gas industry.

RESULTS

In recent years in the process of development of multilayer horizons of gas-condensate fields of the Gogrendag-Ekerem zone of upland (Korpedje, South Gamyshlja) is applied development and design of technology of DCO of two gas-condensate horizons, with leaving production in the tubing string. Well depth and small diameter of production strings significantly limit the possibility of using downhole equipment that meets all the requirements of DCO methods (Deryaev, 2022). The task of analysing the set of equipment available for DCO was to determine the real option of development of gas condensate fields of the area under consideration. The detailed analysis of the equipment set allows us to conclude that it can be used in regional fields at the performance of the functions of each element (above packer) of the equipment complex independently from other elements. Calculations of parameters of DCO of gas-condensate well separately are carried out in the case when in one tubing string the production corresponding to the set of equipment of CGS type is made. The use of DCO technology reduces the number of drilling wells, as well as material and technical costs associated with drilling and development of the entire well in the field under development. In recent years in the process of development of gas condensate deposits at multilayer fields of the Gogrendag-Ekerem zone of rises (Korpedje, Gunorta Gamyshlydzha) design and application of DCO technology of two reservoirs by the lifting of production by one tubing string is practised.

The selection of sites for DCO considers a variety of geological and technical characteristics of the fields (Kongar-Syuryun *et al.*, 2021). These factors include the coincidence of the main components of the productive areas of the horizons intended for DCO. The matching of the volume of gas recovered by an individual well and the absolute values of current reserves is also considered. The distance between the horizons intended for DCO technology and the level of reserves development in these horizons were investigated. Data on reservoir pressure, temperature, reservoir drainage regimes and productive characteristics of reservoirs were considered. In addition, the possibility of reducing the number of wells drilled when implementing this technology was assessed. All these factors were systematically considered to ensure the optimal selection of sites for the successful implementation of the DCO technology following the individual geological and technical characteristics of each field.

Calculation of the parameters of the gas condensate well DCO technology is assumed in the case of lifting the products of two reservoirs through a single tubing string, which corresponds to the use of specialised downhole equipment, such as a gas gathering complex (or gas collection complex, GCC). The sequence of calculations appears to be as follows (Fig. 1).

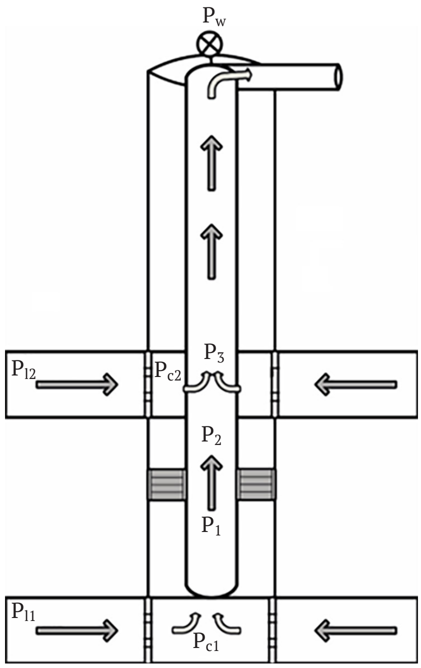

Figure 1. Calculated scheme of DCO technology for lifting the production of two reservoirs through a single tubing string

Note: P_{l1} – lower reservoir pressure; P_{l2} – upper reservoir pressure; P_{c1} – lower reservoir wellbore pressure; P_{c2} – upper reservoir wellbore pressure; P_2 – pre-packer pressure; P_2 – after-packer pressure, P_3 – upper reservoir tubing pressure: P_w – wellhead pressure

Source: developed by the author

It starts with a preliminary calculation of annual and cumulative gas production, as well as a determination of the average gas production rate (q1) of wells for the future for the lower reservoir development scenario using a stand-alone well grid. At known values of cumulative production (Q1), the dynamics of reservoir pressure in the lower reservoir are evaluated using the formula (1). By using filtration coefficients "A_1" and "B_1", at known gas flow rate q1 and reservoir pressure level P_1, wellbore pressure P_{c1} is determined (2). Due to the small size of the distance from the lower reservoir to the packer and from the packer to the upper reservoir, to simplify subsequent calculations, we assume $P_1 = P_{c1}$ and $P_3 = P_2$. In this case, the pressure P_2 is calculated using (3) formula. Considering the pressure loss during gas flow from the upper reservoir into the tubing in the amount of 3 atmospheres, the wellbore pressure P_{c2} is calculated according to the following formula (4). Pressure change in the upper horizon formation is regulated according to the dependence (5). At given values of formation and wellbore pressure, the flow rate of the well from the upper reservoir is determined using the formula (6). The total gas flow rate is (7). Calculation of wellhead pressure in case of gas-liquid mixture lifting from two formations through a single tubing string is carried out by formula (8), where (9):

$$
\begin{gathered}
S_0 = 0.03415\frac{\rho\rho L}{Z_{sr}T_{sr}}:\rho = \phi + (1-\phi)\frac{P_{zh}}{P_g},\\
p = \frac{\rho_g P_{sr} T_{st}}{P_{at} T_{sr}}:\phi \leq \beta = \frac{Q_{zh}}{(Q_g Q_{zh})},\\
Q_g = \frac{Q_g P_{at} T_{sr}}{P_{sr} T_{st}}:Q_{sm} = \frac{G_g + G_{zh}}{(\rho_g)},\\
G_g = Q_g \rho_g; \overline{\rho} = \frac{g}{\rho_v}; T_{st} = 293^0 K,\\
\theta = 1.377\lambda\frac{(Z^2{}_{sr}T^2{}_{sr}}{d^5}(e^{2S}-1).
\end{gathered}
\tag{9}
$$

It is necessary to experimentally determine the true gas volume content as the ratio of the actual gas volume V_u in the well to the borehole volume . However, due to the difficulty of such measurements, it can be estimated based on the flowing gas content β according to formula (9). Since φ is always less than β, using β instead of φ may lead to underestimation of wellbore pressure, especially when the difference between the volume of fluid in the well and the volume of gas flowing out increases (Zou *et al.*, 2021). Differential condensation isotherms under reservoir conditions were used in the calculations, which were approximated in advance by polynomials for the convenience of computer calculations. The hydraulic resistance coefficient λ should be determined based on studies of wells under different regimes. If such data are not available, the value λ = 0.025 for the pipe and λp = 0.0815 for the packer can be used. All parameters (Z_{sr}, ρ_g, Q_g, β), which depend on wellhead pressure P_{sr}, can be determined by using the iteration method. The parameter L included in formulas (9), when using formulas (3) and (8), denotes packer length and tubing length, respectively. The formation of proposals regarding the choice of DCO technology and optimal equipment set corresponds to the general criteria for this method of multilayer reservoir development (Zhou *et al.*, 2021).

According to general standards, DCO solutions should provide optimum flow rates for each of the footings used in the development project. The key factors are the ability to control the total well production rate quickly and with an acceptable ratio of individual footings, to conduct explorations to characterise each formation, and to efficiently perform development and killing operations for the footings and the entire well (Farsi *et al.*, 2021). The ability to perform remedial actions, the availability of devices to prevent the uncontrolled release of fluids from the well, and the ability to apply chemicals to both the fluid flow in the tubing and the production footings, including the use of hydrate inhibitors and other chemicals, are required. Engineering and technology solutions for gas condensate fields can vary considerably depending on the specific conditions (Abad *et al.*, 2022). Nevertheless, fully meeting all of these requirements can be challenging in certain scenarios, especially when considering well depth and casing diameter. Deep wells and small casing diameters can significantly limit the use of downhole equipment that fully meets the design requirements for DCO of gas reservoirs. The analysis of existing DCO equipment packages aimed to determine the best option for developing a gas condensate field in the region under consideration when applying the DCO method for two footings through one well. Different sets of equipment for wells were compared with the characteristics of the design of gas wells in the fields. The main parameters of the process equipment in the analysis were operating pressure, maximum gas withdrawal, pipe and string diameters, packer depth, media characteristics and packer dimensions (Aghbashlo *et al.*, 2021).

The analysis indicates the inapplicability of complexes Fountain Complex Control (FCC), Universal Submersible Gas Pump (USGP) and Gas Well Control (GWC) in the presented modifications for the equipment of gas wells of the fields of this region. This is due to the requirement for a larger diameter of the production string (more than 146-168 mm) and the purpose of these complexes for operation at much lower values of operating pressure. These parallel tubing and concentric tubing packages from various manufacturers available for the modifications under consideration are designed to operate at lower operating pressures and cannot be applied directly to the wells included in this field analysis. A thorough analysis of the GCC equipment suggests that its application to the fields in the region is possible with certain modifications to the overall configuration of the components (Watanabe & Ogata, 2021). This is acceptable as each element of the complex (above the packer) fulfils its functions independently of the other components. This statement is based on the fact that in a simplified implementation of the DCO technology, the known GCC-type equipment complex can effectively perform all its standard functions of gas production from the reservoir located in the sub-packer zone, with the possibility of regulating its flow rate employing a "deep" choke. Thus, the tubing string above the packer can be fed with production from the upper reservoir, provided there is an appropriate structural input unit. In this case, it is necessary to install a tubing string with one circulation valve in the upper reservoir area (for simultaneous development and killing of both reservoirs). Regulation of separate gas extraction from the two reservoirs is performed by changing the pressure in the tubing in the upper reservoir connection area, which provides flow rate control (Shingala *et al.*, 2022; Sargsyan *et al.*, 2023).

If the cross-sectional area of the choke holes (nozzles) at the upper horizon gas inlet to the tubing is known, the gas flow rate from the upper reservoir can be calculated. The lower reservoir flow rate is then calculated based on the total well flow rate measured at the gas gathering station. A key component of this equipment system is a check valve installed in the gas injection chamber from the upper horizon to the tubing string (Panov, 2023; Yazdani *et al.*, 2023). The use of a check valve is justified by the significant differences in reservoir pressures of facilities whose production is integrated into a single tubing string. In this DCO configuration, the ratio of predicted underpressures to active reservoirs becomes the defining technological aspect. Occasionally, raising the products of two footings in a well through a single tubing string can cause significant pressure changes between the filter zone and the wellhead. This requires well temperature calculations to identify possible conditions for hydrate formation at the wellhead. In such cases, known calculation methods can be applied, including the one described by Aarushi *et al.* (2021). If the results of calculations of the temperature regime of good operation indicate the possibility of hydrate formation in the near-wellhead zone, it is necessary to provide for the possibility of introducing a hydrate formation inhibitor into the tubing string, especially in the zone of connection of the upper formation.

When reservoirs have high flow rates and flow rates are highly dependent on small changes in reservoir pressure, wellbore pressure losses in wellbore pressure equipment must be considered. Packers and valves are the most common elements of downhole complexes that affect "additional" pressure losses compared to the total pressure drop in the tubing string. Practical methods exist for determining such wellbore pressure losses in wellbore equipment, as described by H. Gamal *et al.* (2021). Calculations performed using the methodology from the paper by A.R. Deryaev (2023) for the packer, which is part of the GCC complex, showed that the pressure losses do not exceed in the considered example. It was noted that the wellbore pressure losses in the wellbore equipment, compared to the reservoir underbalanced characteristic of the deep horizons of the lower red colour of Turkmenistan, are insignificant. Failure to consider these losses will practically not affect the adopted technical and technological decisions when introducing the option of DCO with the use of GCC complex. The introduction of DCO technology contributes to a significant reduction in the required number of wells drilling, which, in turn, leads to a reduction in material and technical costs associated with the exploration and development of the entire field.

DISCUSSION

DCO technology is a promising approach aimed at increasing the efficiency of gas condensate field development. Simultaneous production of two reservoirs through a single tubing string allows for optimising the operation process and using resources more efficiently. One of the key advantages of this technology is the reduction in the number of drilling wells, which entails a significant reduction in material and technical costs. This is especially relevant in conditions of complex geological formations. In selecting sites for the application of the EPR technology, it is necessary to consider several geological and technical conditions, such as the coincidence of productive areas of formations, quantitative parameters of reserves, temperature, and pressure characteristics, as well as peculiarities of reservoir drainage. Despite the significant advantages, the application of DCO can face certain challenges, such as the need to carefully control production parameters, adapt to the geological characteristics of each field and ensure the safety of operations. The experience of using DCO technology in practical fields and additional research may help to improve the methodology and expand the application of this technology. Assessment of the environmental impacts of the technology is also an important aspect, including the impact on groundwater, greenhouse gas emissions and other aspects that require close monitoring. DCO technology is a promising tool for the efficient development of gas condensate fields, and its implementation requires an integrated approach, consideration of geological and technical peculiarities, and constant monitoring to ensure safe and efficient operation.

According to the results of recent studies by K. Nurgalieva *et al.* (2021), improving the efficiency of oil and gas wells facing the problem of asphalt-smothered paraffin (ASP) deposits is an important issue in the oil and gas industry. ASP deposits can significantly reduce reservoir capacity and well flow rates, which adversely affects the overall productivity of the field. The use of chemicals to prevent and remove deposits has been proposed to address this problem. The development and application of effective inhibitors and dispersants specifically tailored to combat ASP formation play a key role in improving well performance. These chemicals must not only be effective in preventing deposits but also safe for the environment and equipment. Developing technologies to clean wells of already formed ASP deposits is also an important aspect. Effective mechanical and chemical cleaning methods will probably include the use of innovative reagents and techniques, as well as the development of intelligent monitoring systems to prevent future fouling. These findings are consistent with the theses presented in the previous section. The overall approach to solving the fouling problem must include a combination of chemical, mechanical and technological innovations, as well as strategies to keep wells clean and efficient throughout their life cycle.

Referring to the definition of X. Zheng *et al.* (2022), the development of oil and gas production technology in

China is a strategic direction to meet the growing energy demand in the country. As the largest energy consumer in the world, China is actively adopting innovative approaches and advanced technologies to optimise production and ensure energy security. Prospects for technological development include the intensive use of digital technologies and artificial intelligence to monitor and manage production processes. The introduction of smart solutions in drilling, equipment condition monitoring and predicting changes in underground geological structures can improve production efficiency and reduce costs. Overall, China's oil and gas technology development is aimed at balancing the country's growing energy needs, ensuring economic efficiency, and meeting environmental sustainability standards. These efforts also affect the global energy landscape as China plays a key role in the global energy system.

M.B. Sadr & A. Bozorgian (2021) determined that gaseous hydrates are crystalline structures formed under conditions of high pressure and low temperature where gas molecules are enclosed within a framework of water molecules. The study of gas flow in gaseous hydrates is key to effectively managing their formation and preventing problems associated with their formation in pipelines and wells. The intensity of gas transfer in gaseous hydrates varies significantly with environmental parameters, particularly temperature and pressure levels. Under conditions where temperature rises or pressure decreases, hydrates can undergo dehydration, releasing the trapped gas. The reverse process, namely the formation of gaseous hydrates, occurs when temperature is lowered, and pressure is increased. These results support the above study because understanding the mechanisms and parameters of gas flow in hydrates is important for the development of technologies to prevent their formation in pipelines and gas production infrastructure. It also has implications for the safety of operations in environments where gaseous hydrates can pose a risk to the stability and efficiency of gas pipelines and wells. Research is underway to develop innovative hydrate management techniques, such as the use of hydrate inhibitors and heat exchange systems to maintain optimal conditions.

E.H. Al Munif *et al.* (2023) determined that downhole gas-liquid separators are important equipment in the oil and gas industry designed to efficiently separate and treat the gas-liquid mixture produced from wells. In unconventional formations, such as shale or high-viscosity hydrocarbon formations, special solutions are required to ensure optimal separator performance. One of the key challenges in oil and gas production from unconventional reservoirs is the presence of large amounts of impurities such as sand, water, and other solids that can accompany high-viscosity oil and gas flows. Well, separators in this context must be designed to effectively remove such impurities to prevent their deposit in pipelines and equipment. Analyses of results and conclusions indicate that technological innovations in downhole separators for unconventional reservoirs include the development of more efficient filtration systems adapted to handle highly viscous fluids, as well as the application of advanced methods for controlling and monitoring separation processes. These improvements are aimed at improving well performance and ensuring the long-term sustainability of unconventional reservoir production.

As noted by C. Sahu *et al.* (2021), well operation completion, as well as mechanised gas extraction from natural gas hydrate deposits, represent important milestones in the development of methane extraction technology. Well completion operations are necessary to ensure safety, prevent gas leakage and minimise environmental impacts. A comprehensive review of such operations includes a thorough analysis of various well sealing and isolation techniques, as well as strategies for abandoning oil and gas equipment in the field. Mechanised gas production from hydrate reservoirs is a current area of research and development in the context of energy efficiency and environmental sustainability. Methods based on the use of heat, pressure, or chemicals to decompose hydrates and release methane are discussed in detail in this context. However, an important aspect is the optimisation of processes to improve extraction efficiency and reduce costs, which becomes key when addressing the technological and economic challenges in methane hydrate extraction.

T. Van *et al.* (2022) noted the formation of paraffin deposits in gas lift wells is a serious technological and operational challenge. To prevent this phenomenon, an integrated approach involving various technologies and chemicals is required. One of the key methods to prevent wax formation is the use of specialised wax inhibitors. These chemical additives prevent paraffins from crystallising at lower temperatures, thus preventing their deposition in the well. In addition, the use of enriched gases and the introduction of heat transfer fluids into the system can also help reduce the risk of fouling. Additional methods include the use of ultrasound to prevent aggregation of paraffin particles and regular mechanical cleaning of wellbores. An important aspect is to monitor the temperature regime and fluid characteristics of the well to identify potential fouling threats promptly. It is possible to agree with the opinion that the combined approach to the problem of paraffin deposit formation in gaslift wells allows the creation of an effective system providing stable and reliable operation of wells while minimising the risk of technological problems.

CONCLUSIONS

The technology of DCO of two gas condensate reservoirs by lifting products through a single tubing string is an innovative method of developing multilayer fields, which can significantly increase the efficiency of hydrocarbon production. An important advantage of this technology is the possibility of reducing the number of drilling wells and, consequently, reducing overall operating costs. The basic idea behind the DCO is to use a single string of tubing to simultaneously lift production from two gas condensate reservoirs. This is achieved through the use of specialised downhole equipment, such as a GCC-type complex. This approach makes it possible to optimise gas and condensate production, manage the flow rates of individual reservoirs and carry out research work efficiently.

The benefits of this technology cover several key aspects. It reduces the ecological impact on the environment. By reducing the number of drilling wells used for field development, the overall footprint of the oil and gas industry on natural ecosystems is reduced. This is in line with modern requirements for sustainable development and compliance with environmental standards. The DCO technology improves the manageability of the production process. Specialised equipment used in this technology allows for more efficient monitoring and regulation of gas and condensate flow rates from each reservoir. This makes it possible to respond quickly to changes in field conditions and maximise hydrocarbon production. However, despite these advantages, the selection of the optimal DCO configuration must consider a variety of field characteristics. Well depths and diameters, geological and technical features require a tailored approach to ensure the best results and efficient use of the technology.

In general, ORE technology is a promising solution for rational and efficient exploitation of gas condensate fields, reducing operating costs and ensuring more efficient use of resources. To better understand and optimise the technology of DCO of gas condensate reservoirs by lifting production through a single string of tubing, additional research could be aimed at analysing the influence of geological and technical parameters of the field on the efficiency of this technique.

ACKNOWLEDGEMENTS

None.

CONFLICT OF INTEREST

None.

REFERENCES

[1] Aarushi, Singh, A.K., & Krishnakanth, V.V. (2021). A review on onshore drilling for oil and gas production with its safety barriers and well control methods. In *Advances in Environment Engineering and Management: Proceedings of the 1st National Conference on Sustainable Management of Environment and Natural Resource Through Innovation in Science and Technology* (pp. 29-40). Cham: Springer. doi: 10.1007/978-3-030-79065-3_3.

[2] Abad, A.R.B., Ghorbani, H., Mohamadian, N., Davoodi, S., Mehrad, M., Aghdam, S.K.Y., & Nasriani, H.R. (2022). Robust hybrid machine learning algorithms for gas flow rates prediction through wellhead chokes in gas condensate fields. *Fuel*, 308, article number 121872. doi: 10.1016/j.fuel.2021.121872.

[3] Abramovich, O.K., & Hadzhigeldyev, H.B. (2022). *Innovative technologies of the oil and gas refining industry of Turkmenistan*. Retrieved from https://elib.gstu.by/bitstream/handle/220612/28066/180-183.pdf?sequence=1.

[4] Aghbashlo, M., Peng, W., Tabatabaei, M., Kalogirou, S.A., Soltanian, S., Hosseinzadeh-Bandbafha, H., Mahian, O., & Lam, S.S. (2021). Machine learning technology in biodiesel research: A review. *Progress in Energy and Combustion Science*, 85, article number 100904. doi: 10.1016/j.pecs.2021.100904.

[5] Akyev, D.S., & Arazov, T.B. (2022). *Prospects for the development of oil and gas fields in Turkmenistan*. Retrieved from https://elib.gstu.by/bitstream/handle/220612/29387/13.pdf?sequence=1.

[6] Al Munif, E.H., Alhamad, L., Ejim, C.E., & Banjar, H.M. (2023). Review of downhole gas liquid separators in unconventional reservoirs. In *SPE Annual Technical Conference and Exhibition* (article number SPE-215112-MS). San Antonio, Texas, USA. doi: 10.2118/215112-MS.

[7] Deryaev, A.R. (2022). Well design development for multilayer horizons for the simultaneous separate operation by one well. *SOCAR Proceedings*, 1, 94-102. doi: 10.5510/OGP2023SI200874.

[8] Deryaev, A.R. (2023). Forecast of the future prospects for drilling ultra-deep wells in the difficult mining and geological conditions of Western Turkmenistan. *SOCAR Proceedings*, 2, 13-21. doi: 10.5510/OGP2023SI200874.

[9] Farsi, M., Barjouei, H.S., Wood, D.A., Ghorbani, H., Mohamadian, N., Davoodi, S., Nasriani, H.R., & Alvar, M.A. (2021). Prediction of oil flow rate through orifice flow meters: Optimized machine-learning techniques. *Measurement*, 174, article number 108943. doi: 10.1016/j.measurement.2020.108943.

[10] Gamal, H., Abdelaal, A., & Elkatatny, S. (2021). Machine learning models for equivalent circulating density prediction from drilling data. *ACS Omega*, 6(41), 27430-27442. doi: 10.1021/acsomega.1c04363.

[11] Grinkova, E.A., & Abaeva, G.I. (2023). Special payments and taxes for subsoil users. mineral extraction tax. In *Collected papers of the international scientific-practical conference of students "The path to science"* (pp. 468-473). Ural: BKATU named after Zhangir Khan.

[12] Kongar-Syuryun, C., Ubysz, A., & Faradzhov, V. (2021). Models and algorithms of choice of development technology of deposits when selecting the composition of the backfilling mixture. *IOP Conference Series: Earth and Environmental Science*, 684, article number 012008. doi: 10.1088/1755-1315/684/1/012008.

[13] Nurgalieva, K.S., Saychenko, L.A., & Riazi, M. (2021). Improving the efficiency of oil and gas wells complicated by the formation of Asphalt-Resin-Paraffin deposits. *Energies*, 14(20), article number 6673. doi: 10.3390/en14206673.

[14] Ozbekov, N., Ishanov, M., Ataev, D., & Byashimov, A. (2023). The importance of engineering and technical methods in the implementation of the environmental safety strategy of Turkmenistan. In *Collection of articles based on the results of the international scientific and practical conference "Basic and applied research in science and education"* (pp. 61-63). Sterlitamak: Agency of International Research.

[15] Panov, V. (2023). The scientific process of two interferometers (optical) development and the mitigation of external influence. *Scientific Herald of Uzhhorod University. Series "Physics"*, 53, 19-30. doi: 10.54919/physics/53.2023.19.

[16] Sadr, M.B., & Bozorgian, A. (2021). An overview of gas overflow in gaseous hydrates. *Journal of Chemical Reviews*, 3(1), 66-82.

[17] Safarov, F.E., Mamykin, A.A., Vezhnin, S.A., & Thelin, A.G. (2022). Technical solutions for performing operations on RCP-proppant thermal fixing and thermoreagent impact on the bottomhole formation zones of production wells. *Bulletin of the Oil and Gas Industry of Kazakhstan*, 4(1), 69-82.

[18] Sahu, C., Kumar, R., & Sangwai, J.S. (2021). A comprehensive review on well completion operations and artificial lift techniques for methane gas production from natural gas hydrate reservoirs. *Energy & Fuels*, 35(15), 11740-11760. doi: 10.1021/acs.energyfuels.1c01437.

[19] Sargsyan, G., Gukasyan, P., Sargsyan, H., & Poveda, R. (2023). Diffusion flames and a semi-empirical method for estimating the distribution of hydrogen molecules in propane flames. *Scientific Herald of Uzhhorod University. Series "Physics"*, 53, 42-52. doi: 10.54919/physics/53.2023.42.

[20] Shingala, J., Vora, N., & Shah, M. (2022). Emerging the dual string drilling and dual coil tubing drilling technology in a geothermal well applications. *Petroleum*, 8(1), 102-109. doi: 10.1016/j.petlm.2021.03.007.

[21] Van, T.N., Aleksandrov, A.N., & Rogachev, M.K. (2022). An extensive solution to prevent wax deposition formation in gas-lift wells. *Journal of Applied Engineering Science*, 20(1), 264-275. doi: 10.5937/jaes0-31307.

[22] Veysov, S.K., & Hamrayev, G.O. (2023). Comparative characteristics of the wind regime on the sandy massifs of western Turkmenistan and the Mangystau peninsula and its influence on the development of deflation processes. *Geography and Water Resources*, 1, 24-35. doi: 10.55764/2957-9856/2023-1-24-35.3%20.

[23] Watanabe, K., & Ogata, S. (2021). Drag reduction of aqueous suspensions of fine solid matter in pipe flows. *AIChE Journal*, 67(6), article number e17241. doi: 10.1002/aic.17241.

[24] Yazdani, B., Alinejad, S., Ghasemi, E., & Taghikhani, V. (2023). Experimental study of fluid flow in horizontal and deviated wells during the artificial gas lift process. *Journal of Chemical and Petroleum Engineering*, 57(1), 81-95. doi: 10.22059/JCHPE.2023.347272.1401.

[25] Zheng, X., Shi, J, Cao, G., Yang, N., Cui, M., Jia, D., & Liu, H. (2022). Progress and prospects of oil and gas production engineering technology in China. *Petroleum Exploration and Development*, 49(3), 644-659. doi: 10.1016/S1876-3804(22)60054-5.

[26] Zhou, Z., Shen, H., Liu, B., Du, W., & Jin, J. (2021). Thermal field prediction for welding paths in multi-layer gas metal arc welding-based additive manufacturing: A machine learning approach. *Journal of Manufacturing Processes*, 64, 960-971. doi: 10.1016/j.jmapro.2021.02.033.

[27] Zou, Q., Liu, H., Jiang, Z., & Wu, X. (2021). Gas flow laws in coal subjected to hydraulic slotting and a prediction model for its permeability-enhancing effect. *Energy Sources, Part A: Recovery, Utilization, and Environmental Effects*. doi: 10.1080/15567036.2021.1936692.

Аннагули Реджепович Деряєв
Доктор технічних наук, головний науковий співробітник
Науково-дослідний інститут природного газу державного концерну "Туркменгаз"
744036, просп. Арчабіл, 58, м. Ашхабад, Туркменістан
https://orcid.org/0009-0004-8569-6277

Технологія одночасно-роздільної експлуатації двох газоконденсатних пластів підйомом продукції однією колоною насосно-компресорних труб

Анотація. В умовах активного розвитку газоконденсатних родовищ з кількома пластами в районі височини Гогрендаг-Екерем (Корпедже, Південний Гамишлджа), дослідження його технологій є важливим напрямом роботи. Метою даного дослідження є оптимізація технології одночасно-роздільної експлуатації двох газоконденсатних пластів підйомом продукції однією колоною насосно-компресорних труб з підвищенням ефективності видобутку вуглеводнів. Серед використаних методів слід зазначити аналітичний метод, функціональний метод, статистичний метод, метод синтезу та інші. У ході проведеного дослідження було розроблено інноваційну методику одночасно-роздільної експлуатації двох газоконденсатних пластів, що передбачає підйом продукції єдиною колоною насосно-компресорних труб. Ключовим елементом є уточнення здійснених розрахунків. В результаті детального аналізу обладнання, що використовується в зоні Гогрендаг-Екерем, було зазначено, що воно також може бути ефективно застосоване і на інших регіональних родовищах, забезпечуючи справне функціонування кожного елемента вище рівня пакера. При цьому необхідно звертати увагу на різноманітні індивідуальні характеристики родовища для залучення дійсно ефективної конфігурації цієї технології. Нова технологія включає оптимізовані параметри тиску, витрати і контролю для кожного пласта, що в результаті призводить до збільшення ефективності видобутку і зниження енерговитрат. Було виявлено значне скорочення негативного впливу на довкілля та підвищення загальної стійкості виробничого процесу. Ці особливості роблять запропоновану технологію важливим внеском у розвиток нафтогазової промисловості, сприяючи більш ефективному та екологічно стійкому видобутку вуглеводнів та підкреслюють її потенціал для застосування у сучасних умовах розробки родовищ. Практичне значення дослідження полягає у створенні більш ефективної та стійкої технології видобутку вуглеводнів, що не тільки сприяє оптимізації виробничих процесів та зниженню впливу на екологію, але також надає індустрії цінний інструмент для покращення загальної енергетичної ефективності та стійкості в умовах постійно мінливих вимог та викликів у галузі енергетики

Ключові слова: видобуток вуглеводнів; ефективність використання ресурсів; екологічний вплив; покращена методика; стійкість виробничого процесу

Machinery & Energetics
Vol. 14, No. 4. 2023

Journal homepage:
https://technicalscience.com.ua/en

UDC 681.518:621.311.25
DOI: 10.31548/machinery/4.2023.42

Dmytro Belytskyi*
Student
Taras Shevchenko National University of Kyiv
01033, 60 Volodymyrska Str., Kyiv, Ukraine
https://orcid.org/0009-0004-1605-7658

Ruslan Yermolenko
PhD in Physical and Mathematical Sciences, Associate Professor
Taras Shevchenko National University of Kyiv
01033, 60 Volodymyrska Str., Kyiv, Ukraine
https://orcid.org/0009-0000-0854-4668

Kostiantyn Petrenko
Senior Lecturer
Taras Shevchenko National University of Kyiv
01033, 60 Volodymyrska Str., Kyiv, Ukraine
https://orcid.org/0009-0007-2972-4001

Olga Gogota
PhD in Physical and Mathematical Sciences, Junior Researcher
Taras Shevchenko National University of Kyiv
01033, 60 Volodymyrska Str., Kyiv, Ukraine
https://orcid.org/0000-0003-4108-7256

Application of machine learning and computer vision methods to determine the size of NPP equipment elements in difficult measurement conditions

Abstract. The research relevance is determined by the need to improve the processes of measurement of objects size in hard-to-reach conditions. In the modern industrial environment, where high measurement accuracy is critical for ensuring safety and maximizing the efficiency of production processes, the study of this topic is relevant in the context of rapid technological development and increased requirements for production quality. The study aims to evaluate the possibilities of using modern computer vision methods for measuring and reconstructing objects in difficult technical conditions, such as the enclosure of a water-water power reactor. The study employed 3D photogrammetry methods, including Depth from Stereo and Multi-View Stereo, as well as Structure from Motion methods. The study determined that modern computer vision methods, in particular machine learning methods, can be successfully used for measuring and reconstructing objects in hard-to-reach conditions. The study showed that the measurement accuracy can reach values close to 1 mm under ideal conditions and at a distance of 1.5 from the measuring device to the object. At the same time, the Multi-View Stereo method revealed greater uniformity of the spatial distribution of errors compared to the Depth from the Stereo method. In practice, in the conditions of real photos, the Multi-View Stereo method turned out to be more demanding to accurately determine the position of the camera. Due to its low demand for the exact coordinates of the cameras, the Depth from the Stereo method showed better results, showing less error in the measurements. The study highlighted the possibility of using the proposed method to distinguish fluctuations in the height of the surface of

Article's History: Received: 09.07.2023; Revised: 09.10.2023; Accepted: 22.11.2023.

Suggested Citation:
Belytskyi, D., Yermolenko, R., Petrenko, K., & Gogota, O. (2023). Application of machine learning and computer vision methods to determine the size of NPP equipment elements in difficult measurement conditions. *Machinery & Energetics,* 14(4), 42-53. doi: 10.31548/machinery/4.2023.42.

*Corresponding author

the object, which is important for further applications in the field of reactor maintenance and other areas of industry. The practical value of this research lies in the development and validation of methods for measuring and reconstructing objects in conditions where traditional methods become limited or impractical

Keywords: water-water power type reactor; neutron fields; physical properties; binocular system; machine learning

INTRODUCTION

The research on the machine learning and computer vision methods for determining the dimensions of Nuclear Power Plant (NPP) equipment elements under difficult measurement conditions is important for the development of new methods and technologies in the field of computer vision and automated inspection, which can be used in various industries, including nuclear power and industrial automation. The study of this topic is critically important in the context of the development of modern methods of computer vision and automated inspection. The need for accurate and reliable methods of surface measurement in difficult conditions of high radiation background becomes especially relevant in nuclear power, where safety and reliability are crucial. The use of automated systems based on machine learning can reduce human involvement in the measurement process, which can lead to increased speed and efficiency of research. Accurate and efficient measurement of equipment dimensions is an important step in ensuring the safety and reliability of nuclear power plants. The use of advanced technologies can help avoid malfunctions and ensure optimal efficiency. The problem with the study is that there is currently a lack of research in the development and improvement of computer vision and image analysis methods for precision measurement of objects in difficult-to-access environments. In particular, there are problems related to the accuracy and reliability of measurements, especially in conditions of high radiation background. In such conditions, traditional methods may become unsuitable or unsafe for use, and this determines the relevance of the study to develop new, more efficient, and safer measurement approaches in this area.

With the innovative development of technology, a range of new information technologies for image processing is emerging, which opens up new opportunities for further research. A.O. Zelinskyi & V.V. Lisovskyi (2023) are confident that there are many areas for their application, but many of them face the problem of using resources to fully realise their potential. Thus, the development of a system based on a cloud architecture for machine image analysis using modern analytical processing technologies is a relevant area of research. It is not specified how resources affect the full realisation of the potential of image-processing information technologies. It is important to consider economic and technical limitations.

According to T.V. Mosagutova (2021) and V. Levchenko *et al.* (2021), the long-term operation of nuclear power plants is largely determined by the choice of the right structural materials. The development of new technologies for the selection of materials and equipment in the energy sector was based on the experience gained during the long development of conventional thermal power plants. No specific materials and technologies have been identified that are used in new technologies for selecting materials for nuclear power plants.

M.V. Kukhlenko (2023) states that for almost a century of the existence of nuclear reactors, humanity has been using them in various industries, and for Ukraine, they are one of the main sources of electricity. The development of nuclear energy is important because the need for energy increases with the development of civilisation. Therefore, it is important to work on improving and creating new nuclear reactors to meet the needs. The study does not focus on specific aspects of nuclear reactor development and improvement, such as new technologies or safety improvements.

S. Ageiev (2021) has developed an approach for assessing the severity of pipeline erosion and corrosion wear that considers various impacts and geometry. His approach allows us to assess the degree of wear not only by depth but also by considering the length and width of erosion and corrosion wear, which is important for complex pipeline systems. There is no indication of how this approach to assessing erosion and corrosion wear can be applied or implemented in different industrial sectors, or how it can be optimised for specific conditions.

P.O. Sunak *et al.* (2020) substantiate the prospects of using laser scanning technology for the reconstruction of engineering structures and networks, as well as the landscape. This technology makes it possible to obtain high-precision measurements of complex engineering objects, restore project documentation and create a three-dimensional model with sufficient detail for further processing in various software systems. The active implementation of laser scanning technology in construction is in line with the Industry 4.0 concept and provides a modern technical level of solving various problems of sustainable development of cities and amalgamated territorial communities in the context of urbanisation.

According to K. Sytnyk (2020), the formation of new approaches to the organisation of production, and the large-scale implementation of quality management systems significantly increase the requirements for ensuring metrological activities in production. This necessitates the search for ways to improve the quality and efficiency of measurement processes at the stage of product manufacturing and their integration into product quality assurance processes.

Based on the analysis of the scientific literature mentioned above, the selected topic has not been studied sufficiently. Therefore, the study aims to investigate and compare two computer vision methods, namely Depth from Stereo (DFS) and Multi-View Stereo (MVS), for precision measurement of the reactor vessel surface in high radiation background conditions.

MATERIALS AND METHODS

The study considered the BBEP-1000 water-water power reactor (WWPR), namely the problem associated with the swelling of the reactor's internal lining. The subject of the experimental study was a water-water reactor baffle made of stainless steel 08X18H10T. The reconstructed surface was compared with a reference three-dimensional model of the vessel.

The following neural network architectures were selected in the study: transMVSnet for the MVS approach (Ding *et al.*, 2021), and CREstereo for the DFS approach (Li *et al.*, 2022). These neural networks were chosen due to their high efficiency, which they demonstrated during testing on the Middlebury Benchmark (a system for independent testing of various algorithms and neural network architectures) among open-source neural networks. The transMVSnet architecture was chosen because of its use of transformers, which are now showing an advantage over traditional convolutional neural networks, especially in computer vision tasks. This architecture should ensure the stability of the neural network even with low image quality.

There are differences between MVS and DFS that need to be considered. For MVS, it is necessary to accurately determine the position of the cameras for high-quality results, and this can be achieved by placing the camera on a manipulator that can be controlled by encoders and/or stepper motors. However, this poses an engineering challenge, as the long distance from the arm attachment point to the baffle can make it very difficult to design the arm for accurate positioning. As an alternative, the structure from motion (SFM) method is used, which determines the position of the cameras based on the images received. The application of SFM to synthetic data generated in Blender showed positioning accuracy of several centimetres.

For the DFS method, it is critical to accurately calibrate the camera, as the slightest distortion of the camera image will distort the results. Although DFS allows the depth map to be constructed without knowing the camera positions (a stereo camera is used where the relative positions of the cameras are known), the camera position is still required to determine the degree of deformation of the baffle by comparing it to the reference model. Thus, it was important to determine the position of the cameras. This structure was chosen to test neural networks under ideal conditions, where there are no distortion artefacts on the cameras and the exact parameters of their location are known.

The virtual environment for the research was created using Blender software. It included a simplified model of a baffle with no internal channels and Physically Based Rendering (PBR) technology was used for texturing. The texture included a texture layer, a normal map, a height map, and a roughness map. The texture layer was taken from an open source and applied only to the inner surface of the baffle using the UV mapping method. Then, using the nodes UI interface of the shading tab, the material for the surface was configured.

The 4D Light Field Benchmark addon was used to simulate the movement and configure parameters of the virtual camera. The trajectory of the camera was determined using key points. The Cycles (physically based production renderer) graphics engine was used to generate photos, which uses a path-tracking method for realistic lighting simulation (Choi *et al.*, 2021). The add-on saved the camera images to separate files, including a depth map in PFM format and a configuration file (config.cfg) containing the camera parameters and its spatial position. This data can be used to train the neural network from scratch or to fine-tune its parameters. The frames and configuration parameters extracted from the source file are converted by using a script, part of which was applied according to (Meng & Gräbe, 2021), to convert them into a format compatible with the transMVSnet neural network.

The images were processed based on the parameters specified in the bash script, such as resolution, number of images in the batch. The paths to the input data, the fusion method (merging separate point clouds into one large one), the path to the output file, and the path to the Python scripts were specified there either. When processing 50 images in a resolution of 960×704 using a GTX1070 graphics card (manufactured by NVidia, USA), the process took about 10 minutes. The output was a ready-made point cloud in .ply format.

The following methods and approaches were used in the study, namely the Structured Light Method. This method was used for the modelled environment in the Blender software. With the help of structured light, a texture was created, which was used for accurate surface measurements. This method provided accurate height and depth data. For real photographs, the photogrammetry method was used, which is based on the analysis of photographs from different cameras to measure and reconstruct 3D objects. The cameras were pre-calibrated and rectified to obtain accurate results. For real-world photos, a stereo imaging system was used to obtain duplicate images from different cameras. These images were processed to determine the depth and structure of the objects. The research involved the use of neural networks for image analysis and processing. Neural networks were trained on large training datasets and used to solve 3D object reconstruction tasks. Python scripts and bash scripts were used to process the results. These scripts helped to process, analyse, and visualise the data obtained from cameras and neural networks.

These methods were used to perform both virtual and real measurements of surfaces and objects, compare the results and determine their accuracy and efficiency in different conditions. The distance to the object in the study was calculated using formula (1):

$$l = \frac{b \cdot fp}{\Delta d}, \tag{1}$$

where l – distance to a point, b – distance between cameras, Δd – offset between identical pixels, fp – focal length of camera.

The synthesis method was used to create models of the virtual environment in Blender. The results obtained in the study were compared with a reference three-dimensional model of the enclosure.

RESULTS

This study addresses the problem associated with the swelling of the reactor baffle of the Water-Water Power Reactor (WWER-1000). Specifically, the object of study is the effect of powerful neutron fields on the physical properties of stainless steel used for the manufacture of the reactor pressure vessel. These physical properties, including stiffness, ductility, density, and volume, are subject to significant changes under the influence of neutron radiation intensity. This phenomenon is quite dangerous in the context of nuclear reactor operation, since changes in the physical properties of the material can lead to disruption of the normal circulation of coolant in the first reactor circuit or even destruction of fuel assemblies in case of fuel reload. The transformation of material due to neutron irradiation is a complex process, as it depends on several variables in the environment, including temperature, pressure, and energy spectrum of emitting neutrons. Important aspects of this study include the uncertainty of mathematical modelling of material swelling under the influence of neutron fields since existing mathematical models do not always reliably predict material behaviour in VVER-1000 reactor conditions (Qian & Liu, 2023).

Considering the aforementioned circumstances, solving this problem requires regular monitoring of the physical properties of the inner surface of the reactor vessel and further study of the influence of various factors on the material swelling process (Pylypchynets, 2022). These efforts are important for ensuring the safety and efficient operation of VVER-1000 nuclear reactors. This study describes an innovative method of applying 3D photogrammetry for non-contact inspection of the baffle surface. The application of this method involves the use of approaches based on MVS and DFS to obtain depth maps and 3D point clouds (Morgan *et al.*, 2022).

The proposed approach introduces the possibility of measuring the surface of the reactor baffle without the need for physical contact with it. The use of 3D photogrammetry techniques in combination with MVS and DFS methods allows obtaining accurate and objective data on the depth and structure of the object's surface. This approach is particularly useful when monitoring is to be carried out on a shutdown reactor during maintenance when high radiation conditions make traditional measurement methods difficult. The DFS method is based on a binocular system that includes two cameras placed at a certain distance from each other (base). This method is used to determine the distance to an object using the information obtained from both cameras. The basic principle of the method is to identify the same pixels in the images obtained from the right and left cameras and determine the displacement of these pixels. The distance to the object is calculated using a simple formula (1).

Simple computer vision algorithms exist to determine pixel shifts in images, such as the Boyer-Moore algorithm (Faqih *et al.*, 2022). These algorithms work effectively under relatively simple conditions, such as a flat surface that is properly illuminated, no camera lens distortion, and accurate stereo pair rectification. However, they demonstrate limited effectiveness when processing tilted surfaces and scenes that contain a lot of detail. Machine learning methods have undergone significant transformations in recent years, particularly in the field of computer vision. Neural networks trained on large data sets have shown significant improvements in solving computer vision problems. The use of neural networks is of great advantage, but this advantage is only manifested if the network has been trained on large training data sets. Typically, neural networks perform best when the training and test data are of similar origin. However, recent years have seen the development of new neural network architectures that perform well even when the data have different origins. For example, networks trained on synthetic data perform well when applied to real data. Typically, such architectures are based on transformers. However, their main disadvantage is the large number of weighting factors, which requires special approaches to the training process. One of the important differences between algorithms and neural networks is the high resource intensity of the latter. This feature has led to the excellent use of algorithms in robotics, especially in conditions where it is necessary to operate with limited computing resources. However, with the advent of microcomputers equipped with graphics accelerators and supporting parallel computing, it has become possible to use complex neural networks in real-time in robotics.

Unlike DFS, MVS is not self-sufficient and requires accurate information about the relative position of the cameras in a series of measurements to build a depth map. The MVS method is similar to DFS, namely, analysing the source images, identifying the same details, triangulating them, and building a depth map. However, the MVS method has its advantages, including the use of only one camera and the ability to correct occlusions (dead zones) using a series of images, unlike DFS, which uses only two rectified images. Depth maps obtained by DFS or MVS and known camera parameters can be used to build three-dimensional point clouds and further reconstruct a three-dimensional scene in the form of a mesh. For this purpose, ready-made implementations exist, such as in S. Galliani *et al.* (2015) and C. Griwodz *et al.* (2021), which can be used to reconstruct a scene using the MVS method. They are characterised by open source and modular structure, which allows the use of individual components of these programs to create the final three-dimensional scene in combination with other neural networks.

The DFS method requires fewer computing resources and uses only two cameras, so it is suitable for real-time surface research, provided that the appropriate computing hardware is available. The general idea is to 3D reconstruct the visible surface of a piece of equipment from a set of images using machine learning methods. In the case of NPP applications, it is assumed that a radiation-resistant camera is lowered into the area of the shaft in a shutdown reactor with fuel elements removed and photographic data of the selected part of the surface under study is collected from different angles. The water-water reactor baffle is made of stainless steel 08Kh18N10T, so it is possible to reflect a significant part of the light flux energy. Reconstructing reflective surfaces is an extremely difficult task for traditional MVS systems, and new methods such as NeRf or Gaussian splatting have come close to solving this problem, although these methods were created to generate new views from existing ones, research is underway to extract the mesh from the reconstructed scene, the results of which can be seen in projects such as dreamgausian.

The swelling of the baffle metal under the influence of neutron radiation is a long process. During this time, the baffle is covered with oxides and deposits, which causes it to lose its reflectivity, become cloudy and develop textural irregularities that allow the convolutional neural network to better distinguish features and thus improve the accuracy of depth map prediction. Lighting is also an important consideration. As shown by the Blender environment simulation, a point light source near the camera is highly undesirable as it causes flares in the images. The best option is an extended light source placed perpendicular to the camera normal plane. Noise in the image caused by the interaction of ionising radiation with the camera's light-sensitive sensor should also be considered. Moreover, broken pixels can quickly appear. It is also possible that the optics may become cloudy due to high-powered radiation. All of this requires scanning the baffle in a short period (on the order of minutes).

After obtaining satisfactory quality images of the surface, the surface is reconstructed using DFS or MVS algorithms based on neural networks. The resulting reconstructed surface is compared to a reference three-dimensional model of the baffle. For this purpose, an alignment procedure is first performed, which involves the alignment of the model and the resulting point cloud in three-dimensional space. The part of the reactor shaft visible above the baffle from the middle of the core can be used as an undeformed surface against which the alignment is performed. Alignment parameters, such as displacement, rotation, and scale, are selected by approximation methods until the error function reaches an extremum. This procedure requires the definition of seven degrees of freedom. There are other possible variants of the alignment procedure, which will be discussed later.

After the alignment, it is possible to study the deviations of the cloud points from the reference model and estimate the surface deformation. The photographs were taken with a real camera using a lens with minimal distortion (almost zero distortion). The camera was previously calibrated and rectified to create a stereo pair. For the MVS method, the images from the left camera of the stereo pair were used. The photos were taken in bright light during the daytime to obtain high-quality images. The test object was a calibration plate with known geometric characteristics.

To determine the camera positions, the Structure from Motion (SfM) method was used, which was implemented using the COLMAP software package (Schonberger & Frahm, 2016). After that, the point cloud was cropped to the area of the verification plate and a plane was constructed using the least squares method. This plane served as the ground truth for calculating measurement errors for both MVS and DFS approaches (Jin *et al.*, 2023).

The main features of these studies are the absence of image distortion by the camera and the known absolute values of the camera positions, which makes it possible to compare the accuracy of the results for both methods. DFS approach: the results of measurements on a synthetic dataset using a virtual stereo camera for the specified parameters at a distance of 1.5 m from the baffle surface are shown below (Table 1).

To capture the scene, the camera moves in a circular path around a certain point on the surface of the enclosure at a distance of 1.5 m (Fig. 1-3).

Table 1. Camera parameters

Camera parameters	
Resolution:	1280×720
Fp:	1372 (fov 50 degrees)
Baseline:	20 cm
Acquired results	
Avgerror:	0.7 mm
RMS:	1 mm
FWHM:	1 mm

Source: compiled by the authors

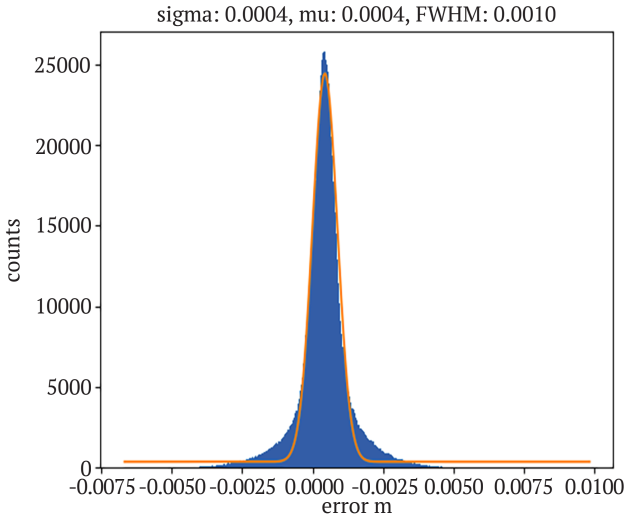

Figure 1. Error distribution histogram

Source: compiled by the authors

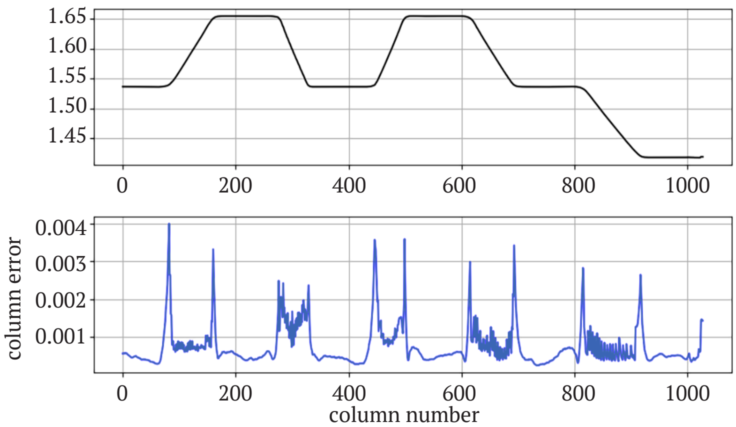

Figure 2. One-dimensional spatial distribution of the error

Source: compiled by the authors

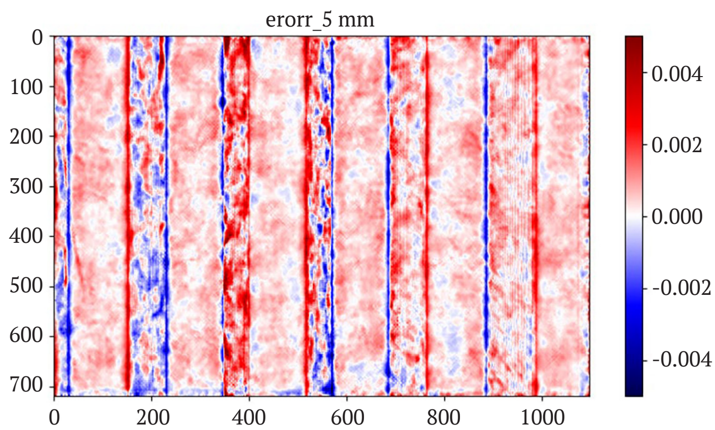

Figure 3. Two-dimensional spatial distribution of error

Source: compiled by the authors

To capture the picture, the camera moves in a circular path around a certain point on the surface of the enclosure at a distance of 1.5 m (Fig. 4)

MVS approach. Research on real data: To verify the results, several images of the test plate were taken at a distance of 0.4 ± 0.1 m in 960×720 resolution (Fig. 5-7).

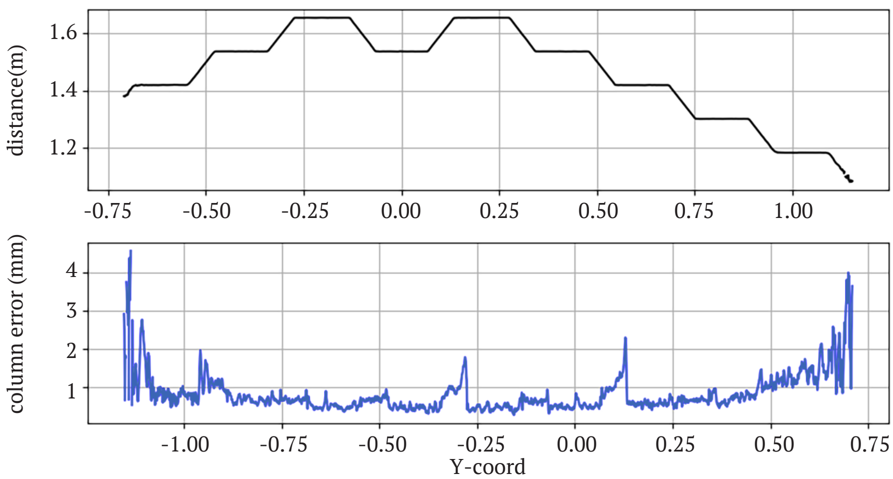

Figure 4. One-dimensional spatial distribution of the error
Source: compiled by the authors

Figure 5. Test plate
Source: compiled by the authors

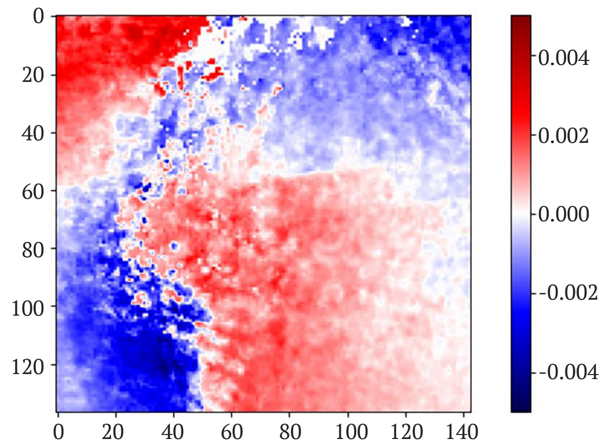

Figure 6. Two-dimensional spatial distribution of error
Source: compiled by the authors

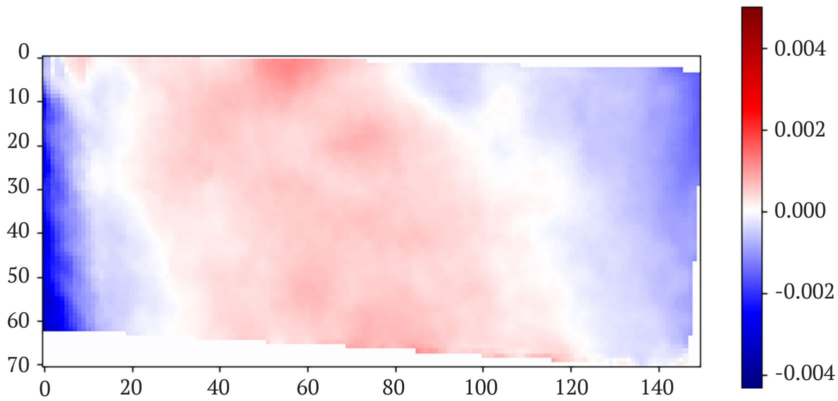

Figure 7. Two-dimensional spatial distribution of error
Source: compiled by the authors

An experimental measurement was carried out to thoroughly analyse the sensitivity of the plane distance method. To accomplish this, a computer numerically controlled machine (CNC) was used to fabricate a test sample, as shown in Figure 8. A given 150×150 mm plate was divided into 9 50×50 mm squares, each of which was recessed into the plate to a variable depth of 2.5 to 0.25 mm. Additionally, two flat surfaces were fitted on both sides of the 150×150 mm square, which were defined as reference surfaces. These surfaces were used to orientate the reconstructed model in space. The depth map shown in Figure 9 was constructed using the acquired images.

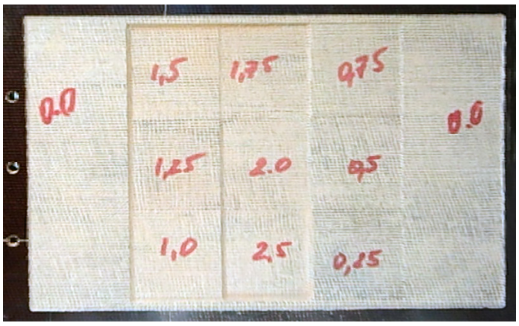

Figure 8. Test sample
Source: compiled by the authors

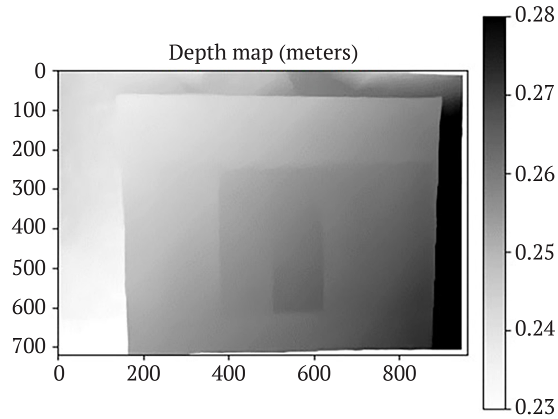

Figure 9. Predicted depth map by DFS method from the tested sample
Source: compiled by the authors

Next, a point cloud was collected using the obtained depth map, similar to the previous experiments. The main goal was to manually measure the depth values in the centres of the 5×5 squares and compare them with the true depth values. To ensure the possibility of measurements, it was decided to place the reconstructed surface in the XY plane. This process is possible both with the help of the built-in tools of MeshLab and with the help of a Python script, as it was implemented in this case.

From the resulting point cloud, only those points that corresponded to zero surfaces were selected. These points were then approximated by a plane using the least squares method. Knowing the equations of the plane, the necessary spatial displacement and rotation transformations were found, which reflect the original point cloud in the XY plane. The obtained measurement results (GT – determined by experts, and DFS measurement results) were systematised and presented in Table 2.

Table 2. Measurement results

GT (true value), mm	1.5	1.25	1	1.75	2	2.5	0.75	0.5	0.25
Measured value, mm	1.3	1.2	1.1	1.6	2	2.2	0.88	0.5	≈0

Source: compiled by the authors

The data obtained were visualised in a bar chart shown in Figure 10. To determine the error due to measurement fluctuations, the following approach was used: the reference side surfaces were approximated by a plane using the least squares method.

The average deviation of the points of the side surfaces from this plane was taken as the value of the error caused by fluctuations. This value was 0.23 mm. The resulting value was displayed on the diagram in the form of an error bars.

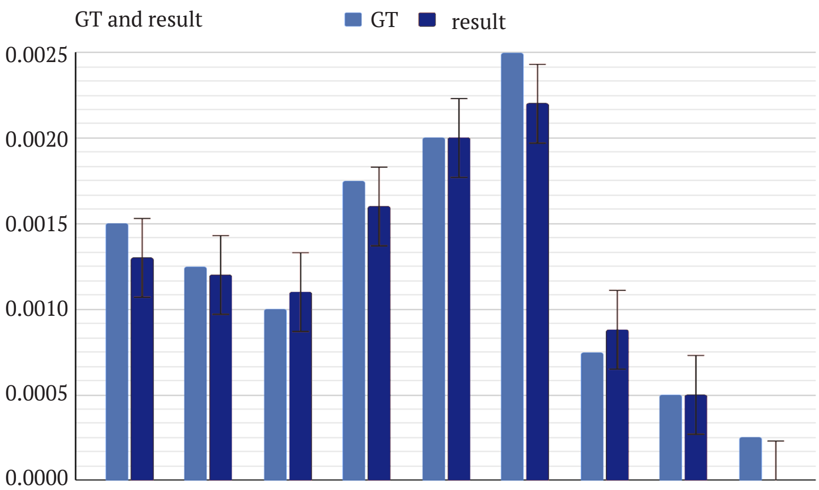

Figure 10. Measurement results
Source: compiled by the authors

The graph shows that the depth of the steps determined by the DFS method generally does not exceed the error value compared to the true value. This indicates that the method can determine the difference between points with an accuracy of 0.5 mm, provided that these points are more than 5 cm apart in the horizontal plane.

DISCUSSION

The study results demonstrate the importance and potential of using modern computer vision systems and neural networks for measurements in difficult conditions, in particular, in conditions of high radiation background, as may occur in nuclear power. Y. Xu *et al.* (2023) focus on the importance of assessing the condition of nuclear power plant (NPP) equipment and points out its significance for improving the safety and efficiency of NPPs. The paper is notable for offering a detailed literature review and highlighting issues that require further research in this area. The researchers emphasise the importance of using machine learning methods to assess the condition of NPP equipment, as this can help improve decisions on their operation and maintenance. The authors assure that this approach can help to detect anomalies in time, predict the remaining service life and diagnose faults. The study includes an analysis of the main types of failures, data sources, maintenance strategies, and their interrelationships. The study places a special emphasis on the use of deep learning methods to assess the condition of NPP equipment. It also highlights current challenges and future research directions in this area. This study is important for the community because it reviews current methods for assessing the condition of NPP equipment and indicates that there are significant opportunities for applying machine learning methods and improving maintenance in this area. Both studies have a common feature – the object of research in both is the use of modern technologies and methods to improve the accuracy and efficiency of measurements and assessments of the condition of objects. In both cases, the importance of choosing the right method and taking into account the specific conditions of measurement or assessment is emphasised. However, they differ in terms of the subject matter and methodology. The study described above is more focused on measuring and controlling surfaces in hard-to-reach environments. It looks at two methods (DFS and MVS) for this purpose and compares their performance. The results emphasise the importance of choosing the right method depending on the conditions and the need for accurate measurements. On the other hand, Y. Xu *et al.* (2023) focus on monitoring the condition of NPP equipment and use machine learning methods for this purpose. Both studies have practical applications in various technology areas, but their subjects and methods differ. The research reported in the results is more focused on surface measurement and control, while the researchers focus on monitoring the condition of NPP equipment using machine learning methods.

The study by Z. Sun *et al.* (2020) proposes a new approach to predicting downtime at nuclear power plants (NPPs) using computer vision and data-driven modelling. The main goal of their research is to automatically detect abnormal behaviour of people or teams during field operation processes and predict possible delays during NPP downtime. The researchers use computer vision algorithms to track people in a video to detect abnormal behaviour. They then create a simulation model of field operation and training processes based on the data. This model uses the anomalies detected in the video to adjust parameters and predict possible delays in the workflow. The results of their research show that delays in task completion often occur in the initial phase of the workflow, and waiting queues build up due to the over-allocation of resources during mid-stage maintenance. Modelling shows that tasks on the critical path are more sensitive to these anomalies and can lead to delays in the workflow. In both cases, the research uses modern technology to improve efficiency and accuracy in a variety of industries, but their goals and methods differ. The research described above focuses on surface measurement and control. It looks at two methods (DFS and MVS) for measurements and compares their performance. On the other hand, the study by Y. Xu *et al.* (2023) focuses on monitoring the condition of NPP equipment and uses machine learning methods for this purpose. The third study by Z. Sun *et al.* (2020) proposes a new approach to predicting outages at NPPs. All these studies are important and have the potential to improve the respective industries.

Y. Yao *et al.* (2020) propose a new approach for fault diagnosis in nuclear power plants (NPPs) using a full-scale state image-based simulator (FDFSSII). The main idea is to create a series of grey images that represent the transient process, including the normal state and the fault state, based on real-time monitoring data. Machine learning (ML) technology is used to extract and classify image features from the analysis of a large amount of historical and synthetic grey image data. The main steps include kernel principal component analysis (KPCA) and classification of image features using developed classifiers in different learning methods. The diagnostic effect is evaluated using the F1 score. The simulation results show that the FDFSSII approach is successfully used for fault diagnosis at NPPs. It simplifies the process of nuclear reactor operation due to a large amount of monitoring data and provides useful auxiliary information to operators. This approach can improve the safety and efficiency of NPPs by facilitating timely fault detection and diagnosis. Although both studies have a common factor in common – the use of modern technology to achieve their goals – their approaches and subjects differ. The study on computer vision systems focuses on improving the accuracy of measurements in hard-to-reach environments by comparing the performance of two methods (DFS and MVS) in different conditions. On the other hand, the researchers diagnosed faults in nuclear power plants by using machine learning to analyse condition images and detect anomalies.

The researchers X. Zhong & H. Ban (2022) consider the problem of classification and diagnosis of faults in the nuclear industry in one of their studies. In their opinion, the main problem is that data on faults and accidents at nuclear power plants are usually limited or difficult to obtain. The researcher proposes a transfer learning method based on a convolutional neural network (CNN) to solve this problem. The method uses a two-level network. The first, shallower level of the network is based on a pre-trained CNN based on the ImageNet database and is designed to automatically extract features. The second, deeper layer of the network is configured for a specific classification problem. Using data on rotating machine faults, the proposed method only requires limited training data but achieves high accuracy. This means that the method can be an effective tool for fault diagnosis and classification in data-constrained environments at nuclear power plants, which can improve their safety and efficiency. Both studies are concerned with the use of advanced technologies to improve efficiency and safety in various industries.

The research described above focuses on the use of computer vision systems for precision measurements in hard-to-reach environments. Two methods (DFS and MVS) are investigated and their accuracy in virtual and real environments. The possibility of distinguishing surface height fluctuations is also investigated. The study by the researchers focuses on the use of convolutional neural networks for the classification and diagnosis of faults in nuclear power plants. The problem of limited fault data is investigated, and a transfer learning method is proposed that allows achieving high diagnostic accuracy with a minimum amount of data. Both studies use modern technologies, including neural networks and computer vision. These studies are helping to improve accuracy and safety in a variety of fields, such as surface measurement and nuclear power plant diagnostics. The research described above focuses on surface measurement and control, particularly in hard-to-reach environments. The study by the researchers focuses on fault diagnosis in nuclear power plants and is used for accident classification and image-based anomaly detection. Both studies can make significant contributions in their respective fields and help to improve processes and safety.

CONCLUSIONS

In this study, the possibility of using modern computer vision systems for precision measurements in hard-to-reach environments was carefully considered. The results of this study provide an important contribution to the development of new methods of measurement and control of surfaces in various fields of science and technology. Experiments conducted in a simulated virtual environment show that the desired level of accuracy is achieved, which is on average 1 mm. It is noticeable that the DFS method shows a significant increase in error on surfaces located at an angle to the camera. In contrast, the MVS method shows a more homogeneous spatial distribution of error. This observation highlights the importance of selecting the appropriate method depending on the specific conditions and the need for accurate measurements.

In real-world conditions, the key limitation of the MVS method was the accurate determination of the camera position. Using the SFM method to determine the position of the camera at a distance of about 1.5 m from the surface allowed us to achieve an accuracy of positioning about 2 cm. On the other hand, the DFS method, which does not require precise camera parameters, demonstrated greater accuracy. The average error over the surface was 0.6 mm for DFS compared to 1.2 mm for MVS. Additionally, a study was conducted to investigate the ability of the proposed method to distinguish between surface height fluctuations. The results show that this approach is promising, as it can simplify the tasks of reactor maintenance and accurate measurements in conditions of high radiation background. Such possibilities open up a wide range of possible applications of this method in various fields of science and technology.

Based on the results of this study, two possible areas for further research can be suggested. Firstly, improving MVS and DFS algorithms can increase their accuracy and speed. Research into new neural network architectures that would be more efficient for 3D reconstruction tasks is one of the possible directions. Secondly, further research is required to investigate the impact of physical conditions on the accuracy and reliability of the methods. Radiation background, lighting and other environmental parameters can affect the results. It is important to determine how these factors affect measurements and how they can be corrected.

ACKNOWLEDGEMENTS

None.

CONFLICT OF INTEREST

The authors declare no conflict of interest.

REFERENCES

[1] Ageiev, S. (2021). Methodology for assessing the allowable wall thicknesses of carbon steel NPP piping under erosion-corrosion wear. *Nuclear and Radiation Safety*, 3(91), 32-42.

[2] Choi, Y., Bae, J.H., & Yeo, D. (2021). Deep-learning-based nuclear power plant fault detection using remote light-emitting diode array data transmission. *Microwave and Optical Technology Letters*, 63(12), 155-61. doi: 10.1002/mop.32974.

[3] Ding, Y., Yuan, W., Zhu, Q., Zhang, H., Liu, X., Wang, Y., & Liu, X. (2021). TransMVSNet: Global context-aware multi-view stereo network with transformers. *Computer Vision and Pattern Recognition.* doi: 10.48550/arXiv.2111.14600.

[4] Faqih, Y., Rahmanto, Y., Ari Aldino, A., & Waluyo, B. (2022). Application of string matching using the Boyer-Moore algorithm in the development of an online book search system. *Bulletin of Computer Science Research*, 2(3), 100-106. doi: 10.47065/bulletincsr.v2i3.172.
[5] Galliani, S., Lasinger, K., & Schindler, K. (2015). Massively parallel multiview stereopsis by surface normal diffusion. In *2015 IEEE International Conference on Computer Vision (ICCV)* (pp. 873-881). Santiago: IEEE. doi: 10.1109/ICCV.2015.106.
[6] Griwodz, C., Gasparini, S., Calvet, L., Gurdjos, P., Castan, F., Maujean, B., De Lillo, G., & Lanthony, Y. (2021). AliceVision Meshroom: An open-source 3D reconstruction pipeline. In *Proceedings of the 12th ACM Multimedia Systems Conference (MMSys '21)* (pp. 241-247). Istanbul: MMSys. doi: 10.1145/3458305.3478443.
[7] Jin, J., Lim, Y., & Bang, C. (2023). Deep-learning-based system-scale diagnosis of a nuclear power plant with multiple infrared cameras. *Nuclear Engineering and Technology*, 55, 493-505. doi: 10.1016/j.net.2022.10.012.
[8] Kukhlenko, M.V. (2023). *Study of two-dimensional stationary problems of thermal conductivity in heat exchangers of nuclear power plants*. Kyiv: National Technical University of Ukraine "Igor Sikorsky Kyiv Polytechnic Institute".
[9] Levchenko, V. (2021). Improvement of thermometric control of Nuclear Power Plant equipment based on the study of the possibility of using intelligent sensors. *Scientific Herald of Uzhhorod University. Series "Physics"*, 49, 26-34.
[10] Li, J., Wang, P., Xiong, P., Cai, T., Yan, Z., Yang, L., Liu, J., Fan, H., & Liu, S. (2022). Practical stereo matching via cascaded recurrent network with adaptive correlation. *Computer Vision and Pattern Recognition*. doi: 10.48550/arXiv.2203.11483.
[11] Morgan, D., Pilania, G., Couet, A., Uberuaga, B.P., Sun, C., & Li, J. (2022). Machine learning in nuclear materials research. *Current Opinion in Solid State and Materials Science*, 26(2), 687-692. doi: 10.1016/j.cossms.2021.100975.
[12] Mosagutova, T.V. (2021). *Regularities of controlling the structure and material properties of pipelines under the conditions of NPP operation*. Kyiv: National Technical University of Ukraine "Igor Sikorsky Kyiv Polytechnic Institute".
[13] Meng, A.B., & Gräbe, P.J. (2021). RailEnV-PASMVS: A perfectly accurate, synthetic, path-traced dataset featuring a virtual railway environment for multi-view stereopsis training and reconstruction applications. *Data in Brief*, 38, article number 107411. doi: 10.1016/j.dib.2021.107411.
[14] Pylypchynets, I. (2022). Optimal scheme for stimulating photofission of shielded nuclear materials on the Microtron M-30: A combination of theoretical and experimental studies. *Scientific Herald of Uzhhorod University. Series "Physics"*, 52, 16-26.
[15] Qian, G., & Liu, J. (2023). Development of deep reinforcement learning-based fault diagnosis method for rotating machinery in nuclear power plants. *Progress in Nuclear Energy*, 152, 408-412. doi: 10.1016/j.pnucene.2022.104401.
[16] Schonberger, J.L., & Frahm, J.M. (2016). Structure-from-motion revisited. In *Proceedings of the IEEE Conference on Computer Vision and Pattern Recognition (CVPR)* (pp. 4104-4114). London: CVPR.
[17] Sun, Z., Zhang, C., Chen, J., Tang, P., & Yilmaz, A. (2020). Predictive nuclear power plant outage control through computer vision and data-driven simulation. *Progress in Nuclear Energy*, 127, article number 103448. doi: 10.1016/j.pnucene.2020.103448.
[18] Sunak, P.O., Siny, S.V., Melnyk, Yu.A., Ksonshkevych, L.M., Krantovska, O.M., & Orešković, M. (2020). Reconstruction of engineering structures and networks, landscape based on laser scanning technology. *Modern Technologies and Methods of Calculations in Construction*, 18, 114-119. doi: 10.36910/6775-2410-6208-2022-8(18)-16.
[19] Sytnyk, K. (2020). *Improvement of technology characteristics measuring accuracy and performance at atomic power station*. Zaporizhzhia: National University "Zaporizhzhia Polytechnic".
[20] Xu, Y., Cai, Y., & Song, L. (2023). Condition assessment of nuclear power plant equipment based on machine learning methods: A review. *Nuclear Technology*, 209(7), 929-962. doi: 10.1080/00295450.2023.2169042
[21] Yao, Y., Wang, J., Xie, M., Hu, L., & Wang, J. (2020). A new approach for fault diagnosis with full-scope simulator based on state information imaging in nuclear power plant. *Annals of Nuclear Energy*, 141, article number 107274. doi: 10.1016/j.anucene.2019.107274.
[22] Zelinskyi, A.O., & Lisovskyi, V.V. (2023). *Software development based on cloud architecture for analysis of machine images*. Ternopil: Ternopil Ivan Puluj National Technical University.
[23] Zhong, X., & Ban, H. (2022). Pre-trained network-based transfer learning: A small-sample machine learning approach to nuclear power plant classification problem. *Annals of Nuclear Energy*, 175, article number 109201. doi: 10.1016/j.anucene.2022.109201.

Дмитро Олександрович Белицький
Київський національний університет імені Тараса Шевченка
01033, вул. Володимирська, 60, м. Київ, Україна
https://orcid.org/0009-0004-1605-7658

Руслан Вікторович Єрмоленко
Кандидат фізико-математичних наук, доцент
Київський національний університет імені Тараса Шевченка
01033, вул. Володимирська, 60, м. Київ, Україна
https://orcid.org/0009-0000-0854-4668

Костянтин Григорович Петренко
Старший викладач
Київський національний університет імені Тараса Шевченка
01033, вул. Володимирська, 60, м. Київ, Україна
https://orcid.org/0009-0007-2972-4001

Ольга Петрівна Гогота
Кандидат фізико-математичних наук, молодший науковий співробітник
Київський національний університет імені Тараса Шевченка
01033, вул. Володимирська, 60, м. Київ, Україна
https://orcid.org/0000-0003-4108-7256

Застосування методів машинного навчання та комп'ютерного зору для визначення розмірів елементів обладнання АЕС в складних умовах вимірювання

Анотація. Актуальність цього дослідження визначається необхідністю вдосконалення процесів вимірювання розмірів об'єктів у важкодоступних умовах. В сучасному промисловому середовищі, де висока точність вимірювань є критичною для забезпечення безпеки та максимізації ефективності виробничих процесів, вивчення цієї теми стає актуальним в контексті стрімкого технологічного розвитку та підвищених вимог до якості виробництва. Мета цього дослідження – оцінити можливості використання сучасних методів комп'ютерного зору для вимірювання та реконструкції об'єктів у складних технічних умовах, таких як вигородка водо-водяного енергетичного реактора. Для досягнення цієї мети використовувалися методи 3D фотограмметрії, включаючи Depth from Stereo та Multi-View Stereo, а також методи структури з руху Structure from Motion. У результаті цього дослідження було виявлено, що сучасні методи комп'ютерного зору, зокрема методи машинного навчання, можуть бути успішно використані для вимірювання та реконструкції об'єктів у важкодоступних умовах. Дослідження показало, що точність вимірювань може досягати значень близьких до 1 мм в ідеальних умовах і при відстані 1.5 від вимірювального пристрою до об'єкту. При цьому метод Multi-View Stereo виявив більшу рівномірність просторового розподілу похибок порівняно з методом Depth from Stereo. На практиці, в умовах реальних фотографій, метод Multi-View Stereo виявився більш вимогливим до точного визначення положення камери. Завдяки своїй невибагливості до точних координат камер, метод Depth from Stereo продемонстрував кращі результати, показуючи меншу похибку у вимірюваннях. Дослідження також вказало на можливість використання запропонованого методу для розрізнення коливань у висоті поверхні об'єкта, що є важливим для подальших застосувань у сфері обслуговування реактора та інших сферах промисловості. Практична цінність цього дослідження полягає в розробці та валідації методів вимірювання та реконструкції об'єктів в умовах, коли традиційні методи стають обмеженими або недоцільними

Ключові слова: реактор водо-водяного енергетичного типу; нейтронні поля; фізичні властивості; бінокулярна система; машинне навчання

Machinery & Energetics
Vol. 14, No. 4. 2023

Journal homepage:
https://technicalscience.com.ua/en

UDC 621.3.067
DOI: 10.31548/machinery/4.2023.54

Roman Chuienko

PhD in Technical Sciences, Associate Professor
National University of Life and Environmental Sciences of Ukraine
03041, 15 Heroiv Oborony Str., Kyiv, Ukraine
https://orcid.org/0000-0002-9339-9764

Viktor Kaplun*

Doctor of Technical Sciences, Professor
National University of Life and Environmental Sciences of Ukraine
03041, 15 Heroiv Oborony Str., Kyiv, Ukraine
https://orcid.org/0000-0001-7040-9344

Svitlana Makarevych

PhD in Technical Sciences, Associate Professor
National University of Life and Environmental Sciences of Ukraine
03041, 15 Heroiv Oborony Str., Kyiv, Ukraine
https://orcid.org/0000-0002-9601-5156

Oleksandr Sytnyk

Postgraduate Student
National University of Life and Environmental Sciences of Ukraine
03041, 15 Heroiv Oborony Str., Kyiv, Ukraine
https://orcid.org/0009-0000-8108-4944

Asynchronous generator replacement scheme with internal capacitive reactive power compensation

Abstract. The relevance of using compensated induction machines in the generator mode of autonomous power supply systems is determined by their ability to provide a stable and reliable power supply even in the absence of an external grid. The research aims to develop a procedure for determining the characteristics of an equivalent circuit of compensated induction generators that considers the mutual influence between the main and additional phase windings of the armature. The theory of an idealised induction machine with the representation of electromechanical energy conversion processes and basic physical parameters in the form of equations of electrical equilibrium and drive motion was used to obtain the calculated characteristics of the generator's operating modes of this class. The generalised system of differential equations made it possible to calculate dynamic and static processes for symmetrical and asymmetrical modes at given machine parameters under different methods of excitation and voltage stabilisation under variable load. For the practical implementation of modelling the parameters of an induction generator, the equations of electrical equilibrium of the stator and rotor circuits for the symmetrical steady-state mode are used, which is a special case of the generalised mathematical model of the machine for both transient and steady-state processes with constant parameters of the substitution scheme. Consideration of the structural and functional features of compensated induction generators was made possible by using a mathematical model with the armature winding divided into two coaxial or spatially offset half-windings. In this case, the number of calculation equations doubles. The use of an autotransformer scheme for switching on the stator phase half-windings to capacitors required the introduction of an additional differential equation

Article's History: Received: 02.08.2023; Revised: 01.11.2023; Accepted: 22.11.2023.

Suggested Citation:
Chuienko, R., Kaplun, V., Makarevych, S., & Sytnyk, O. (2023). Asynchronous generator replacement scheme with internal capacitive reactive power compensation. *Machinery & Energetics,* 14(4), 54-63. doi: 10.31548/machinery/4.2023.54.

*Corresponding author

for the electrical equilibrium of the stator phases. This made it possible to substantiate the values of active and inductive resistances used in the replacement circuit of an induction generator with internal capacitive reactive power compensation. The mutual inductive coupling of the main and additional half-windings of the generator stator phase windings due to both the operating magnetic flux and the magnetic fluxes of dissipation was considered. The practical significance of the obtained results is to increase the efficiency and stability of the power supply, which helps to reduce losses and improve the operation of electric power systems

Keywords: asynchronous machine; internal capacitive compensation; reactive power; active resistance; inductive resistance; mutually inductive coupling

INTRODUCTION

The study and calculation of the characteristics of induction machines (IMs) is an important task, as it helps to develop and improve the electrical industry, contributing to the conservation of energy resources and the creation of more stable and efficient power supply systems. With the development of new materials and production technologies, the design of induction machines needs to be adapted to new designs and functional properties. This helps to create more powerful, efficient, and stable machines. C.A.C. Wengerkievicz *et al.* (2017), the characteristics of an induction machine are calculated using a system of design equations for the electrical equilibrium of the stator and rotor windings, compiled according to Kirchhoff's second law. This system of equations is based on the generally accepted assumptions of the classical theory of electric machines at constant values of stator and rotor resistances and is a special case of the general mathematical model of an induction machine for both steady-state and transient operating modes.

To calculate the characteristics of compensated induction generators (CIG), S.V. Kumar *et al.* (2023) used a mathematical model that considers its new design and functional properties. The manufacture of stator phase windings consisting of two parts that are coaxially or spatially offset by an arbitrary angle necessitates a twofold increase in the electrical equilibrium equations. In addition, H. Terzioğlu & M. Selek (2017) described that the use of an autotransformer scheme for switching on additional stator phase windings to capacitors leads to the need to write an additional differential equation of electrical equilibrium of the stator phases.

An important problem that arises when using a compensated induction generator (CIG) in autonomous power supply systems is voltage stabilisation under variable load. V.I. Mishin *et al.* (2022) established the quantitative and qualitative dependencies of an induction machine analytically, which was carried out considering the classical theory of an idealised induction machine, where the main physical parameters and electromechanical energy conversion processes are represented in the form of equations of electrical equilibrium and drive motion. The presented generalised equation system in differential form in M. Popp *et al.* (2017) makes it possible to calculate dynamic and static processes for symmetrical and asymmetrical modes under given machine parameters and excitation conditions. Physical processes and features of CIG design solutions, caused by the presence of additional spatially displaced electromagnetic circuits with capacitance, complicate the mathematical model and increase the order of the system of differential equations. According to M.M. Tezcan *et al.* (2018), this requires the adoption of additional special conditions and approaches for calculating physical processes in machines of this class.

It is commonly used to calculate the characteristics of induction machines in the L-shaped substitution scheme and to bring them to the equivalent parameters of the T-shaped scheme. The L-shaped scheme is simple, and the magnetisation current is assumed to be constant, independent of the AM load. However, to ensure greater accuracy in reflecting physical processes in an induction machine, the T-shaped substitution scheme should be preferred in our case. According to M. Liu *et al.* (2023), the design of a compensated induction generator differs from the basic asynchronous machine, so the parameters of the replacement scheme of the basic asynchronous machine cannot be used to calculate its characteristics.

O.M. Popovych & M.O. Smahliuk (2014) considered a variant of an induction machine with a compensation winding. The use of such a winding when the machine operates in motor mode allows for controlling its energy efficiency. However, the compensation winding carries only reactive power and does not carry an active load. The study proposes variants of the stator windings of a compensated asynchronous generator, where both the main and additional stator phase windings are carriers of both reactive and active powers.

The study aims to develop a methodology for calculating the parameters of the replacement circuit of compensated asynchronous generators, considering their design features and the mutually inductive connection between the main and additional phase windings of the armature.

MATERIALS AND METHODS

Experimental studies of the compensated asynchronous generator were carried out at the Department of Electrical Engineering, Electromechanics and Electrical Technologies of the Educational and Research Institute of Energy, Automation and Energy Saving of the National University of Life and Environmental Sciences of Ukraine. A Metrix-3252 digital oscilloscope (manufactured by Chauvin Arnoux, France) was used to obtain the waveforms. The following methods were used to substantiate the parameters of the compensated asynchronous generator replacement circuit, considering its design features, and to verify the results obtained: analytical using the theory of a generalised electromechanical energy converter; mathematical and electrical modelling; and experimental. A compensated asynchronous generator manufactured on a serial asynchronous motor AIR71V2 (АИР71В2, Ukraine) was selected as the object of computational and experimental studies.

Studies of A.E. Kravchik *et al.* (1982), J. Rolek & G. Utrata (2018), and A.R. Helonde & M.M. Mankar (2019), which contain information on the parameters of induction machines, were used. At the same time, either an L-shaped replacement scheme (Fig. 1a) or a T-shaped replacement scheme for an induction machine (Fig. 1b) was used. For the L-shaped substitution scheme, the active resistance of the stator phase winding $R_1^/$ and the inductive resistance of the stator phase winding $X_1^/$, as well as the active resistance of the rotor phase winding $R_2^{//}$ and the inductive resistance of the rotor phase winding $X_2^{//}$ were considered. In addition, the inductive resistance due to the mutually inductive coupling between the armature and rotor phase windings in the case of their axes coincidence and the total main inductive resistance of the armature phase winding X_m at the rated load of the combined induction machine was considered.

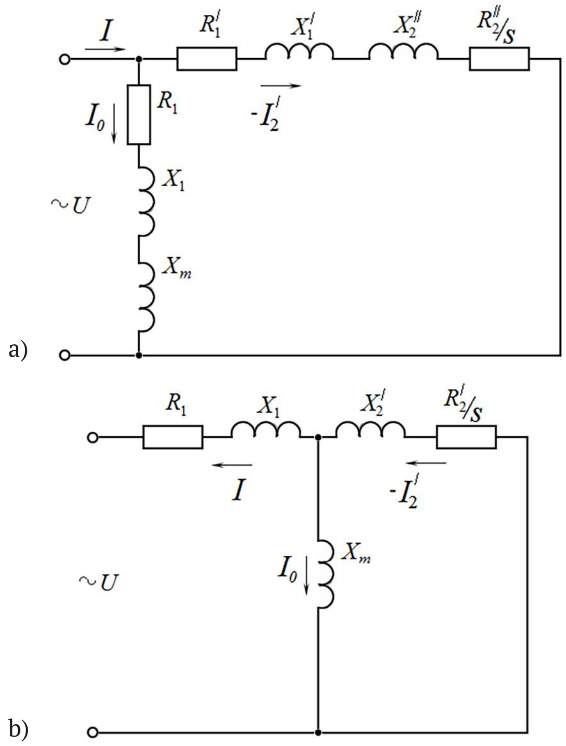

Figure 1. Asynchronous generator replacement scheme
Note: a – L-shaped; b - T-shaped; $R_1^/$ – active resistance of the stator phase winding, $X_1^/$ – inductive resistance of the stator phase winding, $R_1^{//}$ – active resistance of the rotor phase winding, and $X_1^{//}$ inductive resistance of the rotor phase winding, X_m – main inductive resistance of the armature phase winding, *s* – sliding
Source: R. Chuenko & O. Kryvoshey (2014)

To calculate the characteristics of the AG under a steady-state symmetrical load, a T-shaped substitution scheme was used (Fig. 1b), which describes the physical processes occurring in the generator with high accuracy (Mishin *et al.*, 2022). The transition from the active and inductive resistances of the L-shaped substitution scheme to the resistances of the T-shaped substitution scheme was carried out using the following formulas (Mishin *et al.*, 2011):

$$X_1 = \frac{2X_1^/ X_m}{X_m+\sqrt{{X_m}^2+4X_1^/ X_m}} R_1 = R_1^/ \frac{X_1}{X_1^/};\ R_2 = \frac{R_2^{//}}{c^2};$$
$$X_2 = \frac{X_2^{//}}{c^2},\ c \approx 1+\frac{X_1}{X_m}\dot{I}_2 = c\cdot \dot{I}_2'. \tag{1}$$

To express parameters in a system of relative units R_1 (*r.u.*), X_1 (*r.u.*), and R_2 (*r.u.*) it is necessary to have the values of the corresponding resistances in named units and use the following formulas:

$$R_1(r.u.) = \frac{R_1(Ohm)}{Z_n(Ohm)}A;\ X_1(r.u.) = \frac{X_1(Ohm)}{Z_n(Ohm)};$$
$$R_2(r.u.) = \frac{R_2(Ohm)}{Z_n(Ohm)} \dots, \tag{2}$$

where $Z_n = \frac{U_n}{I_n}$ – total resistance of the armature phase winding of an induction machine at rated mode operation in case of star connection of the armature winding, Ohm; $I_n = \frac{P_n}{3\cdot U_n \eta_n \cos\phi_n}$ – current of the armature phase winding at rated operation, A; U_n – phase voltage at rated load, B, η_n – asynchronous machine efficiency, $\cos_{\varphi n}$ – asynchronous machine power factor, P_n – rated asynchronous power output.

RESULTS AND DISCUSSION

Unlike a basic induction machine, each phase winding of a compensated induction generator armature consists of two half-windings: the main winding and the auxiliary winding. The main and auxiliary windings can be connected either in series (Fig. 2a) or in parallel (Fig. 2b).

Depending on the connection scheme of the main and auxiliary windings, the number of turns of the main and auxiliary windings will also change, as well as the possible voltage on the armature terminals of the compensated generator. Accordingly, to conduct numerical studies of the characteristics of the CIG, the corresponding parameters of its substitution scheme should be used. The phase winding of the armature of the base machine contains *w* turns. In the case of using internal capacitive reactive power compensation with a series connection of the main and auxiliary windings, the winding of the base machine is divided into two equal parts with the number of turns *w*/2 each, which are switched on in series. In this case, the resistance of the main and auxiliary windings of the generator armature phases will be equal to $R_1/2$. The inductive resistance due to the presence of magnetic fluxes of the main and auxiliary windings will also be halved compared to the basic machine – $X_1/2$. Similarly, the total main resistance of the main and auxiliary windings of the armature phase of the CIG – $X_m/2$ – will be halved. In this case, the phase replacement scheme of an induction generator with a series connection of half-windings is as shown in Figure 3a.

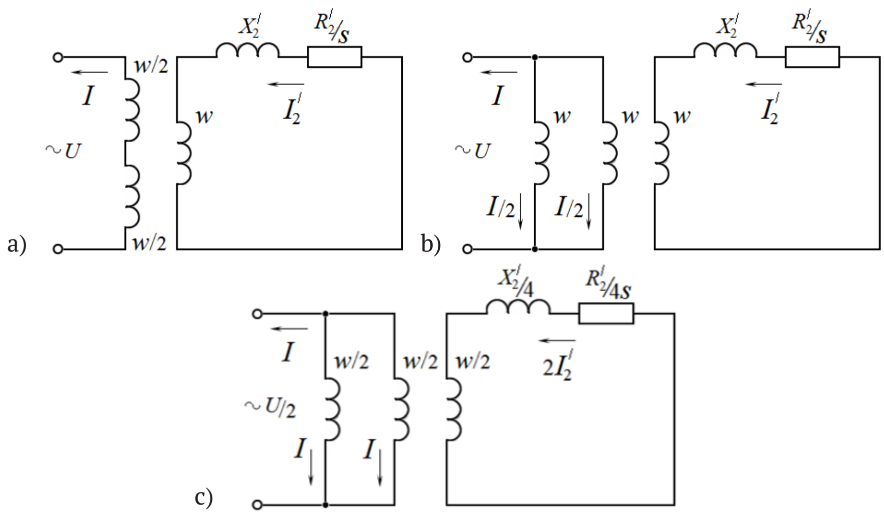

Figure 2. Schematic diagrams of the phase winding of the armature CIG

Note: a – when the main and auxiliary windings of the armature phase are switched on sequentially; b – when the main and auxiliary windings are switched on in parallel; c – for switching the winding of the base machine to a circuit with two parallel windings, where R_1, R_2 – resistance of the main and auxiliary windings of the generator armature phases, X_1, X_2 – inductive resistance of the main and auxiliary windings, w – number of coils, S – sliding, X_m – main resistance of the main and auxiliary windings of the CIG armature phase

Source: compiled by the authors based on R. Chuenko & O. Kryvoshey (2014)

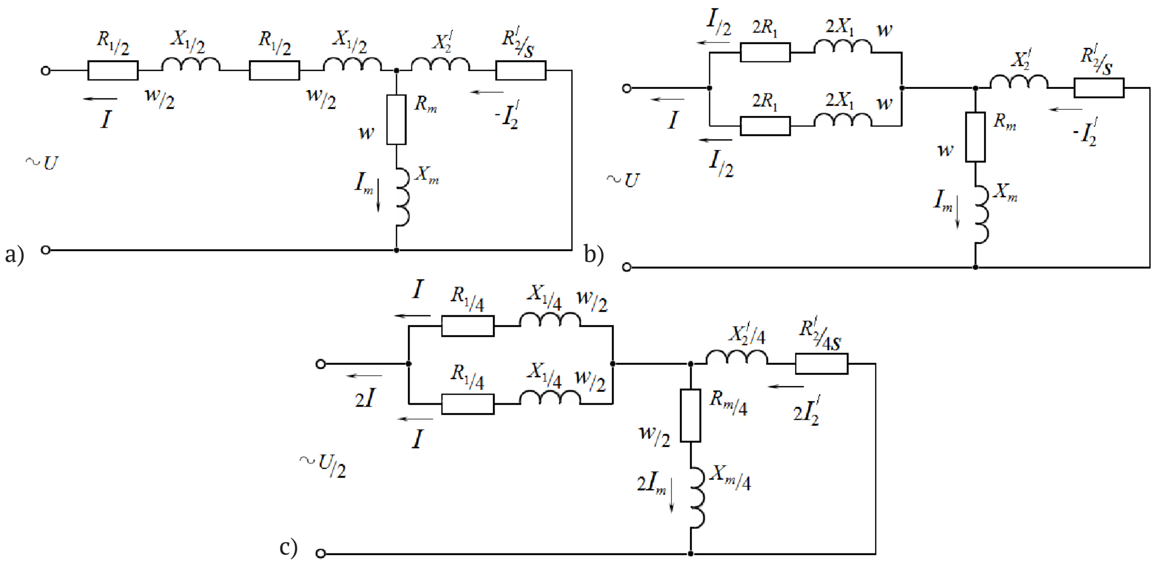

Figure 3. Phase replacement schemes for compensated induction generators

Note: a – the main and additional windings of the armature phase are switched on in series; b – the main and auxiliary windings of the armature phase are switched on in parallel; c – for switching the series winding to two parallel windings, where R_1, R_2 – resistance of the main and auxiliary windings of the generator armature phases, X_1, X_2 – inductive resistance of the main and auxiliary windings, w – number of coils, S – sliding, X_m – main resistance of the main and auxiliary windings of the CIG armature phase

Source: compiled by the authors

The total inductive reactance of the phase winding of an induction machine armature consists of its inductive reactance, the value of which depends directly on the square of the number of windings, and the inductive reactance due to the mutual inductive coupling with neighbouring magnetically coupled windings, which depends on the product of the number of turns of these windings. At the same time, the mutually inductive coupling between the windings by magnetic fluxes is not considered. When the main and auxiliary windings of the armature phases of the CIG are connected in series, their inductive reactance will depend on w^2 and will be determined by the inductive dissipation resistance:

$$X_{1i} = \frac{X_1}{4} \equiv \left(\frac{w}{2}\right)^2, \quad (3)$$

and the main resistance:

$$X_{mc} = \frac{X_m}{4} \equiv \left(\frac{w}{2}\right)^2. \quad (4)$$

The discrepancy between the total resistance of consecutive half-windings $\frac{X_1}{2}$, $\frac{X_m}{2}$ and their values $X_{1c} = \frac{X_1}{4}$, $X_{mc} = \frac{X_m}{4}$ is caused by the mutually inductive connection between the main and auxiliary windings of the armature phases of the CIG as in terms of operating magnetic flux, and terms of magnetic flux dissipation. As a result, the total inductive reactances of the main and auxiliary windings increase by $X_{1b} = \frac{X_1}{4} \equiv \left(\frac{w}{2}\right)^2$ due to the action of the magnetic flux scattering and on the value of $X_{mb} = \frac{X_m}{4} \equiv \left(\frac{w}{2}\right)^2$ due to the action of the main magnetic flux.

Thus, the inductive dissipation resistance of the main and auxiliary windings of the phase winding of the armature of the CIG, which are located without spatial displacement of their axes, will be determined by the following formula: $\frac{X_1}{2} = X_{1i} + X_{1b} = \frac{X_1}{4} + \frac{X_1}{4}$. The main inductive resistance is equal to $\frac{X_m}{2} = X_{mi} + X_{mb} = \frac{X_m}{4} + \frac{X_m}{4}$, and the mutual induction resistance of the stator half-windings with the rotor winding, respectively – $\frac{X_m}{2} \equiv \frac{w}{2} \cdot w$.

In a basic induction machine, there is a mutually inductive connection in terms of operating magnetic flux between all armature and rotor windings of different phases (Rolek & Utrata, 2017; Tezcan *et al.*, 2018). In its turn, the magnetic flux is closed only between the armature half-windings of the same phase. Considering a CIG with sequential switching on of the main and auxiliary windings, which do not have spatial displacement of the axes, the mutually inductive coupling by the magnetic flux should be considered as a component of the inductive resistance $X_{1b} = \frac{X_1}{4}$. If there is a spatial offset between the axes of the main and auxiliary windings by an angle θ, then the inductive resistance component due to the magnetic flux scattering will be equal to $\frac{X_1}{4} \cdot \cos\theta$.

In the case of using the variant of internal capacitive reactive power compensation with a parallel connection of the main and additional windings of the generator armature phase (Fig. 2b), each of these windings will be under the same voltage. Accordingly, if the base machine had the armature winding parameters R_1, X_1, X_m, then the resistances of each of the two parallel branches of the phase winding of the CIG will be equal to $2R_1$, $2X_1$, $2X_m$, respectively, and at the total rated current I_n, the rated current of the main and auxiliary windings will be half the total rated current – $I_n/2$.

If the main and auxiliary windings of the armature phase of the CIG have the same number of turns as the armature phase winding of the base machine w, then the inherent inductive resistance of the scattering and the main inductive resistance, as well as the inductive resistance due to the mutually inductive coupling by the scattering magnetic flux and the operating magnetic flux, will be equal to the corresponding inductive resistances of the base machine winding $X_{1v} = X_{1b} = X_1$, $X_{mv} = X_{mb} = X_m$. In this case, the inductive resistances of the main and additional windings will be $X_{1v} + X_{1b} = 2X_1$, $X_{mv} + X_{mb} = 2X_m$. The rotor parameters remain unchanged R_2, X_2, X_m (Fig. 3b)

In practice, it may be necessary to change the switch scheme of the main and auxiliary windings of the armature phase of an induction generator from series to parallel (Fig. 2c). In this case, the number of turns of the generator armature phase winding will remain unchanged, and the main and auxiliary windings will have $w/2$ coils each. For the generator energy characteristics to remain unchanged under different schemes of switching on the main and auxiliary windings (Fig. 2b) and (Fig. 2c), it is necessary to reduce the generator output voltage ($U/2$) by half and to increase the rated armature current and the rated rotor current by 2 times. The inductive dissipation resistance of the main and additional armature windings will be equal to $\frac{X_1}{2} = \frac{X_{1c}}{4} + \frac{X_{1b}}{4}$, standard resistance $\frac{X_m}{2} = \frac{X_{1c}}{4} + \frac{X_{mb}}{4}$, and the general parameters of the entire stator winding are respectively $\frac{X_1}{4}, \frac{X_m}{4}, \frac{R_1}{4}$. When switching from a real CIG to a reduced CIG, the number of turns of the rotor winding must be reduced by a factor of 2. Accordingly, the inductive dissipation resistance of the rotor of the combined CIG will be equal to $X_2^{/} = \frac{X_2}{4}$. In turn, the active rotor impedance of the combined gas turbine will also be halved $R_2{}^{/} = \frac{R_2}{4}$, as its current has doubled (Fig. 3c).

When a compensated induction machine operates in the motor mode, it consumes active and reactive power from the power supply network and converts electrical energy into mechanical energy (Fig. 4a). When operating in the generator mode as part of an autonomous power supply system, the compensated induction machine itself is a source of active and reactive power for the consumer and converts mechanical energy into electrical energy (Fig. 4b):

$$\begin{aligned}
&1)\ \dot{U}_1 = \dot{E}_1 - \dot{I}_1 z_1 - jx_1 \cos\Theta \cdot \dot{I}_\Delta = \dot{I} \cdot Z,\\
&2)\ \dot{U}_1 = \dot{U}_\Delta - \dot{U}_{c\Delta} = \dot{E}_\Delta - \dot{I}_\Delta z_\Delta - jx_1 \cos\Theta \cdot \dot{I}_1 + jx_{c\Delta} \cdot I_{c\Delta},\\
&3)\ \dot{U}_\Delta = \dot{E}_\Delta - \dot{I}_\Delta z_\Delta - jx_1 \cos\Theta \cdot \dot{I}_1 = -jx_{CK} \cdot \dot{I}_{CK},\\
&4)\ 0 = \dot{E}_2 - \dot{I}_2 z_2.
\end{aligned} \quad (5)$$

The design equations of the CIG phase when operating on a static load in a steady-state process of the symmetrical mode by the schematic diagram of its phase (Fig. 5) are as follows (Mishin *et al.*, 2011):

One of the most common characteristic variants of an autonomous power supply system is the operation of an autonomous generator for an induction motor. In particular, the external characteristics of a compensated induction generator were calculated, from which an induction motor AIR71V2 with a capacity of 0.75 kW is started and powered. The values of the compensating capacitances were equal: external capacity $C = 30$ μF, internal capacitance $C_\Delta = 28$ μF and additional internal capacity $C_k = 10$ μF.

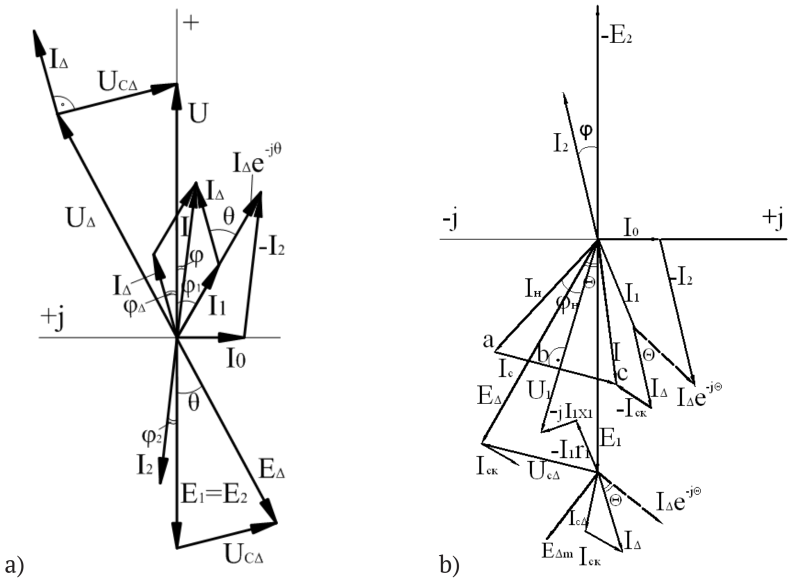

Figure 4. Vector diagrams of a compensated induction motor (a) and a compensated induction generator (b)

Note: U – power supply voltage; U_Δ – voltage on the additional stator winding; $U_{C\Delta}$ – voltage on the internal capacity; E_1 – electromotive force of the main stator winding; E_Δ – electromotive force of the additional stator winding; E_2 – electromotive force of the rotor winding; I – stator current of an induction machine; Z_l – load resistance; I_l – load current; I_C – external capacitance current; I_{Ck} – current of additional internal capacitance; I – stator current of a compensated induction generator; $I_{C\Delta}$ – internal capacitance current; I_Δ – current of the additional stator winding; I_1 – stator main winding current; I_0 – magnetising current of an induction machine; θ – angle of spatial displacement of the main and auxiliary stator phase windings; I'_2 – rotor current of an induction machine; r_1 – active stator resistance of an induction machine; X_1 – inductive resistance of the stator of an induction machine; φ – angle between the stator current and voltage vectors at the stator of an induction machine; φ_1 – angle between the voltage vectors on the stator and the current of the main stator winding of the induction machine; φ_Δ – angle between the voltage vectors on the stator and the current of the additional stator winding of an induction machine; φ_2 – angle between the rotor electromotive force vectors and the rotor current of an induction machine;

Source: compiled by the authors

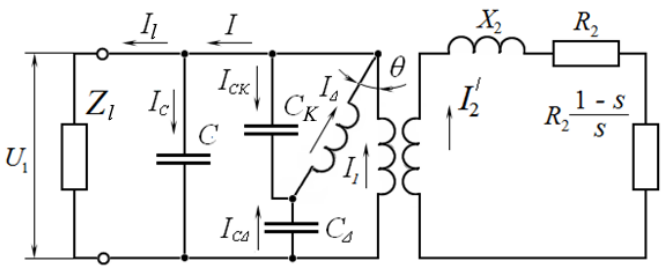

Figure 5. Wiring diagram of CIG phases

Note: U_1 – load voltage; Z_l – load resistance; I_l – load current; C – external capacity; I_C –external capacity current; C_k – additional internal capacity; I_{Ck} – additional internal capacity current; I – stator current of a compensated induction generator; C_Δ – internal capacity; $I_{C\Delta}$ – internal capacity current; I_Δ – additional stator winding current; I_1 – stator main winding current; θ – angle of spatial displacement of the main and auxiliary stator phase windings; I'_2 – generator rotor current; X_2 – inductive resistance of the rotor; R_2 – active rotor resistance; s – sliding

Source: compiled by the authors based on V.I. Mishin *et al.* (2022)

The external characteristic of the compensated induction generator obtained by calculation when operating in conjunction with an induction motor (Fig. 6a), where the voltage drops to 165 V, is confirmed by the experimental oscillogram (Fig. 6b). It was found that the voltage recovery (Fig. 6b) after starting the motor from a compensated induction generator occurs within 0.5 s. The stator current (Fig. 7) of the compensated induction generator when the motor is powered in a steady state is 2 A.

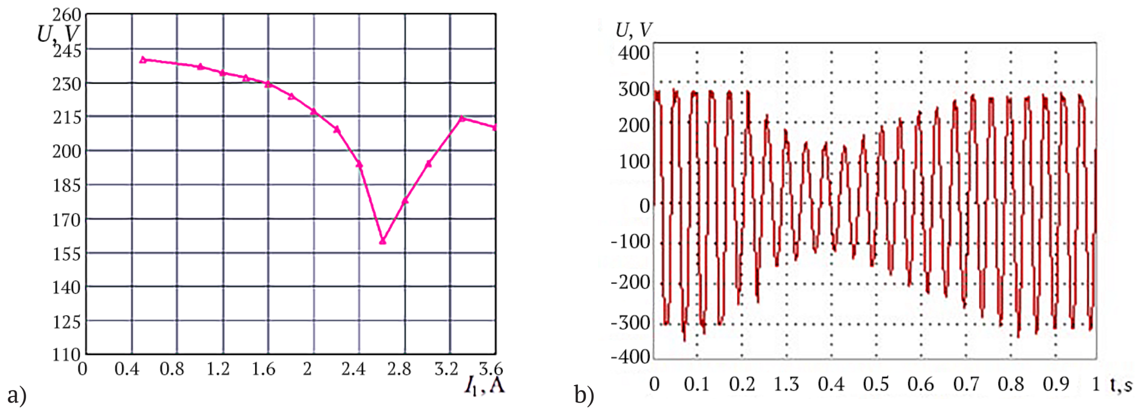

Figure 6. Calculated external compensated asynchronous generator in a joint operation with an induction motor (a) and experimental voltage waveform on the stator of a compensated asynchronous generator (b)
Source: compiled by the authors

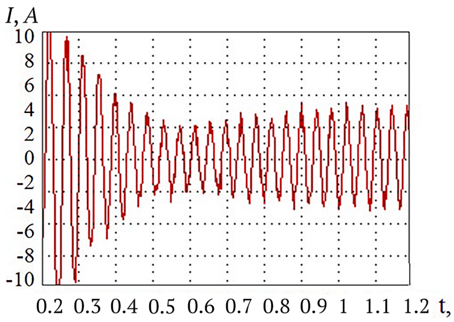

Figure 7. Oscillogram of the stator current of a compensated induction generator when supplying an induction motor
Source: compiled by the authors

The data obtained as a result of calculating the characteristics of compensated induction generators are confirmed with sufficient accuracy by experimental studies. In particular, Figure 8 shows the external characteristics of the compensated induction generator when using the external capacitance C and the internal capacitance C_Δ (curves 1) and when using the external capacitance C, the internal capacitance C_Δ, and the additional internal capacitance C_k (curves 2), based on the calculated and experimental data.

The system of equations for the electrical equilibrium of the stator and rotor circuits of a CIG (Al-Jufout *et al.*, 2018) used the parameters of the substitution scheme (r_1, x_1, r_2, x_2) calculated according to the above methodology. The introduced parameters were the capacitive resistances x_c, $x_{c\Delta}$, x_{ck} and load resistance $Z_n = k_n Z_{nb}$ at $Z_{nb} = r_{nb} + jx_{nb} = 80 + j60 = 100i^{j\varphi}$ Ohm. $Z_n = var$ with a variable load factor k_n, the resistance of the main and auxiliary stator windings was assumed to be the same $z_1 = r_1 + jx_1 = z_\Delta$.

The use of internal capacitive reactive power compensation to improve the characteristics of an induction generator causes changes in the basic electrical circuit of its stator winding. Accordingly, the active and inductive resistances of the stator winding of the compensated induction generator change compared to the basic induction generator, which should be considered in numerical studies.

The parameters of the L-shaped and T-shaped replacement schemes for an induction machine can be found in reference books or the manufacturer's documentation. However, the use of these parameters without considering the operating mode and conditions of the induction machine may be unacceptable or lead to unacceptably large errors in the calculations.

In particular, E.R. Ferrucho-Alvarez *et al.* (2021) considered an induction welding generator with valve excitation. While an L-shaped substitution scheme is used for a conventional induction generator operating in voltage stabilisation mode, it is unacceptable for an induction generator with valve excitation operating on a welding arc. In this case, as in the case of a compensated induction generator, a T-shaped substitution scheme for the basic induction generator is used. The distinctive feature is that the valve excitation system in the replacement circuit is represented by an additional variable capacitive resistance.

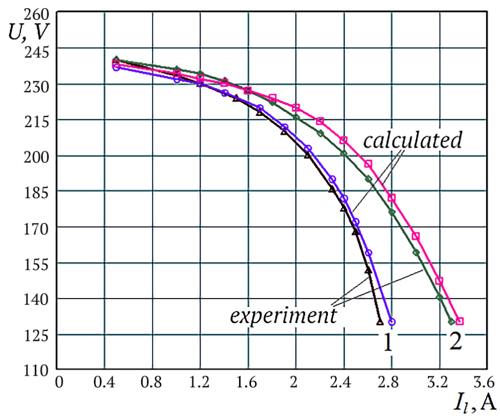

Figure 5. External characteristics of a compensated asynchronous generator obtained by calculation and experiment
Note: curve 1 – when using an external container C and internal container C_Δ; curve 2 – and when using an external container C, internal container C_Δ and additional internal container C_k
Source: compiled by the authors

L.A. Lopes & R.G. Almeida (2006), I. Boldea & S.A. Nasar (2009) noted that the T-shaped replacement scheme for an induction machine is also used to calculate the characteristics of an induction motor with a squirrel-cage rotor that has rotor eccentricity or rotor winding defects. In this case, the T-shaped substitution scheme is supplemented with additional elements that characterise the increase in losses in the damaged motor. The obtained characteristics are used to monitor and predict the condition of motors during their operation, as well as for their diagnosis.

If an induction machine is operated in the motor mode using various speed control devices, the parameters of the L-shaped and T-shaped substitution schemes change, as shown in L. Mazurenko *et al.* (2011), O.M. Popovych & M.O. Smahliuk (2014). This should be considered when calculating the characteristics of an induction motor with a certain method of speed control.

A single-phase substitution scheme for a three-phase induction machine is used to calculate its characteristics in steady-state symmetrical modes with sinusoidal voltages. Depending on the task at hand, the substitution scheme can consider steel losses in the stator cores and rotor, the presence of a double cage in the rotor, changes in machine parameters, such as the surface effect and saturation of the stator and rotor cores. L. Mazurenko *et al.* (2011), and J. Rolek & G. Utrata (2017) considered methods for determining the parameters of an induction machine substitution scheme by alternative methods other than the standard ones (based on the data of no-load and short-circuit experiments). The developed methods for determining the parameters of the induction machine substitution scheme can be used to refine the parameters of the substitution scheme of a compensated induction generator when calculating its characteristics in transient modes. M. Vazifehdan *et al.* (2020) described in detail a complex and high-level control strategy used in the field of electrical engineering and industrial automation. It combines several control methodologies to achieve accurate and efficient control of induction machines, particularly in situations where sensor data is limited or unavailable. They explored sliding control, which helps to make the system state converge to a given sliding surface. This is especially useful in systems with uncertainty and external influences. In this context, sliding control helps maintain precise control of an induction machine.

The determination of the parameters of the induction machine replacement scheme based on the data of no-load and short-circuit experiments carried out using induction machine models implemented in MATAB/Simulink and ETAR environments is the subject of the work by M. Popp *et al.* (2017) Using MATLAB/Simulink models, S. Al-Jufout *et al.* (2018) also proposed a two-step optimisation of the parameters of the induction machine replacement scheme, which ensures the minimum error of the results obtained. The above approaches can also be used to determine the parameters of a compensated induction generator replacement scheme, but for this purpose, it is necessary to develop appropriate MATLAB/Simulink or ETAR models.

CONCLUSIONS

The basic electrical circuit of the stator winding of a compensated induction generator differs from the stator winding circuit of a basic induction machine. It has been shown that the main and additional windings of the stator phase windings of a compensated induction generator can be connected in series or parallel, and their axes can be shifted in space by an arbitrary angle. As a result, the degree of mutual inductive coupling between the windings in terms of operating magnetic flux and dissipation magnetic flux changes. Accordingly, to conduct correct numerical studies of the characteristics of compensated induction generators, the appropriate parameters of the substitution scheme should be used. It has been established that the active and inductive resistances of the stator and rotor windings of a compensated induction generator should be determined by recalculating the parameters of the basic induction machine according to the developed methodology, depending on the connection scheme of the stator phase windings and the generator output voltage. In particular, when the main and auxiliary stator windings of a compensated induction generator are connected in series, their active and inductive impedances must be halved compared to the basic induction machine. If the main and auxiliary stator windings are connected in parallel, the corresponding resistances must be doubled compared to the basic induction machine. The parameters of the rotor winding and the magnetising winding remain unchanged. In the case of using the scheme of parallel connection of the stator phase windings at a halved voltage at the output of the compensated induction generator, the active and inductive resistances of the main and additional stator phase windings, as well as the rotor winding and the magnetisation winding, should be reduced by a factor of 4 compared to the parameters of the basic induction machine. The calculated characteristics of the compensated induction generator, obtained using the appropriately calculated parameters of the substitution scheme, are confirmed with sufficient accuracy by experimental data.

Further research will aim to improve the energy efficiency of induction generators with internal capacitive reactive power compensation as part of autonomous power supply systems. They will focus on analysing the stability and reliability of an autonomous power supply system with a compensated induction generator under different operating conditions and variable load parameters. Particular attention will be paid to the justification of the algorithm for changing the compensating capacities of the generator and to the study of the possibilities of using new switching devices for their switching.

ACKNOWLEDGEMENTS

The work was supported by the National Research Foundation of Ukraine in the competition “Science for the Reconstruction of Ukraine in the War and Postwar Periods”, grant No. 202/0129.

CONFLICT OF INTEREST

None.

REFERENCES

[1] Al-Jufout, S., Al-rousan, W., & Wang, C. (2018). Optimization of induction motor equivalent circuit parameter estimation based on manufacturer's data. *Energies*, 11(7), article number 1792. doi: 10.3390/en11071792.

[2] Boldea, I., & Nasar, S.A. (2009). *The induction machines design handbook* (2nd ed.). Boca Raton: CRC Press. doi: 10.1201/9781315222592.

[3] Chuenko, R.M., & Kryvoshey, O.A. (2014). Determination of the parameters of the replacement scheme of the compensated asynchronous motor. *Scientific Bulletin of the National University Environment and Science of Ukraine. Series: Agricultural Machinery and Energy*, 194(3), 265-270.

[4] Ferrucho-Alvarez, E.R., Martinez-Herrera, A.L., Cabal-Yepez, E., Rodriguez-Donate, C., Lopez-Ramirez, M., & Mata-Chavez, R.I. (2021). Broken rotor bar detection in induction motors through contrast estimation. *Sensors*, 21, article number 7446. doi: 10.3390/s21227446.

[5] Helonde, A.R., & Mankar, M.M. (2019). Identifying three phase induction motor equivalent circuit parameters from nameplate data by different analytical methods. *International Journal of Trend in Scientific Research and Development*, 3(3), 642-645. doi: 10.31142/ijtsrd22934.

[6] Kravchik, A.E., Shlaf, M.M., Afonin, V.I., & Sobolenskaya, E.A. (1982). *Asynchronous motors series 4A*. moscow: Energoizdat.

[7] Kumar, S.V., Kathirvel, C., & Jude, P.S.V. (2023). A new method of sensor-less speed vector control of asynchronous motor drive in model-reference adaptive system. In *Smart grids for smart cities* (vol. 2, pp. 127-141). Hoboken: Wiley.

[8] Liu, M., Chen, L., Sheng, X., Yang, Y., Yu, F., Li, Y., Yuan, X., Li, Y., Wang, Q., & Ma, Q. (2023). Dynamic simulation of life cycle environmental benefits of remanufacturing asynchronous motors to permanent magnet synchronous motors. *Journal of Cleaner Production*, 426, article number 138932. doi: 10.1016/j.jclepro.2023.138932.

[9] Lopes, L.A., & Almeida, R.G. (2006). Wind-driven self-excited induction generator with voltage and frequency regulated by a reduced-rating voltage source inverter. *IEEE Transactions on Energy Conversion*, 21(2), 297-304. doi: 10.1109/TEC.2006.874244.

[10] Mazurenko, L.I., Romanenko, V.I., & Jura, O.V. (2011). Calculation of operating characteristics of an autonomous welding asynchronous generator with valve excitation according to the substitution scheme. *Proceedings of the Institute of Electrodynamics of the National Academy of Sciences of Ukraine: Collection of Scientific Papers*, 28, 64-69.

[11] Mishin, V.I., Kaplun, V.V., & Makarevich, S.S. (2011). Self-contained induction generator with internal capacitive compensation. *Russian Electrical Engineering*, 82, 138-143. doi: 10.3103/S1068371211030060.

[12] Mishin, V.I., Lut, M.T., Makarevych, S.S., & Chuienko, R.M. (2022). *Asynchronous electric machines* (2nd ed.) Kyiv: Komprint Publishing House.

[13] Popovych, O.M., & Smahliuk, M.O. (2014). Research and design of induction motors with internal compensation using simulation and structural modeling. *Bulletin of the National Technical University of Ukraine "Kyiv Polytechnic Institute". Series "Mining"*, 25, 138-144.

[14] Popp, M., Mathis, W., Korolova, O., & Ponick, B. (2017). Modeling and simulation of electrical machines within a CCM framework. In *2017 IEEE International Electric Machines and Drives Conference (IEMDC)* (pp. 1-8). doi: 10.1109/IEMDC.2017.8002174.

[15] Rolek, J., & Utrata, G. (2017). A methodology for electromagnetic parameter estimation of an induction motor equivalent circuit based on the load curve test. In *2017 International Symposium on Electrical Machines (SME)* (pp. 1-6). Naleczow: IEEE. doi: 10.1109/ISEM.2017.7993570.

[16] Rolek, J., & Utrata, G. (2018). An identification procedure of electromagnetic parameters for an induction motor equivalent circuit including rotor deep bar effect. *Archives of Electrical Engineering*, 67(2), 279-2 425/119640.

[17] Terzioğlu, H., & Selek, M. (2017). Determination of equivalent circuit parameters of induction motors by using heuristic algorithms. *Selcuk University Journal of Engineering, Science and Technology*, 5(2), 170-182. doi: 10.15317/Scitech.2017.80.

[18] Tezcan, M.M., Yetgin, A.G., Canakoglu, A.I., Cevher, B., Turan, M., & Ayaz, M. (2018). Investigation of the effects of the equivalent circuit parameters on induction motor torque using three different equivalent circuit models. *MATEC Web of Conferences*, 157, article number 01019. doi: 10.1051/matecconf/201815701019.

[19] Vazifehdan, M., Zarchi, H.A., & Khoshhava, M.A. (2020). Sensorless vector control of induction machines via sliding mode control based model reference adaptive system. In *28th Iranian Conference on Electrical Engineering (ICEE)* (pp. 1-6). Tabriz: IEEE. doi: 10.1109/ICEE50131.2020.9260920.

[20] Wengerkievicz, C.A.C., Elias, R.A., Batistela, N.J., Sadowski, N., Kuo-Peng, P., Sandro Lima, C., da Silva Jr., P.A., & Beltrame, A.Y. (2017). Estimation of three-phase induction motor equivalent circuit parameters from manufacturer catalog data. *Journal of Microwaves, Optoelectronics and Electromagnetic Applications*, 16(1), 90-107. doi: 10.1590/2179-10742017v16i1873.

Роман Миколайович Чуєнко
Кандидат технічних наук, доцент
Національний університет біоресурсів і природокористування України
03041, вул. Героїв Оборони, 15, м. Київ, Україна
https://orcid.org/0000-0002-9339-9764

Віктор Володимирович Каплун
Доктор технічних наук, професор
Національний університет біоресурсів і природокористування України
03041, вул. Героїв Оборони, 15, м. Київ, Україна
https://orcid.org/0000-0001-7040-9344

Світлана Сергіївна Макаревич
Кандидат технічних наук, доцент
Національний університет біоресурсів і природокористування України
03041, вул. Героїв Оборони, 15, м. Київ, Україна
https://orcid.org/0000-0002-9601-5156

Олександр Вікторович Ситник
Аспірант
Національний університет біоресурсів і природокористування України
03041, вул. Героїв Оборони, 15, м. Київ, Україна
https://orcid.org/0009-0000-8108-4944

Схема заміщення асинхронного генератора з внутрішньою ємнісною компенсацією реактивної потужності

Анотація. Актуальність застосування компенсованих асинхронних машин у режимі генератора автономних систем електроживлення полягає в їх здатності забезпечувати стабільне та надійне електропостачання навіть у відсутність зовнішньої мережі. Метою цієї роботи є створення процедури для визначення характеристик еквівалентної схеми компенсованих асинхронних генераторів, яка враховує взаємний вплив між головними та додатковими фазними обмотками якоря. Для одержання розрахункових характеристик режимів функціонування генератора такого класу аналітичним було використано теорію ідеалізованої асинхронної машини з представленням електромеханічних процесів перетворення енергії та основних фізичних параметрів у вигляді рівнянь електричної рівноваги і руху привода. Узагальнена система диференційних рівнянь дала можливість розрахувати динамічні і статичні процеси для симетричних і несиметричних режимів при заданих параметрах машини при різних способах її збудження та стабілізації напруги при змінному навантаженні. Для практичної реалізації моделювання параметрів асинхронного генератора використані рівняння електричної рівноваги кіл статора і ротора для симетричного усталеного режиму, яка є частковим випадком узагальненої математичної моделі машини як для перехідних, так і усталених процесів з постійними параметрами схеми заміщення. Урахування конструктивних та функціональних особливостей компенсованих асинхронних генераторів стало можливим на основі використання математичної моделі з поділом обмотки якоря на дві співвісні або зміщені у просторі напівобмотки. У такому випадку кількість розрахункових рівнянь збільшується удвічі. Використання автотрансформаторної схеми увімкнення напівобмоток фаз статора на конденсатори вимагало введення додаткового диференційного рівняння електричної рівноваги фаз статора. Це дало змогу обґрунтувати величини активних та індуктивних опорів, які використовуються у схемі заміщення асинхронного генератора із внутрішньою ємнісною компенсацією реактивної потужності. При цьому враховувався взаємний індуктивний зв'язок основних і додаткових напівобмоток фазних обмоток статора генератора обумовлений як робочим магнітним потоком, так і магнітними потоками розсіяння. Практичне значення отриманих результатів полягає в підвищенні ефективності та стабільності електроживлення, що сприяє зменшенню втрат та покращенню роботи електроенергетичних систем

Ключові слова: асинхронна машина; внутрішня ємнісна компенсація; реактивна потужність; активний опір; індуктивний опір; взаємоіндуктивний зв’язок

Machinery & Energetics
Vol. 14, No. 4. 2023

Journal homepage:
https://technicalscience.com.ua/en

UDC 539.3
DOI: 10.31548/machinery/4.2023.64

Anastasiia Kutsenko*

PhD in Mathematics and Physics, Associate Professor
National University of Life and Environmental Sciences of Ukraine
03041, 15 Heroiv Oborony Str., Kyiv, Ukraine
https://orcid.org/0000-0003-1808-6773

Oleksii Kutsenko

PhD in Mathematics and Physics, Associate Professor
Taras Shevchenko National University of Kyiv
01033, 60 Volodymyrska Str., Kyiv, Ukraine
https://orcid.org/0000-0001-5089-0409

The gradual removal of Hertz pressure from the surface of elastic half-space

Abstract. Contact stress determination in non-stationary dynamic loading of elastic bodies is crucial for modelling structures at high speeds, but it presents mathematical challenges due to the time-dependent and often unknown contact area size and shape. The study aims to obtain an energy remainder estimation that forms waves during the contact interaction of elastic bodies, based on the exact solutions of non-stationary problems for an elastic half-space. For this purpose, the problem of the instantaneous loading half-space as an additional research problem was reconstructed using the Hankel transform concerning a radial coordinate and the Laplace transform concerning a time variable. The method of derivation of the displacements at an elastic half-space loaded (unloaded) gradually by Hertz's contact pressure has been proposed. Its availability made it possible to pass to the solution of the main problem – the problem of gradual loading of the half-space surface by Hertz pressure. The possibility of changing of the order of differentiation and integration operations in the obtained representation is substantiated based on the integrand properties. The cases when the speed of the indenter was constant when its motion was uniformly accelerated and when the motion corresponded to the law of the first quarter of the cosine period in the time were considered. It was concluded that the distribution of dynamic contact stresses is similar to the Hertz distribution. An estimation of the part of the energy spent on the formation of elastic waves was made for various laws of unloading. The practical significance of this study lies in its development of an effective method for calculating normal displacements on a loading area in dynamic contact interactions of elastic bodies, which can be valuable for modelling structures at high speeds

Keywords: dynamic contact interaction; refinement of the contact distribution; wave energy; Laplace transform; indenter; Hankel transform

INTRODUCTION

The determination of contact stresses, caused by non-stationary dynamic loading of elastic bodies, is one of the practically important problems in the theory of elasticity. The correct consideration of the influence of inertial forces on local deformations in the vicinity of the contact region is necessary for adequate simulation of the operation of a structure or mechanisms, in which components interact in a significant way at significant speeds. Microwave (ultrasonic) motors are typical examples of such mechanical systems. X. Tian *et al.* (2020) concluded that the principle

Article's History: Received: 30.06.2023; Revised: 22.09.2023; Accepted: 22.11.2023.

Suggested Citation:
Kutsenko, A., & Kutsenko, O. (2023). The gradual removal of Hertz pressure from the surface of elastic half-space. *Machinery & Energetics,* 14(4), 64-74. doi: 10.31548/machinery/4.2023.64.

*Corresponding author

of operation of some types of these devices is based on the transfer of kinetic energy from the stator to the rotor by contact forces arising in the process of their periodic collisions. Based on S.P. Wankhede & T.-B. Xu (2021), ultrasonic motors have been widely used in a variety of electronic devices due to their compactness, load torque at moderate rotation speeds and high positioning accuracy. They are widely used in the double-quick development of robotics (Toyama & Nishizawa, 2017). The simultaneous influence of surface and couple stresses on the non-symmetrical frictionless indentation of a linearly elastic, homogenous, and isotropic half-plane under a tilted, rigid, flat-ended indenter with sharp, square corners was investigated by T.M. Le *et al.* (2021) by adopting existing continuum-based models.

B. An *et al.* (2023) broadened the applicability of the vehicle-track dynamics model to account for 3D short-wave irregularities on rail surfaces. The key is developing a meshing grid approach combined with the accurate conjugate gradient (CG) method for contact mechanics under arbitrary 3D contact geometry. Therefore, both the global dynamics and local contact solutions can be provided. In this study, short-pitch rail corrugation is employed for investigating the role of 3D contact geometry in modelling dynamic wheel-rail interaction. The traditional vehicle-track coupled dynamics model using Hertzian spring is used for comparison. The results show that short-pitch rail corrugation contributes two different aspects, i.e., wheel centre trajectory and time-varying contact stiffness. These two aspects are found to be the root causes for explaining the influence of the varying 3D geometry irregularity size on dynamic wheel-rail contact force.

Accounting for the processes that occur during the dynamic contact interaction of solids is also important in the development and design of "classical" machinery. An example is the operation of various crushing machines which were described by B. Doroszuk & R. Król (2022), and Z. Chen *et al.* (2021). In particular, for processing agricultural products, the mechanisms, such as grinding mills, are used. To describe the operation of the crusher more accurately, X. Lv *et al.* (2021), I. Kupchuk *et al.* (2022) addressed the wave processes that occur when parts of the mechanism interact with the crushed material. Many scientists considered similar problems in Ukraine. In particular, the study of V.A. Bazhenov & M.O. Vabishchevich (2020) is relevant to the branch of construction. Similar studies were conducted by V.G. Popov & A.I. Kirillova (2020) in the field of mechanical engineering.

H. Xie *et al.* (2022) noted that the dynamic interaction of a rigid sphere with an elastic half-space should be considered using recently developed particle dynamics. From the provisions of this theory, J. Zhao *et al.* (2021) established that the problem was reduced to a wave equation concerning one of the components of the displacement vector. Based on the mentioned solution, a plausible conclusion was made on the similarity at any time of the distribution of contact stresses to Hertz's distribution. However, the conclusion that the maximum pressure according to Hertz's theory is much less than the calculated holds unresolved issues. According to the given relations, their correlation depends only on Poisson's ratio of the material of the half-space and does not depend on the initial velocity of the sphere. When Poisson's ratio changes from 0 to 0.5, this relation changes from 0.74 to 0.

Thus, it can be concluded that the presented results of previous studies contain several contradictions. Therefore, with the solution to this sort of issue, various numerical methods were used, the finite element method being used most often (Lee & Komvopoulos, 2018; Habchi, 2018). This is also facilitated by the fact that in modern finite element packages, both commercial and freely available, the various algorithms of the contact interaction of finite elements are implemented. However, based on numerical solutions, it is difficult to restore the analytical dependence of the process characteristics on the values of the input parameters. Despite the already fairly long history of research, the important problem of estimation of the contact interaction of the surface of the body under study with measure sensors is open still. Hence, the study aims to determine the energy remainder that causes waves in the case of a contact problem.

MATERIALS AND METHODS

The distribution of normal displacements of surface points under gradual loading of a half-space with a load, according to Heasrtz's law was obtained by using the solution to the corresponding problem of instantaneous loading. Therefore, to present the solution to the problem of gradual loading in a closed form and simplify the perception of the material, the main results of a study by A.G. Kutzenko *et al*. (2001) were employed, which addressed the loading of a half-space by the Hertz's pressure. The elastic half-space $z < 0$ was considered, which at time $t < 0$ had been in static equilibrium, and its surface was not loaded. At the moment of time $t = 0$, the pressure, that was given by Hertz's contact theory, was instantly applied to the surface of the half-space in a circular domain $0 \leqslant r \leqslant a$ (Fig. 1).

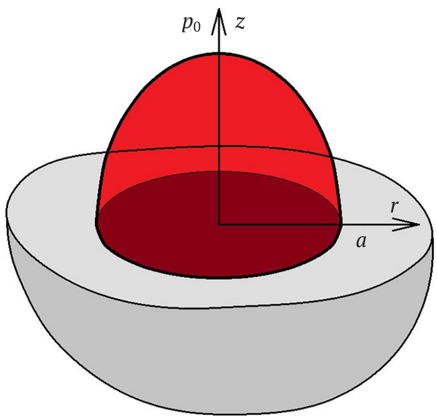

Figure 1. Loading of the elastic half-space by Hertz's pressure

Note: *a – load area radius; z, r – spatial coordinates; p_0 — pressure magnitude*

This pressure was considered a constant variable in the study. It was used to determine the normal displacements of the surface points of the half-space, as a function of time t and radial coordinate *r*. This was an additional task. The corresponding initial and boundary conditions were formulated as follows:

$$w|_{t=0} = u|_{t=0} = 0, \left.\frac{\partial w}{\partial t}\right|_{t=0} = \left.\frac{\partial u}{\partial t}\right|_{t=0} = 0, \tag{1}$$

and

$$\tau_{rz}|_{z=0} = 0, \ \sigma_r|_{z=0} = H(t)\begin{cases} -p_0\sqrt{1-r^2/a^2}, & r < a, \\ 0, & r > a, \end{cases} \tag{2}$$

where w, u – thickness (normal) and radial (tangential) displacements of the points of the half-space; σ_r, τ_{rz} – normal and shear stresses on the surface of a half-space; $H(t)$ – Heaviside function.

The maximum contact pressure was an independent parameter in the boundary conditions (2). However, considering the further extension of the results to cases of gradual loading of a half-space, it was expressed according to Hertz's theory in terms of the radius of the load area a and the radius of curvature of the equivalent indenter R:

$$p_0 = \frac{4Ga}{\pi(1-\nu)R}, \tag{3}$$

where G – shear modulus, ν – Poisson's ratio of the half-space material. All three parameters p_0, a, and R were considered as constant variables in the study. Only one parameter R was considered as a constant in the gradual load issue, as parameters p_0 and a were changed with time.

If the Laplace transform L with was applied concerning time and the Hankel transform H to the spatial coordinate r to Lamé equations of motion respectively, displacements can be represented as multiple integrals of the Riemann-Mellin inversion:

$$\begin{aligned} w(r,z,t) &= \frac{1}{2\pi i}\int_0^\infty J_0(\lambda r)\lambda d\lambda \int_{\delta-i\infty}^{\delta+i\infty} W(\lambda,z,s)\exp(st)ds, \\ u(r,z,t) &= \frac{1}{2\pi i}\int_0^\infty J_1(\lambda r)\lambda d\lambda \int_{\delta-i\infty}^{\delta+i\infty} U(\lambda,z,s)\exp(st)ds. \end{aligned} \tag{4}$$

In this case, the images $W(\lambda, z, s)$ and $U(\lambda, z, s)$ satisfied the system of differential equations:

$$\begin{aligned} &\kappa\frac{d}{dz}\left(\frac{dW}{dz}+\lambda U\right) - \lambda\left(\frac{dU}{dz}+\lambda W\right) = \frac{s^2}{c_2^2}W, \\ &-\kappa\lambda\left(\frac{dW}{dz}+\lambda U\right) + \frac{d}{dz}\left(\frac{dU}{dz}+\lambda W\right) = \frac{s^2}{c_2^2}U, \end{aligned} \tag{5}$$

where $\kappa = 2\frac{1-\nu}{1-2\nu} = \frac{c_1^2}{c_2^2} > 1$, $c_1 = \sqrt{2\frac{1-\nu}{1-2\nu}\frac{G}{p}}$, $c_2 = \sqrt{\frac{G}{p}}$ – the velocities of propagation of tension-compression waves and shear waves, respectively.

The zero initial conditions (1) were considered when equation (5) was deriving. To satisfy the boundary conditions (2), the Laplace and Hankel transformations were also applied:

$$\left.\left(\frac{1-\nu}{1-2\nu}\frac{dW}{dz} + \frac{\nu\lambda}{1-2\nu}U\right)\right|_{z=0} = -\Pi_0(\lambda,s), \ \left.\left(\frac{dU}{dz} - \lambda W\right)\right|_{z=0} = 0, \tag{6}$$

where

$$\begin{aligned} \Pi_0(\lambda,s) &= \Pi_0^i(\lambda,s) = -\mathbf{L}\left(\mathbf{H}(\sigma_z|_{z=0})\right) = \\ &= \frac{2}{\pi(1-\nu)R}\frac{\sin a\lambda - a\lambda\cos a\lambda}{s\lambda^2}. \end{aligned} \tag{7}$$

The general solution of system (4), which satisfies the conditions of boundedness at infinity, was represented as:

$$\begin{aligned} W(\lambda,z,s) &= \lambda\left(\frac{c_2}{s}\right)^2[-\kappa\gamma_1 A\exp(\lambda\gamma_1 s) + B\exp(\lambda\gamma_2 s)], \\ U(\lambda,z,s) &= \lambda\left(\frac{c_2}{s}\right)^2[\kappa A\exp(\lambda\gamma_1 s) - \gamma_2 B\exp(\lambda\gamma_2 s)]. \end{aligned} \tag{8}$$

Submitting it to conditions (6), the expression for the image of normal displacement of boundary points was obtained:

$$\begin{aligned} \tilde{W}^i(\lambda,s,a) &= W^i(\lambda,0,s) = -\Pi_0^i(\lambda,s)\frac{\gamma_1(\gamma_2^2-1)}{2\Delta} = \\ &= \frac{1}{\pi(1-\nu)R}\frac{\gamma_1(\gamma_2^2-1)}{2\Delta}\frac{\sin a\lambda - a\lambda\cos a\lambda}{s\lambda^2}, \end{aligned} \tag{9}$$

where $\gamma_1 = \sqrt{1+s^2/(c_1\lambda)^2}$, $\gamma_2 = \sqrt{1+s^2/(c_2\lambda)^2}$,

$\Delta = \Delta(s/\lambda) = \frac{(\gamma_2^2+1)}{4} - \gamma_1\gamma_2$ – Rayleigh determinant. Its single-valued branch was distinguished on the complex plane s by cutting, as shown in Figure 2.

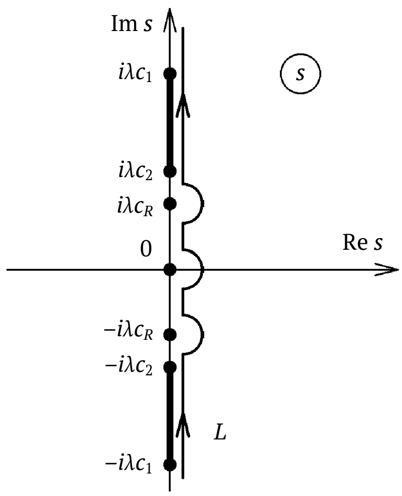

Figure 2. Integration contour in the inverse Laplace transform

Note: c_R – the Rayleigh wave velocity; $s = \pm i\lambda c_R$ are poles of the function W

The radical branches γ_1 and γ_2 were chosen so that their values on the real axis s coincided with the values of the corresponding arithmetic roots. Such selection was used to obtain a representation of the solution in the form of a superposition of waves propagating from the surface into the depths of the half-space, and to ensure that the stress and displacement were clamped at $z \to -\infty$. The index "*i*" in expressions (7) and (9) indicated that the characteristic marked by it corresponded to the problem of *instantaneous* loading.

Since the points of the surface corresponded to a certain (zero) value of the coordinate z, i.e., normal displacements depended only on the variables r and t, this fact in (9) and below was denoted by the symbol "~". In addition, functions, containing the symbol "~" in their designation, were also considered as functions of the parameter a, necessary in the case of gradual loading of the half-space.

Further transformation (9) involved the inversions of the Laplace and Hankel transformations by (4). It was easy to verify that all singular points of expression (9) in the complex plane s stayed within the imaginary axis. According to the selection of branches of the radicals γ_1 and γ_2, the poles corresponded only to the points $s = 0$ and $s = \pm i\lambda c_R$, where c_R was the Rayleigh wave velocity. Therefore, function (9) was an analytic function of a variable parameter s in the right half-plane $Re\ s > 0$, which was used to shift the Laplace inversion contour to the imaginary axis.

Going around the poles of the function W, it was necessary to explicitly select the semi-residues equal to the integrals over the arcs of circles (Fig. 2). Performing this operation and introducing a new integration variable $x = -s_2/(c_2\lambda)^2$, after the pairwise union of the integrals corresponding to the upper and lower parts of the axis $Im\ s$, the normal displacements of points on the surface of the half-space was represented in a form that does not contain complex variables:

$$\tilde{w}^i(r,t,a) = -\frac{a^2}{\pi(1-\nu)R} f(\rho,\tau), \qquad (10)$$

where:

$$\begin{aligned} f(\rho,\tau) = (1-\nu)I(\rho) + \frac{1}{4\pi}\Bigg\{ & \pi\frac{(1-q/2)^2\sqrt{1-q/\kappa}I_C(l,2r)}{(1-q/2)^3-(1+\kappa^{-1}-2q/\kappa)/2} - \\ & -\int_0^1 \frac{\sqrt{1-x/\kappa}I_S\left(\rho,2\tau\sqrt{x/q}\right)}{(1-x/2)^2-\sqrt{(1-x/\kappa)(1-x)}}dx - \\ & -\int_0^\infty \frac{\sqrt{x/\kappa-1}I_C\left(\rho,2\tau\sqrt{x/q}\right)}{(1-x/2)^2+\sqrt{(x/\kappa-1)(x-1)}}dx - \\ & -\int_1^\kappa \frac{(1-x/\kappa)^2\sqrt{1-x/\kappa}I_S\left(\rho,2\tau\sqrt{x/q}\right)}{(1-x/2)^4-(1-x/\kappa)(1-x)}dx - \\ & -\int_1^\kappa \frac{(1-x/\kappa)\sqrt{x-1}I_C\left(\rho,2\tau\sqrt{x/q}\right)}{(1-x/2)^4-(1-x/\kappa)(1-x)}dx \Bigg\}. \end{aligned} \qquad (11)$$

The dimensionless independent variables $\rho = r/a$ and $\tau = (c_R t)/a$ were introduced in the expressions (10)-(11), as well as a parameter $q = c_R^2/c_2^2$ – the square of the ratio of the Rayleigh wave velocity to the shear wave velocity, which was a simple pole of the integrand of the first integral in (11). The index "i" at $\tilde{w}$ indicated, as before, that this distribution of normal displacements corresponded to the problem of *instantaneous* loading. After relocation of the contour of the inverse Laplace transform to the imaginary axis, the integrals of the inverse Hankel transform I, I_S, and I_C were as follows:

$$\begin{aligned} I(\rho) &= \left(1-\frac{\rho^2}{2}\right)I_1(\rho) + \frac{I_2(\rho)}{2}, \\ I_S(l,\xi) &= \left(1-\xi^2-\frac{\rho^2}{2}\right)I_{S1}(l,\xi) + \frac{I_{S2}(l,\xi)}{4}, \\ I_C(l,\xi) &= \left(1-\xi^2-\frac{\rho^2}{2}\right)I_{C1}(l,\xi) + \frac{I_{C2}(l,\xi)}{4}, \end{aligned} \qquad (12)$$

where:

$$\begin{aligned} I_1(\rho) &= \begin{cases} \pi/2, \rho \le 1, \\ arcsin\,\rho^{-1}, \rho \ge 1, \end{cases} \\ I_{S1}(\rho,\xi) &= \frac{1}{2}\begin{cases} ln\left(1+\xi+\sqrt{(1+\xi)^2-\rho^2}\right) - ln\left(|1-\xi| + \sqrt{(1-\xi)^2-\rho^2}\right), & |1-\xi| \ge \rho, \\ ln\left(1+\xi+\sqrt{(1+\xi)^2-\rho^2}\right) - ln\,\rho, & |1-\xi| \le \rho \le 1+\xi, \\ 0, & 1+\xi \le \rho, \end{cases} \\ I_{C1}(\rho,\xi) &= \frac{1}{2}\begin{cases} \pi H(1-\xi), & |1-\xi| \ge \rho, \\ \pi/2 + arcsin((1-\xi)/\rho), & |1-\xi| \le \rho \le 1+\xi, \\ arcsin((1+\xi)/\rho) + arcsin((1-\xi)/\rho), & 1+\xi \le \rho \end{cases} \end{aligned} \qquad (13)$$

and

$$\begin{aligned} I_2(\rho) &= \begin{cases} 0, \rho \le 1, \\ \sqrt{\rho^2-1}, \rho \ge 1, \end{cases} \\ I_{C2}(\rho,\xi) &= \begin{cases} 0, & |1-\xi| \ge \rho, \\ (1+3\xi)\sqrt{\rho^2-(1-\xi)^2}, & |1-\xi| \le \rho \le 1+\xi, \\ (1+3\xi)\sqrt{\rho^2-(1-\xi)^2} + (1-3\xi)\sqrt{\rho^2-(1+\xi)^2}, & 1+\xi \le \rho, \end{cases} \\ I_{S2}(\rho,\xi) &= \frac{1}{2}\begin{cases} sign(1-\xi)\,(1+3\xi)\sqrt{(1-\xi)^2-\rho^2} - (1-3\xi)\sqrt{(1+\xi)^2-\rho^2}, & |1-\xi| \ge \rho, \\ -(1-3\xi)\sqrt{(1+\xi)^2-\rho^2}, & |1-\xi| \le \rho \le 1+\xi, \\ 0, & 1+\xi \le \rho. \end{cases} \end{aligned} \qquad (14)$$

The plots of displacements found based on (10) for various values of the dimensionless time are shown in Figure 3. The analysis highlighted the reason for the selection of Rayleigh as the characteristic velocity in the nondimensionalization of time. This velocity determined the dynamics of transient processes under instantaneous loading of the half-space. After the propagation of the Rayleigh wave excited at the point of the loading area, which is the most distant from the given point of the half-space surface, the static value of the normal displacement was instantly set in the latter one. This important property was used in further transformations.

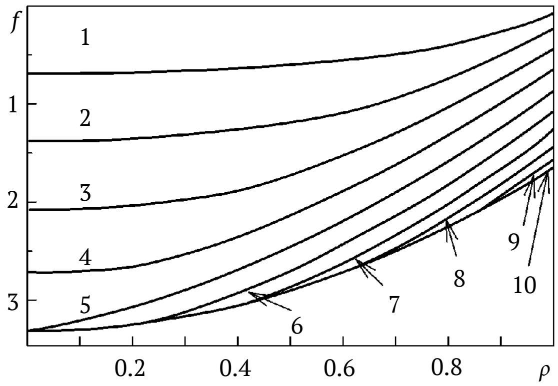

Figure 3. Dimensionless function $f(\rho, \tau)$ for $\nu = 0.3$ at moments of dimensionless time $\tau = n/10$, where n is the number of the curve
Source: developed by the authors

An elastic half-space that was at the initial moment $t = 0$ in an unloaded state of static equilibrium was used. At the given moment an area arises on its surface and then continues to grow, on which the pressure is distributed according to the law:

$$p(r,t) = p_0(t)\sqrt{1 - r^2/a^2(t)}, r \le a(t), t > 0, \quad (15)$$

where $a = a(t)$ is the radius of the loading area. It was the time-respecting variable parameter. In this case, as before, the relation (3) determined the dependence of the maximum pressure $p_0(t)$ on the radius of the loading area. It was required to determine the time evolution of normal displacements on the surface of a half-space.

Since the initial conditions (1) and the first of the boundary conditions (2) were still true, the course of the solution to the given problem did not differ from the aforementioned, until the rest of the boundary conditions were satisfied. The main difference between the boundary conditions concerning the normal component of the stress vector in the problem of instantaneous and in the problem of gradual loading of a half-space was its significant time dependence in the second case. In this case, it was impossible to explicitly run the direct Laplace transform without the specification of the loading area radii dependence concerning time. Therefore, in the general case, instead of (7) and (9), the following was true:

$$\Pi_0(\lambda, s) = \Pi_0^g(\lambda, s) = -L\big(H(\sigma_z|_{z=0})\big) =$$

$$= -\frac{2}{\pi(1-\nu)R\lambda^3}\int_0^\infty (\sin a(\bar{t})\lambda - a(\bar{t})\lambda \cos a(\bar{t})\lambda) exp(-s\bar{t})d\bar{t}, \quad (16)$$

and

$$\widetilde{W}^g(\lambda, s) = -\frac{2}{\pi(1-\nu)R}\frac{\gamma_1(\gamma_2^2-1)}{\lambda^3 \Delta} \times$$

$$\times \int_0^\infty \begin{pmatrix} \sin a(\bar{t})\lambda - \\ -a(\bar{t})\lambda \cos a(\bar{t})\lambda \end{pmatrix} exp(-s\bar{t})d\bar{t}. \quad (17)$$

The index "g" implied that the images of surface pressure and normal displacement correspond to *the gradual* loading of the half-space. It was necessary to apply the inverse Laplace and Hankel transformations to (17) following the first relation in (4) to find the expression of normal displacements. In the general case, it was impossible to run the corresponding integration since the form of the function W itself was unknown. However, since only one of these integrals was singular, they could be introduced under the sign of the integral contained on the right side of (17), i.e., the order of integration could be changed (Gakhov, 2014). Hence, such a permutation could be used to reduce the procedure of taking the internal integrals of the Riemann-Mellin inversion to the calculations made above. It should be remembered that the radius $a(\bar{t})$ acts as an independent parameter in internal integrals. Therefore, the inversion integrals were obtained from the product of the function $\widetilde{W}^i(\lambda, s, a)$ and the parameters. The last multiplier is explained by the absence of the Heaviside function in the boundary conditions under gradual loading. In addition, the exponent of the Laplace inversion kernel contained the difference $t - \bar{t}$ instead of t, which was derived as a result of a rearrangement of the order of integration. Thus, the following was true:

$$\tilde{w}^g(r,t) = \frac{1}{2\pi i}\int_0^\infty d\bar{t}\int_0^\infty J_0(\lambda r)\lambda d\lambda$$
$$\int_{\delta-i\infty}^{\delta-i\infty} \widetilde{W}^i\big(\lambda, s, a(\bar{t})\big)s\, exp\big(s(t-\bar{t})\big)\, ds. \quad (18)$$

The theorem on differentiation of the Laplace transformation original to (18) was applied and $\tilde{w}^i(r, t, a) \equiv 0$ was implied for $t \leqslant 0$, to derive the following:

$$\tilde{w}^g(r,t) = \int_0^t \frac{\partial \tilde{w}^i\big(r, t-\bar{t}, a(\bar{t})\big)}{\partial t} d\bar{t}. \quad (19)$$

It expressed the normal displacements under gradual loading of the half-space in terms of the normal velocities of the surface points under its instantaneous loading. The relationship (19) could be obtained from simpler considerations, based on the incremental approach. Therefore, the process of continuous loading was replaced by a step change in surface pressure at discrete moments separated from each other by a small time interval Δt. A loading area with radius $a_1 = a(t_1)$ was assumed to have arisen on the surface of the half-space at the moment of time $t_1 = \Delta t$. The normal displacements of points on the surface of the half-space were described until the next moment of load change by the expression:

$$\tilde{w}^s(r, t) = \tilde{w}^i(r, t - t_1, a_1), t_1 < t < t_2, \quad (20)$$

where the index "$\underline{s}$" denoted stepwise load change. At the moment of time $t_2 = t_1 + \Delta t$, the radius of the loading area changed abruptly from a_1 to $a_2 = a(t_2)$. It corresponded to instantaneous load removal along the area with the radius a_1 and instantaneous application along the area with radius a_2 at $t = t_2$:

$$\tilde{w}^s(r, t) = \tilde{w}^i(r, t-t_1, a_1) - \tilde{w}^i(r, t - t_2, a^1) + \tilde{w}^i(r, t - t_2, a_2),$$
$$t_2 < t < t_3. \quad (21)$$

The following obtained expression for normal displacements at the N-th step is as follows:

$$\tilde{w}^s(r,t) = \tilde{w}^i(r,t-t_{N+1},a_{N+1}) + \\ +\sum_{k=1}^{N}\left[\tilde{w}^i(r,t-t_k,a_k) - \tilde{w}^i(r,t-t_{k+1},a_k)\right] \approx \\ \approx \tilde{w}^i(r,t-t_{N+1},a_{N+1}) + \sum_{k=1}^{N}\frac{\partial \tilde{w}^i(r,t-t_k,a_k)}{\partial t}\Delta t, \\ t_N < t < t_{N+1}. \tag{22}$$

When the parameter Δt was zero in expression (22), the expression (19) was used instead. In the case when a static load was applied along the radius a_0 to the surface of the half-space, two more terms would be added to the integral on the right side of (19):

$$\tilde{w}^H(r, a_0)\text{-}\tilde{w}^i(r, t, a_0). \tag{23}$$

The first of them described the field of normal displacements in the Hertz contact problem:

$$\tilde{w}^H(r,a_0) = -\frac{2a_0^2}{\pi R}I\left(\frac{r}{a_0}\right). \tag{24}$$

The second term corresponded to the removal of this load at the initial moment. Therefore, the expressions for normal displacements during gradual loading of the half-space due to normal velocities of surface points during its instantaneous loading and normal displacements in contact interaction were obtained.

RESULTS AND DISCUSSION

The relationship (19), addressing (23), was utilised to consider the evolution of normal displacements for different laws of change in the radius of the loading area $a = a(t)$. However, this study only focused on the case when the dependence of the radius of the loading area on time is a monotonically decreasing function, which corresponds to the process of unloading the half-space (Fig. 4).

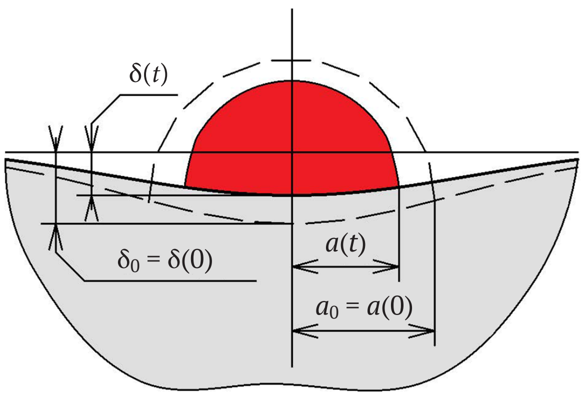

Figure 4. The gradual unloading of the elastic half-space

Note: $a = a(t)$ is the radius of the loading area; $\delta = \delta(t)$ – the law of change in the penetration depth of an equivalent indenter; δ_0 – the initial value of the depth of the penetration

Source: developed by the authors

In this case, to achieve the goals formulated in the introduction, it is sufficient to determine the function (11) and its partial derivative only at $\rho < 1$, since only the normal displacements of points that currently belong to the loading area are considered in this study. In practice, it is better to set not the law of change in the radius of the contact area, but the law of change in the penetration depth of an equivalent indenter δ, which, following the Hertz's theory, is related to the radius by the relation:

$$\delta = a^2/R. \tag{25}$$

Three partial dependencies $\delta = \delta(t)$ will be considered, namely $\delta = \delta_0(1\text{-}t/T)$ – uniform unloading, $\delta = \delta_0(1\text{-}(t/T)^2)$ – uniformly accelerated unloading and $\delta = \delta_0 cos(\pi t/((2\mathrm{T})))$. The last expression accurately approximates the dependence, which follows from Hertz's quasi-static contact theory, of the penetration depth as a function of time during the collision of two elastic balls moving by inertia (Johnson, 2012). Here, δ_0 is the initial value of the depth of the penetration, and T is the period of unloading. In the case of unloading, relation (19) can be represented in a dimensionless form considering (23):

$$\pi\frac{\tilde{w}^g(r,t)}{\delta_0} = -2I(\rho) + \frac{1}{1-\nu}\left[f(\rho,\tau) - \int_0^\tau d(\bar{\tau})f_\tau\left(\frac{\rho}{d(\bar{\tau})},\frac{\tau-\bar{\tau}}{d(\bar{\tau})}\right)d\bar{\tau}\right], \\ \tau < \tau_{max}, \tag{26}$$

where

$$\rho = \frac{r}{a_0} = \frac{r}{\sqrt{R\delta_0}}, \tau = \frac{c_R t}{2a_0} = \frac{c_R t}{2\sqrt{R\delta_0}}, \\ d(\tau) = \sqrt{\frac{\delta(t)}{\delta_0}} = \sqrt{\frac{\delta(2\tau\sqrt{R\delta_0}/c_R)}{\delta_0}}, \\ f_\tau(\rho,\tau) = \frac{\partial f(\rho,\tau)}{\partial \tau}, \ \ \tau\frac{c_R T}{2\sqrt{R\delta_0}}_{max}. \tag{27}$$

During the calculation of the function value, the order of the integration and derivation operations in (11) can be changed and performed analytically. Thus, the determination of f_τ values is reduced to simple (not multiple) integrations, similar to those that arise when calculating the antiderivative of function f. A three-dimensional plot of $-f_\tau(\rho, \tau)$ on the square [0,1]×[0,1] is shown in Figure 5.

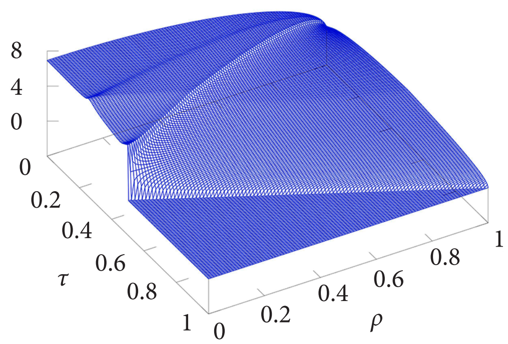

Figure 5. Surface $-f_\tau(\rho, \tau)$ for $\nu = 0.3$

Source: developed by the authors

Figure 6 shows a plot of the same function but in the form of isolines. As can be seen, this function is bounded and continuous everywhere, except for the point $\rho = 0$, $\tau = 1/2$, where a finite gap is present along the axis τ. The advantage of representation (26) in comparison with other possible methods for the solution of the problem of gradual loading/unloading of a half-space is explained by the fact that, in addition to dimensionless variables, the function f_τ depends only on the Poisson ratio as a parameter and can be easily tabulated. Thus, the calculation following (26) is reduced to the integration of a bounded, continuous function.

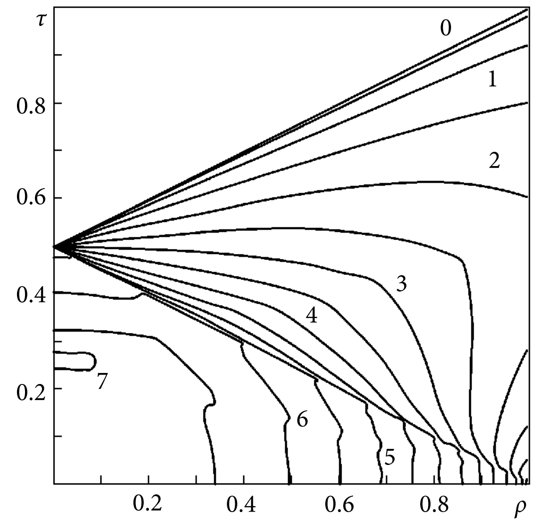

Figure 6. The isolines of a dimensionless function $-f_\tau(\rho, \tau)$
Note: the values of the function are indicated near the isoline
Source: developed by the authors

The representation (26) also shows that the only parameter significant for the process, in addition to the Poisson ratio, is the dimensionless period of unloading τ_{max}, which is equal to the number of diameters of the initial loading area that the Rayleigh wave travels during the unloading time. In addition, based on (26), for random dependence $d = d(\tau)$, which is monotonically decreasing to zero, it can be proved that in the limiting case, when τ_{max}, the distribution of normal displacements tends to the distribution given by Hertz's theory for the current value of the penetration depth. The depth of penetration ($d = \sqrt{1 - \tau/\tau_{max}}$) when $\tau > 1$ is demonstrated in the example of the linear law of decreasing. In this case, the first two terms on the right side of (26) on the loading area completely compensate for each other. However, $f_\tau(\rho, \tau) \neq 0$ at $\rho \leqslant 1$, when $\tau < 1$. Considering the dependence $d = d(\tau)$, it is possible to conclude that the integrand in the remaining term is nonzero on a narrow interval $\tau_1 < \bar{\tau} < \tau$, where $\tau_1 = \tau - \frac{1}{2\tau_{max}}\sqrt{1 - \frac{\tau}{\tau_{max}} + \frac{1}{4\tau_{max}^2}} \approx \tau - \sqrt{1 - \frac{\tau}{\tau_{max}}}$.

Hence, $d(\bar{\tau}) \approx d(\tau)$ and:

$$\pi \frac{\tilde{w}^g(r,t)}{\delta_0} \approx \frac{d(\bar{\tau})}{1-\nu}\left[\int_0^\tau f_\tau\left(\frac{\rho}{d(\bar{\tau})}, \frac{\tau-\bar{\tau}}{d(\bar{\tau})}\right) d(\bar{\tau})\right]. \quad (28)$$

Running the integration in (28), the required results are obtained. It also follows from the above reasons that the magnitude of the deviation of the displacements caused by the gradual removal of the load from Hertz quasi-static displacements is of the order of τ_{max}^{-1}.

Figures 7-10 show the distributions of the displacements "under the indenter", which were calculated using linear (26) (Fig. 7 and 8) and quadratic (Fig. 9 and 10) unloading laws corresponding to different speeds. For comparison analysis, the dashed lines indicate the surface profiles of the loading area given by Hertz's theory for the corresponding penetration depth of the indenter.

Each pair of solid and dashed curves corresponds to a fixed time $0 < \tau < \tau_{max}$. For example, in Figure 7, which corresponds to constant indent speed and τ_{max} the five such pairs for time points $\tau = 1$, $\tau = 3$, $\tau = 5$, $\tau = 7$ and $5 \rightarrow \tau = 9$ are represented. The lengths of curves decrease with time as the size of the load area also decreases. This fact is indicated by the upper dashed outline. The lower dashed contour corresponds to the distribution of displacements in Hertz's static contact problem. The curves in each pair are similar, only slightly shifted relative to each other in the vertical direction. In other words, there is an almost constant vertical gap between them. This gap means that the dynamic distribution of normal displacements lags behind the quasi-static Hertzian distribution. Moreover, for a constant speed of removing the indentor, this lag decreases until the end of the unloading process.

A comparison of Figures 7 and 8 (the latter also shows data for a constant indenter speed but with τ_{max}) indicates that with an increase in the indenter speed, the difference between the dynamic and quasi-static distributions increases.

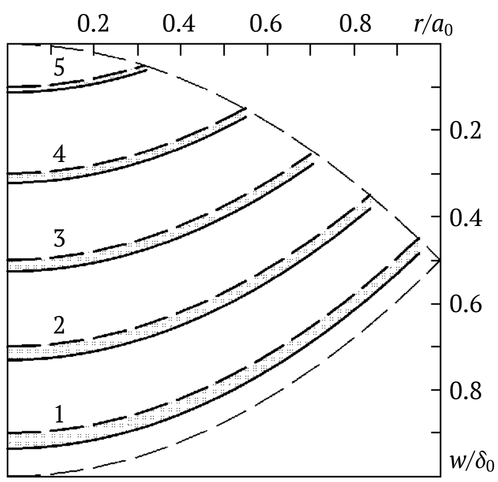

Figure 7. The normal displacements of points of loading area for the law $\delta = \delta_0(1 - \tau/10)$
Note: $1 \rightarrow \tau = 1$, $2 \rightarrow \tau = 3$, $3 \rightarrow \tau = 5$, $4 \rightarrow \tau = 7$, $5 \rightarrow \tau = 9$
Source: developed by the authors

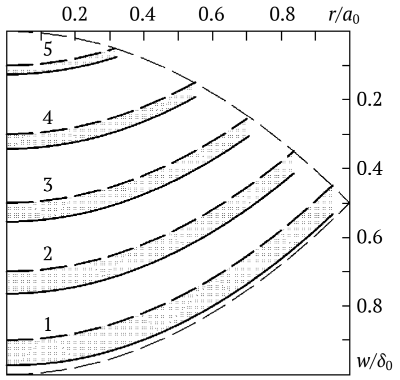

Figure 8. The normal displacements of points of loading area for the law $\delta = \delta_0 (1 - \tau/5)$
Note: $1 \rightarrow \tau = 0.5$, $2 \rightarrow \tau\,1.5$, $3 \rightarrow \tau = 2.5$, $4 \rightarrow \tau = 3.5$, $5 \rightarrow \tau = 4.5$
Source: developed by the authors

This conclusion remains valid even with uniformly accelerated movement of the indenter (see Fig. 9 and 10). Only in this case, the gap between the distributions increases until the end of the unloading process. A similar behaviour of the deviations of normal displacements is also characteristic of the dependence $\delta = \delta_0 \cos(\pi\tau/(2\tau_{max}))$, except that in the last case in the second half of the unloading period, there is a noticeable tendency to their decrease.

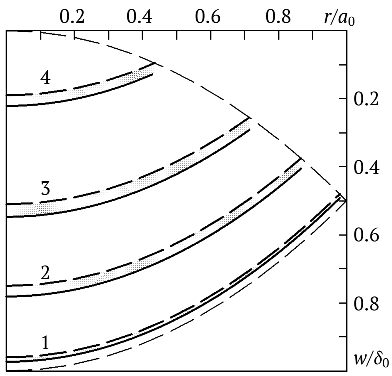

Figure 9. The normal displacements of points of loading area for the law $\delta = \delta_0 (1 - \tau/10)^2$
Note: $1 \rightarrow \tau = 2$, $2 \rightarrow \tau = 5$, $3 \rightarrow \tau = 7$, $4 \rightarrow \tau = 9$
Source: developed by the authors

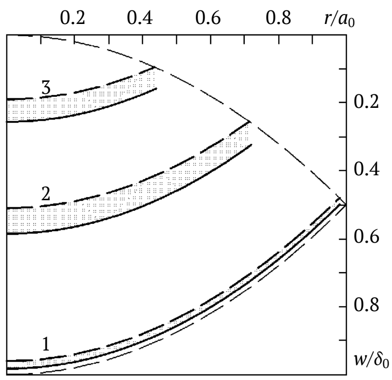

Figure 10. The normal displacements of points of loading area for the law $\delta = \delta_0 (1 - \tau/5)^2$
Note: $1 \rightarrow \tau = 1$, $2 \rightarrow \tau = 3.5$, $3 \rightarrow \tau = 4.5$
Source: developed by the authors

As expected, the deviations between quasi-static movements and movements caused by the gradual removal of the load increase with a decrease in the period of unloading. However, another regularity is noteworthy: at any fixed moment, these deviations are practically independent of the radial coordinate, i.e., the surface profile upon gradual removal of the load repeats the profile of an imaginary stamp, but at a slightly greater depth, depending on time. The latter suggests that by reducing the amplitude of surface forces, but leaving their distribution along the radial coordinate unchanged, it is possible to achieve a match between quasi-static and dynamic displacements. Setting instead of (15) the pressure in the form:

$$p(r,t) = kp_0(t)\sqrt{1 - r^2/a^2(t)}, r < a(t), t > 0, \quad (29)$$

It is necessary to select a coefficient from the condition of the least deviation of the displacement of the points of the surface of the half-space from the profile of the indenter.

Since the magnitude of the deviation varies with time, the coefficient k, in general, should be considered as a function of time. But for sufficiently long periods of unloading, a reasonable solution to the problem can be obtained, assuming that k is constant. In this case, this coefficient is the recovery coefficient during unloading of the half-space. The difference of $1 - k$ is the ratio of the energy carried away by elastic waves from the contact zone during unloading to the total initially accumulated energy of elastic deformation of the half-space.

The calculations were carried out for all three types of half-space unloading according to the proposed scheme. As a criterion for determination of the value of the coefficient k, the coincidence of the normal displacements of the half-space surface points and the corresponding indenter points averaged over the radius and over the complete unloading time was chosen, i.e.:

$$\int_0^T dt \int_0^{a(t)} \left(\widetilde{w}^g(r,t) - \widehat{w}^H(r, a(t))\right) r dr = 0. \quad (30)$$

As such, the value depends not only on the dimensionless period of unloading τ_{max} but also on its nature. For the linear law of change in the depth of penetration the coefficient k is equal:

$$k \approx \frac{0{,}6}{\tau_{max}}, \quad (31)$$

for the other two laws, it is equal:

$$k \approx \frac{0{,}4}{\tau_{max}}, \quad (32)$$

(in the case of uniformly accelerated unloading, the value is slightly less than in the case of inertial movement of the indenter). It should be noted that expressions (31)-(32) make sense only for sufficiently large periods of unloading ($\tau_{max} \geqslant 10$). Otherwise, even for the optimal value, the deviations at certain points in time become comparable with the magnitudes of the displacements themselves.

However, the dimensionless contact period τ_{max} is inversely proportional to the ratio of the speed of insertion/

removal of an imaginary indenter and the speed of elastic waves in elastic space c_0. Therefore, the results obtained qualitatively coincide with those known from the literature, for example, those obtained by I.I. Argatov (2012), stating that the part of the energy spent on the formation of elastic waves increases with increasing this ratio. I.I. Argatov (2012) carried out an asymptotic analysis of the interaction of an elastic half-space with a slowly moving rigid spherical indenter. The superseismic and subsonic phases of interaction were considered separately. For each of them, the expressions for maximum penetration, contact time, and contact force dependence on time are derived. Based on the obtained relations, the above statement on the negligence of the superseismic phase can be questioned.

Therefore, the conclusion reached by H. Xie *et al*. (2022) on the independence of the maximum pressure from the indenter speed could be derived from the method used. At the same time, calculations of this study confirm the conclusion of K.L. Johnson (2012) on the insignificance of the contribution of the superseismic phase to the overall picture of contact interaction. Attempts of rectification of Hertz's theory for the case of dynamic contact were made repeatedly. An analysis of earlier studies was conducted by K.L. Johnson (2012). In particular, the time of the so-called super seismic phase, when the boundary of the contact area moves faster than elastic waves, was determined as negligible. In addition, it is noted that for indenter velocities of an order of magnitude lower than the elastic wave velocities in the half-space, the quasi-static Hertz theory gives a good approximation. The applicability criterion for such an approach, which is called Love's criterion, is given in the fundamental paper of K.L. Johnson (2012). According to this criterion, it has the following formulation: Hertz's theory approximates the real distribution of contact pressure more accurately, that the smaller the ratio of the approach (retreat) velocity of the bodies V to the characteristic value of the elastic wave velocities inside the bodies themselves c_0. The physical implication of this criterion determines that the more times the elastic waves return to the point of impact during the contact time (it is reflected from the distant boundaries of the bodies) the more the deformation process can be like static deformation. As K.L. Johnson (2012) pointed out, this criterion is true even if the dimensions of one of the bodies are so large that during the time of contact, the waves do not have time to return to the point of impact.

C. Zhao (2011), Y. Shen & V. Giurgiutiu (2014) proved that an example of the practical application of the results of dynamic contact mechanics was non-destructive ultrasonic testing and monitoring. However, the determination of contact stresses in the case of the exact formulation of the corresponding boundary value problems of the dynamic theory of elasticity is accompanied by overcoming some mathematical difficulties. H. Jalali & P. Rizzo (2021) concluded that one of the characteristic features of non-stationary contact problems is the dependence of the size, and sometimes the shape of the contact area concerning time, which cannot be deducted in advance. Y. Yang *et al.* (2019) and Q. Peng *et al.* (2021) determined that the absence of relatively simple analytical expressions for contact stresses that consider local dynamic effects is the reason for the practically uncontested use of Hertz's quasi-static theory of impact in applied problems.

Thus, the obtained results of calculations and graphical dependencies obtained on their basis indicate that the gradual removal of the load from the surface of the elastic half-space has been achieved and the Hertzian pressure can be determined sufficiently accurately by the proposed method.

CONCLUSIONS

In the course of the research, an efficient method for calculating normal displacements in the area of loading during dynamic contact interaction of elastic bodies was developed. This method is based on exact solutions to non-stationary problems and holds practical significance for modelling structures operating at high velocities. The only significant parameter in the problem of gradual loading (unloading) of an elastic half-space, excluding the Poisson ratio of the material of the half-space, is the dimensionless loading (unloading) period τ_{max}, which is equal to the characteristic diameter of the loading area, which the Rayleigh wave travels during the loading (unloading) time. With a gradual removal of pressure, the normal displacements of the points of the loading area always lag behind the corresponding quasi-static values given by Hertz's theory, and this lag is proportional to τ^{-1}_{max} for large values of the dimensionless period of unloading. This phenomenon of inertia of points on the surface of the half-space leads to a decrease in the contact pressure compared to the Hertz pressure when the indenter is removed (it is logical to assume that when the indenter is deepened, the inertia of the surface of the half-space leads to an increasing in pressure). For sufficiently long periods of unloading ($\tau_{max} \geqslant 10$), the deviation of normal displacements from its quasi-static value is practically independent of the radial coordinate, i.e., uniform over the loading area, independently of the unloading law. For long periods of unloading, the ratio of the energy spent on the formation of elastic waves to the total energy of the initial elastic deformation is described by the expression $C\tau^{-1}_{max}$, where the constant value of C is different for different laws of unloading.

Considering the rapid development of computing tools, it seems promising to study this problem using the finite element method. This approach will not only allow us to compare numerical results but also suggest the time dependence of the penetration depth of a real, rather than imaginary, stamp. The latter, in turn, will make it possible to perform a more accurate assessment of the energy of elastic waves using the proposed analytical method.

ACKNOWLEDGEMENTS

None.

CONFLICT OF INTEREST

None.

REFERENCES

[1] An, B., Sun, Y., Liu, J., Tao, G., Qian, Y., & Wang, P. (2023). The role of 3D contact geometry in modeling dynamic wheel-rail interaction at short-wave irregularities on rail surface. *Engineering Failure Analysis*, 153, article number 107559. doi: 10.1016/j.engfailanal.2023.107559.

[2] Argatov, I.I. (2012). Slow vertical motions of a spherical indenter on an elastic half-space. *Quarterly Journal of Mechanics and Applied Mathematics*, 65(1), 129-140. doi: 10.1093/qjmam/hbr023.

[3] Bazhenov, V.A., & Vabishchevich, M.O. (2020). Research of nonlinear dynamic deformation of spatial bodies with cracks. *Technology Audit & Production Reserves*, 2(1(52)), 16-23.

[4] Chen, Z., Wang, G., Xue, D., & Cui, D. (2021). Simulation and optimization of crushing chamber of gyratory crusher based on the DEM and GA. *Powder Technology*. 384, 36-50. doi: 10.1016/j.powtec.2021.02.003.

[5] Doroszuk, B, & Król, R. (2022). Industry scale optimization: Hammer crusher and dem simulations. *Minerals*, 12(2), article number 244. doi: 10.3390/min12020244.

[6] Gakhov, F.D. (2014). *Boundary value problems*. New-York: Elsevier.

[7] Habchi, W. (2018). *Finite element modeling of elastohydrodynamic lubrication problems*. Hoboken: John Wiley & Sons. doi: 10.1002/9781119225133.

[8] Jalali, H., & Rizzo, P. (2021). Numerical investigation of the interaction of highly nonlinear solitary waves with corroded steel plates. *International Journal of Mechanical Sciences*, 208, article number 106676. doi: 10.1016/j.ijmecsci.2021.106676.

[9] Johnson, K.L. (2012). *Contact mechanics*. Cambridge: Cambridge University Press. doi: 10.1017/CBO9781139171731.

[10] Kupchuk, I., Poberezhets, J., Kravets, R., & Lavreniuk, P. (2022). Energy intensity of the process of destruction of feed grain in conditions of dynamic contact interaction with the edge of the disc impactor. *Engineering, Energy, Transport AIC,* 117(2), 97-103. doi: 10.37128/2520-6168-2022-2-10.

[11] Kutzenko, A.G., Ulitko, A.F., & Oliynik, V. (2001). Displacements of the elastic half-space surface caused by instantaneous axisymmetric loading. *International Journal of Fluid Mechanics Research,* 28(1&2), 258-273. doi: 10.1615/InterJFluidMechRes.v28.i1-2.190.

[12] Le, T.M., Wongviboonsin, W., Lawongkerd, J., Bui, T.Q., & Rungamornrat, J. (2021). Influence of surface and couple stresses on response of elastic substrate under tilted flat indenter. *Applied Mathematical Modelling*, 104, 644-665. doi: 10.1016/j.apm.2021.12.013.

[13] Lee, A., & Komvopoulos, K. (2018). Dynamic spherical indentation of elastic-plastic solids. *International Journal of Solids and Structures,* 146, 180-191. doi: 10.1016/j.ijsolstr.2018.03.028.

[14] Lv, X., Su, J., Tian, J.-Y., & Ke, L.-L. (2021). Dynamic contact response of an elastic sphere on a piezoelectric half-space, *Applied Mathematical Modelling*, 100, 16-32. doi: 10.1016/j.apm.2021.07.012.

[15] Peng, Q., Liu, X., & Wei, Y. (2021). Elastic impact of sphere on large plate. *Journal of the Mechanics and Physics of Solids,* 156, article number 104604. doi: 10.1016/j.jmps.2021.104604.

[16] Popov, V.G., & Kirillova, A.I. (2020). Mathematical modeling of contact interaction under torsional oscillations. In *International Scientific and Technical Conference "Ship Electrical Engineering, Electronics and Automation"* (pp. 133-136). Odesa: National University "Odessa Maritime Academy".

[17] Shen, Y., & Giurgiutiu, V. (2014) Predictive modeling of nonlinear wave propagation for structural health monitoring with piezoelectric wafer active sensors. *Journal of Intelligent Materials Systems and Structure*. 25(4), 506-520. doi: 10.1177/1045389X13500572.

[18] Tian, X., Liu, Y., Deng, J., Wang, L., & Chen, W. (2020). A review on piezoelectric ultrasonic motors for the past decade: Classification, operating principle, performance, and future work perspectives. *Sensors and Actuators A: Physical*, 306, article number 111971. doi: 10.1016/j.sna.2020.111971.

[19] Toyama, S., & Nishizawa, U. (2017). Micro ultrasonic motor for miniature robot arm. *Vibroengineering PROCEDIA,* 13, 127-131. doi: 10.21595/vp.2017.18999.

[20] Wankhede, S.P., & Xu, T.-B. (2021). The roles of piezoelectric ultrasonic motors in industry 4.0 Era: Opportunities and challenges. *Piezoelectric Actuators – Principles, Design, Experiments and Applications*. doi: 10.5772/intechopen.100560.

[21] Xie, H., Zeng, Z., Su, M., Luo, J., & Dai, G. (2022). On mechanical and motion behavior of the normal impact interface between a rigid sphere and elastic half-space. *Applied Sciences*, 12(21), article number 11094. doi: 10.3390/app122111094.

[22] Yang, Y., Zeng, O., & Wan L. (2019). Dynamic response analysis of the vertical elastic impact of the spherical rock on the metal plate. *International Journal of Solids and Structures*, 158, 287-302. doi: 10.1016/j.ijsolstr.2018.09.017.

[23] Zhao, C. (2011). *Ultrasonic Motors*. Berlin: Springer. doi: 10.1007/978-3-642-15305-1.

[24] Zhao, J., Chen, S., Zhang, K., & Liu, Y. (2021). A review of many-body dissipative particle dynamics (MDPD): Theoretical models and its applications. *Physics of Fluids*, 33, article number 112002. doi: 10.1063/5.0065538.

Анастасія Григорівна Куценко
Кандидат фізико-математичних наук, доцент
Національний університет біоресурсів і природокористування України
03041, вул. Героїв Оборони, 15, м. Київ, Україна
https://orcid.org/0000-0003-1808-6773

Олексій Григорович Куценко
Кандидат фізико-математичних наук, доцент
Київський національний університет імені Тараса Шевченка
01033, вул. Володимирська, 60, м. Київ, Україна
https://orcid.org/0000-0001-5089-0409

Поступове зняття з поверхні пружного півпростору тиску Герца

Анотація. Визначення контактних напружень при нестаціонарному динамічному навантаженні пружних тіл має вирішальне значення для моделювання конструкцій при високих швидкостях, але це пов'язано з математичними труднощами через залежність від часу і часто невідомі розміри та форму контактної області. Основна мета роботи полягала в тому, щоб на основі точних розв'язків нестаціонарних задач для пружного півпростору отримати оцінку величини частини енергії, яка витрачається на утворення хвиль під час контактної взаємодії пружних тіл. Для цього за допомогою перетворення Ханкеля за радіальною координатою та перетворення Лапласа за часовою змінною реконструйовано розв'язок додаткової задачі – задачі про миттєве навантаження півпростору. Запропоновано метод знаходження переміщень у пружному півпросторі, який поступово навантажується (розвантажується) контактним тиском Герца. Його наявність дозволила перейти до розв'язання основної задачі – задачі поступового навантаження поверхні півпростору тиском Герца. Обґрунтовано можливість зміни порядку операцій диференціювання та інтегрування в отриманому представленні на основі властивостей підінтеграла. Розглянуто випадки, коли швидкість індентора постійна, коли його рух рівномірно прискорений і коли рух відповідає закону першої чверті періоду косинуса в часі. Зроблено висновок, що розподіл динамічних контактних напружень подібний до розподілу Герца. Зроблено оцінку частини енергії, що витрачається на формування пружних хвиль, для різних законів розвантаження. Практичне значення роботи полягає в розробці ефективного методу розрахунку нормальних переміщень на ділянці навантаження при динамічній контактній взаємодії пружних тіл, що може бути цінним для моделювання конструкцій, які працюють з високими швидкостями

Ключові слова: динамічна контактна взаємодія; уточнення контактного розподілу; енергія хвиль; перетворення Лапласа; штамп; перетворення Ханкеля

Machinery & Energetics
Vol. 14, No. 4. 2023

Journal homepage:
https://technicalscience.com.ua/en

UDC 621.87
DOI: 10.31548/machinery/4.2023.75

Viacheslav Loveikin*
Doctor of Technical Sciences, Professor
National University of Life and Environmental Sciences of Ukraine
03041, 15 Heroiv Oborony Str., Kyiv, Ukraine
https://orcid.org/0000-0003-4259-3900

Yuriy Romasevych
Doctor of Technical Sciences, Professor
National University of Life and Environmental Sciences of Ukraine
03041, 15 Heroiv Oborony Str., Kyiv, Ukraine
https://orcid.org/0000-0001-5069-5929

Ivan Kadykalo
PhD in Technical Sciences
National University of Life and Environmental Sciences of Ukraine
03041, 15 Heroiv Oborony Str., Kyiv, Ukraine
https://orcid.org/0000-0002-5686-5869

Dynamic analysis of the joint movement of the hoisting and slewing mechanisms of a boom crane

Abstract. To increase the productivity of boom cranes, the operation of individual mechanisms is combined. At the same time, dynamic loads on structural elements, drive mechanisms and loads on a flexible suspension increase, which reduces the reliability of crane operation and increases energy losses. Therefore, the research aims to consider the problem of the dynamics of the joint movement of the mechanisms for load slewing and hoisting of a boom crane. To study the dynamics of the joint movement of the mechanisms, the boom system was represented by a mechanical system with 6DOF, where the basic movement of the mechanisms and the oscillatory movement of the structural links with elastic and dissipative properties, as well as the load on a flexible suspension in the plane of crane slewing and hoisting were considered. For such a mechanical system of a crane, the differential equations of the joint motion of the crane slewing and hoisting mechanisms were developed. The obtained equations are a system of the second order nonlinear differential equations, for solving which a numerical method in the form of a computer program was used. Using the developed program, the dynamics of the joint movement of the mechanisms of a jib crane with specific numerical parameters were calculated. Based on the calculations, a dynamic analysis of the joint movement of the mechanisms for slewing and hoisting the load of a jib crane with a hoisting boom was carried out, which revealed high-frequency vibrations of links with elastic and dissipative properties, as well as low-frequency oscillations of the load on a flexible suspension. The greatest impact of oscillations is observed during the start-up of mechanisms, where high-frequency oscillations dampen during the transient process, and low-frequency oscillations dampen over a fairly significant period. To improve the dynamic properties of the mechanisms for turning and hoisting a load during their joint movement, it is proposed to

Article's History: Received: 20.06.2023; Revised: 29.09.2023; Accepted: 22.11.2023.

Suggested Citation:
Loveikin, V., Romasevych, Yu., & Kadykalo, I. (2023). Dynamic analysis of the joint movement of the hoisting and slewing mechanisms of a boom crane. *Machinery & Energetics,* 14(4), 75-85. doi: 10.31548/machinery/4.2023.75.

*Corresponding author

optimise the mode of movement in the areas of transient processes (start-up, braking). The research results can be used in the development and operation of cranes in mechanical engineering, construction, and other industries

Keywords: tower; drive; slewing; load; flexible suspension; oscillation; amplitude

INTRODUCTION

Heavy loads are moved by various types of cranes: overhead, container, rotary and tower cranes. They are used in industry and construction. To increase the productivity of boom cranes, the combined operation of several mechanisms is often used. T. Yang *et al.* (2019) found that, in particular, it is quite common to combine the operation of the load hoisting mechanism and the crane's slewing mechanism. At the same time, with such operation of crane mechanisms, dynamic loads increase in their drive elements and structures. These loads have a significant impact on the reliability of the structure and energy consumption.

M. Ambrosino *et al.* (2020) traced the relationship between performance and dynamic loads in a crane system. O. Podolyak *et al.* (2022) investigated the dependence of the dynamic load on the crane on the swing movement of the load. Mathematical methods were used to build a mathematical model of motion dynamics describing the transient processes of the DEK-251 diesel-electric crawler crane (Soviet Union). The dynamic loads are estimated according to the design schemes. V. Lovejkin *et al.* (2020) focused on the dynamic analysis of flexible crane systems with programmable constraints. It is established that during the start-up process, oscillations occur that can affect the capacity and reliability of the crane. It is proposed to optimise start-up modes to reduce oscillations and improve performance. Q. Wu *et al.* (2020) considered the dynamic analysis of a crane with a double pendulum and a distributed mass beam.

Therefore, the need to study the dynamics of boom cranes when the mechanisms for hoisting and slewing the crane are in operation is determined. It is necessary to consider the low-frequency oscillations of the load on a flexible suspension and the high-frequency vibrations of links with elastic and dissipative elements.

To improve the efficiency of a crane system (speed and positioning accuracy, etc.), the angular oscillations of the load must be kept within small limits, which is achieved by using a controller (Zhang, 2019). Research on the control of crane systems is widespread and long-term. However, most control methods have been proposed mainly for overhead or container cranes (Jaafar *et al.* 2019), and the number of control methods for tower cranes is much smaller than for overhead cranes. The strength and wear of the crane and its parts: body, jib, and boom, can be assessed by numerical analysis (Buczkowski & Żyliński, 2021).

A. Mohammed *et al.* (2019) suggested a method for controlling the input signal alongside a logic algorithm strategy for tuning the acceleration of a trolley. The polynomial function is defined as an input to accelerate the trolley to move the load along a certain trajectory that meets the system constraints while achieving the desired end conditions. X. Wang *et al.* (2019) proposed a unified symplectic pseudospectral method for motion planning and control of 3D-guided overhead cranes. I. Umaru *et al.* (2021) showed a hybrid control system for oscillation damping and precise positioning of the trolley in gantry crane systems. The hybrid control system combines the formation of an input signal with zero oscillations and the zero derivative of oscillations to suppress oscillations. A. Mohammed *et al.* (2023) demonstrated an optimised controller using a multi-objective genetic algorithmic optimisation strategy. The purpose of the proposed method is to minimise the residual oscillations of the crane load that occur when the load is moved from one position to another, starting from non-zero initial conditions.

Thus, the problem of determining the actual dynamic loads that arise during the joint operation of the crane hoisting and slewing mechanisms is quite relevant, as it reflects the real conditions of boom cranes during operation. Therefore, the research aims to determine the dynamic loads in the elements of boom cranes during the joint operation of the mechanisms of the hoisting and crane slewing.

MATERIALS AND METHODS

The boom system of the crane was represented by a mechanical system consisting of absolutely rigid links of the crane slewing and hoisting mechanisms. At the same time, the traction rope of the hoisting mechanism has elastic and dissipative properties, and the flexible load suspension oscillates in the crane outreach and slewing plane and has dissipative properties. In addition, the slewing mechanism drive has elastic and dissipative properties. All the elements of the drive of the hoisting mechanism were connected to the axis of the drive drum, and the drive of the slewing mechanism to the crane's rotation part (column). The hoist rope forms a poly-sling system in which the load is suspended.

Based on the aforementioned, Figure 1 shows a dynamic model of the boom system with the combined movement of the slewing and hoisting mechanisms, which has 6 degrees of freedom. The generalised coordinates of this system are the angular coordinates of the rotation drive α, the drive of the hoisting mechanism β, the crane rotation part φ, the load slewing ψ and the linear coordinates of the load centre of mass when moving in the plane, where coordinate x changes and hoisting in the vertical plane u.

The boom system is subject to the driving forces of the crane's slewing drive mechanisms M_1 and load hoisting M_2, as well as the torque of the resistance forces in the swivel part of the crane M_0 and the mass of the load with the gripper and the bock-and-tackle system. In addition, elastic and dissipative forces act in the elastic elements of the drive mechanisms and the flexible load suspension.

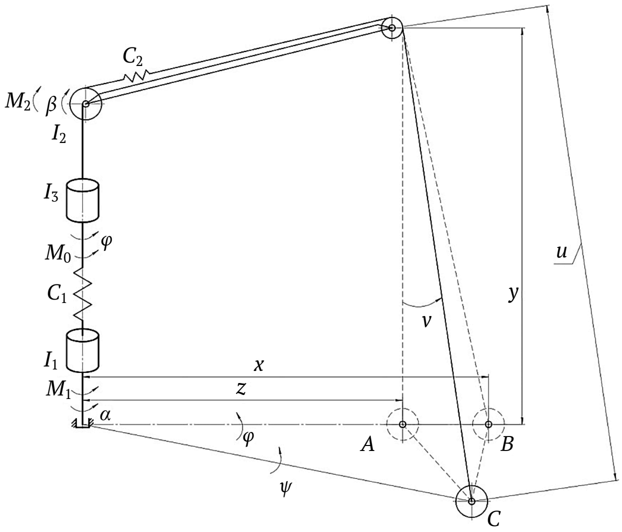

Figure 1. Dynamic model of a boom system with simultaneous movement of the turning and hoisting mechanisms

Note: generalised angular coordinates of the drive of the slewing mechanism α, drive of the load hoisting mechanism β, the rotation part of the crane φ, rotation the load ψ and the linear coordinates of the centre of mass of the load when moving in the plane of starting position change x and hoisting in the vertical plane u; driving forces of the crane slewing drive mechanisms M_1 and load hoisting M_2, moment of resistance forces in the rotation part of the crane M_0; I_1, I_2 – the moments of inertia of the drives of the crane's rotation part and the drive drum of the hoisting mechanism, respectively, are reduced to the axes of the slewing and hoisting mechanisms; I_3 – moment of inertia of the crane slewing part relative to its rotational axis; y – vertical coordinate of the load's centre of mass; z – initial value of the load starting position; v – angular coordinate of deviation from the vertical of the poly-sling system of the load hoisting mechanism; C_1, C_2 – the stiffness coefficients of the drive mechanisms for rotation and hoisting the load are reduced in accordance with the axes of rotation of the crane and the drive drum of the hoisting mechanism; A, B, C - initial, intermediate and final positions of the load during movement

Source: compiled by the authors

To build a mathematical model of the joint movement of the load hoisting and crane slewing mechanisms, represented by the dynamic model in Figure 1, the second order Lagrange equations were applied:

$$\begin{cases} \frac{d}{dt}\frac{\partial T}{\partial \dot{\alpha}} - \frac{\partial T}{\partial \alpha} = M_1 - \frac{\partial P}{\partial \alpha} - \frac{\partial R}{\partial \dot{\alpha}}; \\ \frac{d}{dt}\frac{\partial T}{\partial \dot{\beta}} - \frac{\partial T}{\partial \beta} = M_2 - \frac{\partial P}{\partial \beta} - \frac{\partial R}{\partial \dot{\beta}}; \\ \frac{d}{dt}\frac{\partial T}{\partial \dot{\phi}} - \frac{\partial T}{\partial \phi} = -M_0 - \frac{\partial P}{\partial \phi} - \frac{\partial R}{\partial \dot{\phi}} \\ \frac{d}{dt}\frac{\partial T}{\partial \dot{\psi}} - \frac{\partial T}{\partial \psi} = -\frac{\partial P}{\partial \psi} - \frac{\partial R}{\partial \dot{\psi}}; \\ \frac{d}{dt}\frac{\partial T}{\partial \dot{x}} - \frac{\partial T}{\partial x} = -\frac{\partial P}{\partial x} - \frac{\partial R}{\partial \dot{x}}; \\ \frac{d}{dt}\frac{\partial T}{\partial \dot{u}} - \frac{\partial T}{\partial u} = -\frac{\partial P}{\partial u} - \frac{\partial R}{\partial \dot{u}}, \end{cases} \qquad (1)$$

where T, P, R – are the kinetic and potential energy of the system, respectively, and the Rayleigh dissipative function; M_1, M_2 – driving torques of the drive mechanisms for crane slewing and hoisting, summed up according to the rotation part of the crane and the drive drum of the hoisting mechanism (torques M_1, M_2 are determined from the mechanical characteristics of electric motors according to the Kloss formula (Lovejkin *et al.*, 2020)); M_0 – the moment of resistance forces in the rotary part of the crane, reduced to the rotation axis.

The kinetic energy of the boom system during the joint movement of the mechanisms for rotation and hoisting the load was expressed through generalised coordinates and is represented by the following dependence:

$$T = \frac{1}{2}I_1\dot{\alpha}^2 + \frac{1}{2}I_2\dot{\beta}^2 + \frac{1}{2}I_3\dot{\phi}^2 + \frac{1}{2}m\left(\dot{x}^2 + \dot{y}^2 + \dot{\psi}^2 x^2\right), \qquad (2)$$

where I_1, I_2 – the moments of inertia of the drives of the crane's rotation part and the drive drum of the hoisting mechanism, respectively, are reduced to the axes of the slewing and hoisting mechanisms; m – load mass; I_3 – moment of inertia of the crane slewing part relative to its rotation axis; y – vertical coordinate of the centre of load mass.

The potential energy function of the joint movement system of the slewing and hoisting mechanisms:

$$P = \frac{1}{2}C_1(\phi - \alpha)^2 + \frac{1}{2}C_2(\text{nu-}\beta r)^2 - mgu\cos v, \qquad (3)$$

where C_1, C_2 – the stiffness coefficients of the drive mechanisms for rotation and hoisting the load are reduced following the axes of rotation of the crane and the drive drum of the hoisting mechanism; r – radius of the drive drum of the load hoisting mechanism; n – multiplicity of the load hoisting mechanism; g – free fall acceleration; v – angular coordinate of deviation from the vertical of the block-and-tackle system of the load hoisting mechanism.

The Rayleigh dissipative function is expressed by the following relationship:

$$R=\frac{1}{2}b_1(\dot{\phi}-\dot{\alpha})^2+\frac{1}{2}b_2(n\dot{u}-\dot{\beta}r)^2+\frac{1}{2}b\dot{v}^2, \tag{4}$$

where b_1, b_2, b – Dissipation coefficients of elastic elements, respectively, of the drives of the mechanisms for slewing and hoisting the load, as well as the flexible load suspension.

To find the coordinate of the deviation from the vertical of the load rope (block-and-tackle system) (Fig. 1), the following geometric relationships are used:

$$\mathrm{AB}=\text{x-z};\;\; \mathrm{BC}=x(\phi-\psi);\, \angle\mathrm{ABC}=\frac{\pi}{2}-\frac{\phi-\psi}{2}; \tag{5}$$

$$\begin{aligned}AC&=\sqrt{AB^2+BC^2-2AB\cdot BC\cdot \cos\angle ABC}=\\&=\sqrt{(x-z)^2+x^2(\phi-\psi)^2-2(x-z)x(\phi-\psi)\cdot \sin\frac{\phi-\psi}{2}}.\end{aligned} \tag{6}$$

Since during the operation of cranes, the deviation of the load rope from the vertical does not exceed 12°, then it is possible to assume $\sin\frac{\varphi-\psi}{2}=\frac{\varphi-\psi}{2}$ which will result in:

$$\begin{aligned}AC&=\sqrt{(x-z)^2+x^2(\phi-\psi)^2-x^2(\phi-\psi)^2+zx(\phi-\psi)^2}=\\&=\sqrt{(x-z)^2+zx(\phi-\psi)^2}.\end{aligned} \tag{7}$$

Given the latter expression, the angular coordinate of the deviation of the block-and-tackle system from the vertical was determined by the dependence:

$$v=\frac{\mathrm{AC}}{u}=\frac{1}{u}\sqrt{(x-z)^2+zx(\phi-\psi)^2}, \tag{8}$$

where z – initial load starting position.

Dependencies were used to determine the vertical coordinate and velocity of the centre of mass of the load during the joint operation of the mechanisms for hoisting the load and the crane slewing:

$$y=u\cos v;\; \dot{y}=\dot{u}\cos v-\dot{v}u\sin v. \tag{9}$$

The derivatives of the kinetic energy required for the system of equations (1) are found:

$$\frac{\partial T}{\partial\alpha}=\frac{\partial T}{\partial\beta}=\frac{\partial T}{\partial\phi}=\frac{\partial T}{\partial\psi}=0;\frac{\partial T}{\partial x}=\mathrm{m}x\dot{\psi}^2;\frac{\partial T}{\partial u}=m\dot{y}\frac{\partial\dot{y}}{\partial u}; \tag{10}$$

$$\frac{\partial T}{\partial\dot{\alpha}}=I_1\dot{\alpha};\frac{\partial T}{\partial\dot{\beta}}=I_2\dot{\beta};\frac{\partial T}{\partial\dot{\phi}}=I_3\dot{\phi};\frac{\partial T}{\partial\dot{\psi}}=\mathrm{m}x^2\dot{\psi}; \tag{11}$$

$$\frac{\partial T}{\partial\dot{x}}=\mathrm{m}\dot{x};\;\; \frac{\partial T}{\partial\dot{u}}=m\dot{y}\frac{\partial\dot{y}}{\partial\dot{u}}=m\dot{y}\frac{\partial y}{\partial u}; \tag{12}$$

$$\frac{d}{dt}\frac{\partial T}{\partial\dot{\alpha}}=I_1\ddot{\alpha};\frac{d}{dt}\frac{\partial T}{\partial\dot{\beta}}=I_2\ddot{\beta};\frac{d}{dt}\frac{\partial T}{\partial\dot{\phi}}=I_3\ddot{\phi}; \tag{13}$$

$$\frac{d}{dt}\frac{\partial T}{\partial\dot{\psi}}=\mathrm{m}x^2\ddot{\psi}+2mx\dot{x}\dot{\psi};\frac{d}{dt}\frac{\partial T}{\partial\dot{x}}=\mathrm{m}\ddot{x}; \tag{14}$$

$$\frac{d}{dt}\frac{\partial T}{\partial\dot{u}}=m\ddot{y}\frac{\partial y}{\partial u}+m\dot{y}\frac{\partial\dot{y}}{\partial u}. \tag{15}$$

Several derivatives included in expressions (9)...(15) were found:

$$\begin{aligned}\frac{\partial\dot{y}}{\partial u}&=-\dot{u}\frac{\partial v}{\partial u}\sin v-\left(\dot{v}+u\frac{\partial\dot{v}}{\partial u}\right)\sin v-u\dot{v}\frac{\partial v}{\partial u}\cos v;\\ \frac{\partial y}{\partial u}&=\cos v-u\frac{\partial v}{\partial u}\sin v.\end{aligned} \tag{16}$$

$$\begin{aligned}\ddot{y}&=\ddot{u}\cos v-\dot{u}\dot{v}\sin v-\ddot{v}u\sin v-\dot{u}\dot{v}\sin v-\dot{v}^2u\cos v=\ddot{u}\cos v-\\&-2\dot{u}\dot{v}\sin v-\dot{v}^2u\cos v-\ddot{v}u\sin v.\end{aligned} \tag{17}$$

Partial derivatives of the potential energy of the system were taken, which was expressed by dependence (3):

$$\frac{\partial P}{\partial\alpha}=-C_1(\phi-\alpha);\frac{\partial P}{\partial\beta}=-C_2r(nu-\beta r); \tag{18}$$

$$\frac{\partial P}{\partial u}=C_2n(nu-\beta r)-mg\left(\cos v-u\frac{\partial v}{\partial u}\sin v\right); \tag{19}$$

$$\frac{\partial P}{\partial\phi}=C_1(\phi-\alpha)+mgu\sin v\frac{\partial v}{\partial\phi}; \tag{20}$$

$$\frac{\partial P}{\partial\psi}=mgu\frac{\partial v}{\partial\psi}\sin v;\frac{\partial P}{\partial x}=mgu\frac{\partial v}{\partial x}\sin v. \tag{21}$$

Expressions (18), and (21) contain partial derivatives of the function of the load rope deviation from the vertical by generalised coordinates. These derivatives were determined:

$$\frac{\partial v}{\partial u}=-\frac{1}{u^2}\sqrt{(x-z)^2+zx(\phi-\psi)^2}; \tag{22}$$

$$\frac{\partial v}{\partial\phi}=\frac{1}{u}\frac{zx(\phi-\psi)}{\sqrt{(x-z)^2+zx(\phi-\psi)^2}}; \tag{23}$$

$$\frac{\partial v}{\partial\psi}=-\frac{1}{u}\frac{zx(\phi-\psi)}{\sqrt{(x-z)^2+zx(\phi-\psi)^2}}; \tag{24}$$

$$\frac{\partial v}{\partial x}=\frac{1}{u}\frac{(x-z)+z(\phi-\psi)^2/2}{\sqrt{(x-z)^2+zx(\phi-\psi)^2}}. \tag{25}$$

Partial derivatives of the Rayleigh dissipative function:

$$\frac{\partial R}{\partial\dot{\alpha}}=-b_1(\dot{\phi}-\dot{\alpha});\frac{\partial R}{\partial\dot{\beta}}=-b_2r(n\dot{u}-\dot{\beta}r); \tag{26}$$

$$\frac{\partial R}{\partial\dot{u}}=b_2n(n\dot{u}-\dot{\beta}r)+b\dot{v}\frac{\partial\dot{v}}{\partial\dot{u}}; \tag{27}$$

$$\frac{\partial R}{\partial\dot{\phi}}=b_1(\dot{\phi}-\dot{\alpha})+b\dot{v}\frac{\partial\dot{v}}{\partial\dot{\phi}}; \tag{28}$$

$$\frac{\partial R}{\partial\dot{\psi}}=b\dot{v}\frac{\partial\dot{v}}{\partial\dot{\psi}};\frac{\partial R}{\partial\dot{x}}=b\dot{v}\frac{\partial\dot{v}}{\partial\dot{x}}. \tag{29}$$

Angular rate of deviation of the load rope from the vertical:

$$\dot{v}=\frac{1}{u^2}\left\{\frac{(x-z)\cdot\dot{x}+z[\dot{x}(\phi-\psi)^2/2+x(\phi-\psi)(\dot{\phi}-\dot{\psi})]}{\sqrt{(x-z)^2+zx(\phi-\psi)^2}}\cdot u-\dot{u}\sqrt{(x-z)^2+zx(\phi-\psi)^2}\right\}. \tag{30}$$

The partial derivatives of function (30) are taken, and the result is:

$$\frac{\partial\dot{v}}{\partial\dot{u}}=\frac{\partial v}{\partial u}=-\frac{1}{u^2}\sqrt{(x-z)^2+zx(\phi-\psi)^2}; \tag{31}$$

$$\frac{\partial\dot{v}}{\partial\dot{\phi}}=\frac{\partial v}{\partial\phi}=\frac{1}{u}\frac{zx(\phi-\psi)}{\sqrt{(x-z)^2+zx(\phi-\psi)^2}}; \tag{32}$$

$$\frac{\partial\dot{v}}{\partial\dot{\psi}}=\frac{\partial v}{\partial\psi}=-\frac{1}{u}\frac{zx(\phi-\psi)}{\sqrt{(x-z)^2+zx(\phi-\psi)^2}}; \tag{33}$$

$$\frac{\partial\dot{v}}{\partial\dot{x}}=\frac{\partial v}{\partial x}=\frac{1}{u}\frac{x+z[(\phi-\psi)^2/2-1]}{\sqrt{(x-z)^2+zx(\phi-\psi)^2}}. \tag{34}$$

After substituting expressions (9), (10), (14), (15), (18)..., (21), (26), ... (29) into system (1), a system of differential equations of motion of the joint movement of the mechanisms for slewing and hoisting the load of a boom crane is obtained:

$$\begin{cases} I_1\ddot{\alpha} = M_1 + C_1(\phi-\alpha) + b_1(\dot{\phi} - \dot{\alpha});\\ I_2\ddot{\beta} = M_2 + C_2 r(nu-\beta r) + b_2(n\dot{u} - \dot{\beta} r);\\ I_3\ddot{\phi} = -M_0 - C_1(\phi-\alpha) - mgu\frac{\partial v}{\partial\phi}\sin v - \\ \qquad -b_1(\dot{\phi}-\dot{\alpha}) - b\dot{v}\frac{\partial v}{\partial \phi};\\ mx^2\ddot{\psi} + 2mx\dot{x}\dot{\psi} = -mgu\frac{\partial v}{\partial\psi}\sin v - b\dot{v}\frac{\partial v}{\partial\psi};\\ m\ddot{x} - mx\dot{\psi}^2 = -mgu\frac{\partial v}{\partial x}\sin v - b\dot{v} \frac{\partial v}{\partial x};\\ m(\ddot{u}\cos v - 2\dot{u}\dot{v}\sin v - \dot{v}^2 u\cos v - \ddot{v} u \sin v)\cos v = \\ \quad = -C_2 n(nu-\beta r) + mg(\cos v - u\frac{\partial v}{\partial u}\sin v) - \\ -b_2 n(n\dot{u} - \dot{\beta} r) - b\dot{v}\frac{\partial v}{\partial u}.\end{cases} \qquad (35)$$

The resulting system of second-order differential equations is nonlinear and cannot be solved by analytical methods, so a numerical method is used to solve it, which is presented in the form of a developed computer program in the Wolfram Mathematica software. The following initial conditions for the joint movement of the mechanisms for slewing and hoisting the load are used:

$$\begin{gathered} t=0,\ \alpha = \frac{M_0}{C_1}, \dot{\alpha} = 0, \beta = \frac{u_0 \cdot 4}{r}, \dot{\beta} = 0, \beta = \frac{u_0 \cdot 4}{r}, \\ \dot{u} = 0, x = z = 40m, \dot{x} = 0, \phi = 0, \dot{\phi} = 0, \psi = 0, \dot{\psi} = 0. \end{gathered} \qquad (36)$$

The calculations of the dynamics of the joint movement of the mechanisms for slewing and hoisting the load of a boom crane were performed for the following initial data: I_1 = 71626.115 kg·m²; I_2 = 1249.93 kg·m²; I_3 = 4920738.85 kg·m²; C_1 = 6626669.045 (N·m)/rad; C_2 = 150796 (N·m)/rad; m = 2000 kg; z = 40 m; u = 20 m; r_b=0.25 m; n=4; M_{cr1}=85N·m; M_{cr2}=487.5N·m; M_{n1}=36.8 N·m; M_{n2} = 195 N·m; u_1 = 1355.2; u_2 = 116.56; η_1 = 0.86; η_2 = 0.85; ω_{o1} = 104.67 rad/c; ω_{o2} = 157 rad/c; ω_{n1} = 95.04 rad/c; ω_{n2} = 153.86 rad/c; λ_1 = 2.8; λ_2 = 2.5; $b = 2.1 \cdot 10^5 \frac{Nm}{m/s}$; $b_1 = 1 \cdot 10^5 \frac{Nm}{m/s}$; $b_2 = 1.5 \cdot 10^5 \frac{Nm}{m/s}$; g = 9.81 m/c².

RESULTS AND DISCUSSION

As a result of numerically solving the system of differential equations (35) under the initial conditions of movement of the mechanisms (36) using the developed computer program for a specific hoisting boom crane, graphical dependences of kinematic, dynamic, and energy characteristics were built. Figure 2 shows the graphical dependences of the angular velocities of the drive mechanisms for crane slewing and hoisting, plotted following the axes of rotation of the crane and the drive drum of the hoisting mechanism. The angular velocity graph of the slewing mechanism drive (Fig. 2a) shows that during the 5-second start-up period, there are alternating speed oscillations with an amplitude of -0.09 to +0.07 rad/s and a frequency of 1.4 s^{-1}, followed by reaching a steady-state value within 15 s. This mode of starting the slewing mechanism leads to significant dynamic loads in the drive elements and the rotary column. Since this study considers lowering the load, the drive mechanism for hoisting the load almost instantly (within 0.1 s) acquires the steady-state angular velocity of the drive drum (Fig. 2b). In this case, significant dynamic loads also act, but they take on an instantaneous value and in the steady-state movement section, the angular velocity of the drive drum takes on a constant value.

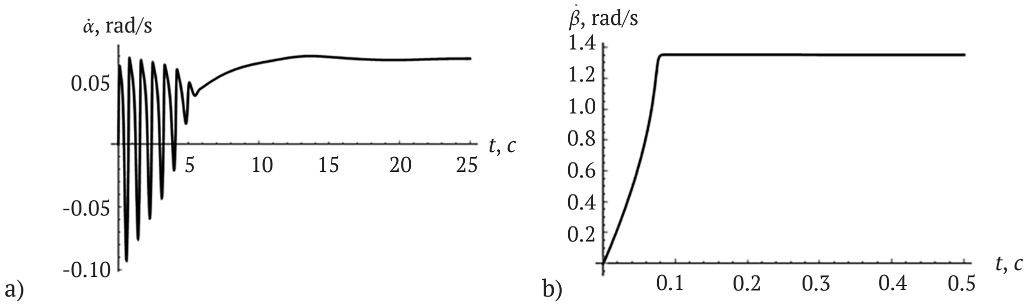

Figure 2. Angular speeds of drive mechanisms

Note: a) slewing; b) hoisting
Source: compiled by the authors

The graphical dependences of the angular accelerations of the drive mechanisms for crane slewing and hoisting (Fig. 3) confirm the results of the analysis of the angular velocities of these mechanisms. From Figure 3a, it can be seen that at the start-up section of the slewing mechanism, the drive elements exhibit alternating oscillations of angular accelerations with a maximum oscillation amplitude of 1.5 rad/s². After the start-up process, the acceleration oscillations of the slewing mechanism drive dampen and are practically zero in the steady-state motion area. When the load hoisting mechanism is started, the angular acceleration of the drive almost instantly increases to a maximum value of 40 rad/s² and then instantly decreases to zero. The instantaneous maximum acceleration of the hoisting actuator is an order of magnitude greater than the instantaneous maximum acceleration of the slewing actuator, but this action is instantaneous without further oscillations, which is not the case with the slewing actuator, which has damped oscillations.

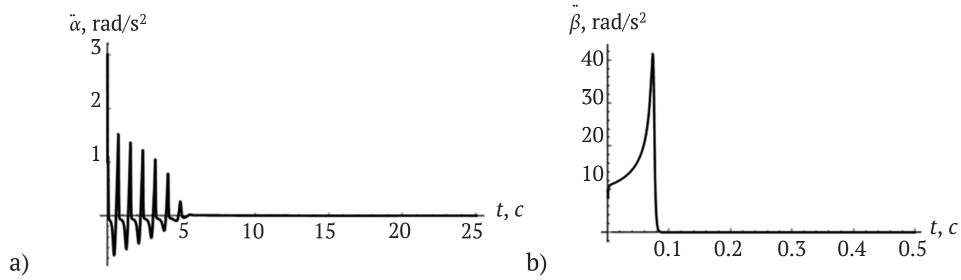

Figure 3. Angular accelerations of drive mechanisms

Note: a) crane slewing; b) load hoisting

Source: compiled by the authors

Figure 4 shows the angular velocity and acceleration of a crane slewing column. Figure 4a shows that the steady-state value of the column's angular velocity is reached after approximately 13 seconds of movement. At the same time, at the beginning of the start-up, within 5 seconds of movement, high-frequency speed oscillations with a small amplitude are observed. Subsequently, during the steady-state movement, there are slight low-frequency fluctuations in the column speed caused by the oscillations of the load on the flexible suspension. At the start-up section, high-frequency alternating oscillations of the column's angular acceleration are observed for 5 seconds of motion (Fig. 4b). Such a change in acceleration leads to the appearance of alternating dynamic loads in the column during the first seconds of start-up. Subsequently, the acceleration of the column decreases with minor low-frequency oscillations and tends to zero by the 25th second of movement.

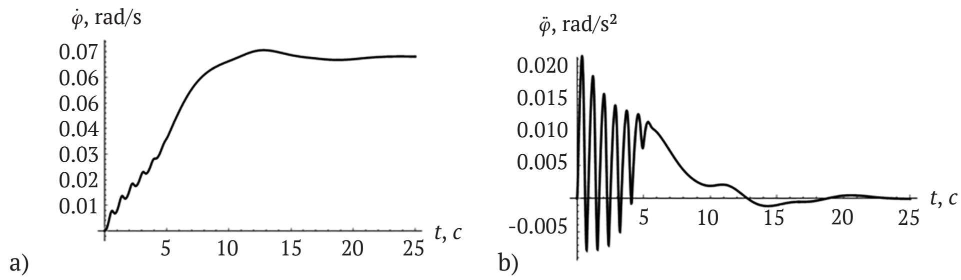

Figure 4. Angular velocity (a) and acceleration (b) of the crane column

Source: compiled by the authors

The linear velocity and acceleration of the axial movement of the load (Fig. 5) have a familiar oscillatory character caused by the centrifugal force when the crane is turning and the action of the horizontal component of the load's gravity when the load rope deviates from the vertical. As can be seen from Figures 5a and 5b, these oscillations require a significant duration of movement to dampen, which is not often enough for cranes to operate. Therefore, at the end of the crane's movement cycle, it is necessary to cease the load oscillations, which takes time and leads to a decrease in the crane's productivity.

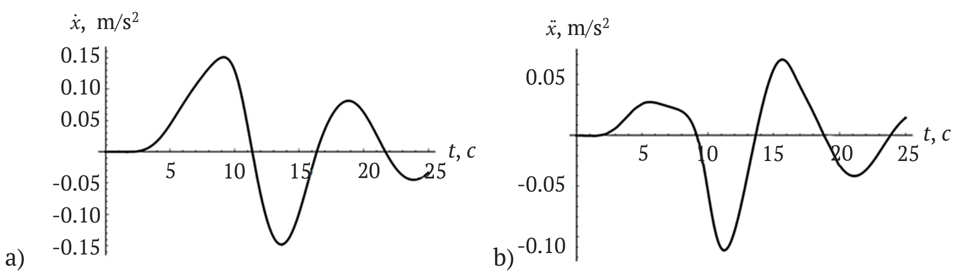

Figure 5. Linear velocity (a) and acceleration (b) of the load in the plane of starting position change

Source: compiled by the authors

Figure 6 shows the graphs of angular displacement, speed, and acceleration of the deviation from the vertical of the block-and-tackle system of the load hoisting mechanism. From Figure 6a, it can be seen that the deviation of the load chain from the vertical initially (during the first five seconds of movement) increases, and then low-frequency oscillations are observed with a decrease in the value of the deviation. At the same time, the deviation of the load hoist from the vertical does not change its sign, which indicates the dominant role of the centrifugal force of the load when the crane is turning. The rate of change of the deviation of the hoist from the vertical (Fig. 6b) consists of low-frequency and high-frequency components of oscillations in a section lasting up to 5 seconds, and then only the low-frequency component of oscillations remains, which fading over time. The angular acceleration of the deviation from the vertical of the load sling (Fig. 6c) also has a familiar high-frequency component of oscillations up to 5 seconds of movement, and after that, insignificant low-frequency oscillations of acceleration are observed, which practically dampen by 25 seconds of movement. Moreover, the amplitude of high-frequency oscillations significantly exceeds the amplitude of low-frequency oscillations of the angular acceleration of the load sling deviation from the vertical.

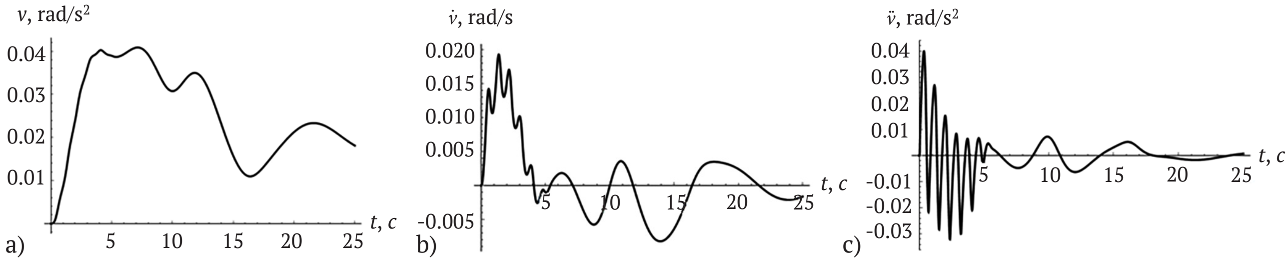

Figure 6. Poly-harness system deviation from the vertical
Note: a) angular changes, b) speed, c) velocity
Source: compiled by the authors

The driving torque of the electric motor (Fig. 7a) and the elastic torque in the transmission mechanism (Fig. 7b) of the rotation drive during the start-up phase change in an oscillatory mode with a high oscillation frequency for up to 6 seconds. Then, these moments decrease and take on steady-state values by the 25th second of movement. The maximum value of the driving torque is 100 kNm, and the elastic torque in the transmission mechanism is 120 kNm. Such a change in the driving torque leads to a significant increase in dynamic loads of an oscillatory nature in the structural elements and the drive, as evidenced by the graph of the elastic moment in the transmission mechanism, where the maximum value of the elastic moment is 20% higher than the maximum value of the driving torque. To reduce the dynamic loads in the elements of the boom system during the joint movement of the mechanisms for turning and hoisting the load, there is a need to eliminate oscillations and increase the smoothness of the change in the driving torques of the drive mechanisms.

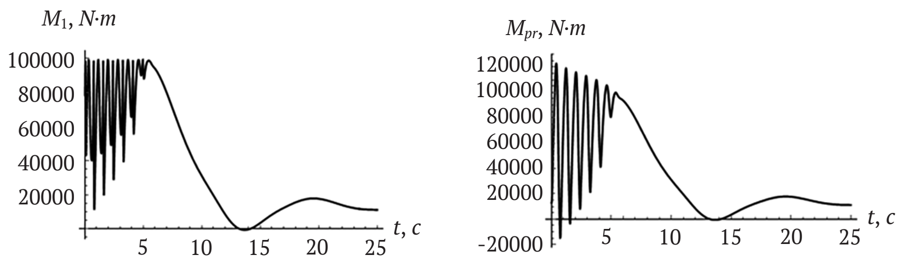

Figure 7. Crane rotational torques
Note: a) driving, b) elastic
Source: compiled by the authors

Figure 8 shows a graph of the power change of the slewing mechanism drive, which shows that at the beginning of the start-up, up to 5 seconds of movement, there is a familiar oscillating character of power change with its maximum value of 4.0 kW. Subsequently, the power changes smoothly and by the 25th second of movement, its steady-state value is established. The reason for the oscillations in the power change of the slewing drive mechanism is the oscillatory nature of the drive torque change, which depends on electromagnetic transients in the electric motor. Therefore, to eliminate oscillatory processes in the boom crane mechanisms, it is necessary to optimally control electromagnetic transients in the drive motors.

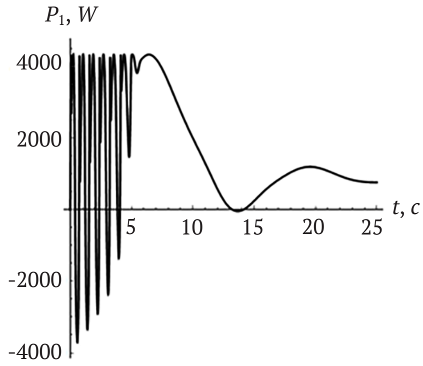

Figure 8. Diagram of power variation of the drive of the turning mechanism
Source: compiled by the authors

The research results obtained were compared with those of other authors. O. Podolyak *et al.* (2022) presented the construction of a mathematical model of the dynamics of the boom crane movement when three mechanisms work jointly: trolley movement, slewing, and load hoisting. Differential equations of motion are presented that describe the joint movement of the mechanisms without considering the elasticity of the links, but no numerical calculations are used in the constructed model. The study considers the elastic-dissipative properties of the drive mechanisms for crane hoisting and turning with the calculation of kinematic, dynamic, and energy numerical characteristics. At the same time, a significant influence of oscillatory processes on the dynamics of movement of the mechanisms for slewing and hoisting loads is shown. V. Lovejkin *et al.* (2020) considered a dynamic model of the motion of two mechanisms for the trolley movement and crane slewing, which considers the oscillations of the load on a flexible suspension, but all other links of the mechanisms are assumed to be rigid bodies. As a result of the calculation, the maximum rotation and acceleration speeds were obtained, which are 0.1 rad/s and 0.03 rad/s^2, respectively, while in the present article, the maximum speed in the slewing mechanism is 0.07 rad/s and the acceleration is 0.022 rad/s^2. N. Sun *et al.* (2019) built a mathematical model of the dynamics of load movement on a flexible suspension. They developed the differential equations of motion and conducted experimental studies, which showed that the maximum deviation of the load from the vertical is 0.11 rad. In the presented study, a similar result is 0.041 rad, which is almost 2.5 times less compared to the result obtained by N. Sun *et al.* (2019). M. Ambrosino *et al.* (2020) developed a mathematical model of the dynamics of movement of crane slewing and boom hoisting mechanisms with load oscillations on a flexible suspension in the plane of the trolley movement and crane slewing. As a result of the calculations, the maximum values of the load rope deviations from the vertical were obtained, which are 0.047 rad, In the proposed article, a similar result is 0.041 rad, which is almost the same as the result obtained by M. Ambrosino *et al.* (2020). R. Miranda-Colorado (2021) presents a new robust controller to dampen the oscillation of the deflection angle of a crane load suspension with a variable cable length. E. Jarzębowska *et al.* (2020) investigated the vibrations of flexible systems with programmable constraints. The automated procedure allows the analysis of both rigid and flexible systems. An example of a crane with a flexible boom and programmable constraints is demonstrated. S. Wang *et al.* (2019) studied an anti-error device with a triple cable mechanism for cranes that eliminates the disadvantages of existing methods of reducing oscillations. J. Wang *et al.* (2022) analysed a three-degree-of-freedom anti-error method for damping crane load oscillations on a ship. I.A. Martin *et al.* (2021) developed an anti-error control system for a crane on a ship with multiple degrees of freedom.

M. Zhang *et al.* (2019) developed a dynamic model of the movement of an overhead crane and simulated the dynamics of the movement of a load on a flexible suspension. The maximum deviation of the load from the vertical was determined to be 0.094 rad, while in the proposed study this value reaches 0.041 rad, which is 2.29 times higher than the result obtained. H. Ouyang *et al.* (2019) presented a dynamic model of an overhead crane, however, which is presented in the form of a double pendulum, and equations of motion describing transient processes (start-up, steady-state motion, and braking) were developed. The motion analysis was performed, and the method proposed by H. Ouyang *et al.* (2019) and the method of continuous sliding mode control (CSMC). The method proposed by H. Ouyang *et al.* (2019) proved to be better than the CSMC method, reducing the maximum values of load oscillations by almost 3.5 times. Comparing the method proposed by H. Ouyang *et al.* (2019) with the results obtained in the proposed study, which are 0.024 rad and 0.041 rad, respectively, it has a 1.7 times lower maximum amplitude of load oscillations, in contrast to the results obtained in the proposed article. However, it should be noted that the method proposed by H. Ouyang *et al.* (2019) is an optimization, while the proposed article was based on the mechanical characteristics of the engine (without optimization).

Considering the results obtained in the research and studies of other authors, it can be stated that the study of the dynamics of movement of crane mechanisms is relevant, and the results obtained in this article are close to those obtained by other authors.

CONCLUSIONS

Based on the results of the study of the dynamics of the joint movement of the mechanisms for boom crane slewing and hoisting, a mathematical model of the dynamics of the joint movement of the mechanisms for slewing and hoisting of the load of a boom crane with a hoisting boom was built, which is a system of six nonlinear second order differential equations. The developed model considers the main motion of the drive mechanisms for the crane slewing and hoisting the load, as well as high-frequency vibrations of the links of these mechanisms with elastic and dissipative properties, as well as low-frequency oscillations of the load on a flexible suspension. The solution of the system of nonlinear differential equations for the joint motion of the crane slewing and hoisting mechanisms was found by the numerical method using a specially developed computer program.

Based on the results of the calculations, a dynamic analysis of the joint movement of the mechanisms for turning and hoisting the load of a boom crane was carried out. The dynamic analysis of the joint movement of the hoisting and slewing mechanisms revealed significant dynamic loads in the elements of the drives and the crane structure during the process of starting the drive mechanisms. In the slewing mechanism elements, which have elastic and dissipative properties, the authors found familiar high-frequency oscillatory processes of kinematic, power, and energy characteristics that dampen rather quickly. At the same time, the low-frequency oscillations of the mechanism links and the load on a flexible suspension decay rather slowly or practically do not decay during the movement cycle. This primarily applies to the load on the flexible suspension, whose oscillations need to be dampened, which takes time and reduces crane productivity. When lowering the load during the start-up process, the hoisting mechanism is subject to instantaneous significant overloads that do not cause oscillations of the mechanism links.

It has been established that one of the reasons for the oscillatory processes in the crane slewing mechanism is the abrupt nature of the change in the drive torque. To reduce oscillatory processes in the crane elements, it is necessary to increase the smoothness of the change in the driving torque of the drive mechanisms. Low-frequency oscillations of crane structural elements, drive mechanisms, and load on a flexible suspension are recommended to be calmed by introducing boundary conditions of movement after the passage of transient processes (start-up, braking). The prospect for further research is to optimise the modes of movement of drive mechanisms to minimise dynamic loads on structural elements and eliminate oscillations of the load on a flexible suspension.

ACKNOWLEDGEMENTS

The research was carried out within the framework of and with the financial support of the TREATY grant project "Nurturing deep tech talents for clean and sustainable energy transition" within the framework of the EIT HEI Initiative "Innovation Capacity Building for Higher Education" No. 230047, Grant Agreement No. 10111303.

CONFLICT OF INTEREST

None.

REFERENCES

[1] Ambrosino, M., Berneman, M., Carbone, G., Dawans, A., & Garone, E. (2020). Modeling and control of a 5-DoF boom crane. In *2020 Proceedings of the 37th ISARC* (pp. 25-30). Kitakyushu, Japan. doi: 10.22260/ISARC2020/0071.

[2] Buczkowski, R., & Żyliński, B. (2021). Finite element fatigue analysis of unsupported crane. *Polish Maritime Research*, 28(1), 127-135. doi: 10.2478/pomr-2021-0012.

[3] Jaafar, H.I., Mahamed, Z., Shamsudin, M.A., Subha, N.A.M., Ramli, L., & Abdullahi, A.M. (2019). Model reference command shaping for vibration control of multimode flexible systems with application to a double-pendulum overhead crane. *Mechanical Systems and Signal Processing*, 115, 677-695. doi: 10.1016/j.ymssp.2018.06.005.

[4] Jarzębowska, E., Urbaś, A., & Augustynek, K. (2020). Analysis of influence of a crane flexible supports, link flexibility, and joint friction on vibration associated with programmed motion execution. *Journal of Vibration Engineering & Technologies*, 8, 337-350. doi: 10.1007/s42417-019-00186-1.

[5] Lovejkin, V., Romasevych, Yu., Loveikin, A., & Mushtyn, D. (2020). Dynamic analysis of roller molding installation taking into account dissipative properties balanced drive mechanism. *Machinery & Energetics*, 11(1), 5-11. doi: 10.31548/machenergy2020.01.005.

[6] Martin, I.A., & Irani, R.A. (2021). Dynamic modeling and self-tuning anti-sway control of a seven degree of freedom shipboard knuckle boom crane. *Mechanical Systems and Signal Processing*, 153, article number 107441. doi: 10.1016/j.ymssp.2020.107441.

[7] Miranda-Colorado, R. (2021). Robust observer-based anti-swing control of 2D-crane systems with load hoisting-lowering. *Nonlinear Dynamics*, 104, 3581-3596. doi: 10.1007/s11071-021-06443-x.

[8] Mohammed, A., Alghanim, K., & Andani, M.T. (2019) An optimized non-linear input shaper for payload oscillation suppression of crane point-to-point maneuvers. *International Journal of Dynamics and Control*, 7, 567-576. doi: 10.1007/s40435-019-00536-7.

[9] Mohammed, A., Altuwais, H., & Alghanim, Kh. (2023). An optimized shaped command of overhead crane nonlinear system for rest-to-rest maneuver. *Journal of Engineering Research*. doi: 10.1016/j.jer.2023.08.012.

[10] Ouyang, H., Hu, J., Zhang, G., Mei, L., & Deng, X. (2019). Decoupled linear model and s-shaped curve motion trajectory for load sway suppression control in overhead cranes with doublependulum effect. *Proceedings of the Institution of Mechanical Engineers, Part C: Journal of Mechanical Engineering Science*, 233(10), 3678-3689. doi: 10.1177/0954406218819029.

[11] Podolyak, O., Khoroshylov, O., & Anenko, K. (2022). Investigation of combined motion of lifting, slewing, and jib length adjustment mechanisms in crane DEK-251. *Engineering*, 28, 18-25. doil: 10.32820/2079-1747-2021-28-18-25.
[12] Sun, N., Yang, T., Fang, Y., Wu, Y., & Chen, H. (2019). Transportation control of double-pendulum cranes with a nonlinear quasi-PID scheme: Design and experiments. *IEEE Transactions on Systems, Man, and Cybernetics: Systems*, 49(7), 1408-1418. doi: 10.1109/TSMC.2018.2871627.
[13] Umaru, I., Bashir, H.A., & Liman, H. (2021). A gantry crane control scheme using hybrid input shaper and pid controller. *Bayero Journal of Engineering and Technology*, 16(1), 93-103.
[14] Wang, J., Liu, K., Wang, S., Chen, H., Sun, Y., Niu, A., & Li, H. (2022). Dynamic analysis and experiment of underactuated double-pendulum anti-swing device for ship-mounted jib cranes. *Polish Maritime Research*, 29(4), 145-154. doi: 10.2478/pomr-2022-0052.
[15] Wang, S., Wu, J., Chen, H., Ji, Y., & Sun, Y. (2019). Dynamic analysis and experiment of the mechanical anti-swing device for ship-mounted cranes. *Journal of Harbin Engineering University*, 40(11), 1858-1864. doi: 10.11990/jheu.201805082.
[16] Wang, X., Liu, J., Zhang, Y., Shi, B., Jiang, D., & Peng, H. (2019). A unified symplectic pseudospectral method for motion planning and tracking control of 3D underactuated overhead cranes. *International Journal of Robust and Nonlinear Control*, 29(7), 2236-2253. doi: 10.1002/rnc.4488.
[17] Wu, Q., Wang, X., Hua, L., & Xia, M. (2020). Dynamic analysis and time optimal anti-swing control of double pendulum bridge crane with distributed mass beams. *Mechanical Systems and Signal Processing*, 144, article number 106968. doi: 10.1016/j.ymssp.2020.106968.
[18] Yang, T., Sun, N., Chen, H., & Fang, Y. (2019). Neural networkbased adaptive antiswing control of an underactuated shipmounted crane with roll motions and input dead zones. *IEEE Transactions on Neural Networks and Learning Systems*, 31(3), 901-914. doi: 10.1109/TNNLS.2019.2910580.
[19] Zhang, M. (2019). Finite-time model-free trajectory tracking control for overhead cranes subjectto model uncertainties, parameter variations and external disturbances. *Transactions of the Institute of Measurement and Control*, 41(12), 3516-3525. doi: 10.1177/0142331219830157.
[20] Zhang, M., Zhang, Y., & Cheng, X. (2019). An enhanced coupling PD with sliding mode control method for underactuated doublependulum overhead crane systems. *International Journal of Control, Automation and Systems*, 17(7), 1579-1588. doi: 10.1007/s12555-018-0646-0.

Вячеслав Сергійович Ловейкін
Доктор технічних наук, професор
Національний університет біоресурсів і природокористування України
03041, вул. Героїв Оборони, 15, м. Київ, Україна
https://orcid.org/0000-0003-4259-3900

Юрій Олександрович Ромасевич
Доктор технічних наук, професор
Національний університет біоресурсів і природокористування України
03041, вул. Героїв Оборони, 15, м. Київ, Україна
https://orcid.org/0000-0001-5069-5929

Іван Олександрович Кадикало
Кандидат технічних наук
Національний університет біоресурсів і природокористування України
03041, вул. Героїв Оборони, 15, м. Київ, Україна
https://orcid.org/0000-0002-5686-5869

Динамічний аналіз сумісного руху механізмів підйому та повороту стрілового крана

Анотація. Задля підвищення продуктивності стрілових кранів здійснюють суміщення роботи окремих механізмів. При цьому зростають динамічні навантаження на елементи конструкції, приводних механізмів і вантажу на гнучкому підвісі, які знижують надійність роботи кранів і підвищують енергетичні витрати. Тому метою статті було розглянути задачу динаміки спільного руху механізмів повороту та підйому вантажу стрілового крану з підйомною стрілою. Для дослідження динаміки спільного руху механізмів стрілова система була представлена механічною системою з шістьома ступенями вільності, де враховано основний рух механізмів та коливальний рух ланок конструкції з пружними та дисипативними властивостями, а також вантажу на гнучкому підвісі в площині повороту крана та підйому вантажу. Для такої механічної системи вантажопідйомного крана складено диференціальні рівняння сумісного руху механізмів повороту та підйому вантажу. Отримані рівняння являють собою систему нелінійних диференціальних рівнянь другого порядку, для розв'язування яких використано чисельний метод у вигляді комп'ютерної програми. За допомогою розробленої програми проведені розрахунки динаміки спільного руху механізмів стрілового крана з конкретними числовими параметрами. На основі проведеного розрахунку здійснено динамічний аналіз спільного руху механізмів повороту та підйому вантажу стрілового крана з підйомною стрілою, в результаті якого встановлені високочастотні коливання ланок з пружними та дисипативними властивостями, а також низькочастотні коливання вантажу на гнучкому підвісі. Найбільший вплив коливань спостерігається в процесі пуску механізмів, де високочастотні коливання затухають протягом перехідного процесу, а низькочастотні коливання затухають протягом достатньо значного проміжку часу. Для покращення динамічних властивостей механізмів повороту та підйому вантажу під час їх спільного руху запропоновано здійснювати оптимізацію режиму руху на ділянках перехідних процесів (пуск, гальмування). Результати досліджень можуть бути використані при розробленні та експлуатації вантажопідйомних кранів в машинобудуванні, будівництві та інших галузях виробництва

Ключові слова: башта; привод; обертання; навантаження; гнучкий підвіс; коливання; амплітуда

Machinery & Energetics
Vol. 14, No. 4. 2023

Journal homepage:
https://technicalscience.com.ua/en

UDC 621.039.5
DOI: 10.31548/machinery/4.2023.86

Juliya Malogulko*
PhD in Technical Sciences, Associate Professor
Vinnytsia National Technical University
21021, 95 Khmelnytske Highway, Vinnytsia, Ukraine
https://orcid.org/0000-0002-6637-7391

Olena Sikorska
PhD in Technical Sciences, Senior Lecturer
Vinnytsia National Technical University
21021, 95 Khmelnytske Highway, Vinnytsia, Ukraine
https://orcid.org/0000-0001-7341-9724

Vira Teptia
PhD in Technical Sciences, Associate Professor
Vinnytsia National Technical University
21021, 95 Khmelnytske Highway, Vinnytsia, Ukraine
https://orcid.org/0000-0002-2792-0160

Kateryna Povstianko
Graduate Student
Vinnytsia National Technical University
21021, 95 Khmelnytske Highway, Vinnytsia, Ukraine
https://orcid.org/0000-0002-5501-662X

Natalia Ostra
PhD in Technical Sciences, Associate Professor
Vinnytsia National Technical University
21021, 95 Khmelnytske Highway, Vinnytsia, Ukraine
https://orcid.org/0000-0002-8245-2937

Research and analysis of new generation nuclear reactors in the world

Abstract. The research of new nuclear reactors is gaining urgent importance worldwide due to the need for continuous improvement of technologies to ensure safety, efficiency, and emissions reduction. This is crucial in the context of climate change and rapid technological development, which demand constant updating and improvement of nuclear energy. The objective of the study was to analyse next-generation reactors worldwide and identify their advantages and potential prospects for the future. The research utilized statistical, comparative, and analytical methods. The results of the analysis considered contemporary technological and safety parameters related to the operation of such reactors, including their ability to optimize fuel usage, enhance operational safety, and effectively manage radioactive waste. As a result of the study, fourth-generation nuclear reactors were analysed, including fast neutron reactors using gas cooling, very high-temperature reactors, reactors using sodium as a coolant, fast neutron reactors with lead cooling, reactors where the reaction occurs

Article's History: Received: 05.07.2023; Revised: 02.10.2023; Accepted: 22.11.2023.

Suggested Citation:
Malogulko, J., Sikorska, O., Teptia, V., Povstianko, K., & Ostra, N. (2023). Research and analysis of new generation nuclear reactors in the world. *Machinery & Energetics,* 14(4), 86-100. doi: 10.31548/machinery/4.2023.86.

*Corresponding author

in molten salt, and supercritical water-cooled reactors. Each of these reactors has its unique features that make them distinctive in their application. For example, gas-cooled reactors have high productivity due to their ability to achieve high temperatures without significant pressure. On the other hand, molten salt reactors offer flexibility in using different types of fuel, including spent fuel, and can help reduce the level of radioactive waste through the use of special materials. During the analysis, it was noted that fourth-generation reactors, using various cooling and reaction-slowing technologies, are characterized by high efficiency, low accident risk, and the ability to produce stable electricity. Improved methods of reaction control open up new possibilities for the efficient production of electricity and increased safety in nuclear energy. The practical significance of the research lies in the opportunity to enhance modern electricity production technologies and ensure greater safety and efficiency in the field of nuclear energy

Keywords: nuclear energy; electricity generation; optimization of fuel use; cooling technologies; retarder; reactions

INTRODUCTION

Research on next-generation nuclear reactors plays a critical role in the development of the energy sector and ensuring stable and secure energy supply. The increasing interest in this topic is driven by the constant need for excellent, environmentally friendly, and efficient energy sources in the context of global challenges related to climate change, energy security, and sustainable development. In the modern world, urgent questions arise concerning the search for a sustainable and environmentally clean energy source. The development of nuclear energy and next-generation nuclear reactors plays a key role in addressing these issues. The study and exploration of this topic aim to ensure the safety and efficiency of nuclear energy use in the future. The accelerated development of new technologies in this field can open up new opportunities for energy development, reduce CO_2 emissions, and create a more resilient energy supply system. However, alongside the potential of next-generation nuclear reactors, there are serious challenges that require comprehensive consideration. In particular, safety issues arise concerning the effective management of nuclear materials and reactions. The development of new safety and monitoring systems, the search for optimal materials for reactor construction, and effective management of radioactive waste all require in-depth research and innovative solutions. It is important to address these aspects to create reliable and safe nuclear energy systems capable of meeting the energy needs of the modern world while caring for the environment.

According to the findings of I. Korduba & Zh. Patlashenko (2023), a promising type of next-generation nuclear reactor is a sodium-cooled reactor, due to its potential to provide a high level of energy production efficiency. The researchers note that this system has significant advantages in terms of nuclear fuel usage and ensures a more efficient energy generation process compared to other alternatives. The sodium-cooled reactor is known for its relatively high safety, a key aspect in considering new nuclear reactor technologies. Its ability to operate at high temperatures and maintain reaction stability reflects its potential as a long-term solution for efficient electricity generation.

In the studies of O. Yefimov *et al.* (2023), it was also emphasized that the sodium-cooled reactor demonstrates high efficiency in using recycled fuel and reducing the amount of waste. Its high degree of heat utilization and the ability to use spent nuclear fuel highlight its advantages in terms of sustainable and environmentally friendly solutions in nuclear energy. This type of reactor has the potential to enhance safety and reliability due to the specificity of its technical characteristics and operating principles.

In the work of E.M. Pysmennyi (2018), the importance of improving technological aspects of the supercritical water-cooled reactor was noted. He focuses on the necessity of developing and implementing innovative approaches aimed at increasing the efficiency, safety, and reliability of this type of reactor. The researcher emphasizes that this plays a crucial role in ensuring the stability and efficiency of nuclear energy, contributing to the development of more resilient and safe energy production technologies.

As noted by M. Ladan *et al.* (2023), a lead-cooled reactor based on fast neutron reactions is distinguished by an increased neutron slowing-down coefficient, contributing to higher spent fuel yield and reduced risks of reaction temperature escalation. According to statements, such a characteristic influences the overall safety of the reactor and extends its operational lifespan. The study also highlighted that the use of lead cooling contributes to the reduction of corrosion impact and enhances the reactor's resistance to external factors.

V.D. Polyakov & T.V. Donyk (2019) assert that a lead-cooled reactor utilizing the supercritical Rankine steam cycle demonstrates significant potential for efficient electricity generation. This approach creates conditions for the optimal utilization of the reactor's thermal energy potential, leading to an overall increase in efficiency. It was noted that the use of the Rankine cycle in combination with lead cooling contributes to the elevation of the working fluid temperature and ensures stability in the reactor's operation at high temperatures. These factors contribute to increased energy output and enhanced overall reactor productivity.

According to N.R. Kostyak (2022), another important aspect in the context of researching the new generation of nuclear reactors is not only the development of technological solutions but also the consideration of social and environmental requirements. The emphasis is placed on the need to implement strategies aimed at reducing environmental impact and increasing societal acceptability. Such an approach will promote not only the development of the energy sector but also the creation of more sustainable and acceptable energy solutions in the future.

Since the mentioned works did not conduct a detailed investigation into the specifics of all types of next-generation nuclear reactors, the aim of this research is to analyse all characteristics that determine the efficiency and safety of such reactors. Considering the wide range of factors influencing the operation of nuclear installations, this work aims to examine each reactor type to identify their distinctive features. A thorough analysis of specific details of different constructions will help determine the optimal direction for the further development of nuclear reactors. This approach will systematically evaluate the impact of each reactor type on meeting energy needs and ensuring environmental safety in the future.

MATERIALS AND METHODS

Within the conducted research, six main types of fourth-generation nuclear reactors were considered. These variations include:

1. Fast neutron reactor using gas cooling (GFR).
2. Reactor with very high temperatures (VHTR).
3. Reactor using sodium as a coolant (SFR).
4. Reactor with lead cooling (LFR).
5. Reactor with reactions occurring in molten salt (MSR).
6. Supercritical water-cooled reactor (SCWR).

The methods employed in the research encompassed statistical analysis, comparative analysis, as well as system-functional approach. These methods were applied to process and interpret data, providing deeper insights into the characteristics and operational features of next-generation nuclear reactors. The analysis of the obtained data allowed the identification of key aspects influencing their efficiency and safety, determining optimal directions for further refinement and optimization of reactor operations. The statistical method was utilized to assess data obtained during the investigation of nuclear reactors. This facilitated the identification of relationships between various reactor parameters and their functioning, as well as the determination of statistically significant dependencies among factors affecting their performance and safety. This method enabled the identification of potential and critical points in reactor operation, defining their operational characteristics and efficiency.

The comparative method allowed the extraction and identification of fundamental distinctions between different types of next-generation nuclear reactors. This method unveiled the advantages and disadvantages of each type, highlighting key characteristics influencing their efficiency and safety. The results of the comparative assessment can serve as a basis for selecting the most promising solutions for further advancements in new reactors. Additionally, this method emphasized important aspects that aided in a better understanding of the specific features and potential capabilities of each reactor, guiding directions for further research for maximizing the effectiveness of nuclear systems. System-functional approach, in turn, facilitated a deeper exploration of the specifics of each reactor type, including their main technical characteristics and parameters such as average power density, coolant mass flow rate, pressure inside the reactor, maximum coolant temperature, and others. This method revealed the dynamics of each reactor's operation, indicating their capabilities and limitations under specific operating conditions. It also allowed attention to be focused on critical aspects affecting the safety and reliability of reactor operations, as well as their overall efficiency.

Through the analysis, it was also determined that different types of reactors have their advantages and limitations. For example, high-temperature reactors with gas cooling may be more efficient in electricity and hydrogen production, while water-cooled reactors may offer greater versatility and have a smaller environmental impact. The obtained data formed the foundation for conducting further research and identified the main directions for improving reactor parameters to maximize their productivity and ensure the highest level of safety. Thus, statistical and comparative methods, along with system-functional approach, underscore the significance of further research and refinement in the field of next-generation nuclear reactors. These aspects reveal key factors influencing their efficiency and safety, emphasizing the need for exploring new solutions to ensure stability and enhance their functional characteristics.

RESULTS

The growing demand for clean and sustainable energy in the modern world stimulates continuous efforts to develop new technologies. The development of a new generation of nuclear reactors has become a priority to ensure efficient electricity production. One key aspect of this process is to increase the thermal efficiency of reactors, contributing to the optimization of converting nuclear energy into electricity. This is essential for expanding electricity production with minimal impact on the environment and natural resources (Şahin & Şahin, 2021).

Innovative development in nuclear energy aims to create a new generation of reactors with improved energy output while simultaneously minimizing negative environmental impact. Modern advanced technologies and reactor designs focus on increasing their thermal efficiency. This means that the efficiency of converting nuclear energy into electricity will be higher, making nuclear energy more competitive and suitable for widespread use. Such development opens perspectives for an energy system that demonstrates high stability and environmental preservation. This form of energy could be a significant step towards reducing carbon emissions and other pollutants, contributing to the preservation of environmental cleanliness.

Currently, the efforts of leading countries (such as the United States, Canada, Japan, and others) in the field of nuclear energy are directed towards creating the next generation of reactors within the framework of international initiatives. The main goal of this project is a significant increase in the thermal efficiency of nuclear power plants. Modern reactors have an efficiency of ~30%, while new Generation IV reactors have the potential to achieve rates of 45% and higher. This step could have immense significance for future energy consumption, providing a more sustainable and productive use of nuclear energy (Pioro *et al.*, 2019).

This significant collaboration between countries aims not only to expand electricity production, but also to transform this process into a more efficient and environmentally sustainable one. In particular, the initiative to develop new systems involves creating and implementing innovative systems aimed at increasing the utilization of nuclear fuel. It is expected that with the increase in the thermal efficiency of reactors, electricity production will be more efficient using the same amount of fuel.

It is worth noting that the creation of a new generation of Generation IV reactors has a broad spectrum of goals, including improving the safety and reliability of reactor systems. In addition to increasing energy production, these reactors are oriented towards using advanced technologies to minimize potential risks of nuclear accidents. Their innovative approaches cover not only technical aspects, but also the creation of comprehensive control and protection systems aimed at preventing potential problems. This fundamental development has significant potential to improve safety and reliability standards, contributing to stable and safe electricity production worldwide.

The International Generation IV Forum program has consolidated possible design concepts for nuclear reactors into six main types (Kamide *et al.*, 2021). These variations of nuclear reactors differ from each other in design, neutron type, reagents used, coolant, operating temperatures, and pressures, providing them with unique characteristics.

Gas-cooled fast reactor. GFR (HTR) is a complex system based on the use of fast neutrons to generate electricity. The power of this system lies not only in the generation of electricity, but also in the possibility of using it to produce hydrogen (Fig. 1).

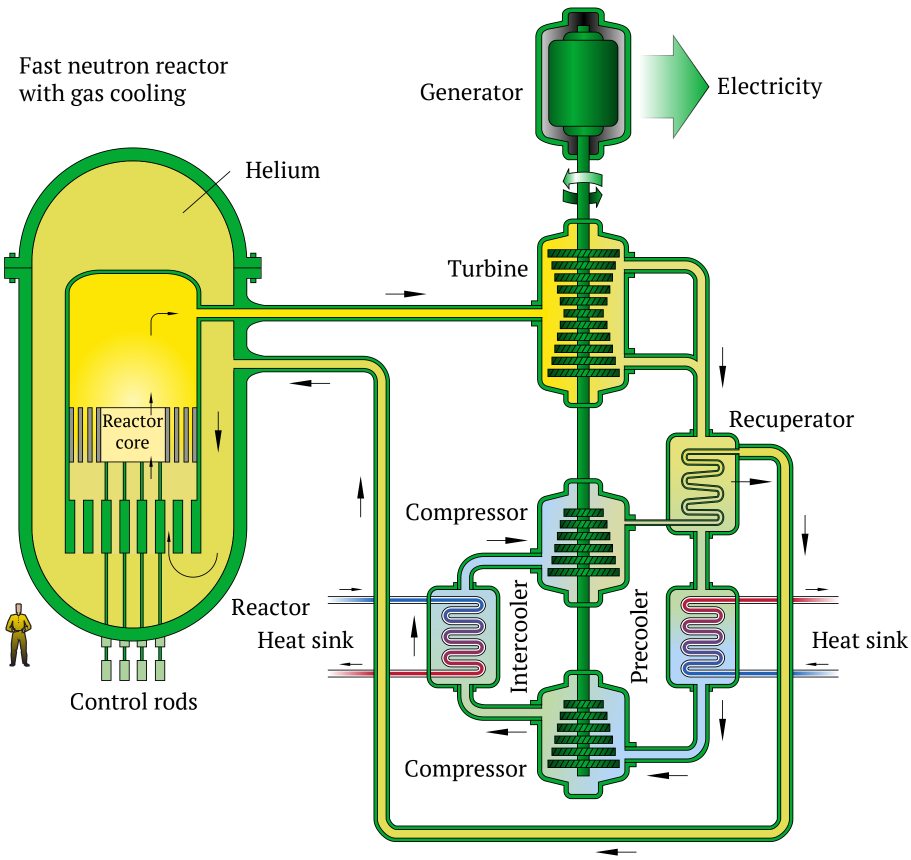

Figure 1. The concept of a nuclear power plant based on GFR

Source: W. Jung (2023)

Helium is the primary coolant in this concept. The net thermal efficiency of this system is approximately 48%. The main characteristics and parameters of this concept are provided in Table 1. It is also noteworthy that due to the challenges associated with implementing the direct Brayton gas turbine cycle with helium used in this system, alternative options using indirect cycles and other technological solutions are being considered. Transitioning to indirect cycles means moving from the direct use of helium gas, which operates directly in the turbine system, to the use of heat exchangers that facilitate interaction between the reactor and the working fluid of the gas turbine systems. This implies that the heat generated in the reactor is first transferred through a heat exchanger, where it is used to heat another working fluid, and only after that is this working fluid utilized to increase steam pressure in turbines that generate electricity (Čížek *et al.*, 2021).

Table 1. The main design parameters of the GFR concept

Reactor parameters	Unit of measurement	Reference value
Reactor power	MW	600
Coolant inlet/outlet temperature	°C	490/850
Pressure	MPa	9
Mass consumption of the coolant	kg/s	320
Standard fuel mixture	-	Uranium-plutonium ceramics (70/30%)
The net efficiency of the installation	%	48

Source: W. Jung (2023)

This allows for improved heat exchange and heat exchanger performance, allowing more efficient use of the heat generated in the reactor to produce electricity. Such a transition may be more difficult to implement due to the need to create an additional heat exchange system and process optimization, but it can provide an opportunity to improve the working process and increase the overall efficiency of the reactor.

Very-high-temperature reactor. VHTR is a reactor used to generate electricity and produce hydrogen through high-temperature electrolysis (Fig. 2).

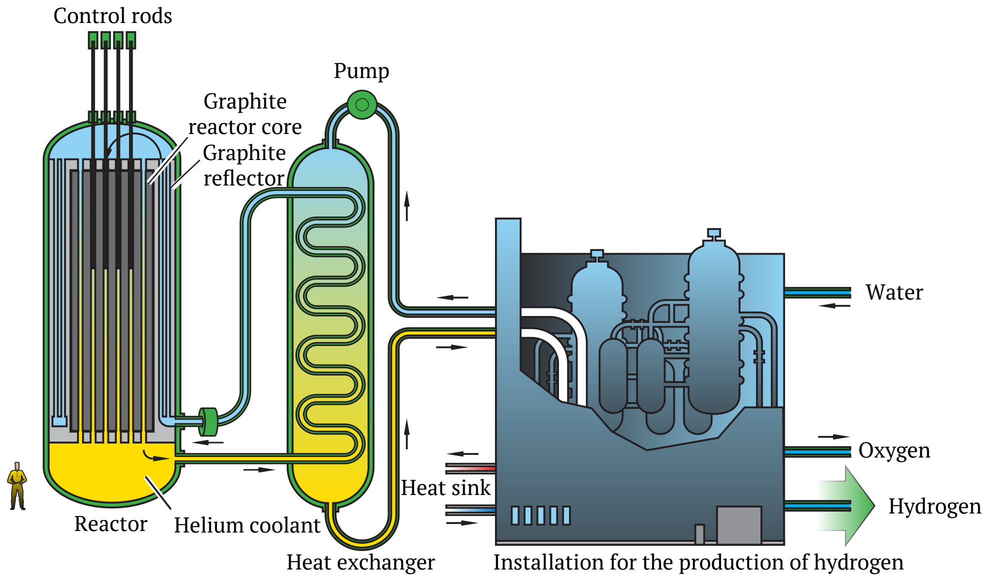

Figure 2. Concept of a facility with a VHTR combined with hydrogen production
Source: G. Baccaglini *et al.* (2003)

The foundation of this design is the use of a graphite moderator and helium as the coolant. During reactor operation, helium is heated to a temperature of 640°C at the inlet and 1000°C at the outlet at a pressure of 7 MPa. This ensures a high level of thermal efficiency exceeding 50%. More detailed parameters and structural characteristics of the VHTR are provided in Table 2.

SFR, which is like the GFR in certain aspects, is another unique reactor operating with fast neutrons. The primary objectives of this reactor type include electricity generation and the management of high-level radioactive waste. However, the distinctive feature of the SFR lies in its ability to use liquid sodium as a coolant, maintaining a temperature range from 530°C to 550°C at atmospheric pressure. The uniqueness of this approach lies in the reactor's capability to work with various types of fuels, including both oxide and metal fuels, making it more versatile in application and operation (Ohshima & Kubo, 2023). It is worth noting that Japan has been utilizing SFR at the Monju Nuclear Power Plant for an extended period (Fig. 3).

Table 2. The main design parameters of the concept of a VHTR

Reactor parameters	Unit of measurement	Reference value
Power	MW	600
Inlet coolant temperature	°C	640
Outlet coolant temperature	°C	1000
Heat carrier consumption/mass consumption	kg/s	Helium/320
Reference fuel composition	-	ZrC-coated particles
The net efficiency of the installation	%	More than 50

Source: G. Baccaglini *et al.* (2003)

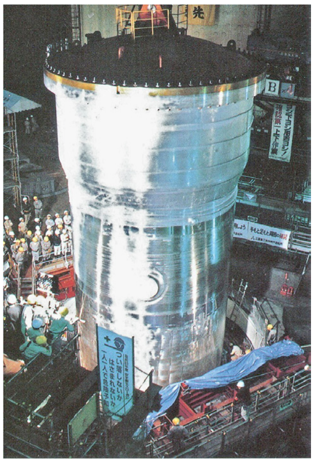

Figure 3. Photo of the SFR reactor housing at the Monju NPP (Japan)
Source: I. Pioro & P. Kirillov (2013)

In the aforementioned systems, electricity generation occurs through heat exchange within the system. Utilizing heat exchangers, high-temperature SFRs interact with sodium as a coolant. This process takes place at low pressure, generating thermal energy used to produce steam. Subsequently, the steam is employed in the Rankine steam cycle, where it expands, performs work, and adds energy to steam generators. The aim of such a system is to optimize the efficiency of converting the thermal energy resulting from the reaction in SFR into usable electricity by utilizing the Rankine steam cycle under low pressure (Fig. 4). The key parameters of the overall SFR concept are outlined in Table 3.

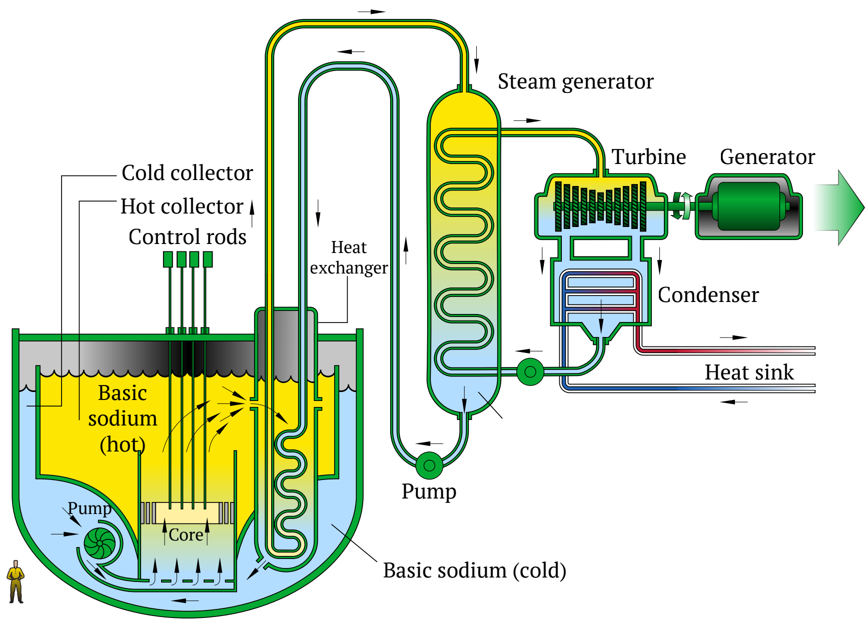

Figure 4. The concept of a nuclear power plant based on fast neutrons (SFR)
Source: R.M. Meyer *et al.* (2013), M. Wang *et al.* (2020)

Table 3. Key design parameters of the overall SFR concept

Reactor parameters	Unit of measurement	Reference value
Reactor power	MW	500-1000
Thermal efficiency	%	40-42
Coolant	-	Sodium
Melting temperature of the coolant		98
Boiling temperature of the coolant	°C	883
The maximum temperature of the coolant at the outlet	°C	530-550
Reference fuel composition	-	Metal alloy(oxide)
Facing	-	Ferritic with oxide particles

Source: R.M. Meyer *et al.* (2013)

Sodium, as a highly reactive metal, has the property of reacting with water, which leads to the release of hydrogen and heat. This reaction can cause spontaneous combustion when sodium comes into contact with water. In addition, at high temperatures, sodium can ignite in some conditions. Thus, the operation of reactors of this type requires taking special safety and caution measures. One such measure is the use of a three-flow circuit with an intermediate sodium loop between the reactor coolant system (primary sodium) and water, which acts as the working fluid in the power cycle.

Lead-cooled fast reactor, molten salt reactor and supercritical water-cooled reactor. LFR is a type of fast neutron reactor that uses lead as a coolant to transfer heat from nuclear reactions (Fig. 5). This technology uses lead for cooling and simultaneously shielding against radiation, which ensures stable and safe operation of the reactor. An alloy of lead and bismuth can also be used as a coolant. It operates at an outlet coolant temperature of approximately 550°C, but it can reach up to 800°C under atmospheric pressure. The primary fuel type for this reactor is nitride fuel, utilized for its optimal performance (Sargsyan *et al.*, 2023).

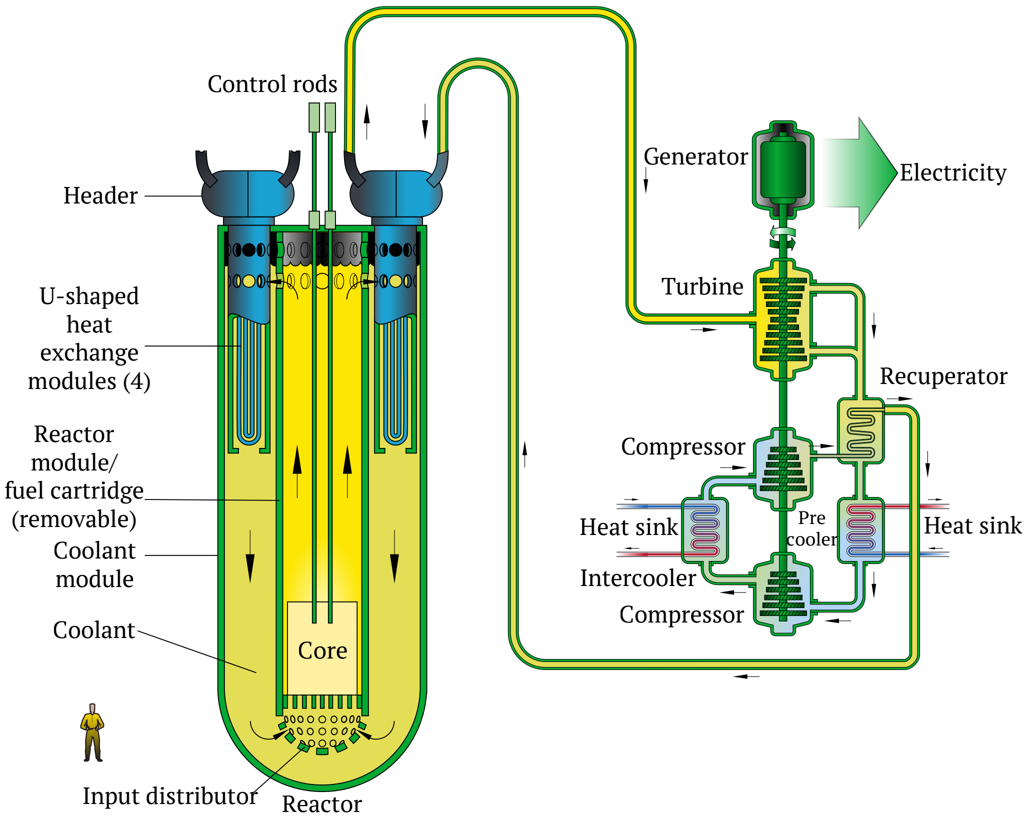

Figure 5. The concept of a nuclear power plant based on LFR

Source: M. Tarantino *et al.* (2021)

In the United States, for example, the supercritical carbon dioxide Brayton gas turbine cycle has been chosen as the primary for this type of reactor. At the same time, in some countries, the supercritical Rankine steam cycle is considered as the main option (Table 4). The difference in the choice of power cycle in different countries reflects the diversity of approaches in implementing technologies for LFR and emphasizes the importance of finding optimal solutions for its improvement and safety in various contexts.

Table 4. Main design parameters of LFR

Reactor parameters	Unit of measurement	Brest-300	Brest-1200
Thermal power	MW	700	2800
Electrical power	MW	300	1200
Thermal efficiency	%	43	
Melting temperature of the coolant	°C	328	
Boiling temperature of the coolant	°C	1743	
Coolant inlet temperature	°C	420	
Coolant outlet temperature	°C	540	
Mass consumption of the coolant	t/s	40	158
The maximum speed of the coolant	m/s	1.8	1.7
Fuel	-	Uranium nitride + plutonium nitride	
Fuel loading	t	16	64
Fuel residence time in the reactor	years	5	5-6
The maximum facing temperature	°C	650	
Temperature at the inlet/outlet of the steam generator	°C	340/520	
Power of the steam generator	t/s	0.43	1.72
The term of operation of the reactor	years	30	60

Source: I. Pioro & P. Kirillov (2013)

MSR is a thermal neutron facility that utilizes liquid fluoride salt with dissolved uranium, and graphite serves as the moderator. Upon introducing the fuel-salt mixture, the temperature at the inlet is approximately 565°C, but upon exiting the reactor, it can reach 700°C. Considering the option of hydrogen cogeneration, the temperature of the fuel-salt mixture at the outlet may even rise to 850°C. The efficiency of the facility, measured by the thermal efficiency, ranges from 45 to 50%. The installation scheme is detailed in Figure 6, and key parameters are provided in Table 5.

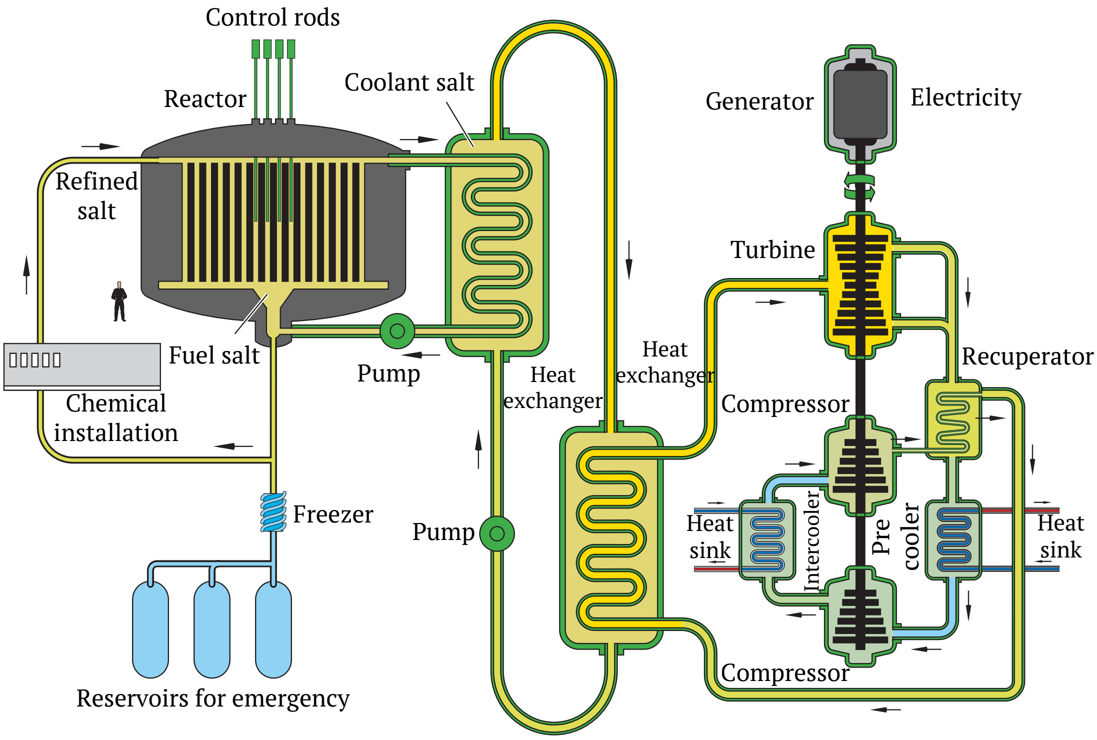

Figure 6. Concept of a nuclear power plant with a MSR
Source: M.P. Dion *et al.* (2020), V. Levchenko *et al.* (2023)

Table 5. Key design parameters of the MSR concept

Reactor parameter	Unit of measurement	Reference value
Reactor power	MW_{el}	1000
Net thermal efficiency	%	44-50
Average power density	MW_t/m^3	22
The temperature of the fuel-salt solution at the inlet/outlet	°C	565/700 (800)
Retarder	-	Graphite
Burner of the neutron spectrum	-	Thermoactinide

Source: M.P. Dion *et al.* (2020)

SCWR is considered an evolution of modern water-cooled nuclear reactor systems. In comparison to traditional nuclear reactors, the SCWR offers a new approach, utilizing water under supercritical pressure and high temperatures. The SCWR aims to surpass limitations PWR faced by achieving even higher pressures and temperatures (Krykova *et al.*, 2021).

In the case of BWR, steam is directly supplied from the nuclear reactor to the turbine. The SCWR, on the other hand, is designed to operate at supercritical pressure and high temperatures, enabling more efficient and optimal energy utilization. This technology employs the concept of nuclear superheating of steam, providing an outlet temperature exceeding the critical temperature but at a pressure lower than the critical pressure. Modern supercritical pressure turbines used in coal-fired power plants have demonstrated successful results for over fifty years, operating at pressures around 25 MPa and high inlet temperatures approaching 600°C. However, in the context of the SCWR, the use of water under supercritical conditions defines a new frontier of efficiency, potentially allowing for even more effective energy utilization and higher productivity (Novotny & Guzonas, 2020).

The classification of SCWR can be considered from various perspectives, such as the maximum pressure, neutron spectrum, and moderator material. One classification method based on maximum pressure divides PWR into two main categories: Pressurized Vessel (PV) and Pressurized Tube (PT) or Pressurized Channel (PCh). To ensure optimal operation of pressurized heavy-water underwater reactors, pressurized tubes of approximately 50 cm thickness are required, capable of withstanding supercritical pressure. The diagram of a nuclear power plant with a PV-type SCWR reactor is presented in Figure 7.

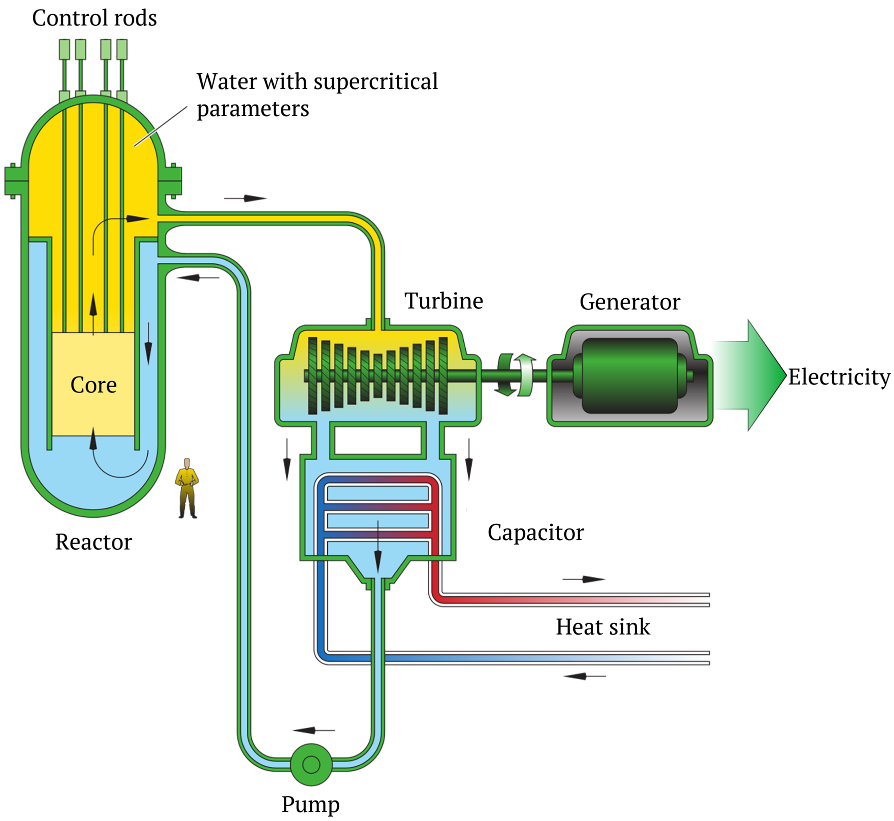

Figure 7. Concept of a nuclear power plant with a PV SCWR

Source: M. Krykova *et al.* (2021)

The active zone of reactors with pressurized tubes consists of channels with distributed pressure, which can be placed vertically (or horizontally). This approach is similar to the construction principles of reactors such as the Canada Deuterium Uranium (CANDU) and the High-Power Channel-type Reactor (HCCR or RBMK). For instance, the SCWR-CANDU reactor comprises 300 fuel channels that placed horizontally (Fig. 8). The option with a vertically oriented active zone should also not be ruled out (Fig. 9).

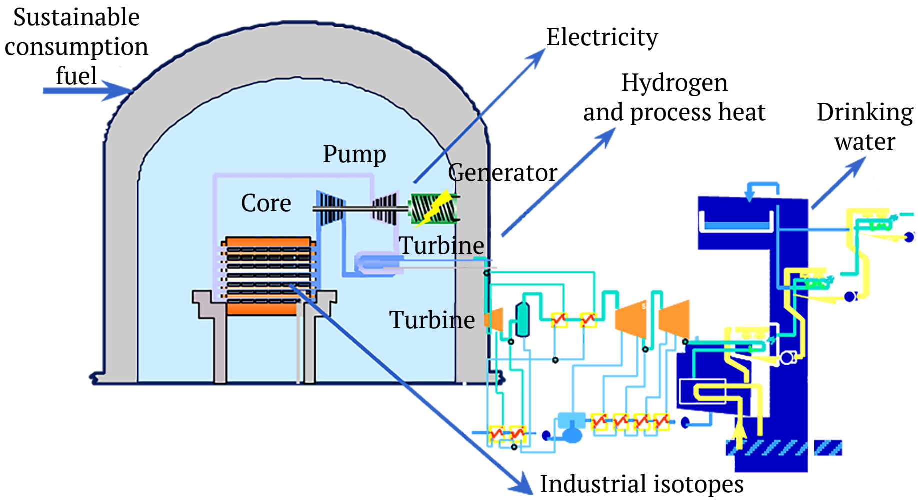

Figure 8. Concept of a nuclear power plant with a SCWR-CANDU type reactor with PT under pressure
Source: I. Pioro & P. Kirillov (2013)

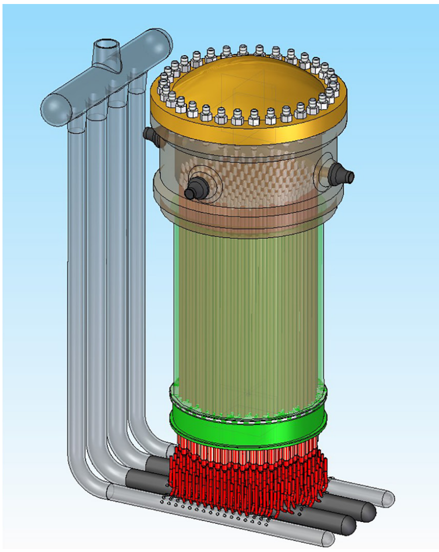

Figure 9. Variant of the vertical configuration of the active zone of the PT SCWR-CANDU reactor
Source: I. Pioro & P. Kirillov (2013)

The specifications of SCWR reactor designs indicate that the majority of these systems belong to the thermal neutron spectrum category. This means they operate in a neutron spectrum where thermal neutrons predominate, which is a typical choice for many modern SCWRs. However, variations also allow for the use of fast neutron spectrum designs, providing greater flexibility and diversity (Yamaji *et al.*, 2023). In SCWR designs with a thermal neutron spectrum, various types of moderators – liquid or solid – can be employed. Options include light or heavy water, graphite, among others. This diversity enables the exploration and implementation of various concepts, considering the specificity of each material and its interaction with the reactor's energy processes. A crucial aspect is that the concept of a liquid moderator can be applied in both pressurized and gas-water variations of the reactor, offering versatility in the operation of these systems.

In pressurized water reactors, the moderator and the coolant are isolated, creating many variations to select the optimal moderator depending on the specific needs of the reactor. The diversity of moderator options in pressurized water reactors creates a broad spectrum for experimentation and innovation in nuclear power, allowing for the exploration of different methods and approaches to improve the efficiency and safety of reactor installations.

Considering options for improving safety in PT SCWRs is the use of a liquid moderator, as this approach can have a number of advantages. This liquid moderator plays an important role in improving reactor safety and provides an additional layer of protection in emergency situations. However, significant drawbacks of this approach include increased heat losses resulting from heat transfers. This is relevant in SCWR systems, where high temperature and pressure present certain challenges in managing thermal processes and heat dissipation. These aspects require further research and technology refinement to mitigate the negative impact of increased heat losses and improve the efficiency of this reactor type (Ibrahim *et al.*, 2019).

It's worth noting that the use of a solid moderator is also a possibility. In RBMK, HTR, and other type reactors, graphite is currently used. This approach may have some peculiarities, as it is important to take into account that graphite can explode under certain conditions. Therefore, alternative variants are being considered as alternatives. The use of such materials can help reduce heat losses. However, it's essential to consider that these moderators do not provide a passive safety system that automatically reacts in emergency situations. While these materials have their advantages in terms of efficiency, they require systematic control and management to ensure the safety and efficiency of the reactor system.

In SCWR-type reactors, the high operating temperatures impose significant thermal loads on fuel elements. This is particularly relevant in Light Water Reactors (LWR) and Pressurized Heavy Water Reactors (PHWR), where uranium dioxide (UO_2) is used as the primary fuel. However, UO_2 has limited thermal conductivity, and overheating may occur in the central regions of the reactor core. Therefore, various alternative fuel types with higher thermal conductivity are being studied. One approach is the use of compounds such as UO_2-BeO, UO_2-SiC and others. The notable feature of these materials is their thermal conductivity properties, which can contribute to better heat distribution in the reactor system and prevent overheating (Peiman *et al.*, 2023).

The use of alternative fuel materials allows for temperature control in the reactor, minimizes the risks of overheating in areas with high heat flux, and ensures a more efficient operation of the reactor system.

DISCUSSION

Researching and analysing next-generation nuclear reactors is a crucial step in the development of modern nuclear energy. This underscores the need for efficient energy resource utilization and ensuring environmentally sustainable electricity production. Fourth-generation nuclear reactors represent a transition from old reactor models to new, innovative systems aimed at improving efficiency and safety. A detailed analysis of these reactors is essential for understanding their operation, efficiency, and environmental impact. Each reactor type is expected to increase the thermal efficiency, reduce the risk of accidents, and minimize radioactive releases. Research helps identify the advantages and disadvantages of each type and determines directions for further improvement. An important feature is that each type of nuclear reactor has unique characteristics defining its efficiency, safety, and environmental sustainability. Different technologies are used for energy production, with variations in heat conversion methods, construction materials, and nuclear process control. These differences determine not only reactor performance but also potential risks and opportunities for further development. Each reactor type requires a unique approach to management, waste storage, and safety measures, necessitating further scientific research and analysis for optimal nuclear facility functioning.

According to F. Osuský *et al.* (2020), a significant feature of gas-cooled reactors is their thermodynamic and thermophysical characteristics, ensuring highly efficient and safe nuclear facility operation. One key advantage of using gas is its resistance to ionizing radiation generated during nuclear reactions. This means that the reactor's gas system has high resilience to damage resulting from radiation exposure. Additionally, gas-cooled reactors may achieve higher efficiency compared to other types due to the gas's high heat transfer and mass exchange characteristics, enabling the conversion of nuclear reaction energy into useful electricity. The work by the researchers indicates the efficiency advantage of gas-cooled reactors, making them attractive for increasing nuclear energy productivity. This study further expands the knowledge presented by the authors by delving deeper into complex influences that can impact the choice of reactor type, providing a more comprehensive comparative analysis and additional crucial aspects to consider in selecting the optimal reactor type for specific conditions and needs.

According to M. Singh *et al.* (2022), a supercritical water-cooled reactor also has defining features and advantages, making it appealing in the field of nuclear energy. The use of water as a coolant reflects its high heat capacity, allowing effective heat dissipation from nuclear reactions. This makes it efficient in controlling the reactor's temperature. Safety is another notable advantage of such a reactor, as the research indicates its potential for high-speed heat removal even in the event of cooling system failure, making it less vulnerable to accidents. This study complements the conclusions mentioned earlier by providing a more in-depth understanding of various aspects compared to other types of nuclear reactors. Since this study reveals not only thermophysical and thermodynamic characteristics but also other aspects, this analysis allows for a broader spectrum of the impact of different reactor types on nuclear energy, facilitating a more thorough comparative analysis and providing additional important considerations when choosing the optimal reactor type for specific conditions and needs.

Research by Z. Zhao *et al.* (2022) reveals important aspects of a supercritical water-cooled reactor equipped with different types of moderators. Since moderators in reactors, such as graphite, beryllium, heavy water, or others, are key components in controlling nuclear reactions, the study emphasizes that using liquid moderators in supercritical water-cooled reactors has the potential to enhance nuclear technology. This improvement can result in efficient use of nuclear fuel and reduce the risks of accidents. The authors' research sheds light on the significance of various moderator types in supercritical water-cooled reactors. By examining liquid moderators like graphite, beryllium, heavy water, and others as crucial components for nuclear reaction control, the author identifies their importance in advancing nuclear technology. This approach may contribute to increased resource utilization efficiency in nuclear facilities and reduce environmental impact, promoting the adoption of safer and more stable technologies in nuclear energy.

According to S.A. Alameri & A.K. Alkaabi (2020), water-graphite reactors with supercritical coolant parameters represent an interesting direction in nuclear technology where water and graphite serve as key components for regulation and control of nuclear reactions. The researchers note that such reactors have the potential to provide high efficiency in nuclear fuel utilization. The combination of water and graphite allows achieving optimal reaction parameters, reducing losses of nuclear materials, and ensuring efficient energy utilization. Comparing the results of research by the authors with the present study, it is noteworthy that the latter examines various aspects of nuclear reactors, including not only water-graphite but also other reactor types. The study comprehensively analyses diverse technologies, materials, and constructions used in nuclear facilities to understand their advantages and limitations. This approach focuses on the specificity of water-graphite reactors with supercritical coolant parameters and their potential contribution to increasing the efficiency of nuclear fuel utilization. Simultaneously, this research aims to provide a general overview and comparison of different reactor types, considering their advantages and potential limitations in the context of efficiency and safety.

As per the research by Y. Wang *et al.* (2021), sodium-cooled reactors, despite several advantages, also present challenges and peculiarities requiring attention and management for optimizing their efficiency and safety. One primary characteristic is the chemical activity of sodium. Since sodium, used as a coolant, is highly chemically active, its interaction with water or air can create reactions with high energy and speed, posing a potential threat to reactor safety in case of accidents. The aspects mentioned in the researchers' research underscore the need for continuous work and improvement in sodium-cooled reactor technology. This highlights the importance of significant efforts in developing new technologies and control methods to ensure the safety and efficiency of such reactors. High attention to these aspects is necessary for continually reducing potential risks arising during operation and ensuring the reliability and stability of these systems.

Further research in the field of nuclear energy is crucial for the gradual development of this technology. It will allow a deeper understanding of various reactor types, their advantages, and limitations, contribute to the development of new control methods that enhance the safety and efficiency of nuclear energy utilization. Moreover, research can focus on reducing environmental impact and optimizing resource utilization, which are key aspects in the modern energy landscape. The development of new technologies and an in-depth understanding of nuclear facility principles play a vital role in ensuring sustainable and safe use of nuclear energy in the future.

CONCLUSIONS

Summarizing the results of the conducted research, it should be emphasized that the development of nuclear technologies is of great significance for the present and future energy landscape. Nuclear energy is considered a substantial source due to its potential to provide electricity over extended periods, even considering its non-renewability. However, it is important to bear in mind that modern nuclear power plants generate radioactive waste, requiring careful control and storage. In this context, fourth-generation reactors can not only reduce the amount of generated radioactive waste but also optimize fuel utilization and decrease the risks of accidents. Their key advantage lies in the use of advanced technologies allowing the processing of waste, reducing their radioactivity and storage duration. Additionally, new reactors may feature improved cooling systems and automated control mechanisms, enhancing their safety and reliability.

During this study, six main types of nuclear installations were thoroughly analysed, including: GFR (HTR), VHTR, SFR, LFR, MSR and SCWR. Among the critical aspects, the study also delved into various types of reactor cooling, analysing possibilities for reducing radioactive waste and addressing safety risks associated with nuclear installations. Furthermore, attention was given to exploring promising directions in the development of new reactors, aiming for more efficient nuclear fuel utilization and reduced radioactivity of waste. These aspects were investigated to identify key trends and opportunities for the further development of nuclear technologies to ensure a sustainable and secure energy future.

Major directions for further research into next-generation reactors may include the optimization of cooling systems to enhance heat exchange efficiency and ensure better temperature control, the development of monitoring systems for constant control of reactor parameters, and the improvement of emergency systems to minimize potential adverse consequences. Equally important is the advancement of methods for managing radioactive waste, including reduction and further processing. All these research directions have the potential to reshape the paradigm in nuclear energy, directing its development toward a more sustainable, secure, and efficient future.

ACKNOWLEDGEMENTS

None.

CONFLICT OF INTEREST

None.

REFERENCES

[1] Alameri, S.A., & Alkaabi, A.K. (2020). Fundamentals of nuclear reactors. In *Nuclear Reactor Technology Development and Utilization* (pp. 27-60). London: Woodhead Publishing. doi: 10.1016/B978-0-12-818483-7.00001-9.

[2] Baccaglini, G., Ball, S., Burchell, T., Corwin, B., Fewell, T., LaBar, M., MacDonald, P., Rittenhouse, P., Shaber, E., Southworth, F., & Vollman, R. (2003). *Very High Temperature Reactor (VHTR). Survey of materials research and development needs to support early deployment*. Retrieved from https://inldigitallibrary.inl.gov/sites/sti/sti/2559926.pdf

[3] Čížek, J., Kalivodová, J., Janeček, M., Stráský, J., Srba, O., & Macková, A. (2021). Advanced structural materials for gas-cooled fast reactors – A review. *Metals*, 11(1), article number 76. doi: 10.3390/met11010076.

[4] Dion, M.P., Worrall, L.G., Croft, S., & Scott, L.M. (2020). *Molten salt reactor signatures and modeling study*. Retrieved from https://info.ornl.gov/sites/publications/Files/Pub149085.pdf.

[5] Ibrahim, R., Bujis, A., & Luxat, J. (2019). Assessment of the long-term storage of PT-SCWR fuel bundle in CANDU Deep Geological Repository. In *Nuclear energy's value: Aligned with community expectations 39th Annual CNS conference and 43rd CNS/CNA student conference* (article number 52027508). Canada: Canadian Nuclear Society.

[6] Jung, W. (2023). Gas-cooled fast reactor. In *Nuclear Power Reactor Designs* (pp. 245-257). London: Academic Press. doi: 10.1016/B978-0-323-99880-2.00012-6.

[7] Kamide, H., Rodriguez, G., Guiberteau, P., Kawasaki, N., Hatala, B., Alemberti, A., & Loewen, E. (2021). *Annual Report 2020*. Retrieved from https://inis.iaea.org/search/search.aspx?orig_q=RN:52054138.

[8] Korduba, I., & Patlashenko, Zh. (2023). Prospects of technological enhancement nuclear environmental safety and efficiency of nuclear energy. *Open Journal of Ecology*, 13(8), 75-79. doi: 10.32846/2306-9716/2023.eco.1-46.13.

[9] Kostyak, N.R. (2022). Influence of radioactive pollution on the human organization. In *XIX All-Ukrainian Scientific and Practical Conference of Students, Postgraduates and Young Scientists "Youth: Education, Science, Spirituality"* (pp. 254-255). Kyiv: University "Ukraine".

[10] Krykova, M., Schulenberg, T., Arnoult Růžičková, M., Sáez-Maderuelo, A., Otic, I., Czifrus, S., Cizelj, L., & Pavel, G.L. (2021). European research program on supercritical water-cooled reactor. *Journal of Nuclear Engineering and Radiation Science*, 7(2), article number 021301. doi: 10.1115/1.4048901.

[11] Ladan, M.M., Bondar, B.S., & Donik, T.V. (2023). High-temperature helium reactor of the fourth generation as the future of Ukrainian energy. In *XXI All-Ukrainian Scientific and Practical Conference of Students, Postgraduates and Young Scientists "Theoretical and Applied Problems of Physics, Mathematics and Informatics"* (pp. 95-98). Kyiv: Igor Sikorsky Kyiv Polytechnic Institute.

[12] Levchenko, V., Pogosov, O., & Kravchenko, V. (2023). Cobalt application in repair tools for maintenance and modernisation of NPP equipment. *Scientific Herald of Uzhhorod University. Series "Physics"*, 53, 31-41. doi: 10.54919/physics/53.2023.31.

[13] Meyer, R.M., Ramunhalli, P., Coble, J.B., Mitchell, M.R., Wootan, D.W., Hirt, E.H., Berglin, E.J., Bond, L.J., & Henager, C.H. (2013). Prognostics health management for advanced small modular reactor passive components. *Annual Conference of the Prognostics and Health Management Society*, 5(1), 1-9.

[14] Novotny, R., & Guzonas, D. (2020). Material research for the supercritical water-cooled reactor – summary and open issues. In *Nuclear Corrosion* (pp. 403-435). London: Woodhead Publishing. doi: 10.1016/B978-0-12-823719-9.00012-3.

[15] Ohshima, H., & Kubo, S. (2023). Sodium-cooled Fast Reactors (SFRs). In *Handbook of Generation IV Nuclear Reactors* (pp. 173-194). London: Woodhead Publishing. doi: 10.1016/B978-0-12-820588-4.00006-2.

[16] Osuský, F., Čerba, Š., Lüley, J., Vrban, B., Haščík, J., & Nečas, V. (2020). On gas-cooled fast reactor designs – Nuclear data processing with sensitivity, uncertainty and similarity analyses. *Progress in Nuclear Energy*, 128, article number 103450. doi: 10.1016/j.pnucene.2020.103450.

[17] Peiman, W., Pioro, I.L., Gabriel, K.S., & Hosseiny, M. (2023). Thermal aspects of conventional and alternative nuclear fuels. In *Handbook of Generation IV Nuclear Reactors* (pp. 613-663). London: Woodhead Publishing. doi: 10.1016/B978-0-12-820588-4.00003-7.

[18] Pioro, I., & Kirillov, P. (2013). Generation IV nuclear reactors as a basis for future electricity production in the world. In *Materials and Processes for Energy: Communicating Current Research and Technological Developments* (pp. 818-830). Madrid: Formatex Research Center. https://www.semanticscholar.org/paper/Generation-IV-Nuclear-Reactors-as-a-Basis-for-in-Pioro-Kirillov/e2797915d6acfc5f0d57edec9e2029377168cdba.

[19] Pioro, I., Duffey, R.B., Kirillov, P.L., Pioro, R., Zvorykin, A., & Machrafi, R. (2019). Current status and future developments in nuclear-power industry of the world. *Journal of Nuclear Engineering and Radiation Science*, 5(2), article number 024001. doi: 10.1115/1.4042194.

[20] Polyakov, V.D., & Donyk, T.V. (2019). Nuclear power plants and their development paths. In *XXI All-Ukrainian Scientific and Practical Conference of Students, Postgraduates and Young Scientists "Theoretical and Applied Problems of Physics, Mathematics and Informatics"* (pp. 90-92). Kyiv: Igor Sikorsky Kyiv Polytechnic Institute.

[21] Pysmennyi, E.M. (2018). *Investigation of heat transfer in the simulators of fuel bundles and passive heat-removal systems for strengthening of safety barriers in nuclear power engineering*. Kyiv: Igor Sikorsky Kyiv Polytechnic Institute.

[22] Şahin, S., & Şahin, H.M. (2021). Generation-IV reactors and nuclear hydrogen production. *International Journal of Hydrogen Energy*, 46(57), 28936-28948. doi: 10.1016/j.ijhydene.2020.12.182.

[23] Sargsyan, G., Silveistr, A., Lysyi, M., Mokliuk, M., & Sargsyan, H. (2023). The appearance of standing wave structures in the reaction medium during the diffusion development of the chain reaction process. *Scientific Herald of Uzhhorod University. Series "Physics"*, 54, 36-46. doi: 10.54919/physics/54.2023.36.

[24] Singh, M.P., Saeed, M., & Berrouk, A.S. (2022). Non linear stability analysis of supercritical water cooled reactor: Parallel channels configuration. *Progress in Nuclear Energy*, 147, article number 104194. doi: 10.1016/j.pnucene.2022.104194.

[25] Tarantino, M., Angiolini, M., Bassini, S., Cataldo, S., Ciantelli, C., Cristalli, C., Del Nevo, A., Di Piazza, I., Diamanti, D., Eboli, M., Fiore, A., Grasso, G., Lodi, F., Lorusso, P., Marinari, R., Martelli, D., Papa, F., Sartorio, C., Utili, M., & Venturini, A. (2021). Overview on lead-cooled fast reactor design and related technologies development in ENEA. *Energies*, 14(16), article number 5157. doi: 10.3390/en14165157.

[26] Wang, M., Chen, J., Zhang, D., Zhang, J., Tian, W., Su, G.H., & Qiu, S. (2020). Numerical study on the thermal stratification characteristics in the upper plenum of sodium-cooled fast reactor (SFR). *Annals of Nuclear Energy*, 138, article number 107222. doi: 10.1016/j.anucene.2019.107222.

[27] Wang, Y., Wang, M., Zhang, J., Qiu, S., Tian, W., & Su, G. (2021). Large eddy simulation on the mixing characteristics of liquid sodium at the core outlet of sodium cooled fast reactors (SFR). *Annals of Nuclear Energy*, 159, article number 108347. doi: 10.1016/j.anucene.2021.108347.

[28] Yamaji, A., Matsuoka, K., Sumida, K., & Funatsu, K. (2023). Scope of conceptual development of Resilient supercritical Light water-cooled reactor (SCWR-R). *Nuclear Engineering and Design*, 416, article number 112756. doi: 10.1016/j.nucengdes.2023.112756.

[29] Yefimov, O.V., Pylypenko, M.M., Tiutiunyk, L.I., Harkusha, T.A., Yesipenko, T.O., & Motovilnik, A.V. (2023). *Reliable reactor systems and concepts of the next IV generation after 2030*. Retrieved from https://repository.kpi.kharkov.ua/server/api/core/bitstreams/2a1ef34e-c863-46e1-8fb8-4ab35f8b662d/content.

[30] Zhao, Z., Shi, J., Sun, B., Chen, Y., Wu, W., & Fu, H. (2022). The influence of four-wire structure on the flow and heat transfer process in supercritical water-cooled reactor fuel assembly. *Applied Thermal Engineering*, 203, article number 117941. doi: 10.1016/j.applthermaleng.2021.117941.

Юлія Володимирівна Малогулко
Кандидат технічних наук, доцент
Вінницький національний технічний університет
21021, Хмельницьке шосе, 95, м. Вінниця, Україна
https://orcid.org/0000-0002-6637-7391

Олена Вікторівна Сікорська
Кандидат технічних наук, старший викладач
Вінницький національний технічний університет
21021, Хмельницьке шосе, 95, м. Вінниця, Україна
https://orcid.org/0000-0001-7341-9724

Віра Володимирівна Тептя
Кандидат технічних наук, доцент
Вінницький національний технічний університет
21021, Хмельницьке шосе, 95, м. Вінниця, Україна
https://orcid.org/0000-0002-2792-0160

Катерина Олександрівна Повстянко
Аспірант
Вінницький національний технічний університет
21021, Хмельницьке шосе, 95, м. Вінниця, Україна
https://orcid.org/0000-0002-5501-662X

Наталя Вікторівна Остра
Кандидат технічних наук, доцент
Вінницький національний технічний університет
21021, Хмельницьке шосе, 95, м. Вінниця, Україна
https://orcid.org/0000-0002-8245-2937

Дослідження та аналіз ядерних реакторів нового покоління у світі

Анотація. Дослідження нових ядерних реакторів набуває невідкладного значення у світі через потребу постійного вдосконалення технологій для забезпечення безпеки, ефективності та зменшення викидів. Це важливо в контексті кліматичних змін і швидкого технологічного розвитку, що вимагають постійного оновлення й удосконалення ядерної енергетики. Метою роботи було проаналізувати реактори нового покоління у світі, а також визначити їхні переваги та можливі перспективи в майбутньому. Методами, що використовувалися під час дослідження, були статистичний метод, порівняльний метод, а також аналіз. Результати проведеного аналізу врахували сучасні технологічні та безпечні параметри, що стосуються роботи таких реакторів, зокрема їхню здатність до оптимізації використання палива, підвищення безпеки експлуатації, та ефективного управління радіоактивними відходами. В результаті роботи було проаналізовано ядерні реактори IV покоління, що включали в себе: реактор із швидкими нейтронами, що використовує газове охолодження; дуже високотемпературний реактор; реактор, де натрій використовується як теплоносій; реактор на швидких нейтронах зі свинцевим охолодженням; реактор, де реакція відбувається в розплавленій солі; та надкритичний водяний реактор. Кожен з цих реакторів має свої особливості, що роблять їх унікальними в своїй сфері застосування. Наприклад, реактори з газовим охолодженням мають високу продуктивність завдяки здатності досягати високих температур без значного тиску. В свою чергу реактори на розплавленій солі володіють гнучкістю у використанні різних видів палива, включаючи відпрацьоване, та можуть допомогти знизити рівень радіоактивних відходів завдяки використанню спеціальних матеріалів. В процесі аналізу було відзначено, що реактори IV покоління, використовуючи різні технології охолодження та сповільнення реакцій, позначаються високою ефективністю, низьким ризиком аварій та здатністю до виробництва стабільної електроенергії, а також вдосконалені методи контролю реакцій, відкривають нові можливості для ефективного виробництва електроенергії та підвищення безпеки в ядерній енергетиці. Практичне значення дослідження полягає в можливості удосконалення сучасних технологій виробництва електроенергії та забезпеченні більшої безпеки та ефективності у галузі ядерної енергетики

Ключові слова: атомна енергетика; генерація електроенергії; оптимізація використання палива; технології охолодження; сповільнювач; реакції

Machinery & Energetics
Vol. 14, No. 4. 2023

Journal homepage:
https://technicalscience.com.ua/en

UDC 629.017:631.3
DOI: 10.31548/machinery/4.2023.101

Andrii Novytskyi *

PhD in Technical Sciences, Associate Professor
National University of Life and Environmental Sciences of Ukraine
03041, 15 Heroiv Oborony Str., Kyiv, Ukraine
https://orcid.org/0000-0001-7789-8531

Oleksandr Bannyi

PhD in Technical Sciences, Associate Professor
National University of Life and Environmental Sciences of Ukraine
03041, 15 Heroiv Oborony Str., Kyiv, Ukraine
https://orcid.org/0000-0003-0505-166X

Yurii Novytskyi

Postgraduate Student
National University of Life and Environmental Sciences of Ukraine
03041, 15 Heroiv Oborony Str., Kyiv, Ukraine
https://orcid.org/0000-0003-1115-1747

Maxim Antal

Master's Student
National University of Life and Environmental Sciences of Ukraine
03041, 15 Heroiv Oborony Str., Kyiv, Ukraine
https://orcid.org/0009-0009-6928-2388

A study of mixer-feeder equipment operational reliability

Abstract. Modern livestock development trends in the agricultural production structure include the use of feed mixers and distribution equipment. However, a stream of malfunctions and failures is reported for mixer-feeders due to factors that are specific to agricultural enterprises in Ukraine, which reduce the operational reliability of feed mixers and distributors. The study aims to evaluate the quantitative indicators of the in-service reliability of mixer-feeders and develop methods to improve them. The reliability test plan [NMT] was used, which implies a certain number of research objects (*N*)*,* objects undergoing repair in case of performance loss (*M*), and tests terminated when the operating time (*T*) is reached. Initial information was collected and processed, and empirical data on the time between failures of KUHN PROFILE 12.2 DS and PROFILE 14.2 DS mixer-feeders in Ukraine were analysed. The analysis established that the faulty condition of mixers-feeders in the initial operation period is caused by the second complexity group failures. Failures related to the loss of the grinding and mixing mechanism, which limits the average time between failures of the feed mixture and distribution equipment, were identified among the second complexity malfunction group. A statistical analysis of the mixer-feeder failure occurrence was carried out. The failure probability of the grinding-mixing mechanism of the feed mixer was determined to be within the normal distribution law. The main parameters of the given theoretical distribution law were determined by calculation results. The calculations determined that the average time between failures is 3152.0 motor-hours; the standard deviation is 902.6 motor-hours; and the coefficient of variation is 0.40. An average time between failures of the study objects was proved to be consistent with the normal distribution law following Kolmogorov's agreement criterion. Calculations determined that the average reliability index value, according to the normal distribution law, is within the confidence intervals: 1964.2 motor-hours – lower confidence limit; 4339.8 motor-hours – upper confidence limit. The obtained results may be used to improve the mixer-feeder operational reliability

Keywords: mixer-feeder; grinding-mixing mechanism; reliability indicators; time between failures; operation

Article's History: Received: 01.08.2023; Revised: 03.11.2023; Accepted: 22.11.2023.

Suggested Citation:
Novitskyi, A., Banniy, O., Novitskyi, Yu., & Antal, M. (2023). A study of mixer-feeder equipment operational reliability. *Machinery & Energetics,* 14(4), 101-110. doi: 10.31548/machinery/4.2023.101.

*Corresponding author

INTRODUCTION

One of the main branches of agriculture is livestock farming. Preparation and distribution of feed is one of the most important tasks in livestock production. At all stages of the task, efforts should be focused on reducing feed consumption, improving its physical and mechanical properties, enhancing its quality and ensuring that it meets zootechnical requirements. Y. Chen *et al.* (2017) suggest using a nutrient-balanced diet based on the physiological needs of ruminants, including cattle, goats and sheep, at different stages of growth. The rationale for these diets by animal nutrition experts includes roughage, chopped to appropriate lengths, concentrates and various additives that are fully mixed in specific proportions. S. Morrone *et al.* (2022) noted that the use of balanced ration technologies is an effective methodology for cattle and sheep farming, and the implementation of the transition from traditional to modern feeding. The justification of feeding technologies and the development of appropriate feed preparation and distribution equipment are key to its effective application.

In many countries with developed livestock production, research has been conducted on the technological processes of preparing feed mixtures, improving existing ones and developing modern feed preparation machines (Astanakulov *et al.*, 2020). Studies of the operating characteristics of feed preparation and distribution equipment have shown that, along with the increased load on each feed mixer, many factors cause a significant dispersion of technical and economic use indicators (Khmelovskyi *et al.*, 2020), machine reliability parameters (Ruzhylo *et al.*, 2022), and the durability of working bodies. In this regard, one of the most important criteria for the quality of the operation of feed preparation and distribution equipment is its reliability. The scientific and technical literature emphasises the importance of using feed preparation and distribution equipment on cattle farms (Lo *et al.*, 2019).

O. Voinalovych *et al.* (2019) presented a methodology for assessing the residual life of tractors and their units. The metrics covered in the paper reflect the results of the long-term operation of objects based on the data of flaw detection. The presented methodology is based on the use of Markov random processes in the study of a complex man-machine-environment system. To implement the model, the values of failure intensities and recovery intensities are required, which are calculated based on the use of the values of time between failure and recovery recorded during operation. The methodological approaches implemented in the article can be used to study the operational reliability of trailed and self-propelled vehicles for feed preparation and distribution.

The presented problematic issues of ensuring reliability need to be studied and implemented based on the analysis of guidelines for the use of feed preparation and distribution equipment. Foreign and Ukrainian feed mixers have recommended operating instructions, but they often differ in the range of such mechanical parameters of feed mixtures as the sequence of loading feed components; mixing time; and feeding speed. Z. Ruzhylo *et al.* (2022) argued that most guidelines for the use of feed preparation and distribution equipment lack information on the level of machine reliability, limit state criteria, and recommendations for maintaining performance. Alongside stationary feed preparation machines and trailed feed dispensers, cattle farms in Ukraine use self-propelled foreign-made feed preparation and distribution equipment. The analysis shows that some manufacturers of these machines do not provide consumers with values of qualitative and quantitative reliability indicators. An important component of the assessment of the operational reliability of feed mixers that requires detailed study is the study of the impact of the human operator as a component of the complex technical system "Man-Machine-Environment" (Novitskyi *et al.*, 2016).

I.L. Rogovskii *et al.* (2022) presented a methodology for determining the patterns of change in the technical condition of Slavutych KZTs-9F combine harvesters (self-propelled combine harvester, Ukraine) during operation. The research paper presents the results of operational studies of combined harvesters' performance and identifies mechanisms and systems that limit reliability. A list of working bodies and parts whose technical condition requires constant monitoring and, if necessary, restoration in case of loss of performance is substantiated. T. Yezekyan *et al.* (2020) reflected the technical parameters of grain harvesters and forage harvesters and developed reference models for determining technical and economic parameters. The authors put forward a variant of linear models, which are reference models for determining the size of equipment and key parameters, and are the basis for development or modernisation. The proposed solution made it possible to justify the choice of machine design and ensure the rational use of economic and environmental resources. The use of modelling will provide a forecasting capability for determining the technical and economic parameters of machines.

To ensure the serviceability or operability of feed mixers, it is necessary to perform a set of maintenance and repair measures. Therefore, researching assessing and ensuring the operational reliability of feed mixers is a rather urgent problem. The study aims to evaluate the quantitative indicators of the reliability of feed mixers in operation and develop measures to improve it.

LITERATURE REVIEW

The tendency is towards the widespread use of feed mixers with horizontal and vertical grinding-mixing designs. In most countries with developed livestock production on cattle farms, considerable attention has been focused on the development of stationary or trailed vertical single-screw and horizontal twin-screw feed mixers-feed dispensers of feed mixtures (Li *et al.*, 2017; Norton *et al.*, 2019; Yezekyan *et al.*, 2020). T. Fuyang *et al.* (2020) argued that the hopper of these devices can be either horizontal trapezoidal or vertical in the shape of a cut cone. Mixer-feeders may also include auxiliary mechanical equipment in their design, including mills for loading and chopping feed or grabs only for loading it and weighing devices for weighing components. T. Yezekyan *et al.* (2020) noted that the design of milling drums of farm combines makes it possible to load and grind silage, haylage from storage, hay in rolls, concentrated feed in film sleeves, etc. It should be noted that, according to P. Ma *et al.* (2020), the working bodies of feed mixers mounted on horizontal augers provide better feed chopping quality than vertical augers. At the same time, machines with vertical grinding and mixing mechanisms are characterised by a higher level of reliability and efficiency. In recent years, research has mainly focused on improving the design of stationary and trailed feed mixers.

Because the livestock industry in many countries of Europe and Asia is developing effective, scientific and practical research on the processes of preparation, transportation, distribution and dosing of feed mixtures by self-propelled and trailed vehicles, stationary equipment is becoming crucial in the technologies of feeding cattle and poultry. U. Moallem *et al.* (2020) noted that mixed diets are used on livestock farms in Israel and the United States. The quality of the overall mixed diet depends on the level and cost of feed, the appropriate diet formulation, and the specifics of preparation. Through practical research, the authors of the scientific article determine the impact on the quality of the feed mixture of the parameters of the equipment used for mixing and dispensing, the professionalism of the operator, control systems, and the sequence of loading of feed components. The issues of testing feed preparation machines need to be clarified.

L. Li *et. al.* (2017) noted that in China, for the most part, stationary or trailed vertical single-screw and horizontal twin-screw mixers are used for feed preparation. Separate studies have been conducted on silage loaders and belt conveyors. At the same time, practical issues of processing information on the efficiency and reliability of these objects need to be clarified. G. Bekele (2020) presented a stationary poultry feed mixer developed, tested, and evaluated by the author. The results of experimental studies indicate that the coefficient of variation has decreased, the degree of mixing has improved, and, accordingly, the mixer shaft speed and mixing time have increased. These indicators minimise the cost of preparing the feed mixture.

S. Morrone *et al.* (2022) noted the relevance and importance of research in precision animal husbandry, which has spread around the world since its formation in 2003, using the achievements of Industry 4.0 and IoT technologies. This modern technological approach to livestock farming covers ethical, economic and logistical aspects. The authors of this paper note that the successful and sustainable development of the livestock industry requires the use of modern feeding technologies and the development of new and improvement of existing means for the preparation and distribution of feed. Among the main resources that ensure high-quality preparation and dosed distribution of feed mixtures are the following: computerisation of the technological process; and on-demand service.

P. Najafi *et al.* (2015) pointed out that the performance of a sugarcane harvester as a complex system depends on the reliability of its component subsystems or mechanisms. When calculating reliability, the authors considered the possible impact of the environment, the effectiveness of maintenance, the specifics of the work process, and the experience of farmers. Therefore, to identify bottlenecks in the harvester system and search for components or subsystems, an analysis of mechanisms with low reliability is necessary. G. Jia *et al.* (2017) proposed a general stochastic formula for analysing the life cycle of wearing engineering systems. The authors note that parametric and emergency failures of an engineering system can be caused by operating conditions, extreme loads, or the influence of environmental conditions. These methodological approaches can be used to restore the parameters of technical mixer-feeders. C. Leangsuksun *et al.* (2022) pointed out that there is a gap between the design process and the modelling of the research objects, which can be compensated by using analytical methods for reliability assessment and assurance. At the same time, additional theoretical and experimental studies are needed to make it possible to realise the property of using these methods and methodologies for forming the reliability of feed mixers at certain stages of the life cycle.

MATERIALS AND METHODS

The study was carried out at the National University of Life and Environmental Sciences of Ukraine (NULES). The objects of the study were mixer-feeders PROFILE 12.2 DS and PROFILE 14.2 DS (Auduro S.A. plant, KUHN Group, France) of KUNH Ukraine LLC (Operator's manual..., 2018; Operator's manual. Mixer feeder wagon. PROFILE. 2DS, 2019) (Fig. 1a) and the grinding-mixing mechanism (Fig. 1b).

a)

b)

Figure 1. PROFILE 14.2 DS feed mixer (a) and chopping and mixing mechanism (b)
Source: compiled by the authors

The reliability of 25 PROFILE 12.2-14.2 feed mixers, which were operated in agricultural enterprises of Ukraine during 2015-2022, was monitored during the research. During the test, PROFILE feed mixers were distributed by region as follows: Khmelnytsky – 9 machines; Zhytomyr – 3 machines; Cherkasy – 3 machines, Vinnytsia – 6 machines; Volyn – 1 machine; Chernihiv – 2 machines; Poltava – 1 machine.

Failures of the PROFILE 12.2 DS and PROFILE 14.2 DS feed mixers are distributed by subsystems of the feed mixer: chopping and mixing mechanism; feed mixture unloading mechanism; running system; frame; and control system. The test mode at the site was set as operational. The reliability test plan [NMT] (DSTU 3004-95..., 1995) was adopted, which provides for the presence of a certain number of research objects *N,* objects are restored in case of loss of efficiency *M*, tests are terminated when the corresponding operating time *T.* That is, for the presented test plan [NMT], the initial parameters are: number of observation objects *N*, pieces; property of objects to be restored in case of loss of efficiency *M*; duration of observations *T*, motor-hours. To determine the minimum number of observations, the initial data that indicates the accuracy of the research results is set. The initial data include the confidence probability, which is assumed to be $\gamma = 0.9$, and the maximum relative error $\delta = 0.15$. The distribution of failures of feeder mixers according to a priori data follows the law of normal distribution (DSTU 3004-95..., 1995). Using reference tables, the minimum number of objects to be set up for testing was determined to be $N_{min} = 21$ (DSTU 3004-95..., 1995). $N = 25$ feed mixers were accepted. The established duration or time of observation is 4880 motor-hours. This value was determined under the assumption that the distribution of failures follows a normal distribution law, with $\gamma = 0.9$ and $\delta = 15$.

The methodology included checking the correspondence between the theoretical law and the empirical distribution of the time between failures of the mixer-feeder according to the agreement criterion λ by O.M. Kolmogorov (Chornovil *et al.*, 2010) The number of objects required for reliability testing was calculated using the following formula by M.I. Chornovil *et al.* (2010):

$$n = \frac{\sigma^2 t_\beta^2}{\Delta^2}, \tag{1}$$

where *n* – required number of parts for inspection, pieces; σ^2 – statistical variance, motor hour.; t_β^2 – a tabular coefficient that depends on the accepted confidence level, β; Δ^2 – the magnitude of the permissible error (when studying the wear failures of parts, assume $\Delta = 0.8$ of the interval value).

The results obtained on the occurrence of failures of the PROFILE 12.2 DS and PROFILE 14.2 DS feed mixers were taken from the reporting regulatory and technical documentation of the official dealer of KUHN equipment in different regions of Ukraine. Statistical analysis methods and experimental data processing techniques were used to obtain the following indicators: mean time between failures; standard deviation; coefficient of variation; theoretical distribution law; and scattering intervals.

RESULTS AND DISCUSSION

Based on the results of the analysis of regulatory and technical documentation, failures were recorded for 25 machines and the time between failures was determined. The results of the failure distribution are shown in the diagram (Fig. 2). Analysis of the diagram shows that most of the failures relate to the grinding and mixing mechanism: wear and damage to the knives; loss of efficiency of the working auger with knives; wear of the hopper body; oil leakage from the gearbox; short circuit of electrical equipment. Failures were distributed as follows: auger, auger with knives – 48%; hopper – 44%; other reasons – 8%.

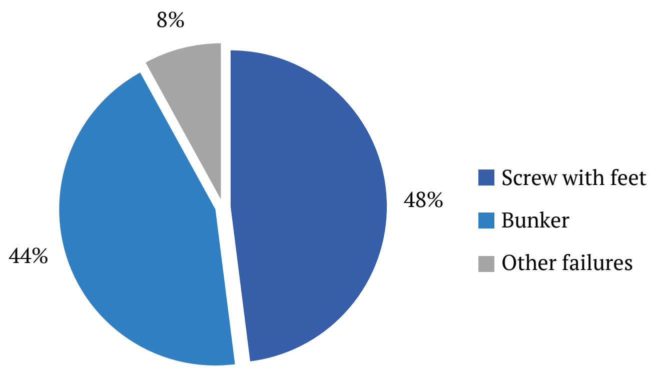

Figure 2. Failure distribution of PROFILE 12.2 DS and PROFILE 14.2 DS feed mixers
Source: compiled by the authors

Failures that limit the reliability of feed mixers were identified. For systematisation, finding ways to analyse and eliminate them, the failures were divided into complexity groups. The analysis of the diagram (Fig. 2) shows that 92% of failures of PROFILE 12.2 DS and PROFILE 14.2 DS feed mixers belong to the second group of complexity. These failures can be eliminated by replacing or repairing easily accessible components and assemblies. To eliminate these failures, it is necessary to open the internal cavities of the units without disassembling them or to perform extraordinary maintenance operations. The diagram shown in Figure 2 also confirms that the most typical failures that limit the reliability of the research objects are failures of the grinding and mixing mechanism.

Statistical data of the tests of the PROFILE 12.2 DS and PROFILE 14.2 DS feed mixers were obtained in the course of the research. A table of statistical information was compiled to process the experimental data on the time between failures of the feed mixers. After grouping the test results by intervals, the failure rate was specified and the accumulated experimental probability was determined. The results of the empirical distribution of the time between failures of feed mixers are presented in Table 1 in the form of a statistical series of information and are graphically shown in Figure 3.

Table 1. Statistical series of time between failures of feed mixers

No. pp	Boundaries of intervals	Interval median	Occurrence rate, m_i	Probability, P_i	Accumulated probability of experimental results, ΣP_i
1	1250-1976	1613	4	0.16	0.16
2	1976-2702	2339	2	0.08	0.24
3	2702-3428	3065	7	0.28	0.52
4	3428-4154	3791	10	0.4	0.92
5	4154-4880	4517	2	0.08	1.0

Source: compiled by the authors

The histogram analysis shown in Figure 3 demonstrates that in the initial period of operation of the feed preparation and distribution equipment, which corresponds to the operating time in the range of 1250-1976 motor-hours, knife failures were recorded, and in the range of 2702-3428 motor-hours – failures of augers with knives. Failures of feed mixers, which were recorded in the range of 3428-4154 motor-hours, correspond to the loss of efficiency of the feed mixer hopper.

After processing the information, the obtained array of experimental data is characterised by the following indicators:

- average wear per failure, $\bar{t} = 3152.0$ motor-hours;
- average square deviation, $\sigma = 902.6$ motor-hours;
- variation coefficient, $\upsilon = 0.40$.

The occurrence of failures of the grinding and mixing mechanism of the PROFILE 12.2 DS and PROFILE 14.2 DS feed mixers is subject to the law of normal distribution (DSTU 3004-95..., 1995). The correspondence between the theoretical law and the empirical distribution of the time between failures of the mixer-feeder was checked by Kolmogorov's criterion of agreement λ. Since $P(\lambda) = 0.9972$ is greater than the accepted significance level for the law of normal distribution, the accepted condition of the possibility of matching the Weibull-Gnedenko law with the empirical distribution of operating time is rejected (DSTU 3004-95..., 1995).

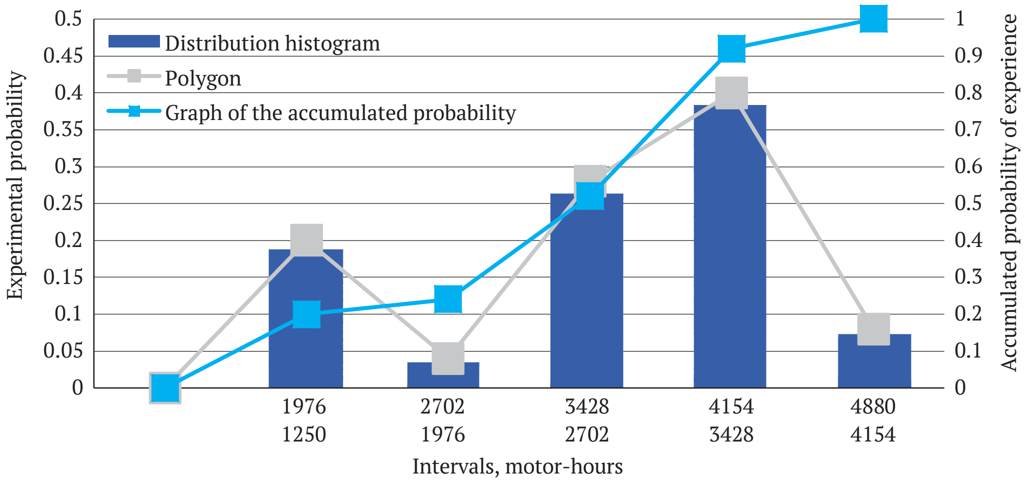

Figure 3. Histogram of distribution, distribution polygon, the graph of the accumulated experimental probability of time between failures of PROFILE 12.2 DS and PROFILE 14.2 DS feed mixers

Source: compiled by the authors

The boundaries of confidence intervals and the size of the scattering interval of the mean time between failures of PROFILE feed mixers for the normal distribution law were calculated using the formulas (DSTU 3004-95..., 1995; Chornovil *et al.*, 2023). The results of these values were respectively:

1. $t^l_{90} = 1964.2$ motor-hours – lower acceptable limit;
2. $t^u_{90} = 4339.8$ motor-hours – upper acceptable limit;
3. $I_{90} = 2375.6$ motor-hours – interval value.

The number of objects required for the tests was calculated. The results of the calculations showed that 9 objects were sufficient for the research according to the test plan

[NMT]. The operational reliability of 25 feed mixers was investigated.

The reliability of the chopping and mixing mechanism (Fig. 4) is limited by the knives, auger sets with knives and the hopper body. The PROFILE 12.2 DS and PROFILE 14.2 DS feed mixers are equipped with two A5336551 augers (Auduro S.A., KUHN Group, France). Each auger is fitted with a corresponding number of knives, according to the design of the PROFILE 12.2 DS or PROFILE 14.2 DS. The knives of the chopping and mixing mechanism can be installed in two ways (Fig. 4). The small knife A5362450 (Auduro S.A., KUHN Group, France), shown in Figure 4a, contains 7 teeth and is installed on the lower turns, and the large knife A5303620 (Auduro S.A., KUHN Group, France), shown in Figure 4b, contains 9 teeth and is fixed on the upper turns of the grinding and mixing mechanism screw. The number of knives mounted on one screw is 6 for small ones and 2 for large ones.

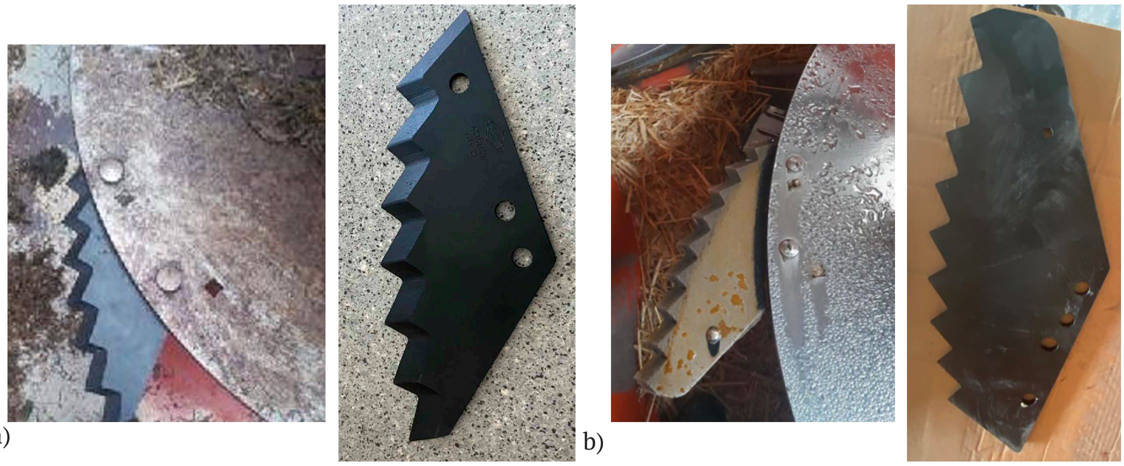

Figure 4. Knives of the PROFILE 12.2 DS and PROFILE 14.2 DS feed mixers in operation and assessment of their technical condition

Note: a – small blade A5362450; b – large blade A5303620

Source: compiled by the authors

Based on this, to prevent the occurrence of mixer-feeder failures during operation, it is necessary to provide for the possibility or include in the list of maintenance activities for the elements of the grinding and mixing mechanism the operation of assessing the technical condition and restoring the hopper's performance at 3000-3100 motor-hours. The inclusion of this operation in the complex maintenance and repair works will increase the availability of the mixer-feeder, reduce the downtime of the vehicle and reduce the cost of restoring performance in case of failure of the grinding and mixing mechanism.

From the analysis of theoretical materials and the results of experimental studies of the operational reliability of feed preparation and distribution equipment, it can be concluded that most authors conducted a scientific search to establish the design parameters and functional and operational parameters of feed mixers. V. Loveikin *et al.* (2022) note that the process of preparing a feed mixture by a feed preparation device is carried out in a single-stream way by a cone-shaped screw working body. The functioning of the device is carried out due to the simultaneous movement and operation of the screw mechanism of grinding and mixing. In this case, dynamic forces arise that lead to the movement of the feed preparation device in the transverse and longitudinal directions, relative to its axis and wear of the elements of the specified mechanism and the chassis. The authors of the article substantiate a rational design of the grinding-mixing mechanism in the form of a two-stroke conical screw. These proposals for changes in the design of the mechanism will intensify the technological process of feed preparation by a mobile feed preparation unit, and improve the balance of the mechanism and the durability of tyres. It would also be advisable to clarify how changes in design parameters will affect the quantitative and qualitative indicators of the reliability of the grinding and mixing mechanism and the durability of the working bodies.

The tendency towards the widespread use of feed mixers with horizontal and vertical grinding-mixing designs is evident. In most countries with developed livestock production on cattle farms, considerable attention is focused on the development of stationary or trailed vertical single-screw and horizontal twin-screw feed mixers-feed dispensers of feed mixtures (Norton *et al.*, 2019). The hopper of these machines can be either horizontal trapezoidal or vertical in the form of a cut cone. Mixer-feeders may also include auxiliary mechanical equipment in their design, including cutters for loading and chopping feed or grabs only for loading it and weighing devices for weighing components. T. Yezekyan *et al.* (2020) found that the design of milling drums of farm combines makes it possible to load and grind silage, haylage from storage, hay in rolls, concentrated feed in film sleeves, etc. It should be noted that the working bodies of feed mixers mounted on horizontal augers provide better feed-chopping quality than vertical augers (Ma *et al.*, 2020). At the same time, machines with vertical grinding and mixing mechanisms are characterised by a higher level of reliability and efficiency of use.

The following combine harvesters have been tested in livestock production in Western European countries and China: Sam 5 490/95 by Seko (Italy), Solomix 2 12VL3 by TRIOLIET (Netherlands), Roto-mix 354-12 by Roto-mix (USA), and 12 St by De Laval (Sweden). However, the scientific and technical literature still lacks information on the performance characteristics of the presented equipment, and research on the technological processes of loading feed components, mixing, transporting and distributing both farm combines and trailed vehicles.

Due to the increase in the volume of foreign agricultural machinery, there is an urgent need to ensure its efficient use in Ukrainian farms, to study the impact of technical and operational parameters of agricultural machinery on the efficiency of its operation, to assess its operational reliability (Najafi *et al.*, 2015), and to use a systematic approach to ensure its performance (Leangsuksun *et al.*, 2022). Strategies for repairing and restoring the operability of machines to increase the reliability and functionality of a complex technical system during operation are proposed in an article by G. Jia *et al.* (2017).

In this aspect of research, the materials provided in the test report of the German testing organisation DLG (DLG Test Report 6418, 2016) for the Siloking Self Line 4.0 Premium 2215 self-propelled mixer-dispenser (Germany) are worthy of attention. This manual opens up the prospects for its use not only to ensure its operational efficiency but also to formulate and develop test plans for similar feed preparation and distribution equipment.

The absence of uniform technical requirements and recommendations for the use of feed mixers leads to a decrease in the quality of mixing feed components and the uniformity of feed distribution to animals. This problem is partially reflected in some scientific articles. However, these studies do not fully reflect the reliability indicators and recommendations for their improvement for feed mixers, including KUHN (France), Seko (Italy), Roto-mix (USA), Trioliet (Netherlands), Siloking and Strautmann (Germany), Delaval (Sweden), which are used in Ukraine. This is because these products are used in different regions, on livestock farms with different livestock, for the preparation of feed mixtures for different groups of livestock and different rations.

V. Khmelovskyi *et al.* (2020) substantiate that for the preparation and distribution of feed mixtures for 51-400 cattle heads, mobile feed preparation equipment should be used with the mixture being fed to feed tables. The paper presents a study of the process of self-cleaning of screw turns at different rotational speeds. The analytical studies and several experiments made it possible to determine the optimal angle of inclination of the turns and the speed of rotation of the screw, which should be at least 25 min^{-1}. The importance of the results for improving the functioning of the grinding-mixing mechanism is confirmed by the possibility of intensifying the process of the feed mixture descent from the screw turns. At the same time, it would be interesting to conduct research aimed at establishing the relationship between these recommendations on the modes of use of the feed preparation agent and its reliability in operation.

The results of studies of feed mixers and self-propelled feed mixers presented in a paper by D. Wang *et al.* (2017) can be useful for the optimal design and optimisation of machines for the preparation and distribution of feed. The researchers presented a justification for the parameters of the auger with the angle of the coils, and the design of the hopper body and determined their impact on the effective preparation of the mixture. The article recommends maintaining the speed of rotation of the auger of the grinding and mixing mechanism close to 32.5 min^{-1}, which will make it possible to prepare a high-quality feed mixture in 4.7 minutes. At the same time, operators need to know how these changes in the design and operation of the grinding and mixing mechanism will affect the performance and reliability of feed mixers. T. Fuyang *et al.* (2020) recommend improving the design and technological parameters of self-propelled feed mixers using the methodology and results of optimising the vertical auger of the grinding and mixing mechanism. The authors of the research paper note that to ensure the quality of preparation and uniformity of the dosed feed mixture, the screw rotation speed should be 22...26 min^{-1}. The recommended time for mixing feed components with self-propelled mixers should be within 6...8 minutes.

S. Postelga *et al.* (2021) presented the results of a comprehensive evaluation of the Siloking SelfLine 4.0 Premium 2215 self-propelled mixer-distributor (Germany) in the process of using it in operation. According to the results of the research, the author found that during the mixing of 5 types of feed, a high-quality homogeneous feed mixture was obtained, with a moisture content of 59.5%, bulk density of 405 kg/m^3, and an average particle size of 17.4 mm. The tests confirmed the effectiveness of the self-propelled mixer-feeder, which ensured 94.3% uniformity of feed mixing and 95.5% uniformity of feed distribution. The test results show that the mixer-dispenser satisfactorily and efficiently performs the technological process of preparing and distributing the feed mixture. However, as the analysis of the test results of Siloking SelfLine 4.0 Premium 2215 (Germany) shows, the article does not sufficiently reflect the reliability of the mixer-dispenser in operation.

V. Bulgakov *et al.* (2017) presented theoretical studies of the parameters of auger working bodies of agricultural machinery and equipment. The authors investigated the movement of a material particle along the working body of an agricultural machine in the form of a vertical auger limited by a coaxial fixed cylinder and proposed for use in the development and improvement of mixer-feeders the dependencies of changes in the speed of transport of a material particle under the influence of the coefficient of friction of the particle on the surface of the auger and the surface of the limiting vertical cylinder. V.M. Baranovsky *et al.* (2018) presented the results of a study of technological operations for transporting agricultural production materials in closed fixed buildings. The study of the operations of transporting these materials by screw conveyors described in the article was not only highly appreciated and efficient but also confirmed the possibility of using them in the design of loading and unloading mechanisms for agricultural machinery. The research results obtained in the articles can be used to substantiate the design parameters and ensure the operational reliability of feed preparation and distribution equipment.

The human factor as a component of the complex technical system “man-machine-environment” is of particular importance in ensuring the operability of machines and equipment. H.-W. Lo *et al.* (2019) and R.M. Amaya-Toral *et al.* (2022) pointed out that increasing the operational reliability of machines and reducing the possible risks of failures during the production process also depends on the reliability of the human operator. It is also necessary to take advantage of the experience of using analytical methods and methods of expert assessment of specialists in calculating and ensuring the reliability of technical systems “man-machine-environment”. The results of scientific work have confirmed the possibility of using analytical methods and test results to ensure the reliability of not only feed preparation and distribution equipment but also service and repair and technological equipment.

During the study of the operational reliability of feed mixers, it was found that some failures were caused by the lack of information in the regulatory documentation on the criteria for the limited state of the working bodies of the grinding and mixing mechanism, including knives and auger elements. The practice of using PROFILE 12.2 DS and PROFILE 14.2 DS has established that one of the first causes of failures of the grinding and mixing mechanism is a deviation from the frequency of assessment of the technical condition of working bodies and parts. Other reasons for mechanism failures are a decrease in the reliability of the human-operator system and insufficient control over the parameters of the technical condition of the mixer-feeder as a complex technical system. Most of the analysed articles are aimed at the design improvement of units and machines in general to ensure efficient operation and reliability. At the same time, the analysed sources do not reflect the level of reliability of mixer feeders both at the stage of manufacture and during operation. The methodology proposed in the article and the results obtained confirm the possibility of assessing and calculating quantitative reliability indicators during the operation of machines for the preparation and distribution of feed.

CONCLUSIONS

Based on the research results, information was obtained on the time between failures of 25 feed mixers under operating conditions. The obtained data set of time between failures of the PROFILE 12.2 DS and PROFILE 14.2 DS feed mixers are characterised by the following indicators: average time between failures, $t = 3152.0$ motor-hours; standard deviation, $\sigma = 902.6$ motor-hours; coefficient of variation, $\upsilon = 0.40$; theoretical law of distribution – the law of normal distribution. The correspondence between the theoretical law and the empirical distribution of the time between failures of the mixer-feeder according to Kolmogorov’s criterion of agreement was established. The calculations have established that the values of the mean time between failures of the objects of study, which are consistent with the law of normal distribution, are within the confidence intervals: $t^u_{90} = 1964.2$ motor-hours – lower acceptable limit; $t^l_{90} = 433.8$ motor-hours – upper acceptable limit.

According to the KUHN recommended frequency of scheduled maintenance and repairs of the PROFILE 12.2 DS and PROFILE 14.2 DS feed mixers, it was found that in the initial period of operation of the machine, which corresponds to an operating time of 1250-1976 hours, knife failures were recorded, and in the range of 2702-3428 hours – failures of augers with knives. Failures of feed mixers, which were recorded within the operating time between failures of 3428-4154 motor-hours, are associated with the loss of efficiency of the hopper. It is proposed to include in the complex of works on maintenance and repair of the operation an assessment of the technical condition and restoration of the hopper’s operability, which will ensure an increase in the availability of the mixer-feeder.

Further research will consider analytical methods for assessing the reliability of the grinding-mixing mechanism of feed mixers as complex technical systems “man-machine-environment” and develop measures to reduce the likelihood of failures depending on the influence of the human factor. Another promising area for further research is the formation of feedback from machine manufacturers and technical service representatives on the development and implementation of a programme to ensure the reliability of feed preparation and distribution equipment at the stage of operation.

ACKNOWLEDGEMENTS

None.

CONFLICT OF INTEREST

None.

REFERENCES

[1] Amaya-Toral, R.M., Piña-Monarrez, M.R., Reyes-Martínez, R.M., de la Riva-Rodríguez, J., Poblano-Ojinaga, E.R., Sánchez-Leal, J., & Arredondo-Soto, K.C. (2022). Human-machine systems reliability: A series-parallel approach for evaluation and improvement in the field of machine tools. *Applied Sciences*, 12(3), article number 1681. doi: 10.3390/app12031681.

[2] Astanakulov, K.D., Gapparov, Sh., Karshiev, F., Makhsumkhonova, A., & Khudaynazarov, D. (2020). Study on preparation and distribution of forage by chopping coarse feed. In *IOP Conference Series: Earth and environmental science 1st international conference on energetics, civil and agricultural engineering* (vol. 614, article number 012158). Tashkent: IOP.

[3] Baranovsky, V.M., Hevko, R.B., Dzyura, V.O., Klendii, O.M., Klendii, M.B., & Romanovsky, R.M. (2018). Justification of rational parameters of a pneumoconveyor screw feeder. *INMATEH: Agricultural Engineering,* 54(1), 15-24.
[4] Bekele, G. (2020). Development of livestock feed mixer. *International Journal of Scientific and Research Publications*, 10(10), 481-486. doi: 10.29322/IJSRP.10.10.2020.p10665.
[5] Bulgakov, V., Holovach, I., Bandura, V., & Ivanovs, S. (2017). A theoretical research of the grain milling technological process for roller mills with two degrees of freedom. *INMATEH. Agricultural Engineering,* 52(2), 99-106.
[6] Chen, Y., Tian, F., Yan, Y., Song, Z., Li, F., & Zhang, Z. (2017). Research progress of domestic and foreign TMR feeding technologies and mixers. *Journal of Chinese Agricultural Mechanization*, 38(12), 19-29.
[7] Chornovil, M.I. (Ed.). (2010). *Reliability of agricultural machinery*. Kropyvnytskyi: CODE.
[8] DLG Test Report 6418. (2016). *Self propelled vertical feed mixer wagon SILOKING SelfLine 4.0 Premium 2215-19*. Retrieved from https://cdn2.hubspot.net/hubfs/4411355/Verkkosivut/Siloking/Tekniset%20tiedot/Siloking%20SelfLine%20DLG-test.pdf.
[9] DSTU 3004-95. (1995). *Reliability of equipment. Methods of estimating reliability indicators based on experimental data*. Kyiv: State Standard of Ukraine.
[10] Fuyang, T., Yuhua, C., Zhanhua, S., & Yinfa, Y. (2020). Finite element simulation and performance test of loading and mixing characteristics of self-propelled total mixed ration mixer. *Journal of Engineering,* 12, 1-15. doi: 10.1155/2020/6875816.
[11] Jia, G., Tabandeh, A., & Gardoni, P. (2017). Life-cycle analysis of engineering systems: Modeling deterioration, instantaneous reliability, and resilience. In *Risk and reliability analysis: Theory and applications* (pp. 465-494). Cham: Springer International Publishing.
[12] Khmelovskyi, V., Otchenashko, V., Voloshyn, S., & Pinchevska, O. (2020). Providing processes of preparation and distribution of feed for cattle on animal husbandry farms. In *Engineering for rural development* (pp. 778-783). Jelgava, Latvia.
[13] Leangsuksun, C., Song, H., & Shen, L. (2003). Reliability modeling using UML. In *Proceedings of the international conference on software engineering research and practice* (pp. 259-262). Las Vegas, USA.
[14] Li, L., Wang, D., & Jiang, Z. (2017). Comparison of detection methods for mixing uniformity of rotary total mixed rations mixer. *Journal of Gansu Agricultural University*, 52(3), 136-139.
[15] Lo, H.-W., Liou, J.J.H., Huang, C.-N., & Chuang, Y.-C. (2019). A novel failure mode and effect analysis model for machine tool risk analysis. *Reliability Engineering and System Safety,* 183, 173-183. doi: 10.1016/j.ress.2018.11.018.
[16] Loveikin, V., Khmelovskyi, V., Lukach, V., & Achkevych, V. (2022). Improving efficiency of mobile combined feed mixer. In *Engineering for rural development* (pp. 853-859). Jelgava, Latvia.
[17] Ma, P., Li, L., Wen, B., Xue, Y., Kan, Z., & Li, J. (2020). Design and parameter optimization of spiral-dragon type straw chopping test rig. *International Journal of Agricultural and Biological Engineering*, 13(1), 47-56.
[18] Moallem, U., & Lifshitz, L. (2020). Accuracy and homogeneity of total mixed rations processed through trailer mixer or self-propelled mixer, and effects on the yields of high-yielding dairy cows. December 2020. *Animal Feed Science and Technology,* 270, article 114708. doi: 10.1016/j.anifeedsci.2020.114708.
[19] Morrone, S., Dimauro, C., Gambella, F., & Cappai, M.G. (2022). Industry 4.0 and precision livestock farming (PLF): An up to date overview across animal productions. *Sensors*, 22(12), article number 4319. doi: 10.3390/s22124319.
[20] Najafi, P., Asoodar, M.A., Marzban, A., & Hormozi, M.A. (2015). Reliability analysis of agricultural machinery: A case study of sugarcane chopper harvester. *AgricEngInt: CIGR Journal*, 17(1), 158-165. doi: 10.22616/ERDev2019.18.N387.
[21] Norton, T., Chen, C., Larsen, M.L.V., & Berckmans, D. (2019). Review: Precision livestock farming: Building "digital representations" to bring the animals closer to the farmer. *Animal,* 13(12), 3009-3017. doi: 10.1017/S175173111900199X.
[22] Novitskyi, A.V., & Banniy, A.A. (2016). Logic and probabilistic modeling of reliability of complex agricultural machinery. *MOTROL. Commission of Motorization and Energetics in Agriculture*, 18(3), 191-199.
[23] Operator's manual. Mixer feeder wagon. PROFILE 12.2-13.2 DS. (2019). Retrieved from. https://nubip.edu.ua/sites/default/files/u132/an112bgb_a_profiie_12.2-13.2.pdf.
[24] Operator's manual. Mixer feeder wagon. PROFILE. 2DS. (2018). Retrieved from https://nubip.edu.ua/sites/default/files/u132/an101bgb_a.pdf.
[25] Postelga, S. (2021). Self-propelled mixer-distributor siloking selfline 4.0 premium 2215 testing. *Agricultural Machinery and Equipment: Forecasting, Design, Testing*, 28(42), 150-161.
[26] Rogovskii, I.L., Titova, L.L., Voinash, S.A., Troyanovskaya, I.P., & Sokolova, V.A. (2021). Change of technical condition and productivity of grain harvesters depending on term of operation. *Earth and Environmental Science*, 720, article number 012110. doi: 10.1088/1755-1315/720/1/012110.
[27] Ruzhylo, Z., Novitskii, A., Milko, D., Bulgakov, V., Beloev, I., & Rucins, A. (2022). Mathematical model for reliability assessment of device for preparation and distribution of animal feed as "Man-Machine". In *Engineering for rural development* (pp. 911-917). Jelgava, Latvia.

[28] Voinalovych, O., Hnatiuk, O., Rogovskii, I., & Pokutnii, O. (2019). Probability of traumatic situations in mechanized processes in agriculture using mathematical apparatus of Markov chain method. In *Engineering for rural development* (pp. 563-569). Jelgava, Latvia. doi: 10.22616/ERDev2019.18.N245.

[29] Wang, D., Li, C., Li, L., Li, B., Wang, G., & Lin, Y. (2017). Mechanism analysis and parameter optimization of blade-type feed mixer. *Transactions of the Chinese Society for Agricultural Machinery*, 48(12), 98-104. doi: 10.6041/j.issn.1000-1298.2017.12.011.

[30] Yezekyan, T., Marinello, F., Armentano, G., Trestini, S., & Sartori, L. (2020). Modelling of harvesting machines' technical parameters and prices. *Agriculture*, 10(6), article number 194. doi: 10.3390/agriculture10060194.

Андрій Валентинович Новицький
Кандидат технічних наук, доцент
Національний університет біоресурсів і природокористування України
03041, вул. Героїв Оборони, 15, м. Київ, Україна
https://orcid.org/0000-0001-7789-8531

Олександр Олександрович Банний
Кандидат технічних наук, доцент
Національний університет біоресурсів і природокористування України
03041, вул. Героїв Оборони, 15, м. Київ, Україна
https://orcid.org/0000-0003-0505-166X

Юрій Андрійович Новицький
Аспірант
Національний університет біоресурсів і природокористування України
03041, вул. Героїв Оборони, 15, м. Київ, Україна
https://orcid.org/0000-0003-1115-1747

Максим Васильович Антал
Студент магістратури
Національний університет біоресурсів і природокористування України
03041, вул. Героїв Оборони, 15, м. Київ, Україна
https://orcid.org/0009-0009-6928-2388

Дослідження експлуатаційної надійності засобів для приготування і роздавання кормів

Анотація. Тенденції розвитку сучасного тваринництва в структурі аграрного виробництва передбачають використання засобів для приготування і роздавання кормів. Але завдяки факторам, які характерні аграрним підприємствам України, для змішувачів-кормороздавачів відмічається поява потоку несправностей і відмов, які знижують показники експлуатаційної надійності засобів для приготування і роздавання кормів. Метою даної статті була оцінка кількісних показників надійності змішувачів-кормороздавачів в умовах експлуатації та розробка заходів щодо її підвищення. Для цього було використано план випробувань на надійність [NMT], який передбачає наявність певної кількості об'єктів дослідження (*N*), об'єкти при втраті працездатності відновлюються (*M*), випробування припиняються при досягненні відповідного напрацювання (*T*). Виконано збирання, обробку вихідної інформації та аналіз емпіричних даних наробітку на відмову змішувачів-кормороздавачів PROFILE 12.2 DS та PROFILE 14.2 DS компанії KUHN в Україні. Під час аналізу було встановлено, що в початковий період експлуатації змішувачів-кормороздавачів, їх несправний стан викликаний відмовами другої групи складності. Серед відмов другої групи складності була виділена несправність, що пов'язана з втратою працездатності механізму подрібнення-змішування, який лімітує середнє напрацювання на відмову засобу для приготування і роздавання кормів. Проведено статистичний аналіз виникнення зазначених відмов змішувачів-кормороздавачів. Встановлено, що ймовірності виникнення відмови механізму подрібнення-змішування засобу для приготування і роздавання кормів підпорядкований закону нормального розподілу. За результатами проведених розрахунків визначені основні параметри представленого теоретичного закону розподілу. Розрахунками встановлено, що середнє напрацювання на відмову становить 3152,0 мото-год.; середнє квадратичне відхилення – 902,6 мото-год.; коефіцієнт варіації – 0,40. Доведено, що середнє напрацювання на відмову об'єктів дослідження узгоджується із законом нормального розподілу за критерієм згоди Колмогорова. Розрахунками встановлено, що середнє значення показника надійності згідно закону нормального розподілу знаходитися в довірних інтервалах: 1964,2 мото-год. – нижня довірна межа; 4339,8 мото-год. – верхня довірна межа. Отримані результати дали можливість підвищити експлуатаційну надійність змішувачів-кормороздавачів

Ключові слова: змішувач-кормороздавач; механізм подрібнення-змішування; показники надійності; напрацювання на відмову; експлуатація

Machinery & Energetics
Vol. 14, No. 4. 2023

Journal homepage:
https://technicalscience.com.ua/en

UDC 681.518.3
DOI: 10.31548/machinery/4.2023.111

Vitaliy Lysenko

Doctor of Technical Sciences, Professor
National University of Life and Environmental Sciences of Ukraine
03041, 15 Heroiv Oborony Str., Kyiv, Ukraine
https://orcid.org/0000-0002-5659-6806

Taras Lendiel

PhD in Technical Sciences, Associate Professor
National University of Life and Environmental Sciences of Ukraine
03041, 15 Heroiv Oborony Str., Kyiv, Ukraine
https://orcid.org/0000-0002-6356-1230

Ihor Bolbot

Doctor of Technical Sciences, Professor
National University of Life and Environmental Sciences of Ukraine
03041, 15 Heroiv Oborony Str., Kyiv, Ukraine
https://orcid.org/0000-0002-5708-6007

Serhii Pavlov*

Postgraduate Student
National University of Life and Environmental Sciences of Ukraine
03041, 15 Heroiv Oborony Str., Kyiv, Ukraine
https://orcid.org/0009-0001-3343-5508

Mobile system for monitoring plant environment parameters for biogas production

Abstract. The main sources of biomass for biogas units can be organic waste, grain, hay, manure, various plant materials, etc. Anaerobic digestion, which consists of a series of complex biological reactions, is a challenging process that requires detailed parameter control to prevent possible losses and to make best use of the material. Therefore, the purpose of this study was to consider the possibility of developing a mobile unit for monitoring the parameters of the plant environment during biogas production with the possibility of storing data and using them in the construction of a mathematical model for predicting gas yield. The algorithm was created based on the principles of fuzzy logic and the structure of neural networks. The architecture of a mobile system for monitoring plant environment parameters for biogas production was proposed. The developed circuit diagram of such a system was presented. The system's operation was presented in the form of a created algorithm for searching and identifying connected devices on the 1-Wire bus. This bus is used to poll sensors and measure process parameters. Software was developed for interfacing several types of sensors, transferring and saving data to the cloud storage with the subsequent possibility of processing it. The biomass can be photographed using the built-in camera. Using the principle of Internet of Things technology, remote access to measured data is provided. The measured process parameters and photos are transferred to the control system server for further analysis, which will allow for a more accurate assessment of the biomass preparation process for fermentation. The obtained results allow improving the control and decision support systems for biomass loading into a biogas unit

Keywords: measurement; control; camera; sensor; biomass

Article's History: Received: 10.07.2023; Revised: 11.10.2023; Accepted: 22.11.2023.

Suggested Citation:
Lysenko, V., Lendiel, T., Bolbot, I., & Pavlov, S. (2023). Mobile system for monitoring plant environment parameters for biogas production. *Machinery & Energetics,* 14(4), 111-120. doi: 10.31548/machinery/4.2023.111.

*Corresponding author

INTRODUCTION

Considering the growing interest in environmentally friendly energy sources and the need to conserve resources, a mobile plant monitoring system is becoming a valuable tool for modern agriculture. Biogas production is a vital component of renewable energy that helps reduce dependence on hydrocarbon fuels. Monitoring of the plant environment contributes to increasing the productivity and efficiency of biogas production, which is important for sustainable energy development and energy conservation, as reported in V.O. Ferreira *et al*. (2023) and K. Gioulounta *et al.* (2023). Biogas production is becoming increasingly popular in today's environment, both in Ukraine and the European Union. 2021 was a record year for the annual increase in biomethane production (almost 6.1 TWh or 0.6 m^3 more than in 2020). In total, the volume of biomethane produced in Europe in 2021 was 37 TWh or 3.5 m^3 (EBA Statistical Report, 2022). The methods of monitoring operating parameters and finding links between them used in biogas plants are insufficiently effective. For instance, O.O. Olakanmi *et al.* (2021) discusses a smart biogas unit that includes a controlled biophysical system that uses both thermofluidic devices and IoT devices to acquire data and control electromechanical subsystems. However, the above study does not include systems for monitoring the condition of biomass undergoing preparation before being loaded into a biogas unit.

Systems based on neural networks (NNs) and Big Data are widely used to find best solutions in various types of production. A.H. Abdurrahman *et al.* (2020) found that such systems make it possible to collect data for everything that creates the conditions for using proportions and operating modes for maximum biogas production. However, this study does not make provision for the use of a camera for external analysis of biomass, which will allow its contactless assessment, since it involves the processing of large amounts of data using computer-integrated technologies. At the same time, L. Zemite *et al*. (2022), A.A. Siyal *et al*. (2023) proved that modern installations, including the one described in this paper, cannot provide the ability to collect data on system parameters at each stage online.

It should also be borne in mind that scientists are looking for ways to increase biogas production using different approaches. For instance, V.M. Polishchuk *et al.* (2021) discusses the issue of increasing the productivity of biogas production through combined fermentation of raw materials. However, in this paper, the authors evaluate the fermentation process by means of laboratory measurements in separate phases of research. Considering the continuity of the fermentation process, it is necessary to constantly monitor technological parameters for a qualitative assessment of the development of new approaches to increase the productivity of biogas production. Approaches to their solution are considered in the studies of M. Zhou & Z. Zou (2018), M. Silwadi *et al.* (2023), where it is argued that this requires obtaining accurate and high-quality data for a long time. As a result, in the future, it is planned to process large amounts of data and train the system on correctly formed models with correctly set goals. At the same time, modern biogas units do not have the ability to collect information on process parameters online at every stage of production. It is proposed to improve the existing control systems of biogas units by monitoring the parameters of the plant environment before they are loaded into the plant.

The purpose of this study was to develop software and hardware for a system for monitoring plant environment parameters for biogas production.

MATERIALS AND METHODS

The production technology was analysed during 2023 based on the Bioenergy Complex of the Astarta-Kyiv agricultural holding, which is characterised by the following indicators: the complex processes 1,200 tonnes of beet pulp per day, 225 tonnes of sugar beet leaf silage and pig manure, and produces about 150,000 m^3 of biogas per day, the equivalent of 75,000 m^3 of natural gas. The design of the plant environment monitoring system was based on the design features of the process equipment and the biomass pretreatment process. Based on the design results, a model of the monitoring system was created. The theoretical stage of the study included an analysis of the works of H. Rahadian *et al*. (2015), V.M. Reshetiuk *et al*. (2016), T. Lendiel *et al*. (2021). Thanks to the review of these studies, the best methods and techniques for the practical stage of the research were selected.

The algorithm was based on fuzzy logic rules and neural network models. The creation of a system for collecting and storing data for long-term storage for further processing and predicting the quality of the plant environment to be fermented began with the architecture of such a system. This architecture included a control device with temperature, air and soil humidity sensors, a camera, and a cloud-based platform for uninterrupted data acquisition and storage.

The NodeMCU v3 module (Espressif Systems, China) was chosen as the control device, built based on the ESP8266 microcontroller (Espressif Systems, China) with the Xtensa L106 processor (Tensilica Inc, USA), which is based on the RISC architecture, uses a frequency of 80 to 160 MHz, which allows for computing and data processing, and is suitable for battery power. One of the key features of the ESP8266 microcontroller was the built-in Wi-Fi module. It supports 802.11 b/g/n standards, which allows devices to connect to wireless networks and share data over the Internet. The ESP8266 features digital and analogue general-purpose input (GPIO) pins that can be used to connect to a variety of devices such as sensors, LEDs, etc. The ESP8266 microcontroller has a Universal Asynchronous Receiver and Transmitter (UART) and a Serial

Peripheral Interface (SPI), which allows it to interact with other devices and microcontrollers when it is necessary to synchronise the operation of devices with each other. The built-in micro-USB port allows connecting the microcontroller to a computer to download the program code.

Temperature measurements on the platform were implemented by several types of sensors:

1) DS18B20 (Analog Devices, USA) is a digital temperature sensor in a waterproof, insulated housing (IP67), which makes it suitable for temperature measurement in various environments. The DS18B20 can measure temperatures from -55°C to +125°C with an accuracy grade of 0.0625°C. The DS18B20 digital interface is based on the 1-Wire protocol, which allows data to be read from the sensor using only one wire.

2) DHT 22 (Aosong Electronics Co Ltd, China) is a universal temperature and humidity sensor. The humidity measurement range is from 0% to 100% with a resolution of 0.1%, and the temperature range is from -40°C to +125°C with a resolution of 0.1°C.

The moisture content of the raw materials will be measured by a moisture sensor combined with a two-channel comparator LM393 (Texas Instruments, USA). The module has both digital and analogue outputs and a potentiometer for threshold adjustment. The moisture sensor consists of two probes that are used to determine the moisture content of the soil. The moisture sensor probes are coated with immersion gold, which protects the nickel from oxidation. These two probes are used to pass current through the soil, which creates the conditions for determining moisture content.

The state of the incoming biomaterial was recorded by the OV2640 camera module (ArduCam China) mounted on the ESP32 microcontroller (Espressif Systems, China). The maximum resolution of the video module's matrix is 1600 by 1200 pixels at 15 frames per second. The colour depth is 8 bits, i.e., the maximum number of colours that can be displayed simultaneously is 256, and the supported formats include 8/10-bit Raw RGB, YUV(422/420), RGB565/555.

The proposed device allowed storing information from sensors with address binding, which makes it possible to accurately monitor changes in parameters in real time. All data is stored in the cloud and can be further processed and used to develop a forecasting model. The code was created and debugged in the Arduino environment.

RESULTS AND DISCUSSION

Systems for monitoring plant environment parameters for biogas production will open opportunities to create effective control solutions for best biogas unit utilisation using advanced IoT technologies. This approach allows for reliable monitoring of plant environment parameters in real time, which helps to optimise and increase the productivity of biogas production. It will be able to introduce innovative approaches to the control and management of biogas processes, ensuring efficient use of resources and increasing the degree of automation of these processes. The component diagram of the system (architecture) is presented in Figure 1.

A part of the code and a fragment of the data flow are presented in Figure 2. In the console, one can see the temperature and humidity data in real time.

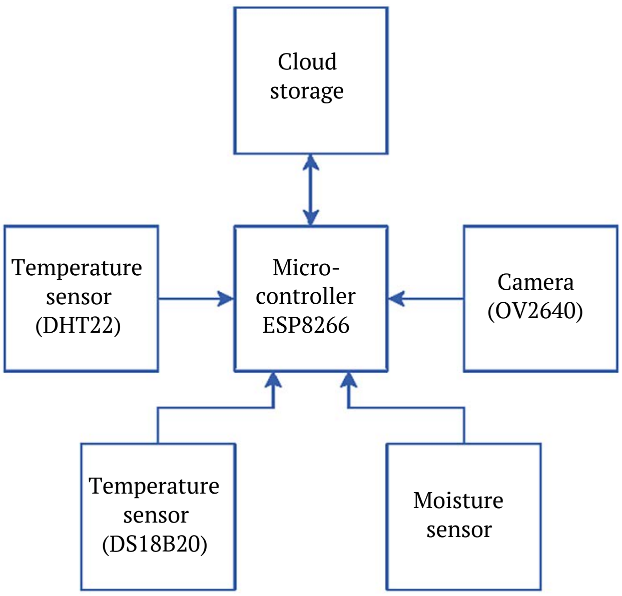

Figure 1. Component diagram (architecture) of the system

Source: compiled by the authors of this study a)

```
OneWire  ds(D1);
#define DHTPIN D2
#define DHTTYPE DHT22
DHT dht(DHTPIN, DHTTYPE);
void setup(void) {
  Serial.begin(9600);
  pinMode(D5, OUTPUT);
  pinMode(D4, OUTPUT);
  digitalWrite(D5, HIGH);
  dht.begin();
}

void loop(void) {
  byte i;
  byte present = 0;
  byte type_s;
  byte data[12];
  byte addr[8];
  float celsius, fahrenheit;

  if ( !ds.search(addr)) {
    Serial.println("No more addresses.");
    digitalWrite(D4, HIGH);

    Serial.println();
    ds.reset_search();
    delay(1000);
    return;
  }

  Serial.print("ROM =");
  for( i = 0; i < 8; i++) {
    Serial.write(' ');
```

b)

```
01:00:02.108 ->   Temperature = 27.00 Celsius, 80.60 Fahrenheit
01:00:02.150 -> Humidity: 49.60%  Temperature: 26.60°C °F  Heat index: 27.03°C No more addresses.
01:00:02.227 ->
01:00:03.125 -> ROM = 28 FF C4 6A B5 16 5 E
01:00:03.161 ->   Chip = DS18B20
01:00:19.750 ->   Data = 1 B0 1 4B 46 1F FF 1F 10 B2  CRC=B2
01:00:19.750 ->   Temperature = 27.00 Celsius, 80.60 Fahrenheit
01:00:19.750 -> Humidity: 49.60%  Temperature: 26.60°C °F  Heat index: 27.03°C No more addresses.
01:00:19.750 ->
01:00:19.750 -> ROM = 28 FF C4 6A B5 16 5 E
01:00:19.750 ->   Chip = DS18B20
01:00:19.750 ->   Data = 1 B0 1 4B 46 1F FF 1F 10 B2  CRC=B2
01:00:19.750 ->   Temperature = 27.00 Celsius, 80.60 Fahrenheit
01:00:19.750 -> Humidity: 49.60%  Temperature: 26.50°C °F  Heat index: 26.95°C No more addresses.
01:00:19.750 ->
01:00:19.750 -> ROM = 28 FF C4 6A B5 16 5 E
01:00:19.750 ->   Chip = DS18B20
01:00:19.750 ->   Data = 1 B0 1 4B 46 1F FF 1F 10 B2  CRC=B2
01:00:19.750 ->   Temperature = 27.00 Celsius, 80.60 Fahrenheit
01:00:19.750 -> Humidity: 49.60%  Temperature: 26.50°C °F  Heat index: 26.95°C No more addresses.
01:00:19.750 ->
01:00:19.750 -> ROM = 28 FF C4 6A B5 16 5 E
01:00:19.750 ->   Chip = DS18B20
01:00:19.750 ->   Data = 1 B0 1 4B 46 1F FF 1F 10 B2  CRC=B2
01:00:19.750 ->   Temperature = 27.00 Celsius, 80.60 Fahrenheit
01:00:19.750 -> Humidity: 49.50%  Temperature: 26.50°C °F  Heat index: 26.94°C No more addresses.
```

Figure 2. Software of the measuring system for monitoring the parameters of the plant environment for biogas production

Note: a – a fragment of the programme code; b – a fragment of the data obtained

Source: compiled by the authors of this study

The 1-Wire protocol used for DS18B20 sensors is a data communication protocol developed by Maxim Integrated that uses a single physical wire for data and power, which substantially saves wiring on an extensive sensor network. All data transfer operations start with bit synchronisation between the transmitter and receiver. At the beginning, a short pause is generated, followed by the "START" bit, after which the factual data is transmitted. Notably, several detectors can be connected to one device, creating a parallel network of consumers. A unique 64-bit code is used to identify each sensor. It creates the conditions for determining the address of the device. To transmit bits, time pulses are used, where a short pulse represents a logical "0" and a long pulse represents a "1". This method allows transmitting information without using additional conductors. After a bit or byte is transmitted, the receiver sends an ACK or NACK signal, depending on the success of the transmission.

The search and identification of devices connected to the same bus takes place in several stages and using a binary tree is an efficient approach to searching, especially when there are many connected devices. The binary tree helps to reduce the number of checks and operations on the bus, reducing detection time (Fig. 3).

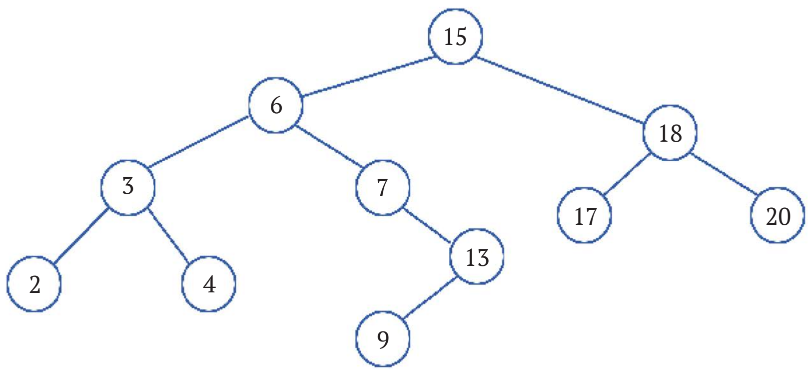

Figure 3. Queries in a binary tree

Source: compiled by the authors of this study

At the first stage of the binary tree functioning, initialisation takes place, and a reset signal (Reset Pulse) is sent to the bus. In response, the device sends a signal confirming its presence. The binary tree algorithm (Zhuang *et al.*, 2009) with options for possible device addresses is divided into two parts from the range of possible addresses. The simplest binary tree can be represented as nodes. Each node includes two children (branches) and a parent (root key). The distribution of node elements can be described as follows: x is a node in the binary search tree, and node y is in the left branch of node x, then the key y is smaller than the key x. If node y is in the right branch of node x, then the key x is smaller than the key y. The binary tree can be displayed as presented in Fig. 3, where 15 is the parent element and branches from it are 2, 3, 4, 6, 7, 13, 9 on the left, which do not exceed the parent element, and 17, 18, 20 on the right, which are larger values.

The first step of the tree check sends a search signal (0F –Search ROM), when the device responds, the algorithm moves to the branch where it occurred and starts dividing again. Thus, the identification will move until it finds all the addresses of the connected devices (Zhuang *et al.*, 2009). Subsequently, one can associate device addresses and physical locations for further monitoring. The OV2640 camera module is configured and calibrated through the module's software interface (Fig. 4).

The camera was set to the parameters presented in Table 1.

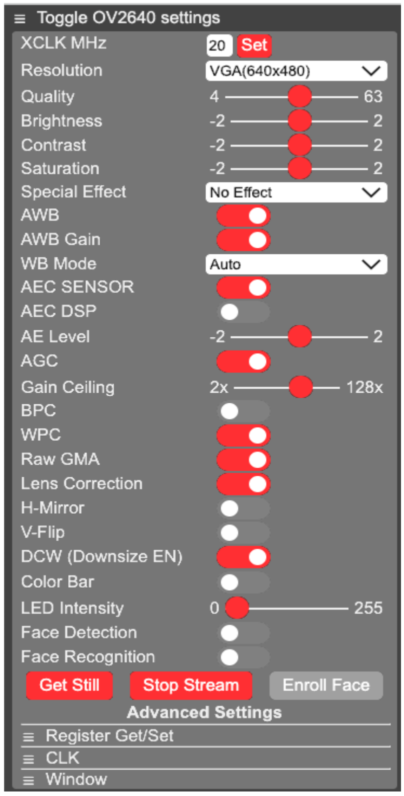

Figure 4. OV2640 camera module configuration software interface
Source: compiled by the authors of this study

Table 1. Calibration options for the OV2640

Parameter name	Designation	Value
XCLK frequency	xclk	20
Pixel format	pixformat	4
Frame size	framesize	8
Quality	quality	38
Brightness	brightness	0
Contrast	contrast	0
Saturation	saturation	1
Sharpness	sharpness	0
Special effect	special_effect	0
White balance mode	wb_mode	0
Automatic white balance	awb	1
White balance gain	awb_gain	1
Automatic exposure	aec	1
Exposure level	ae_level	0
Exposure value	aec_value	168
Automatic gain	agc	1
Gain ratio	agc_gain	0
Maximum gain	gainceiling	4
Correction of black pixels	bpc	0
White pixel correction	wpc	1
GMA settings for RAW	raw_gma	1
Lens correction	lenc	1

Source: compiled by the authors of this study

The photos are synchronised with the temperature, humidity, and soil parameters, and stored in the cloud. Data is transferred via Wi-Fi to the AWS S3 Bucket storage service. Further forecasting of biogas yields will be based on the Weighted Ensemble algorithm. Two separate models are being built for this purpose:

- forecasting based on the results of parameter measurements;
- prediction based on photo analysis of the input material.

After that, the weights of the influence of each of the parameters in the models are distributed, combined in the Weighted Ensemble algorithm, and the model training begins (Dang *et al.*, 2021). The algorithm of the system is presented in Figure 5.

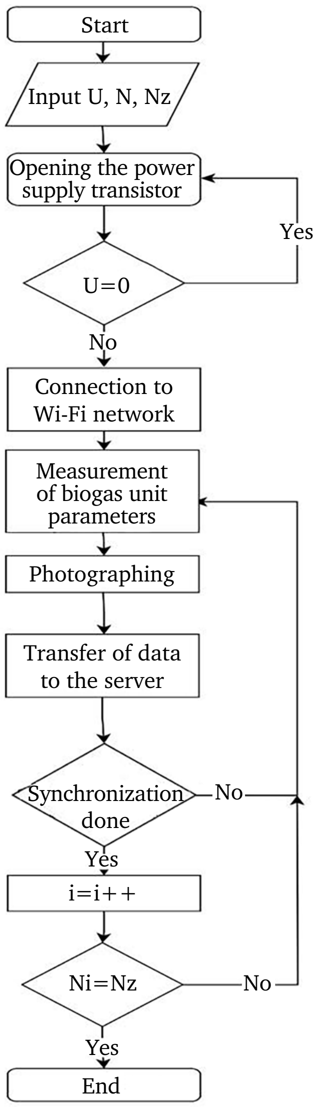

Figure 5. Algorithm for measuring parameters of biomaterial for fermentation
Source: compiled by the authors of this study

The algorithm starts with power supply to the controller and its output contacts. The presence of voltage (U) on the controller is checked, and if there is no voltage, the device is switched on again. According to the algorithm, measurements of Ni (where i = 1..z) are carried out, including measurement of technological parameters and creation of photographs, after which the information is transmitted to the cloud environment to the appropriate address. To ensure the integrity of data transmission, a data synchronisation subroutine is used. Ni measurements are performed until the set number of measurements Nz is reached. After that, the algorithm is completed. A circuit diagram was developed for the interaction and layout of the device, a fragment of which is presented in Figure 6.

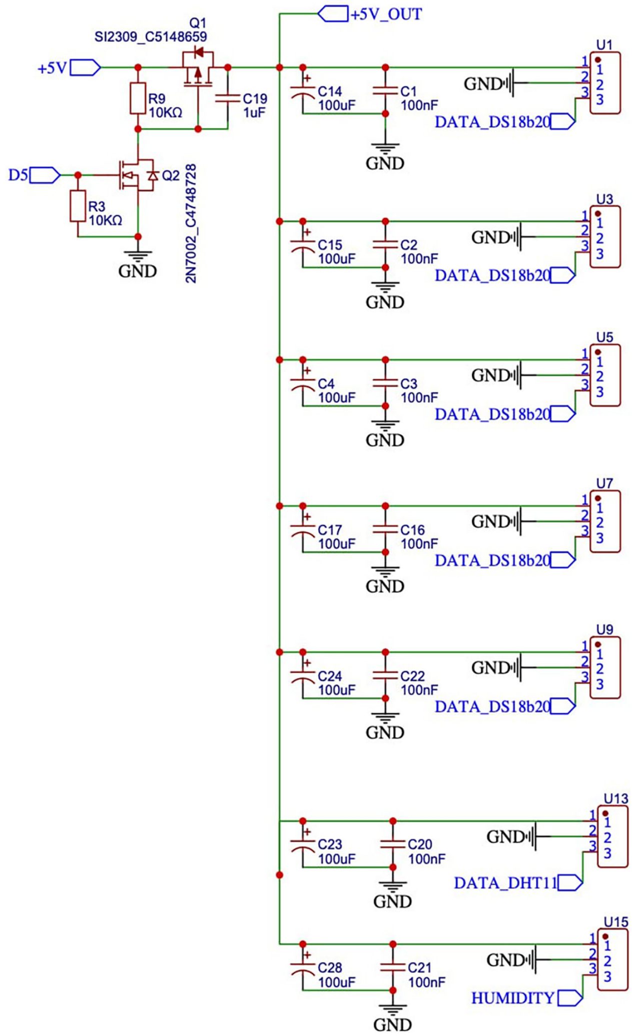

Figure 6. A fragment of the schematic diagram of the mobile monitoring system
Source: compiled by the authors of this study

In the above diagram, the cascade of transistors Q1 and Q2 is required to control the opening of the current to the sensor unit. Elements R9 and R3 are reference resistors that create a low signal level at the logic input to which the wire is connected. Pairs of capacitors C14, C1; C15, C2; C4, C3; C17, C16; C24, C22; C23, C20; C28, C21 are shunt capacitors for current filtering and reducing the influence of some circuit elements on those that ensure correctness of sensor measurements. Mounting connectors U1, U3, U5, U7, U9, U13, U15 are used for quick connection of information sensors for bolted connection.

The data is stored and further processed on the Amazon Web Services Internet of Things (AWS IoT Core) platform (Kianijaya & Hasanuddin, 2022). This platform is used to connect devices to the AWS cloud infrastructure to collect, process, analyse, and manage data generated in real time from various devices operating in the IoT. The device connection begins in the Device Gateway, which is the entry point for connecting IoT devices to AWS. The Device Gateway manages all active device connections and implements semantics for multiple protocols to ensure that devices can securely and efficiently communicate with AWS IoT Core. Devices can be connected using the Message Queue Telemetry Transport (MQTT), WebSockets, and HyperText Transfer Protocol Secure (HTTPS) protocols. The MQTT connection protocol was selected for the device (system). The MQTT protocol recognises two types of network objects: MQTT broker and MQTT client. An MQTT broker is a server that receives all messages from clients and then routes these messages to the respective designated clients or services for further processing. An MQTT client can be any device that uses the MQTT library and connects to an MQTT broker via a network. The information is organised in a hierarchy of topics. When the sender has a new set of data to distribute, it sends a control message with the data to the connected broker. The broker sends information to all clients who have subscribed to this topic. The sender does not need to know the number or location of subscriptions, and vice versa, customers do not have to configure any sender data. If a broker receives a message on a topic for which there are no active clients, the broker discards the message unless the sender has marked it as saved. A saved message is a regular MQTT message with the save flag set to 1. The broker saves the last saved message and the corresponding quality of service (QoS) level for the selected topic. Every customer who subscribes to a topic with saved messages receives them immediately after subscribing. The broker stores only one saved message for each topic. This allows newly subscribed customers to receive the most up-to-date incoming information without waiting for the next update from the sender. If it is the first time a data publishing lead client connects with a broker, they can set up a standard incoming message. In the event of an unforeseen disconnection of the lead client from the broker, the broker will send this message to other clients. Clients interact only with a broker, but the system can include several brokers that exchange data based on the topics to which their current clients subscribe. The minimum MQTT control message contains only two bytes of data, and if necessary, control messages can carry up to 256 megabytes of data. MQTT is based on the TCP protocol for data transmission, and it transmits data for connectivity in plain text format, which allows for convenient data processing after it is stored (Yassein *et al.*, 2017).

The problems of building a qualitative model for the formation of a management decision for biogas production include the following:

1) Insufficient data – machine learning models often require a large amount of data to train. If the amount of data is insufficient, the model may be under-trained and have a high error on the test data;

2) data unevenness – data may be uneven, i.e., some values may be represented much more frequently than others. This can lead to the model being over-trained on some values and under-trained on others;

3) Data faultiness – the data may contain errors, omissions, or incorrect values; this can lead to the model being trained on erroneous data, resulting in a result with low accuracy when tested;

4) Incorrect data placement – data placement can affect the model results; e.g., if the data contains multiple sets from different sources, there may be an issue with incompatibility;

5) incorrect choice of features – it is important to choose the right features to train the model; if the features are not selected correctly, the model may be under-trained;

6) overfitting – a problem when a model overlearns on training data and cannot generalise to new data; overfitting can occur if the model is too complex or if there is not enough data to train;

7) Underfitting is a problem when a model is not trained enough to predict new data accurately enough; underfitting can occur if the model is too simple or if insufficient data is used for training;

8) Noise – data can contain noise, i.e., additional details or random deviations that can prevent the model from learning from the data correctly;

9) Outliers – some values in the data may be outliers, i.e., values that are significantly different from other values; this can affect model training and lead to inaccurate results.

There are studies that suggest different approaches to developing a storage platform. For instance, in M.R. Kianijaya & M.O. Hasanuddin (2022), a web-based IoT solution aimed at monitoring and analysing data in the agricultural sector. The purpose of the presented solution is to simplify the monitoring of production processes in this industry using IoT technologies. Real time is achieved based on the MQTT protocol using a brokered publish/subscribe, which is described in detail. This avoids the limitations that arise from the use of networks in rural areas. The information from the sensors is displayed and stored in the web part of the information system. The architecture of a web application is described as a three-tier client-server architecture in which the graphical user interface (presentation tier), application functions and logic (application tier), and computer data storage (database tier) are developed and maintained as independent modules on separate platforms. This solution is based on a platform that is fully managed in-house.

Otherwise, K. Grgić *et al.* (2016) propose a solution for storing such data using both local and online storage. The system has several subsystems, including data transmission, data storage, and power management. It will use a real-time clock to keep track of time, the Internet for data transmission based on the MQTT protocol, both local storage and a cloud database for data storage, and a power supply system with automatic switching between the main power supply and the backup power supply in the event of an unforeseen event such as a power outage. The cloud database will be available through the AWS cloud service. Using cloud services allows for more flexibility when choosing technologies, as all services are ready to use immediately and do not require additional settings and work on data backup. Data security and accessibility stay important. AWS guarantees a high level of data availability and reliability, and since it will be replicated across multiple regions, it ensures fault tolerance and data security.

The advantages of the MQTT protocol in comparison with other protocols, such as HTTPS, as indicated in the studies of A. Al-Fuqaha *et al*. (2015) and allow opting for it when choosing a data transmission protocol. Most of the protocols used in Internet of Things (IoT) networks are based on data transmission via TCP (Transmission Control Protocol) or UDP (User Datagram Protocol). These protocols include XMPP (Extensible Messaging and Presence Protocol), CoAP (Constrained Application Protocol), DDS (Data Distribution Service, MQTT and AMQP (Advanced Message Queuing Protocol), which are widespread and used in various fields. Each of these protocols has its own concrete functional characteristics and is used to solve specific problems.

This overview will focus on one of the most common application layer protocols, MQTT. The aspects covered include the architecture, message format, scope, and Quality of Service (QoS) for MQTT layers. MQTT is used primarily as a channel for transmitting binary data and provides flexibility in communication patterns. The main goal of MQTT is to provide a publisher-subscriber messaging protocol with minimal bandwidth requirements. Data is transported using the Transmission Control Protocol (TCP). According to M.B. Yassein *et al*. (2017), the advantages of MQTT are as follows: no additional parameters, which makes the protocol less bulky and more efficient for data transmission with a low quality Internet connection; asynchronous data exchange makes it possible to send data regardless of the recipient's state; scalability – the transmission channel does not limit the number of connections, all sent messages are processed in turn; long connection duration without the need to spend resources on reconnection.

The proposed approach will make it possible to form a control decision on the loading of the plant medium into the biogas unit. This uses Internet of Things technologies that provide real-time monitoring of parameters in the system.

CONCLUSIONS

This study proposed the architecture of a system for monitoring the parameters of the plant environment for biogas production. This will contribute to a more accurate assessment of the future biomass fermentation process; and the development of effective management solutions to increase biogas production. Based on the results of this study, a schematic diagram of the mobile monitoring system was developed; an algorithm for searching and identifying connected devices on the 1-Wire bus; software for interacting with different types of sensors, transferring and storing data in the cloud storage with the subsequent possibility of processing them. The data is transferred via Wi-Fi to the AWS S3 Bucket for storage, and further prediction of the biogas yield will be carried out using the Ensemble algorithm, using two separate models: one based on the results of parameter measurements and the other based on the analysis of the input material photo. The developed system of remote monitoring of biomass parameters before its fermentation creates conditions for modernisation of the biogas production process control system in biogas units.

Further research will focus on the development of monitoring technologies, including the development of more accurate and sensitive sensors for measuring plant environment parameters such as methane levels, temperature, soil moisture, and other important parameters. A significant area for further research is to optimise the system for collecting and transmitting data from sensors to central processing and monitoring. It will explore data transmission technologies, including wireless networks and the Internet of Things (IoT), which provide reliable and fast real-time data collection. An essential component of the research is the development of a predictive model of plant environment parameters based on the collected data, which will help optimise the biogas production process and increase its productivity.

ACKNOWLEDGEMENTS

None.

CONFLICT OF INTEREST

The authors of this study declare no conflict of interest.

REFERENCES

[1] Abdurrahman, A.H., Kirom, M.R., & Suhendi, A. (2020). Biogas production volume measurement and Internet of Things based monitoring system. In *2020 IEEE International Conference on Communication, Networks and Satellite (Comnetsat)* (pp. 213-217). Batam: IEEE. doi: 10.1109/Comnetsat50391.2020.9328948.

[2] Al-Fuqaha, A., Guizani, M., Mohammadi, M., Aledhari, M., & Ayyash, M. (2015). Internet of things: A survey on enabling technologies, protocols, and applications. *IEEE Communications Surveys & Tutorials*, 17(4), 2347-2376. doi: 10.1109/COMST.2015.2444095.

[3] Dang, T., Nguyen, T.T., Francisco Moreno-García C., Elyan E., & McCall, J. (2021). Weighted ensemble of deep learning models based on comprehensive learning particle swarm optimization for medical image segmentation. In *2021 IEEE Congress on Evolutionary Computation (CEC)* (pp. 744-751). Kraków: IEEE. doi: 10.1109/CEC45853.2021.9504929.

[4] EBA Statistical Report 2022. (2022). Retrieved from https://www.europeanbiogas.eu/SR-2022/EBA/.

[5] Ferreira, V.O., Junior, D.S., de Melo, K.R.B., Blais, B., & Lopes, G.C. (2023). Prediction of the bed expansion of a liquid fluidized bed bioreactor applied to wastewater treatment and biogas production. *Energy Conversion and Management*, 290, article number 117224. doi: 10.1016/j.enconman.2023.117224.

[6] Gioulounta, K., Matska, M., Piskilopoulos, A., & Stamatelatou, K. (2023). Greenhouse residues' potential for biogas production. *Applied Sciences*, 13(9), article number 5445. doi: 10.3390/app13095445.

[7] Grgić, K., Špeh, I., & Heđi, I. (2016). A web-based IoT solution for monitoring data using MQTT protocol. In *2016 International Conference on Smart Systems and Technologies (SST)* (pp. 249-253). Osijek: IEEE. doi: 10.1109/SST.2016.7765668.

[8] Kianijaya, M.R., & Hasanuddin, M.O. (2022). Implementation of data storage for the monitoring system for biogas production optimization. In *2022 8th International Conference on Wireless and Telematics (ICWT)* (pp. 1-5). Yogyakarta: IEEE. doi: 10.1109/ICWT55831.2022.9935447.

[9] Komarchuk, D.S., Opryshko, O.A., Shvorov, S.A., Reshetiuk, V., Pasichnyk, N.A., & Lendiel, T. (2021). Forecasting the state of charging batteries on board the UAV on the basis of neuro-fuzzy network using. In *2021 IEEE 6th International Conference on Actual Problems of Unmanned Aerial Vehicles Development, APUAVD 2021* (pp. 188-194). Kyiv: IEEE. doi: 10.1109/APUAVD53804.2021.9615413.

[10] Lendiel, T., Lysenko, V., & Nakonechna, K. (2021). Computer-integrated technologies for fitomonitoring in the greenhouse. In *Data-centric business and applications* (vol. 5, pp. 711-729). Berlin: Springer. doi: 10.1007/978-3-030-43070-2_30.

[11] Olakanmi, O.O., Nnoli, K.P., Odeyemi, K.O. & Benyeogor, M.S. (2021). Enhanced secure process control and data routing for multi-plant biogas production system in IoT environment: A practical approach to securing smart bio-energy infrastructure. In *International Symposium on Networks, Computers and Communications (ISNCC)* (pp. 1-5). Dubai: IEEE. doi: 10.1109/ISNCC52172.2021.9615644.

[12] Polishchuk, V.M., Shvorov, S.A., Flonts, I.V., & Davidenko, T.S. (2021). Increasing the yield of biogas and electricity during manure fermentation cattle by optimally adding lime to extruded straw. *Problems of the Regional Energetics*, 49(1(49)), 73-85. doi: 10.52254/1857-0070.2021.1-49.02.

[13] Rahadian, H., Sutopo, B., & Soesanti, I. (2015). TGS2611 performance as biogas monitoring instrument in digester model application. In *2015 International Seminar on Intelligent Technology and Its Applications (ISITIA)* (pp. 119-124). Surabaya: IEEE. doi: 10.1109/ISITIA.2015.7219965.

[14] Reshetiuk, V.M., Lendel, T.I., & Kulyak, B.V. (2016). Electrical measuring system for monitoring parameters of biometric state of the plant and the microclimate in the greenhouse. *Bulletin of Petro Vasylenko Kharkiv National Technical University of Agriculture*, 176, 51-53.

[15] Silwadi, M., Mousa, H., Al-Hajji, B.Y., Al-Wahaibi, S.S., & Al-Harrasi, Z.Z. (2023). Enhancing biogas production by anaerobic digestion of animal manure. *International Journal of Green Energy*, 20(3), 257-264.

[16] Siyal, A.A., Shamsuddin, R., Komiyama, M., Manogaran, M.D., & Soehartanto, T. (2023). Control strategies for enhanced biogas production from chicken manure. *ChemBioEng Reviews*, 10(4), 423-440. doi: 10.1002/cben.202200057.

[17] Yassein, M.B., Shatnawi, M.Q., Aljwarneh, S., & Al-Hatmi, R. (2017). Internet of Things: Survey and open issues of MQTT protocol. In *2017 international conference on engineering & MIS (ICEMIS)* (pp. 1-6). Monastir: IEEE. doi: 10.1109/ICEMIS.2017.8273112.

[18] Zemite, L., Kleperis, J., Mezulis, A., Bode, I., Vempere, L., Jasevics, A., & Jansons, L. (2022). Biogas production support systems for the production and use of biomethane. In *2022 IEEE International conference on environment and electrical engineering* (pp. 1-6). Prague: IEEE. doi: 10.1109/EEEIC/ICPSEurope54979.2022.9854739.

[19] Zhou, M., & Zou, Z. (2018). Design of an intelligent control system for rural biogas engineering. In *2018 2nd IEEE advanced information management, communicates, electronic and automation control conference (IMCEC)* (pp. 1636-1639). Xi'an: IEEE. doi: 10.1109/IMCEC.2018.8469547.

[20] Zhuang, W., Fang, G., & Yuan, L. (2009). Binary tree for 1-Wire technology in the ROM search". In *International forum on information technology and applications (IFITA)* (pp. 15-17). Chengdu: IEEE. doi: 10.1109/IFITA.2009.215.

Віталій Пилипович Лисенко
Доктор технічних наук, професор
Національний університет біоресурсів і природокористування України
03041, вул. Героїв Оборони, 15, м. Київ, Україна
https://orcid.org/0000-0002-5659-6806
Тарас Іванович Лендєл
Кандидат технічних наук, доцент
Національний університет біоресурсів і природокористування України
03041, вул. Героїв Оборони, 15, м. Київ, Україна
https://orcid.org/0000-0002-6356-1230
Ігор Михайлович Болбот
Доктор технічних наук, професор
Національний університет біоресурсів і природокористування України
03041, вул. Героїв Оборони, 15, м. Київ, Україна
https://orcid.org/0000-0002-5708-6007
Сергій Григорович Павлов
Аспірант
Національний університет біоресурсів і природокористування України
03041, вул. Героїв Оборони, 15, м. Київ, Україна
https://orcid.org/0009-0001-3343-5508

Мобільна система моніторингу параметрів рослинного середовища для виробництва біогазу

Анотація. Основними джерелами біомаси для біогазових установок можуть бути органічні відходи, зерно, сіно, гній, різноманітні рослинні матеріали та інше. Процес анаеробного зброджування, який складається з послідовних складних біологічних реакцій, є актуальним і потребує детального контролю параметрів, щоб запобігти можливим втратам і оптимально використати закладений матеріал. Тому метою дослідження було розглянути можливість розробки мобільної установки для моніторингу параметрів рослинного середовища при виробництві біогазу з можливістю збереження даних і подальшого використання їх при побудові математичної моделі для прогнозування виходу газу. Створення алгоритму базувалося на принципах нечіткої логіки та структурі нейронних мереж. Запропоновано архітектуру мобільної системи моніторингу параметрів рослинного середовища для отримання біогазу. Наведено розроблену принципову електричну схему такої системи. Роботу системи представлено у вигляді створеного алгоритму пошуку та ідентифікації підключених пристроїв на шині 1-Wire. За названою шиною виконується опитування давачів та відповідно вимірювання технологічних параметрів. Розроблено програмне забезпечення для взаємодії давачів різних типів, передачі та збереження даних в хмарне сховище з подальшою можливістю їх обробки. Передбачено фотографування біомаси завдяки вбудованій фотокамері. Використавши принцип технології інтернет речей передбачено дистанційний доступ до виміряних даних. Виміряні технологічні параметри та фотографії передаються на сервер системи керування для подальшого аналізу, що дозволить точніше оцінити процес підготовки біомаси для зброджування. Отримані результати дають можливість удосконалити системи керування та підтримки прийняття рішень при завантаженні біомаси в біогазову установку

Ключові слова: вимірювання; керування; фотокамера; давач; біомаса

Machinery & Energetics
Vol. 14, No. 4. 2023

Journal homepage:
https://technicalscience.com.ua/en

UDC 621.316
DOI: 10.31548/machinery/4.2023.121

Irina Bandura
PhD in Technical Sciences, Associate Professor
Lutsk National Technical University
43018, 75 Lvivska Str., Lutsk, Ukraine
https://orcid.org/0000-0003-2166-4909

Mykola Romaniuk*
PhD in Technical Sciences, Associate Professor
Lutsk National Technical University
43018, 75 Lvivska Str., Lutsk, Ukraine
https://orcid.org/0000-0002-1039-1004

Nataliya Komenda
PhD in Technical Sciences, Associate Professor
Lutsk National Technical University
43018, 75 Lvivska Str., Lutsk, Ukraine
https://orcid.org/0000-0002-5944-8665

Andrii Hadai
PhD in Technical Sciences, Associate Professor
Lutsk National Technical University
43018, 75 Lvivska Str., Lutsk, Ukraine
https://orcid.org/0000-0002-4195-7218

Vladyslav Volynets
PhD in Technical Sciences, Associate Professor
Lutsk National Technical University
43018, 75 Lvivska Str., Lutsk, Ukraine
https://orcid.org/0000-0002-9192-2785

Optimisation of energy solutions: Alternative energy, reactive power compensation, and energy efficiency management

Abstract. The relevance of the problem under study is determined by the need to create a sustainable, efficient and environmentally safe energy complex. The growth of the world population, industrial development, and overall energy demand endanger the provision of society's energy needs, making the need for research urgent at the present time. The purpose of the study is to examine optimal energy optimisation strategies, including alternative energy, compensation of reactive power, and energy efficiency management, to ensure the stable and efficient functioning of the energy complex. Among the methods used, analytical, classification, functional, statistical, and synthesis methods were applied. In investigating the optimisation of energy solutions, a thorough analysis of various aspects of alternative energy, reactive power compensation, and energy efficiency management was conducted. This analysis encompassed various aspects and parameters related to these areas, including technical, economic, and environmental indicators. As a result of the study,

Article's History: Received: 20.06.2023; Revised: 27.09.2023; Accepted: 22.11.2023.

Suggested Citation:
Bandura, I., Romaniuk, M., Komenda, N., Hadai, A., & Volynets, V. (2023). Optimisation of energy solutions: Alternative energy, reactive power compensation, and energy efficiency management. *Machinery & Energetics,* 14(4), 121-130. doi: 10.31548/machinery/4.2023.121.

*Corresponding author

it was established that alternative energy has significant potential for ensuring sustainable development of the energy system. It can serve as a reliable source of energy that does not harm the environment and is not dependent on limited resources. In addition, reactive power compensation was recognised as an effective way to avoid energy losses in the system. This strategy helps to ensure more efficient energy use and reduce losses during transmission and distribution. Energy efficiency management also proved to be a key aspect in achieving energy supply sustainability. This allows optimising resource utilisation, reducing energy costs, and mitigating the negative impact on the environment. The practical value of the study lies in the development of innovative recommendations and strategies for energy optimisation, which will contribute to the creation of a stable, efficient, and environmentally safe energy complex and enhance its compliance with current and future challenges, making a considerable contribution to the development of science and the energy sector

Keywords: sustainable development; environmental safety; minimisation of losses; resource conservation; reduction of negative impact

INTRODUCTION

The examination of optimisation of energy solutions, in particular alternative energy, reactive power compensation and energy efficiency management, is critical in the modern world. The increase in population, rapid industrialisation, and continuous growth in energy demands pose significant challenges for effective and sustainable energy supply. Transitioning to alternative energy sources becomes imperative to reduce dependence on depleting natural resources, mitigate environmental pollution, and address climate change issues. Exploring alternative energy sources such as solar, wind, geothermal, and hydroelectric power aids in developing new technologies and approaches for creating a stable and environmentally friendly energy infrastructure. Reactive power compensation and energy efficiency management are vital aspects of energy optimisation. Implementing efficient compensation methods reduces energy losses, enhances supply quality, and ensures the stability of electrical networks. Energy efficiency management facilitates optimal resource use and reduces energy consumption, positively impacting the economy and the environment. Research in this area significantly contributes to science and technology, fostering innovative approaches in the energy sector and ensuring society's sustainable development amidst the growing challenges of the modern world. The investigation of energy solution optimisation is a crucial component in shaping the future, where efficient and sustainable energy supply underpins successful societal development.

The problem under study lies in resolving complex challenges related to effective and sustainable energy provision for contemporary society. One key issue is finding a balance between high energy demand and limited natural resources. The increasing population, industrial development, and widespread use of energy-dependent technologies jeopardise the stability of energy systems, necessitating the exploration of new and efficient solutions. Another problem involves transitioning to alternative energy sources and establishing a robust infrastructure for their integration. The adoption of alternative sources such as solar, wind, and hydroelectric power necessitates the development of new technologies and storage/transmission systems, along with investments in their advancement. Addressing the technical and economic aspects to ensure the effectiveness and stability of alternative sources is exceptionally crucial. Furthermore, the research problem encompasses energy security and the resilience of the energy system. The implementation of new technologies and the enhanced role of alternative sources must guarantee a reliable and stable energy supply, which is critical for the functioning and development of contemporary society. Reducing the negative environmental impact is a complex challenge in energy optimisation research. Finding solutions to minimise environmental pollution and reduce emissions of harmful substances into the atmosphere during energy production and consumption is crucial. The problem under study requires an integrated approach, considering technical, economic, environmental, and social aspects to ensure a sustainable, efficient, and environmentally friendly energy complex for present and future generations.

According to a study by M.L. Lysychenko *et al.* (2021), the effective compensation of reactive power can lead to reduced energy losses and improved operation of power systems, especially in industrial and commercial enterprises. This promotes more rational use of electric power and reduces energy resource consumption, contributing to sustainable development and enhanced energy efficiency. O. Salavor *et al.* (2022) emphasise that the development of solar and wind energy is vital for achieving sustainable development and mitigating the negative impact on climate change since these alternative energy sources are environmentally safe and do not emit harmful gases contributing to global warming. Encouraging the use of solar and wind energy can bring significant positive changes in the energy sector and environmental conservation, fostering sustainable economic and ecological development.

S.P. Denisyuk *et al.* (2022) highlight that implementing energy-efficient technologies can reduce energy costs and ensure a stable and reliable energy future. This can enhance economic efficiency, reduce dependence on exhaustible resources, and decrease the environmental impact of the energy sector. G. Kostenko & C. Zgurovets (2023) illuminate that integrating solar panels, wind turbines, and other alternative energy sources into the power grid is a critical step toward ensuring reliable and stable energy supply. This expansion of the resource base reduces dependence on conventional raw materials, contributing to a more resilient and environmentally balanced energy system.

Yu.A. Veremiychuk *et al.* (2020) emphasise the significance of developing intelligent energy management systems and their implementation in construction and industry to ensure more efficient use of energy resources and reduce energy consumption. This enhances energy efficiency and competitiveness of enterprises, reduces environmental impact, and promotes sustainable development. Results by N. Gelich *et al.* (2020) confirm that alternative energy sources, especially solar and wind, are becoming increasingly competitive compared to conventional sources like coal or gas. This has led to their increased utilisation, fostering the development of sustainable and environmentally friendly energy, ensuring a more efficient and stable energy supply.

The purpose of the study is to explore specific challenges such as ensuring an effective and sustainable energy supply, developing alternative energy sources, and reducing the negative environmental impact for further optimisation of energy solutions.

MATERIALS AND METHODS

The analytical method facilitates in-depth analysis of complex data in the context of alternative energy efficiency. With the use of this method, it was possible to identify the relationship between energy sources, analyse the influence of factors on the efficiency of solar and wind installations, and put forward recommendations for the further development of sustainable energy. The analytical method also assisted in evaluating the economic benefits of using alternative energy sources and determining their influence on reducing dependence on coal and other finite resources. Comparing data on production costs and investments with expected economic benefits allowed understanding the prospects of alternative energy development and transitioning towards a more resilient and efficient energy system.

Using the statistical method, key performance indicators of alternative energy sources, such as solar and wind energy, were determined in comparison with conventional sources. The statistical method also enabled identifying dependencies between factors affecting the efficiency of alternative energy sources and isolating key factors influencing their productivity. Analysing statistical data facilitated the development of optimisation strategies aimed at enhancing the efficiency and stability of alternative energy sources, thereby improving their reliability and economic feasibility.

By employing the functional method, crucial aspects of alternative energy efficiency were elucidated concerning their functionality and interaction with the energy infrastructure. The study disclosed optimal ways to integrate solar and wind installations within existing electrical systems, ensuring reliable and uninterrupted energy transmission. This method allowed focusing on analysing the impact of alternative sources on network capacity, peak load support efficiency, and backup power capabilities. It facilitated the identification of potential advantages of employing alternative sources in local and global energy systems, emphasising optimal planning for the development of modern, sustainable energy networks. The structural-functional method aided in the detailed analysis of the interaction between alternative energy sources and the existing energy system, delineating functional blocks, and assessing the influence of each element on the overall system's efficiency. This study enabled the development of optimal integration strategies for alternative sources, aimed at ensuring the stability and balance of the energy infrastructure.

The deduction method played a pivotal role in formulating general principles and theoretical models, providing the basis for analysing the efficiency of alternative energy sources. This method unveiled fundamental dependencies and regularities defining the functioning and advantages of solar and wind installations. It established a systematic theoretical framework for further research on the efficiency of alternative energy sources, isolating critical factors and influential variables contributing to their enhancement. The analysis of deductive research results can serve as a foundation for developing innovative technologies and effective strategies in the field of alternative energy, fostering a more sustainable and resilient energy future.

By employing the synthesis method, innovative solutions and comprehensive strategies were developed for the integration of solar and wind energy into the power system. This method facilitated the amalgamation of diverse components and technologies, ensuring optimal direction for the development of alternative energy sources to guarantee a sustainable and efficient energy future. The synthesis method also aided in identifying optimal locations for solar and wind installations, considering landscape, climatic conditions, and electricity consumers. Integrating data from the synthesis method enabled the development of global and local projects for the advancement of alternative sources, contributing to climate change mitigation and ensuring stable and sustainable energy supply.

RESULTS AND DISCUSSION

Advancements in alternative energy technologies and strategies for sustainable development

Alternative energy represents a concept in the energy sector's development based on utilising energy sources distinct from conventional coal, oil, and gas resources. This form of energy includes solar, wind, hydro, biomass, geothermal energy, and other sources that occur naturally or are inexhaustible. The advancement of alternative energy holds significant importance in the context of sustainable development and the preservation of natural resources. It plays a crucial role in ensuring energy security, reducing greenhouse gas emissions, and mitigating the adverse effects of climate change. Furthermore, it aids in diversifying the energy mix and reducing dependence on the import of precious energy resources. The implementation of alternative energy necessitates continuous innovation, technological development, and encourages investment in the energy sector. Alternative energy stands as a promising industry, gaining increasing popularity and support from governments and society. The introduction and development of alternative energy sources contribute to the creation of new jobs, the development of technologies, the improvement of energy efficiency, and energy cost reduction. An important aspect is the integration of alternative energy sources into the existing energy infrastructure and the development of effective management mechanisms for energy systems. However, it is necessary to address the technical, economic, and socio-cultural challenges associated with changing the conventional energy approach and promoting awareness of the importance of alternative energy for ensuring sustainable development and a sustainable future energy system.

Referring to the definition of U. Sorimsokov (2022), the use of alternative energy to reduce electricity losses and increase voltage is a relevant and promising strategy in the modern energy sector. This trend is geared towards minimising the adverse environmental impacts of conventional methods of electricity production and consumption while improving the quality of the electrical system. One of the key advantages of utilising alternative energy lies in its renewability and continuity. Solar, wind, hydrothermal, and geothermal energy sources provide reliable energy supply over extended periods with minimal fluctuations. This diminishes dependence on conventional sources such as coal or gas and reduces energy consumption for their operation and transportation. An important advantage is the ability to produce alternative energy on-site Solar panels on building rooftops, wind turbines in rural areas, or hydro generators in rivers contribute to reducing electrical losses during transportation and distribution, a common factor in overall loss reduction. However, there are some challenges and limitations to consider when using alternative energy. For instance, solar and wind energy are weather-dependent and may be unstable sources in specific regions. Hydroelectricity can impact river and waterbody ecosystems, necessitating careful planning. Furthermore, infrastructure for alternative energy production and distribution requires investments and technological advancements. Energy consumption is a vital aspect of various human activities, including heating and lighting homes, cooking, providing transportation, and supporting industrial and agricultural sectors. While developed countries transition from thermal power plants to innovative energy extraction technologies, other nations, such as Ukraine, continue to actively use coal to power thermal power plants.

The combustion of coal and oil resources releases hydrogen sulphide, CO_2, toxic gases, nitrogen oxides, particulates, and so on, leading to significant environmental pollution. Mining coal in quarries and extracting peat lead to the degradation of natural landscapes and, in specific cases, their complete destruction. Spills of oil and petroleum products during their extraction and transportation can cause massive environmental damage, including the pollution of large territories and water bodies (Singh *et al.*, 2020). Current energy trends emphasise the developed countries' focus on reducing their dependence on expensive organic energy sources and increasing the use of alternative energy sources in their energy balances. The main driving factors for alternative energy development include the high cost of energy obtained, which is due to the equipment cost such as photovoltaic cells and wind turbines, as well as a relatively long payback period. The service life of photovoltaic cells is about 5 years, while for wind turbines, it ranges from 2 to 3 years, depending on local natural conditions.

Researchers U. Mirzayev & J.T. Tulakov (2019) identified that modern methods of utilising alternative energy sources represent a key area aimed at ensuring a sustainable and environmentally friendly energy future. These methods allow the efficient utilisation of natural resources, reduce dependence on depleting fuels, and contribute to reducing greenhouse gas emissions, a crucial aspect given the increasing awareness of climate change. Solar energy, using solar panels to convert sunlight into electrical energy, provides an accessible and efficient alternative. Wind turbines installed in wind farms harness wind energy to generate electricity, offering a stable source of electrical power. Hydroelectricity utilises water flow to rotate turbines, while geothermal energy uses the Earth's underground heat for heating and electricity. Biomass utilisation, such as wood and agricultural waste, transforms waste into valuable energy, making strides in waste management. Tidal energy, using tidal forces from seas and oceans, provides an additional avenue for clean energy production. These modern methods of using alternative energy sources are aimed at reducing the negative impact of the energy sector on the environment, increasing energy independence, and ensuring sustainable energy supply for future generations.

Most European countries are successfully developing the field of alternative energy with active support from the state. European Union countries, both at international and national levels, are implementing programmes and strategies for the development of renewable energy and providing financial and organisational support to companies operating in this sector. Growing challenges such as the depletion of global hydrocarbon reserves, rising energy prices, and worsening environmental conditions compel many developed countries to actively develop their energy strategies focused on alternative energy sources. According to the International Energy Agency, Ukraine is expected to double its electricity production from alternative sources by 2030 compared to current figures, which currently account for approximately 16% of the total production (Wałowski, 2021).

There are a significant number of innovative technologies that use renewable energy sources. These technologies are constantly improving, and new ones are being developed to enhance efficiency. Special solar collectors and solar batteries are used to store solar energy. The operation of solar collectors is based on the concept of focusing solar radiation on a transparent tube through which a liquid passes and is heated. On the other hand, solar batteries operate based on the photovoltaic effect, where semiconductor components, photovoltaic converters, generate electric current when exposed to solar radiation. These photovoltaic components are grouped into batteries of various sizes, which are then installed on solar panels (Kilgo *et al.*, 2022). These solar collectors and batteries are typically applied to obtain thermal energy in individual buildings and as additional sources in combined heating and water heating systems.

Various technologies are used for the production of energy from biomass and biogas, such as composting, processing in bioreactors, and forming briquettes from dry residues. In places with a large accumulation of biomass, powerful biogas reactors are often constructed. The obtained biogas can be used by direct combustion to obtain thermal energy or in gas generators to produce electricity. For instance, in Poland, there are currently 21 power plants generating energy from biomass with a total capacity of 485.5 MW and 178 power plants using biogas with a capacity of 111.8 MW. The placement of wind energy facilities depends on the presence of "wind corridors," which have uneven seasonal characteristics. Before the construction of wind stations, extensive studies of wind flows at heights ranging from 90 to 100 m were conducted, and the results of these studies influenced the adoption of appropriate techno-economic decisions. Wind turbines with capacities ranging from 500 to 2000 kW are grouped in specific areas, and the generated electric power is supplied to centralised electrical grids (Weiss *et al.*, 2021).

Small hydropower utilises the potential energy of small rivers and water bodies. Generating turbines of small hydropower plants are located near the base of the dam or at the outlet of the derivation channel to maximise water flow utilisation and efficient conversion into electric energy. The use of alternative energy sources proves to be very effective in many countries, significantly improving their economic and environmental situations. However, despite the evident advantages, these sources can have a negative impact on the environment. The operation of stations using renewable energy sources is associated with the acquisition of significant land plots and can cause changes in landscapes. Some of these power plants can create noise and pollute the environment.

According to the results of recent studies by M.G. Prina *et al.* (2020), one of the key aspects of multi-objective investment optimisation is considering various goals and constraints in decision-making. This may include minimising costs, maximising energy production, ensuring stability and efficiency, reducing environmental impact, and ensuring supply reliability. Considering these diverse objectives allows for a more comprehensive and balanced approach to the development of the energy system. Due to high temporal and spatial resolution, it is possible to more accurately account for the dynamics of energy demand and production in different geographic areas and time intervals. This enables optimal allocation of resources, the use of different energy sources based on their availability and demand, and efficient utilisation of energy storage systems to compensate for variations in demand. This issue also involves the application of advanced modelling and data analysis technologies. High resolution requires the use of precise and detailed data on production, consumption, energy distribution, and the interaction of various sources and system components. Modern data analysis and information processing tools allow considering these parameters for more accurate and well-founded decision-making.

Multi-objective investment optimisation for high-temporal and high-spatial-resolution energy system models opens up new opportunities for the development of sustainable, efficient, and environmentally friendly energy. This approach helps balance different goals and constraints, allowing the creation of an optimal and long-term sustainable energy system. For example, wind power stations are efficient during strong winds but can be vulnerable to hurricanes. Solar boiler plants require large areas, and solar panels can pose environmental issues as waste. Power plants using geothermal energy can be profitable only if thermal sources are close to the surface, considering the potential impact of construction on seismic activity. Biomass can be used to generate energy by burning plant material, but this method is also accompanied by the emission of carbon dioxide and soot, which can have a negative impact on the environment. Therefore, the effective utilisation of renewable energy sources requires careful balancing between the benefits and negative consequences for the environment.

V. Suresh *et al.* (2020) demonstrated through their research that modelling and optimising autonomous hybrid renewable energy systems for rural electrification are important areas in modern energy research. This opens up possibilities to ensure a sustainable and reliable power supply in rural areas where access to conventional energy sources may be limited or costly. Hybrid renewable energy systems combine different sources, such as solar panels, wind turbines, hydro generators, batteries, to ensure continuous and stable electricity supply. Modelling such systems allows determining the optimal combination of sources and their parameters, ensuring maximum efficiency and minimum costs. The optimisation process of a hybrid system includes analysing energy consumption in rural areas, forecasting renewable energy production based on weather conditions and other factors, and determining optimal energy storage and distribution parameters. It is also crucial to consider economic feasibility factors, including equipment cost, maintenance, and system operation.

One of the key challenges in modelling and optimising hybrid systems is the uncertainty of weather conditions and the variability of renewable energy production. This can lead to energy shortages or excess, requiring the development of control and storage algorithms to ensure system stability. In addition, the efficiency of bioturbines is relatively low, leading to high implementation costs, and the use of biomass is often not cost-effective. An excellent alternative solution is the conversion of plant mass into gas, such as methane. Methane can then be burned using gas turbines, which operate much more efficiently. This method holds promise where a large amount of agricultural waste is available. Methanol and ethanol obtained during biomass fermentation can also be used as alternative fuels for vehicles. Recent years have seen increasing concerns among policymakers and the general population due to the worsening global environmental issues such as acid rain and climate change, and the consequences of these phenomena on the environment. Despite existing more environmentally friendly methods of energy production, such as using renewable sources like solar, wind, thermal energy, wood, and agricultural waste, it is crucial to understand that there is no perfect energy production method that does not negatively impact the environment.

O.A. Al-Shahri *et al.* (2021) identified that solar photovoltaic energy is one of the most promising sources of alternative energy; however, its optimisation poses certain challenges and issues. One optimisation method involves improving the manufacturing technology of solar panels to increase their efficiency and reduce production costs. The development of new materials and designs can contribute to capturing more solar energy and enhancing its utilisation. However, this can be associated with high costs for research and development. Another problem is the dependency on weather conditions; solar panels achieve high efficiency only in sunny weather. This issue is related to the lack of a constant energy supply, necessitating the development of storage systems to provide electricity during cloudy days or at night.

Infrastructure aspects can be an additional hurdle for optimising solar photovoltaic energy. A developed grid network is needed for the transmission and distribution of generated electricity, as well as monitoring and control systems for the efficient use of solar panels (Table 1).

Table 1. Energy potential of renewable energy sources in Ukraine

Energy sources	Theoretical potential, MW × (h/year)	Utilisation, MW × (h/year)	Technical capacity, MW × (h/year)
Solar energy	$7.2*10^{11}$	$8.1*10^{4}$	$0.13*10^{9}$
Wind power	$9.65*10^{11}$	$0.8*10^{3}$	$0.36*10^{9}$
Geothermal energy	$5.13*10^{12}$	$0.4*10^{3}$	$1.4*10^{10}$
Bioenergy	$1.25*10^{7}$	$0.14*10^{2}$	$6.1*10^{6}$
Small hydroenergy	$1.74*10^{7}$	$0.5*10^{6}$	$6.4*10^{6}$

Source: O.Yu. Niskhodovska & N.L. Korzhenivska (2023)

In Ukraine, there is a need and opportunity to develop energy based on renewable sources, which is due to several factors (Rabbi *et al.*, 2022):

1. The presence of a shortage of conventional fuel and energy resources in Ukraine.
2. Imbalance in the development of Ukraine's energy complex, with a significant focus on electricity production at nuclear power plants (up to 25-30%).
3. Suitable climatic and meteorological conditions for the efficient use of major renewable energy sources.
4. Ability to produce diverse equipment for renewable energy on existing industrial infrastructure, despite significant damage due to the war with Russia.

Table 1 provides information on the resources of renewable energy sources in Ukraine, their potential energy productivity, and utilisation volumes. An important legislative step in the latest stage of alternative energy development is providing tax incentives to energy companies utilising alternative energy sources. As noted by M.J. Mayer *et al.* (2020), the eco-economic multicriteria optimisation of household-level hybrid renewable energy systems using genetic algorithms is a crucial step toward creating sustainable and efficient energy solutions based on alternative energy sources. Hybrid systems that combine multiple renewable energy sources such as solar panels, wind turbines, and batteries can be an effective option for household electrification. However, the optimal selection of parameters for such a system can be challenging, as it needs to consider not only environmental but also economic factors. Multicriteria optimisation considers various criteria, such as cost, reliability, efficiency, and environmental impact, allowing for a compromise between these factors. In this context, genetic algorithms are powerful tools as they enable the search for optimal solutions in the space of possible parameters for hybrid systems. One of the main challenges in this approach is the complexity of determining the weights of different criteria since they may have different levels of importance for different users or situations. It is also essential to consider the uncertainty of certain parameters, such as weather conditions and energy consumption.

Energy audit, efficiency management, and reactive power compensation: Insights into insulation technical condition

The compensation of reactive power is a technical process aimed at reducing or eliminating undesirable reactive power in electrical systems. Reactive power arises due to inductive or capacitive consumption of electrical energy in distribution networks and electrical installations (Tazky *et al.*, 2021). This forces electrical systems to operate with excessive loads and increased electricity consumption, leading to reduced energy efficiency and increased electrical losses.

Reactive power compensation involves eliminating excess reactive power by implementing compensating devices such as capacitors. These devices generate reactive power, compensating for excessive reactive power consumption and ensuring a balance between active and reactive power. The advantages of reactive power compensation include increased energy efficiency, reduced electricity costs, and increased power transmission capacity. In addition, reactive power compensation helps maintain the stability of electrical systems, reduce equipment overload, and increase the technical lifespan of electrical installations. Successful reactive power compensation requires accurate calculation of reactive power, well-designed and installed compensating devices, and continuous monitoring of electrical systems. This process helps optimise the operation of electrical power systems, enhance the reliability and stability of electrical installations, and contribute to efficient and stable power supply. The technical condition of insulation relates to the assessment of the quality and effectiveness of insulation materials used to protect electrical conductors and electrical devices in electrical systems. This is a crucial aspect in ensuring the safe and stable operation of electrical installations. The assessment of the technical condition of insulation involves the diagnosis and measurement of the state of insulation materials to identify potential issues (Frizzo Stefenon *et al.*, 2020). This may include checking for cracks, wear, contamination, or damage on the surface of insulation materials. The technical condition of insulation is measured by parameters such as insulation resistance, indicating the effectiveness of insulation and its ability to prevent current leakage.

It is worth noting that the technical condition of insulation can change over time due to various factors such as humidity, temperature, mechanical loads, and electrical voltages. Regular inspections and maintenance of insulation materials are critical to ensure effective and safe operation of electrical systems. Preserving proper insulation conditions helps prevent potential accidents, reduces repair costs, and enhances the reliability of electrical installations. The technical condition of insulation is crucial for electrical safety, efficiency, and the lifespan of electrical devices and systems. Therefore, its regular monitoring and maintenance are essential tasks for all energy systems and industrial enterprises.

An energy audit is a comprehensive technical process aimed at assessing and analysing the energy consumption of enterprises, buildings, organisations, or other energy-dependent objects. The purpose of an energy audit is to identify opportunities for reducing energy costs, improving energy efficiency, and saving energy resources. An energy audit involves collecting and analysing data on electricity, thermal energy, gas, water, and other energy resources consumption, and checking the operation of technical equipment and energy supply systems (Chakravarty *et al.*, 2022). Based on the obtained data, the energy audit assesses the efficiency of systems and proposes recommendations for optimising energy consumption and implementing energy-efficient technologies. Conducting an energy audit helps identify energy losses, inefficient resource usage, technical deficiencies, and weaknesses in energy supply systems. This allows for the development of a strategy and action plan to ensure more efficient and economical energy use. Energy audits help reduce energy costs, mitigate environmental impact, and enhance the competitiveness of enterprises. This process may also include calculating the economic efficiency of proposed measures, assessing their impact on reducing energy consumption, and determining the payback periods of investments. Energy audit is a vital tool in implementing energy policies, resource-efficient utilisation, and ensuring sustainable development.

Energy management is a comprehensive approach to managing energy resources and energy efficiency aimed at optimising energy consumption, reducing energy costs, and improving the efficiency of energy processes. The goal of energy management is to ensure the sustainable and efficient operation of energy systems and reduce negative environmental impact. Energy management includes planning, monitoring, analysis, and control of energy resource usage, defining energy needs, developing effective energy strategies and supply policies. This approach involves the rational use of energy, implementation of energy-efficient technologies and processes, and planning and implementation of energy-saving measures. Scientists T. Bauwens *et al.* (2022) have found that Energy management is typically performed at various levels, from individual enterprises or organisations to city or national energy systems. Successful implementation of energy management requires cooperation among all departments and units within an organisation, including production, technical maintenance, finance, and administration. The main objectives of energy management include ensuring sustainable energy supply, increasing the efficiency of energy resource utilization, reducing energy costs, and minimising negative environmental impact. Energy management also contributes to ensuring energy security, reducing dependence on imported energy resources, and developing domestic energy potential. Successful implementation of energy management helps businesses and organisations achieve effective, stable, and economically viable operation of energy systems and positively contribute to addressing energy efficiency and environmental issues.

In the current context of escalating environmental and energy problems, rising costs of conventional energy resources, and the need to reduce environmental impact, optimising energy solutions becomes a key focus. One of the most promising industries in this context is alternative energy. Alternative energy encompasses the use of renewable energy sources such as solar, wind, hydroelectric power, and biomass. These sources are natural and renewable, reducing dependence on limited natural resources and lowering the environmental footprint. Optimising alternative energy involves selecting optimal solutions for placing solar panels, wind turbines, and hydroelectric power stations, considering geographic and climatic conditions, and developing efficient energy storage and distribution systems.

Reactive power compensation is a crucial component of energy system optimisation. Reactive power arises from the use of electrical equipment with capacitive and inductive properties. Excessive reactive power can lead to increased electricity consumption and decreased system efficiency. Reactive power compensation involves managing its level, reducing energy losses, and improving the power factor. Energy efficiency management is a key aspect of optimising energy solutions. It involves the implementation of technologies and practices aimed at reducing energy consumption while preserving or enhancing productivity. Energy efficiency can be achieved through the deployment of energy-efficient equipment, optimisation of system operation modes, and the use of modern technologies in construction and industry. However, it is essential to recognise that achieving absolute energy efficiency is impossible without compromise. The choice of optimal solutions must consider economic, social, and environmental aspects. Optimising energy solutions is a complex task that requires collaboration between government agencies, research institutions, businesses, and society. Overall, optimising energy solutions is an integral part of sustainable societal development. The introduction of alternative energy sources, reactive power compensation, and energy efficiency management can help reduce energy dependence, improve the environment, and ensure sustainable economic growth.

CONCLUSIONS

Optimisation of energy solutions, focusing on the development of alternative energy, reactive power compensation, and energy efficiency management, has become a crucial component of modern energy strategy. The growing awareness of issues related to climate change and the depletion of conventional energy resources stimulates the implementation of innovative technologies and methods based on alternative energy sources. The development of alternative energy offers potential from various sources such as solar, wind, hydro, and biomass. Research results show that energy derived from these sources can become a sustainable and reliable complement to conventional sources like coal and oil. In addition, it is environmentally friendly and has a low impact on the environment, making it an attractive alternative for sustainable development and reducing dependence on harmful sources. Another important aspect is reactive power compensation, which helps address issues related to inefficient energy usage. The use of smart compensation systems avoids excessive energy consumption and reduces energy losses. This leads to an increase in the efficiency of energy systems and a reduction in energy costs for enterprises and consumers. Energy efficiency management is also becoming a crucial factor in achieving sustainable development. The introduction of intelligent management and monitoring systems helps optimise energy resource utilisation, identify potential energy expenditures, and enhance the efficiency of energy infrastructure. This contributes to supporting a stable and effective energy supply, forming the basis for the development of modern society.

One of the most important aspects of optimising energy solutions is the development of alternative energy. The high competitiveness and continuous supply of solar and wind installations demonstrate their significance in ensuring a stable and effective energy system. Integrating alternative sources allows expanding the resource base and reducing dependence on conventional sources, contributing to climate change mitigation and environmental preservation. Reactive power compensation issues are becoming increasingly relevant in the context of growing electricity consumption. The application of modern compensation technologies allows reducing energy losses, improving supply quality, and enhancing the efficiency of energy systems. The implementation of automated reactive power compensation tools will help maintain a stable and consistent voltage level, providing optimal conditions for all consumers' operations. Energy efficiency management is a necessary component to ensure energy stability and economic efficiency. The use of intelligent management systems enables optimising energy consumption, identifying energy losses, and more effectively distributing energy resources. Increasing energy efficiency can contribute to reducing energy costs, enhancing the competitiveness of businesses, and mitigating environmental impact. All these aspects of optimising energy solutions interact and are interconnected, forming a comprehensive system that promotes sustainable development and stability in the energy sector. Ensuring a reliable and stable energy supply, reducing negative environmental impact, and ensuring economic efficiency are crucial for modern society.

Further studies in the field of optimising energy solutions require an innovative approach and collaboration between scientists, industry enterprises, and government bodies. The development of new technologies and the implementation of advanced practices will enable an effective and stable energy supply, fostering sustainable development and resource conservation for future generations.

ACKNOWLEDGEMENTS

None.

CONFLICT OF INTEREST

None.

REFERENCES

[1] Al-Shahri, O.A., Ismail, F.B., Hannan, M.A., Lipu, M.S.H., Al-Shetwi, A.Q., Begum, R.A., Al-Muhsen, N.F.O., & Soujeri, E. (2021). Solar photovoltaic energy optimization methods, challenges and issues: A comprehensive review. *Journal of Cleaner Production*, 284, article number 125465. doi: 10.1016/j.jclepro.2020.125465.

[2] Bauwens, T., Schraven, D., Drewing, E., Radtke, J., Holstenkamp, L., Gotchev, B., & Yildiz, Ö. (2022). Conceptualizing community in energy systems: A systematic review of 183 definitions. *Renewable and Sustainable Energy Reviews*, 156, article number 111999. doi: 10.1016/j.rser.2021.111999.
[3] Chakravarty, K.H., Sadi, M., Chakravarty, H., Alsagri, A.S., Howard, T.J., & Arabkoohsar, A. (2022). A review on integration of renewable energy processes in vapor absorption chiller for sustainable cooling. *Sustainable Energy Technologies and Assessments*, 50, article number 101822. doi: 10.1016/j.seta.2021.101822.
[4] Denisyuk, S.P., Beloha, G.S., Cherneshchuk, I.S., & Lysiy, V.V. (2022). Global trends in implementation of renewable energy sources and features of their implementation during the recovery of Ukraine's economy. *Power Engineering: Economics, Technique, Ecology*, 4, 7-23. doi: 10.20535/1813-5420.4.2022.273360.
[5] Frizzo Stefenon, S., Zanetti Freire, R., Henrique Meyer, L., Picolotto Corso, M., Sartori, A., Nied, A., Rodrigues Klaar, A.C., & Yow, K.C. (2020). Fault detection in insulators based on ultrasonic signal processing using a hybrid deep learning technique. *IET Science, Measurement and Technology*, 14(10), 953-961. doi: 10.1049/iet-smt.2020.0083.
[6] Gelich, N., Panasiuk, Y., & Onishchyk, V. (2020). Alternative energy in Ukraine: Status and development prospects. *Economic Journal of Lesya Ukrainka Volyn National University*, 2(22), 143-151. doi: 10.29038/2411-4014-2020-02-143-151.
[7] Kilgo, M.K., Anctil, A., Kennedy, M.S., & Powell, B.A. (2022). Metal leaching from Lithium-ion and Nickel-metal hydride batteries and photovoltaic modules in simulated landfill leachates and municipal solid waste materials. *Chemical Engineering Journal*, 431, article number 133825. doi: 10.1016/j.cej.2021.133825.
[8] Kostenko, G., & Zgurovets, O. (2023). Current state and prospects for development of renewable distributed generation in Ukraine. *System Research in Energy*, 2(73), 4-17. doi: 10.15407/srenergy2023.02.004.
[9] Lysychenko, M.L., Handola, Y.M., & Huzenko, V.V. (2021). Development of an automated technological line of production of feed for livestock with the adjustment the quality of the end product. *Engineering of Nature Management*, 4(22), 89-93. doi: 10.5281/zenodo.6967587.
[10] Mayer, M.J., Szilágyi, A., & Gróf, G. (2020). Environmental and economic multi-objective optimization of a household level hybrid renewable energy system by genetic algorithm. *Applied Energy*, 269, article number 115058. doi: 10.1016/j.apenergy.2020.115058.
[11] Mirzayev, U., & Tulakov, J.T. (2019). The modern methods of using alternative energy sources. *Central Asian Problems of Modern Science and Education*, 4(2), article number 74.
[12] Niskhodovska, O.Yu., & Korzhenivska, N.L. (2023). The energy potential of biomass is a source of energy sustainability of Ukraine. In *Proceedings of VIII International Scientific and Practical Conference "Scientific Research in the Modern World"* (pp. 541-548). Toronto: Perfect Publishing.
[13] Prina, M.G., Casalicchio, V., Kaldemeyer, C., Manzolini, G., Moser, D., Wanitschke, A., & Sparber, W. (2020). Multi-objective investment optimization for energy system models in high temporal and spatial resolution. *Applied Energy*, 264, article number 114728. doi: 10.1016/j.apenergy.2020.114728.
[14] Rabbi, M.F., Popp, J., Máté, D., & Kovács, S. (2022). Energy security and energy transition to achieve carbon neutrality. *Energies*, 15(21), article number 8126. doi: 10.3390/en15218126.
[15] Salavor, O., Bublienko, N., Nychyk, O., & Voytenko Palgan, Y. (2022). Jean Monnet Project: EU renewable energy strategy as a roadmap for Ukraine. In *Proceedings of the IV International Conference on European Dimensions of Sustainable Development* (pp. 120-121). Kyiv: National University of Food Technology.
[16] Singh, H., Bhardwaj, N., Arya, S.K., & Khatri, M. (2020). Environmental impacts of oil spills and their remediation by magnetic nanomaterials. *Environmental Nanotechnology, Monitoring and Management*, 14, article number 100305. doi: 10.1016/j.enmm.2020.100305.
[17] Sorimsokov, U. (2022). Use of alternative energy to reduce power losses and improve voltage. *Gospodarka i Innowacje*, 23, 20-25.
[18] Suresh, V., Muralidhar, M., & Kiranmayi, R. (2020). Modelling and optimization of an off-grid hybrid renewable energy system for electrification in a rural areas. *Energy Reports*, 6, 594-604. doi: 10.1016/j.egyr.2020.01.013.
[19] Tazky, M., Regula, M., & Otcenasova, A. (2021). Impact of changes in a distribution network nature on the capacitive reactive power flow into the transmission network in Slovakia. *Energies*, 14(17), article number 5321. doi: 10.3390/en14175321.
[20] Veremiychuk, Yu.A., Opryshko, V.P., Prytiskach, I.V., & Yarmolyuk, O.S. (2020). *Optimizing the functioning of integrated energy supply systems for consumers*. Kyiv: Publishing House "KYY".
[21] Wałowski, G. (2021). Development of biogas and biorafinery systems in Polish rural communities. *Journal of Water and Land Development*, 49, 156-168. doi: 10.24425/jwld.2021.137108.
[22] Weiss, R., Saastamoinen, H., Ikäheimo, J., Abdurafikov, R., Sihvonen, T., & Shemeikka, J. (2021). Decarbonised district heat, electricity and synthetic renewable gas in wind-and solar-based district energy systems. *Journal of Sustainable Development of Energy, Water and Environment Systems*, 9(2), article number 1080340. doi: 10.13044/j.sdewes.d8.0340.

Ірина Олександрівна Бандура
Кандидат технічних наук, доцент
Луцький національний технічний університет
43018, вул. Львівська, 75, м. Луцьк, Україна
https://orcid.org/0000-0003-2166-4909

Микола Валентинович Романюк
Кандидат технічних наук, доцент
Луцький національний технічний університет
43018, вул. Львівська, 75, м. Луцьк, Україна
https://orcid.org/0000-0002-1039-1004

Наталія Володимирівна Коменда
Кандидат технічних наук, доцент
Луцький національний технічний університет
43018, вул. Львівська, 75, м. Луцьк, Україна
https://orcid.org/0000-0002-5944-8665

Андрій Валентинович Гадай
Кандидат технічних наук, доцент
Луцький національний технічний університет
43018, вул. Львівська, 75, м. Луцьк, Україна
https://orcid.org/0000-0002-4195-7218

Владислав Ігорович Волинець
Кандидат технічних наук, доцент
Луцький національний технічний університет
43018, вул. Львівська, 75, м. Луцьк, Україна
https://orcid.org/0000-0002-9192-2785

Оптимізація енергетичних рішень: Альтернативна енергетика, компенсація реактивної потужності та управління енергоефективністю

Анотація. Актуальність досліджуваної проблеми визначається необхідністю створення сталого, ефективного та екологічно безпечного енергетичного комплексу. Зростання чисельності населення планети, розвиток промисловості та загальний попит на енергоресурси ставлять під загрозу забезпечення енергетичних потреб суспільства, що робить необхідність проведення досліджень актуальною на сучасному етапі. Метою дослідження є вивчення оптимальних стратегій оптимізації енергетики, включаючи альтернативну енергетику, компенсацію реактивної потужності та управління енергоефективністю, для забезпечення стабільного та ефективного функціонування енергетичного комплексу. Серед використаних методів – аналітичний, функціональний, статистичний та синтезу. При дослідженні оптимізації енергетичних рішень було проведено ретельний аналіз різних аспектів альтернативної енергетики, компенсації реактивної потужності та управління енергоефективністю. Цей аналіз охоплював різні аспекти та параметри, пов'язані з цими сферами, включаючи технічні, економічні та екологічні показники. В результаті дослідження було встановлено, що альтернативна енергетика має значний потенціал для забезпечення сталого розвитку енергосистеми. Вона може слугувати надійним джерелом енергії, що не завдає шкоди навколишньому середовищу та не залежить від обмежених ресурсів. Було визнано, що компенсація реактивної потужності є ефективним способом уникнення втрат енергії в системі. Ця стратегія допомагає забезпечити більш ефективне використання енергії та зменшити втрати під час передачі та розподілу. Управління енергоефективністю також виявилося ключовим аспектом у досягненні сталості енергопостачання. Це дозволяє оптимізувати використання ресурсів, зменшити витрати на енергію та пом'якшити негативний вплив на навколишнє середовище. Практична цінність дослідження полягає в розробці інноваційних рекомендацій та стратегій оптимізації енергоспоживання, які сприятимуть створенню стабільного, ефективного та екологічно безпечного енергетичного комплексу та підвищенню його відповідності сучасним і майбутнім викликам, що є вагомим внеском у розвиток науки та енергетичної галузі

Ключові слова: сталий розвиток; екологічна безпека; мінімізація втрат; ресурсозбереження; зменшення негативного впливу

Machinery & Energetics
Vol. 14, No. 4. 2023

Journal homepage:
https://technicalscience.com.ua/en

UDC 621:004.8
DOI: 10.31548/machinery/4.2023.131

Volodymyr Khotsianivskyi*
Postgraduate Student
National Aviation University
03058, 1 Liubomyr Huzar Ave., Kyiv, Ukraine
https://orcid.org/0000-0003-0415-777X

Victor Sineglazov
Doctor of Technical Sciences, Professor
National Aviation University
03058, 1 Liubomyr Huzar Ave., Kyiv, Ukraine
https://orcid.org/0000-0002-3297-9060

Robotic manipulator motion planning method development using neural network-based intelligent system

Abstract. The research relevance is determined by the constant development of industry and the use of robotic manipulators in production processes. The study aims to develop an approach to planning the trajectory of a manipulator robot using an intelligent system based on neural networks. An analysis method, as well as special methods such as design, machine learning, integration strategies, and optimisation techniques, were used to achieve this goal. The main results of the study cover a wide range of achievements in the development of methods for planning the motion of robotic manipulators and their integration into real production conditions. The analysis of existing methods for planning the motion of robotic manipulators and a review of intelligent control systems provided a comprehensive picture of the current state of the art. The developed methods of robot manipulator trajectory identified effective control strategies that consider both dynamic and static scenarios. Training a neural network to plan the optimal path of movement made it possible to detect, track and avoid obstacles in real-time. Hierarchical path planning, adaptive neural network control, genetic algorithms for path optimisation, and dynamic prediction for obstacle avoidance were used to integrate the developed methods into a real production environment. The optimisation and improvement of the created approaches have shown positive results in improving the safety and performance of robotic manipulators, reducing the risk of collisions, and avoiding damage to robots. In addition, the implementation of hierarchical trajectory planning and adaptive neural network control contributed to a significant increase in the accuracy and stability of manipulator movements in various production process scenarios. The practical significance of the study is to develop an intelligent control system and methods for planning the movement of robotic manipulators, which contributes to the efficiency and safety of their operation in real production conditions

Keywords: motion trajectory; industrial automation; mechatronic structures; smart technologies; deep learning models

INTRODUCTION

With the growing use of robotic manipulators in manufacturing, a need for improved methods of planning their movement to ensure the efficiency and accuracy of tasks is growing. The relevance is determined by the existing approaches that often have limitations and are unable to provide flexibility in dealing with dynamic production

Article's History: Received: 13.07.2023; Revised: 05.10.2023; Accepted: 22.11.2023.

Suggested Citation:
Khotsianivskyi, V., & Sineglazov, V. (2023). Robotic manipulator motion planning method development using neural network-based intelligent system. *Machinery & Energetics,* 14(4), 131-145. doi: 10.31548/machinery/4.2023.131.

*Corresponding author

scenarios. The development of an intelligent system based on neural networks opens up prospects for adaptive and autonomous robot motion planning, which is key to increasing productivity and reducing costs in modern production environments.

The research problem is the need to improve planning methods for the robotic manipulator movement in production conditions. Existing approaches often do not provide optimality and adaptability to changing conditions, which can lead to conflicts and unforeseen situations when robots interact in common areas or with dynamic obstacles. The problem also lies in the limited ability of existing robot control systems to respond to changes in the production environment, such as physical deformations of robot components or dynamic changes in the working environment.

Other studies on this topic should be considered for a more thorough analysis. As such, O. Nalobina *et al.* (2022) emphasised that the low robot adoption rate is due to a lack of research on the feasibility and efficiency of their use compared to traditional technologies. The absence of theoretical design frameworks, efficiency assessment methods, and insufficient training emphasises the need for further research in this area, aimed at developing methods for determining the feasibility and training of personnel for the introduction of robotics in agriculture. The authors also analysed the turning movement of the robot and determined its centre of mass speed and the turning radius. V. Khotsyanivskyi and V. Sineglazov (2023) discussed the use of machine learning for the autocalibration of moving elements of robotic systems, in particular, for the control of stepper motors. The described auto-calibration algorithm uses machine learning to improve the accuracy of stepper motors. The authors emphasised that the use of machine learning methods in solving the tasks of calibrating the moving elements of robotic systems can improve their accuracy and efficiency, ensuring more efficient system operation.

M.V. Bogdanovsky (2020) examined the key technical parameters of industrial robots, such as movement speed, load capacity, degrees of mobility, positioning errors, and working area. The author analysed the classification distribution of robots by speed and accuracy to determine their characteristics. He also investigated the impact of the manipulation system's movement on the accuracy of an industrial robot and analysed the types of errors, considering their design features and factors that affect the robot's functioning. The analysis of the study conducted by O. Litvin and S. Pankov (2021) showed limitations of the study on special-purpose robotic manipulators and, as such, this study contributes to the improvement of their systems. Determination of special-purpose robotics and specification of the parameters of new robots are the main tasks for further research and development. As a result of the study, a concept for improving existing and developing new prototypes of robotic mechanisms was set.

P. Koruniak *et al.* (2023) focused on the improvement of equipment, technological processes, and mechanisation, which comprehensively affects product quality and reduces labour costs. The use of industrial robots, including those with remote and automatic control, in flexible automated systems and automation of assembly processes is a promising area. The development of industrial robots equipped with additional coordinate degrees of mobility expands their versatility and technological capabilities but raises new challenges in terms of simplifying structural elements and maintenance systems. In turn, V. Zalypka (2023) developed a new approach to improving the performance of multifunctional manipulators on the platform of multipurpose robotic platforms using Abenics technology. The proposed method allowed the manipulators to perform the functions of both predefined and walking or wheeled propulsion. The author also conducted a three-dimensional modelling and analysis of structural features.

The above studies did not address the issues related to the use of intelligent systems and neural networks for the movement of robotic manipulators. The absence of these aspects requires additional research to develop methods that will effectively use intelligent systems based on neural networks in motion planning for such robots. To solve the stated problem, this study developed methods for planning robot movement using neural networks.

MATERIALS AND METHODS

The study used analytical methods and special techniques: design, machine learning, integration strategies and optimisation methods. To conduct the analysis, a systematic review of scientific publications related to robot manipulator trajectory planning and intelligent control was conducted. The analysis was based on the identification of the advantages and disadvantages of existing approaches, which forms the basis for the development of new methods. In particular, the study included an analysis of the design of algorithms and system architecture to develop effective trajectory planning methods. These trajectory planning methods are aimed at improving the accuracy and speed of manipulators in production environments, providing optimal and efficient solutions to meet the challenges of the industry.

The design method was used to develop proprietary robot trajectory methods for the manipulator. It included careful design of algorithms, development of the optimal system architecture, and creation of highly efficient trajectory planning solutions. It is necessary to note that this method covers not only the technical aspects of the algorithms but also an integrated system that determines the optimal path for the robot to follow. This ensures a high level of productivity and the avoidance of conflicts in the production environment through intelligent motion planning and the selection of optimal paths.

To train the neural network, machine learning methods were used, where the optimal trajectories were used as input data. The main technical aspects of this method include a detailed study of various types of neural network training, such as supervised learning, unsupervised learning, and deep reinforcement learning (DRL) subtasks. In this context, a neural network can predict optimal solutions for manipulator movement, opening up prospects for improving machine learning-based trajectory planning methods and ensuring high efficiency in manipulator control.

Integration strategies were used to effectively combine the developed methods into a single system. The main technical component of this method involves the careful integration of trajectory planning algorithms and the control system. This process is aimed at ensuring their interaction, which leads to the stability and optimal functioning of robotic manipulators in a real production environment. This approach solves the problem of coordination and synchronisation between different stages of the system, increasing the overall productivity and reliability of automated processes.

Optimisation methods were used to systematically improve the efficiency and accuracy of the developed methods. System parameters and algorithms were optimised to achieve optimal results. These approaches have contributed to a significant improvement in the quality of robot trajectory planning and minimisation of the risk of collisions, which is particularly important in production processes. As a result of this optimisation approach, the functionality of the system has been improved, and its suitability for successful application in real-world production conditions has been increased.

The study included a table with a comparative analysis of existing approaches to planning the robotic manipulator motion, namely geometric trajectory planning, inverse kinematics, dynamic programming, random positions, and optimisation methods. Unity3D was chosen to model the movements of the robot manipulator, and MoveIt and UnityRoboticsHub were used for controls. The robot movements via Selective Compliance Articulated Robot Arm (SCARA) were considered. The Rapidly Exploring Random Trees (RRT) interpolation algorithm was used to compare the variables of the joint angle, velocity, and acceleration. Additionally, tables of obstacles in static and dynamic environments, relative errors of the trained model in predicting movement and the time of real movement were used. In addition, the study included the development of our ways to move robotic manipulators, analysis, and description of the architectures of various neural networks, schemes of neural networks for manipulators, recurrent neural networks and long-term memory layers, a schematic diagram of the network for determining controlled influences, and a formula for the space of locally feasible solutions.

The space of locally feasible solutions was calculated using the formula:

$$f_{local}\,(x_k, \phi_k | x_{goal} \,\big|\!\rightarrow u_k), \qquad (1)$$

where: f_{local} – the space of locally possible solutions; x_k – current robot state; ϕ_k – environment state; x_{goal} – target state; u_k – control command.

RESULTS

Analysis of existing and custom robotic manipulator motion planning methods and review of intelligent control systemscustom

The analysis of traditional methods of manipulator motion planning involves key techniques such as geometric trajectory planning, inverse kinematics, dynamic programming, as well as random positions and optimisation methods. Geometric path planning determines the robot's movement based on the geometric characteristics of the workspace. This method can be used to set the exact position and orientation of the manipulator but can be limited by the complexity of solving problems for complex configurations. In addition, geometric trajectory planning is one of the commonly used methods for industrial robot control. It is typically based on the assignment of high-level commands, such as moving from point to point. While this approach provides user-friendliness, it has its limitations, particularly in the area of adaptation to changing conditions.

The inverse kinematics method is used to determine the input angles or positions of a manipulator to reach a specific position or trajectory. This method is effective in solving problems for specific points in space but can lose accuracy in complex problems due to the large number of possible solutions. It is also used in most industrial robot control systems. The inverse kinematics method can be used to determine the kinematic parameters of a robot based on its position and orientation. Dynamic programming considers the movement of the manipulator as a sequence of actions to minimise criteria. This method is effective for optimisation problems and trajectory planning, particularly in cases where the dynamic constraints of the robot are important. However, it is possible to be computationally expensive for real-time applications in complex environments, especially when there are many dimensions of the solution space and complex problems. Regarding random positions and optimisation methods, these approaches often use random points to reduce the number of intermediate points in trajectories or optimisation techniques to achieve optimal solutions.

To perform a comparative analysis of the above approaches, a table showing their main characteristics and differences was compiled (Table 1).

Table 1. Comparative analysis of existing approaches

Appro ach	Peculiarities	Advantages	Limitations
Geometric trajectory planning	Determines robot movement by workspace parameters	Provides accurate position and orientation data	Difficult to use for complex configurations
		Easy user-manipulation	Limited adaptation to variable conditions

Continued Table 2.

Appro ach	Peculiarities	Advantages	Limitations
Inverse kinematics	Determines input angles or manipulator position to change to target state	Effective in determining specific points	Loss of accuracy in complex tasks
		Used in most movement control systems	High number of possible solutions in complex tasks
Dynamic programming	Implies manipulator movement as a sequence of actions with minimized criteria	Effective for trajectory optimization and planning	Computational-heavy for real-time processing
		Can be used to address robot dynamic restrictions	Hard to use in real-time operation
Random positions and optimization methods	Random-point	Reducing the number of intermediate points in trajectories	Dependency on initial random-point selection
	Optimization methods employment	Achievement of optimal solutions	Need for computing resources, especially for complex tasks

Source: compiled by the authors

Intelligent control systems play a key role in improving and optimising the motion of manipulators. One of the most advanced technologies is the use of neural networks to solve trajectory planning and motion control tasks. Neural networks prove to be effective in solving complex control problems, providing flexibility and adaptability to changing conditions. Deep learning models allow neural networks to automatically learn complex relationships and solve motion planning problems that may be difficult to solve using traditional methods. One of the main advantages of intelligent control systems is their ability to learn and adapt to new conditions. This makes it possible to optimise the operation of manipulators in real-time and increase their productivity. Other types of intelligent systems used to control the motion of manipulators include expert systems, genetic algorithms, and fuzzy logic control systems. Each of these approaches has its advantages and peculiarities when applied to robotics. The integration of intelligent control systems into the motion of manipulators opens up new opportunities for autonomous and adaptive robotic systems. Such systems can effectively adapt to changes in the working environment and perform a variety of tasks with high accuracy.

To achieve the goal of developing an intelligent system based on neural networks for planning the trajectory of a manipulator, it is worth proposing a new approach that considers the key aspects of motion optimisation and control. This approach can include such methods as a hierarchical trajectory planning method, a neural network for adaptive control, a genetic algorithm for trajectory optimisation, and dynamic prediction for obstacle avoidance. The hierarchical trajectory planning method operates on the principle of dividing the original task into successive stages, at each of which the corresponding trajectory is determined and planned. This allows us to divide complex tasks into smaller, more manageable subtasks, which contributes to the effective control of the manipulator's movement in real-time. A neural network for adaptive control is a method that uses a neural network to adaptively control the motion of a manipulator depending on changing environmental conditions. The neural network receives input about the state of the workspace and maintains the optimal path of movement, considering dynamic constraints.

The genetic algorithm for trajectory optimisation creates a population of potential trajectories that evolve to achieve optimal solutions. This allows for a variety of factors to be considered and improves the quality of traffic planning. Dynamic Obstacle Avoidance predicts future environmental conditions and uses this information to adjust the trajectory in real-time. Thus, the developed methods aim to improve the accuracy and speed of planning the trajectory of the manipulator, providing an optimal and adaptive approach to control.

Training a neural network to plan the optimal movement path

When considering the use of neural networks for robot manipulator motion planning systems, it is important to focus on analysing and describing architectures that optimally address the characteristics of these systems. For robot manipulator motion planning systems, the most suitable neural networks are convolutional neural networks, recurrent neural networks, deep neural networks, and autoencoders (Fig. 1).

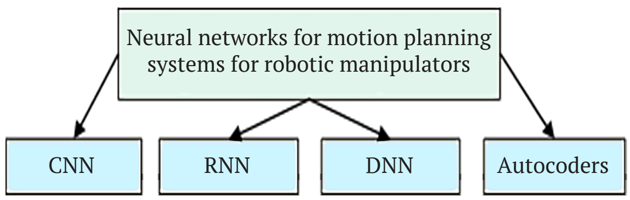

Figure 1. Neural networks for robotic manipulators
Note: CNN – Convolutional neural network; RNN – Recurrent neural network; DNN – Deep neural network
Source: compiled by the authors

CNN is suitable for object recognition. The use of CNNs allows for efficient real-time object recognition, which is key to planning the safe movement of the manipulator around objects in the workspace. The CNN architecture can be modified to include additional layers to accurately determine the position and shape of objects. RNNs are used to model motion dynamics. RNNs are suitable for considering time dependencies and modelling the dynamics of the manipulator's motion, which allows for predicting future states of the system. By applying RNNs to input data that includes previous and current states, the optimal control can be determined accurately. In turn, DNN is best used for trajectory optimisation. The use of DNNs allows optimising the manipulator's trajectories, considering geometric and dynamic constraints. Deep perceptrons can be used to solve complex path-planning problems involving a large number of parameters. For efficient feature extraction, autoencoders can be used. They can help in the efficient extraction of important features from the input data about the manipulator's working environment. The use of autoencoders helps to obtain a latent representation that is useful for analysing objects and obstacles in space.

The functionality of the neural network for determining the trajectory of the manipulator is focused on avoiding collisions and ensuring safe movement. Input data, such as the position and speed of each of the robot's axes and information about obstacles, are processed through the layers of the neural network to identify patterns. The network generates an optimal trajectory, avoiding collisions, by considering geometric constraints and safety limits. The output data, which includes new values for positions and velocities, is used to control the manipulator's motion. The neural network is trained on training data that includes various motion and obstacle scenarios to detect patterns and make the right decisions for a safe trajectory. In addition, it is important to emphasise the advantages of using a neural network to determine a collision avoidance path. These advantages include the ability to consider geometric constraints and the working area of the manipulator, automatic planning of collision avoidance paths, and the ability to adapt to changing environments and different motion scenarios. This ensures the safe and efficient operation of the manipulator in conditions where unpredictable dynamics of changes in its environment are observed.

In general, the analysis and description of these architectures provide an understanding of how neural networks can be adapted to solve specific challenges related to robot motion planning in manufacturing and industrial environments. Although all of these networks are suitable for robot manipulator motion planning, the best is the recurrent neural network. It is used to identify, process, and understand a large amount of visual information, such as analysing dynamic and static scenes. Moreover, RNNs can be used to solve the problem of determining the trajectory to avoid collisions in a manipulator (Fig. 2). The basic concept is that it will be used to model the dynamics of the manipulator's motion, capable of predicting future positions of the robot's axes based on the current state, which is achieved using long short-term memory (LSTM) layers.

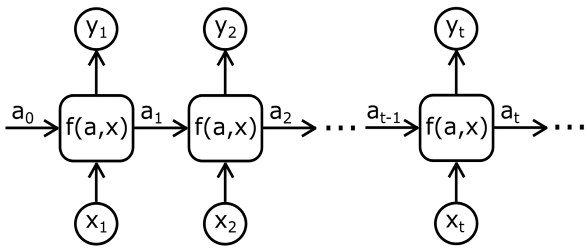

Figure 2. RNN architecture

Source: D. Lazar (2021)

The structure of an RNN consists of repeating blocks that allow information to be transmitted through successive time steps. Each such block contains components such as an input layer, a hidden layer, an output layer, and feedback. Input data, such as the current state of the robot, is entered through the input layer. In the case of trajectory determination, it can be a vector containing information about the positions and velocities of each axis of the manipulator. The hidden layer consists of neurons that perform calculations and transmit information in time steps. This layer can model the dynamics of the manipulator's movement and consider dependencies on previous states. The information from the hidden layer is transmitted to the output layer, which generates the predicted values of the positions of each axis of the manipulator at the next time step. The RNN also includes feedback loops that allow information to be passed back along the time axis. This allows the model to use the information from previous time steps to make more accurate predictions.

As for the LSTM, its structure of manipulator movement consists of an input layer, a repeating block, an output layer, feedback, and trajectory parameterisation (Fig. 3). The input layer accepts a vector containing the current state of the manipulator, including the positions and velocities of each axis. The repetitive block contains an LSTM layer that models the dynamics of the manipulator's movement and transmits information in time steps. The output layer generates the predicted values of the positions of each axis of the manipulator at the next time step. Feedback allows information to be passed from the output layer back to the repeating block to consider the context from previous time steps. Trajectory parameterisation means that the initial values of the positions of each axis can be expressed as trajectory parameters in the form of integer values.

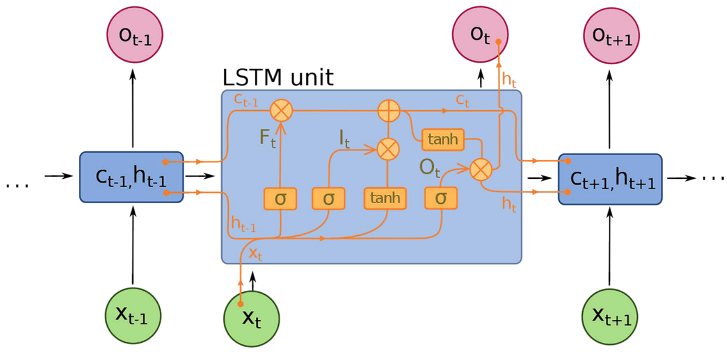

Figure 3. LSTM architecture
Source: M. Zulqarnain *et al*. (2021)

The movements planned via this approach correspond to standard motion commands. After generating the trajectory, it is important to determine the control influence and transform it into the commands required to execute the movement of the robot manipulator. Thus, the actuator control network plays a key role in the motion control system by converting high-level commands into specific control signals. The structure of the controlled action network includes an input layer that receives high-level commands to determine the desired movement; hidden layers that perform calculations and information processing; an output layer that generates controlled actions to implement the movement; feedbacks that adapt the network parameters based on the output signal and movement results; and action parameterisation, where output values can be adapted to meet the requirements of the actuators, such as force or controlled signals (Fig. 4).

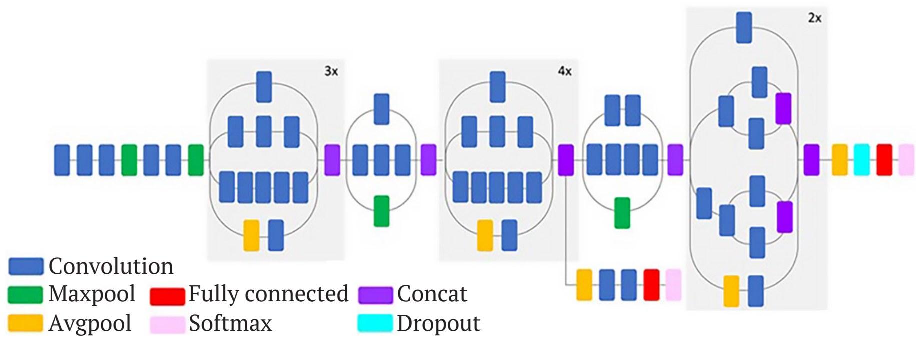

Figure 4. Schematic diagram of the managed impacts identification network
Source: compiled by the authors

The use of a neural network to determine the trajectory of the manipulator helps to increase the safety and efficiency of its operation, minimise the risk of collisions and avoid possible damage to both obstacles and the robot itself.

Ways to integrate the developed methods into a real production environment

The system described above requires a significant amount of data for training and realistic robot movements performed by the control system. However, simulating such movements in a real environment is resource and time-consuming. Thus, the Unity3D environment developed by Unity Software in the United States of America is used to achieve this goal (Fig. 5).

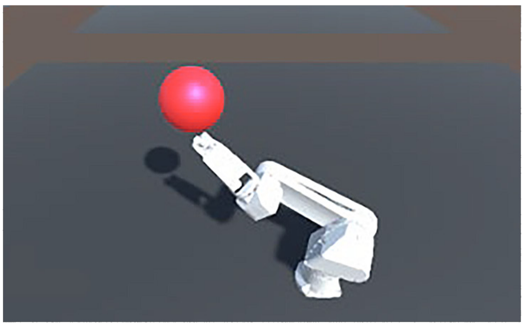

Figure 5. Using the Unity3D environment to model the movements of a robot arm
Source: compiled by the authors

MoveIt and UnityRoboticsHub motion planners were used to control the robot. Some robot movements were generated using high-level motion commands that were programmed manually. To evaluate the proposed approach, two robots will perform the task of picking up and placing objects in different environments that include static and dynamic obstacles (Table 2). It is important to note that, despite the presence of two SCARA robots, motion planning is performed for only one robot, while the other robot is treated as a static or dynamic obstacle.

Table 2. Static and dynamic interference in four environments

Environment type	Static interference	Dynamic interference
Simple static environments	Robot and a cube	None
Complex static environments	Robot and 3 cubes	
Simple dynamic environments	Cube	Movable robot
Complex dynamic environments	3 cubes	

Source: compiled by the authors

Table 2 shows the static and dynamic interference in the four different categories of environments. To evaluate the proposed approach, 100 environments were created that were not used during training. In each environment, 20 pairs of start and target coordinates were randomly generated. The performance of the proposed approach was evaluated in terms of validity, trajectory execution time, and computation time. In an application where the movements of SCARA robots are planned by different planners in an offline mode, the validation was performed only in visual aspects.

The robot can move along an incorrectly generated trajectory, or it can follow the planned trajectory exactly (Fig. 6).

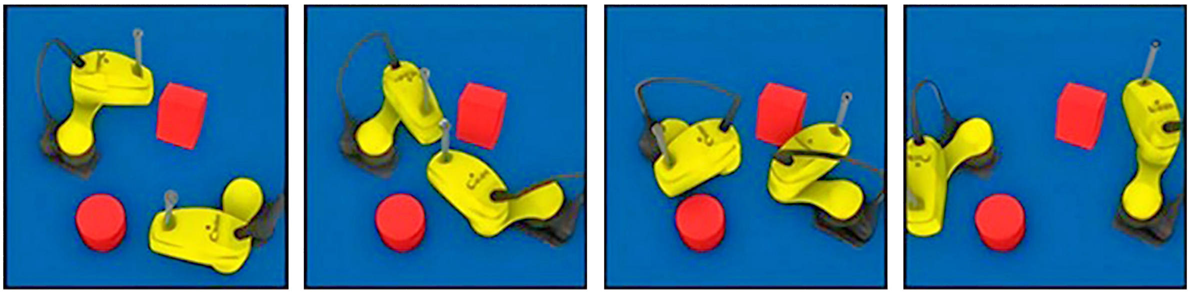

Figure 6. An example of the correct trajectory of the SCARA robot
Source: compiled by the authors

Figure 6 shows that when a robot accurately follows a given trajectory, the other robot moving from the right side crosses the common area earlier than the one moving from the left. Since exploring the full solution space is a complex and scalable task for other challenges, the proposed approach is to start with exploring the local solution space. The locally feasible solution space is the set of all possible control strategies that are constrained only by the state of the local system and guide the robot from the current state to the target area with the help of a specific control command at a certain stage of the search. The task of analysing the environment to determine its characteristics should also be considered, and it is advisable to use a convolutional neural network to solve this problem. In a dynamic scene, objects move or change their state over time. A neural network can be used to detect, track, and determine the speed and direction of movement of these objects. A static scene, on the other hand, describes the state of objects without their movement. The use of a convolutional neural network can be effective for object segmentation in an image, which means highlighting individual objects or regions in a scene.

The YOLOv7 neural network can be used to analyse dynamic and static scenes (Fig. 7). The YOLOv7 object detection algorithm is based on the use of neural networks to recognise objects in images and videos. This algorithm is widely used in the field of computer vision and image processing due to its speed and accuracy in detecting objects. It is safe to assume that YOLO is one of the most popular architectures for object detection and localisation, and YOLOv7 represents a modern modification of this architecture.

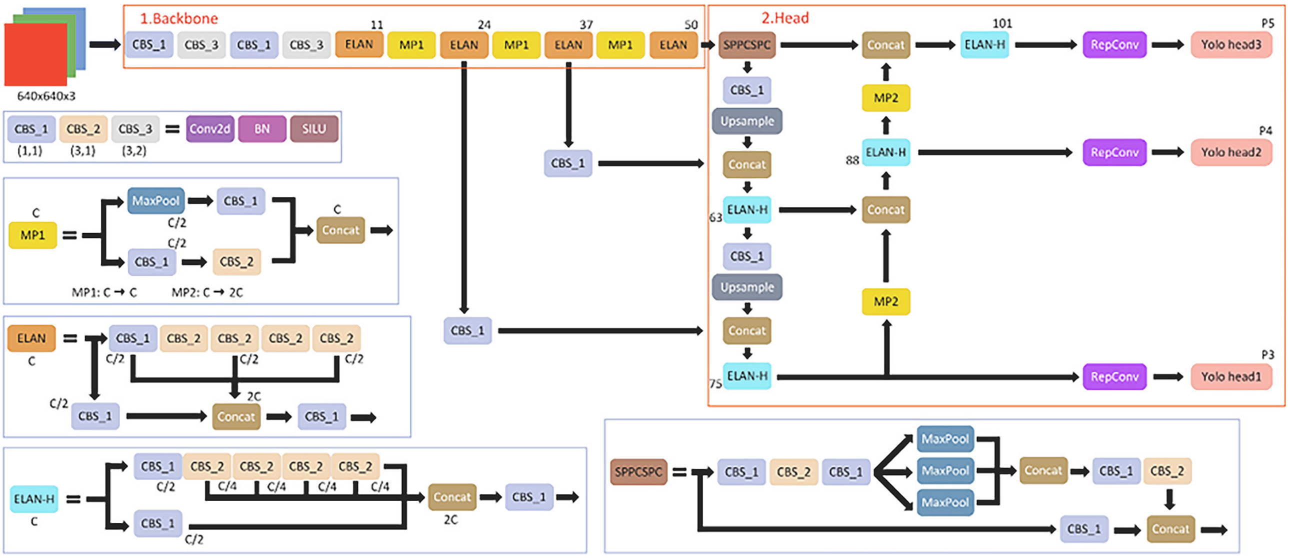

Figure 7. Structure of the YOLOv7 neural network

Source: W. Zhu *et al.* (2022)

YOLOv7 effectively detects objects in images, working with both dynamic and static scenes. Its main advantage is the high speed and accuracy of object detection, allowing it to be used in real-time. To analyse dynamic scenes using YOLOv7, the neural network can be trained on a wide range of videos with moving objects. Once trained, the model can automatically detect and track moving objects in the video, which is useful in video surveillance systems, transport systems, or autonomous vehicles where it is important to analyse moving objects in real-time. As for static scene analysis, YOLOv7 is used to segment and classify objects in an image. Thus, its architecture enables the network to efficiently detect and localise various objects, regardless of their degree of blur or shape, such as cars, people, animals, furniture.

In general, the integration of the developed methods into a real production environment requires a careful approach to ensure the efficiency and reliability of the manipulator. The integrated use of the obtained methods can ensure optimal and reliable planning of the manipulator's trajectory in real production conditions.

Comparison and optimisation of created approaches

After testing in 100 created environments, only 5 trajectories generated by the proposed approach contain errors (Table 3).

Table 3. Relative errors of the trained model when predicting the movement and the execution time of the actual movement

The values of the minimum and maximum possible robot speed, %	Average time error when performing a movement		Average trajectory prediction error	
	Point-to-point movement, %	Linear movement, %	Point-to-point movement, %	Linear movement, %
0-25	2.71	4.4	0.232	0.574
25-50	2.89	5.78	0.473	0.789
50-75	4.38	6.65	0.481	0.862
75-100	6.11	7.17	0.653	0.912

Source: compiled by the authors

Thus, in all scenarios of the experiment, the average discrepancy between the actual and predicted execution time of high-level movement commands is approximately 5%. It is also worth comparing the interpolation algorithm used to convert the planned robot movement into high-level commands, including RRT, with the trajectory generated by the developed system (Fig. 8). It is important to note that the runtime of the robot's trajectory varies significantly depending on the distance between the start and end points of the movement. Thus, for the test cases, it is necessary to classify distances into three categories: small distance (less than 30% of the robot's manipulator range); medium distance (more than 30% but less than 60%); and large distance (more than 60%).

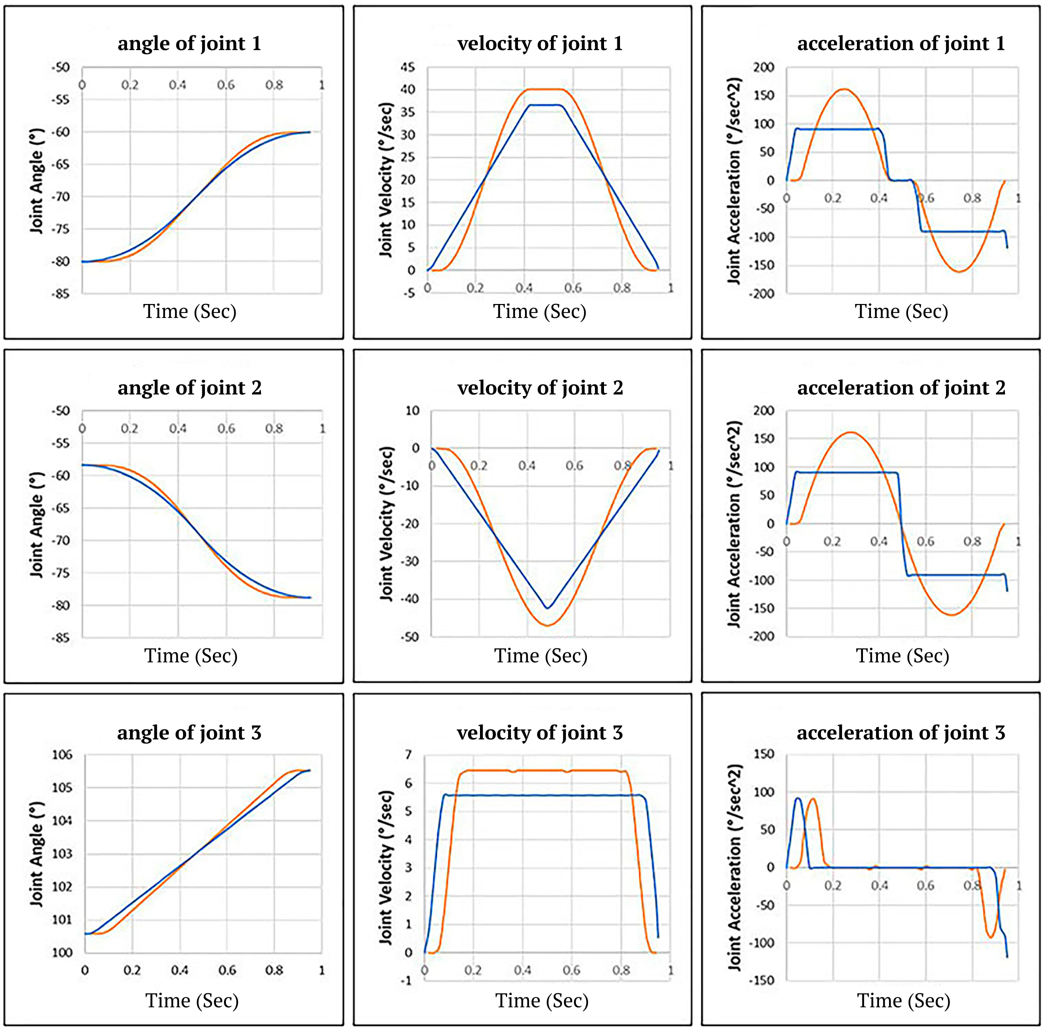

Figure 8. Joint movement at short, medium, and long distances
Note: blue line – joint movement planned via the existing approach; orange line – joint movement performed by the proposed approach
Source: compiled by the authors

Figure 8: "angle of joint 1, 2, 3" – change the angle of rotation of the joint; "velocity of joint 1, 2, 3" – change the velocity of the joint; "acceleration of joint 1, 2, 3" – change the acceleration of the joint. Thus, it is possible to calculate the execution time of the trajectories generated by the approach when using YOLOv7 and RRT (Table 4).

Table 4. Comparative table of the execution time of trajectories generated by the approach using YOLOv7 and RRT

Environment	Distance between start-point and end-point	Average runtime, ms		
		Proposed approach	RRT	Improved RRT
Simple static environments	Low	221	212	213
	Average	422	543	515
	High	659	836	694
Complex static environments	Low	291	372	304
	Average	603	797	663
	High	732	904	756
Simple dynamic environments	Low	244	272	277
	Average	496	581	558
	High	734	958	826
Complex dynamic environments	Low	419	462	465
	Average	765	975	829
	High	1071	1294	1113

Source: compiled by the authors

Therefore, the robot motion planned by the existing system is significantly different from the motion proposed by the trajectory planning system. This is because the RRT control algorithm used in the planning phase is different from the control algorithm described in this paper. In the planning phase, RRT assumes that the joints can reach their maximum acceleration, while the actual robot control system uses only 60% and 45% of the maximum acceleration for the respective robot axes. In general, the developed methods for planning the motion of manipulators already demonstrate significant advantages in solving the problems of obstacle avoidance and trajectory optimisation. However, to achieve an even higher level of efficiency and flexibility, it is worth suggesting several optimisation directions. For example, tuning the hyperparameters of neural networks. Further research and tuning of model parameters will help to achieve an optimal balance between speed and accuracy. Optimising the weights and architecture of the networks can help improve training results and prediction accuracy.

It is necessary to use deep reinforcement learning or DRL. The use of DRL will allow the robot manipulator to learn in real-time, adapting its strategies to new conditions. This can improve the robot's ability to quickly adapt to unpredictable scenarios in a production environment. There is also the integration of additional sensors and real-world data. Incorporating additional sources of information, such as additional cameras or sensors, can improve the robot's perception of its surroundings and provide a more accurate model of the work environment. It is worth paying attention to the improvement of genetic algorithms. Exploring different variants of genetic algorithms and adapting them to the specific requirements of the production process will allow for a better balance between speed and trajectory optimisation capability. Additionally, defining and using clear metrics to evaluate system performance will help to accurately measure the improvements achieved. Metrics can include robot speed, prediction accuracy, and reaction time to changes in the environment. Identifying opportunities includes the use of quantum computing to optimise the large amounts of computation involved in training deep networks and optimising trajectories. These areas of improvement are aimed at expanding the capabilities and improving the motion planning system of manipulators, ensuring that they can effectively adapt to a variety of production process

Based on the study results, several recommendations for practical application in the field of motion planning for manipulative robots emerge. First of all, it is recommended to implement the developed approach in modern production processes that require autonomy and adaptability in the operation of manipulators. It is important to focus on staff training in the use of this technology to optimise workflows. Additionally, it is recommended to conduct other experiments and research aimed at improving the efficiency and speed of manipulative robots in real production conditions. This will expand the scope of the technology and increase its competitiveness. For practical implementation, it is recommended to cooperate with manufacturers of robotic equipment to integrate the proposed approach into new and existing manipulators. This will increase the availability and speed of implementation of this technology on production lines.

DISCUSSION

The study results demonstrate the success of the developed approach to motion planning for manipulative robots. This approach uses an intelligent system and neural networks and is highly accurate and flexible in performing various tasks. For a deeper understanding of this topic, it is worth analysing similar studies conducted by other researchers in this field.

For instance, W. Si *et al.* (2021) investigated composite dynamic movement primitives (DMPs) based on neural networks with radial basis functions for teaching robot skills through human demonstrations. These DMPs can simultaneously encode skills for manipulating position and orientation for transfer from human to robot. Since a robotic manipulator needs to perform tasks under uncertainty, Adaptability to new situations is a requirement. DMPs have been successfully used for various tasks, such as trajectory planning and obstacle avoidance, due to their adaptability to uncertainties and the ability to scale in space and time. In this study, the authors presented a composite DMP framework for simultaneously modelling pose and orientation for robot skill training using neural network techniques. The proposed approach was successfully validated through simulation and experiments. Thus, the common aspects between the present study and the above-mentioned one include the use of neural networks to teach robots movements and manipulation skills. In both cases, the authors aim to achieve robot adaptability in uncertain environments and to train them to perform a variety of tasks. On the other hand, the differences lie in the focus of this study on the use of neural networks for real-time robot manipulator trajectory planning, while the other study focuses more on modelling pose and orientation for teaching specific skills.

In the work of T. Rakhimov *et al.* (2023) emphasised that robots and robotic systems with innovative intelligent control are widely used in industrial production, but their diversity and complexity of control negatively affect working time and productivity. The authors considered a method of position-speed control of a manipulator based on an intelligent mechatronic module. They have developed a block diagram of the control system that calculates the relative speeds of the manipulator's links. They proposed requirements for the control system and methods for eliminating transients during control. They also showed the advantages of time saved and the method of position-speed control of the manipulator by the operator. Common aspects of both studies include an emphasis on the use of innovative technologies in production to improve efficiency. They examine the use of robots and intelligent control systems in industrial production. However, this study focuses on the development of a motion planning method using an intelligent system based on neural networks. Secondly, it focuses on improving the methods of controlling robotic systems in the context of a particular industry.

H. Kalani *et al.* (2017) developed the kinematics of a parallel robot and presented an improved hybrid method for more accurate and faster analysis of the forward kinematics problem (FKP) of parallel manipulators. Artificial neural networks and a 3rd order numerical algorithm are combined to obtain an approximate solution to the FKP problem, which is used as a starting point for the Newton-Raphson numerical technique. Applying this approach to a parallel Stewart-Gough manipulator shows a reduction in the number of iterations to achieve the desired accuracy and a corresponding reduction in FKP analysis time. The result is an innovative algorithm suitable for any rectangular kinematics of serial or parallel robots. Both studies describe innovative technologies to improve the performance of robotic manipulators. However, the research on rectangular kinematics of parallel robots is aimed at optimising motion analysis, in particular, rectangular kinematics analysis. This research focuses on developing ways to move robotic manipulators using an intelligent system based on neural networks.

W.F. Latorre *et al.* (2023) highlighted that a robot manipulator can learn from its environment using the method of reinforcement learning. Each movement of the robot is recorded and compared with past data to determine the best way to achieve the goal in the future. This makes robots more efficient, as they are constantly looking for the best path to follow. At the same time, a trajectory planning method is implemented to control the various movements of the three-stage manipulator in the workspace. The resulting trajectories are stored and used to train the movements, which allows the robot to analyse and compare them to determine the optimal performance of programmed tasks. Both studies aim to improve the movements of robotic manipulators but use different methods to achieve this goal.

Researchers Z. Zhang *et al.* (2023) proposed a new fuzzy recurrent neural network (FRNN) to overcome the internal spurious noise of robots that arises when performing effector tasks, which was developed and implemented on the programmable field of the studied arrays. The pipeline implementation guarantees the sequence of operations, and data processing based on the interaction between clock domains contributes to the acceleration of computing blocks. Compared to traditional gradient neural networks and null neural networks, the proposed FRNN is characterised by a faster convergence rate and more correct operation. In other words, both studies point to the use of innovative approaches in the field of robotics and neural networks to solve important problems. The common aspects include the use of neural networks in robotics to optimise and improve performance. The differences lie in the specifics of the tasks being solved: the above study focuses on improving the robot's internal stability by applying FRNNs to optimise control and overcome spurious noise, while this study aims to develop a method for planning the movement of robotic manipulators using an intelligent system and neural networks.

J. Mężyk (2016) emphasised that industrial manipulators have been replacing humans in production for many years, increasing productivity and product quality. However, the introduction of robotics is often complicated by high costs. The concept of an intelligent tool exchange system offers a solution to this problem. The system enables rapid tool changes by using a decision-making module to self-configure the manipulator, which assesses the situation, identifies the product, and makes decisions about operations and tools. This solution is suitable for variable production and short runs, particularly for small businesses that cannot afford multiple robots. Hence, both studies relate to industrial manipulators and focus on improving production efficiency. However, this study is concerned with the development of a motion planning approach using an intelligent system based on neural networks, while the other focuses on the development of the intelligent system itself for tool exchange and self-configuration of manipulators.

H.S. Kumhar and V. Kukshal (2022) recorded that industrial manipulators play an important role in intelligent manufacturing systems, ensuring high productivity and quality of manufactured products. However, the complex problems of inverse kinematics of industrial robotic manipulators with multiple degrees of freedom require new methods. In this study, a 6-degree-of-freedom manipulator is modelled, and its kinematic parameters are analysed. A CNN is used to solve the inverse kinematics problem, and the network is trained and tested, and performance and training graphs are examined. The results obtained indicate the high efficiency of the method in solving the inverse kinematics problem for a robot with 6 degrees of freedom. Thus, both papers discuss robotic manipulators and intelligent systems, as well as convolutional neural networks. However, this study uses different neural networks. In addition, unlike the other study, there are no specific kinematic parameters.

The archive management robot studied by J. Cui *et al.* (2021) can effectively increase productivity by providing autonomous access to different levels of archives without the need to change their structure or install additional devices. The robot uses a mobile navigation platform a motion algorithm based on laser sensing and a map to move independently. The bionic manipulator simulates the movement of manual access to archives and is attached to the robot's working arm to access different layers of archives. The robot can identify and access files at different levels using an industrial camera to read barcodes. Also, the developed robot was tested in an archival repository, demonstrating efficiency and cost-effectiveness compared to existing solutions for robotic access to archives. In other words, both studies are aimed at improving the movements of robotic manipulators. However, the aforementioned study focuses on the ability of the robot to perform tasks without modifying the structure of the archives, while this study focuses on creating ways to plan the movement of robotic manipulators.

Scientists D. Galvan-Perez *et al.* (2022) worked on the problem of controlling the trajectories of anthropomorphic manipulators in a disturbed environment using output feedback and artificial neural networks. The proposed adaptive robust control scheme uses three-layer artificial neural networks and time-series modelling to improve the efficiency of anthropomorphic manipulator trajectory tracking in high-precision applications such as laser cutting or welding. The system allows the robotic system to autonomously navigate, identify and access archives at different levels without the need to modify the storage or use additional devices. This approach uses neural networks to reduce the dependence on detailed modelling of robotic systems and does not require real-time estimation of uncertain dynamic interference. Both studies address the problems of robotic motion control and neural networks. However, this study focuses on robotic manipulators, while the other study focuses on anthropomorphic manipulators.

Furthermore, X. Wang *et al.* (2023) pointed out that the robotics industry and its applications are playing an important role in modern manufacturing. With the intelligent development of the manufacturing industry, the use of collaborative robots and human-robot cooperation technology is gaining popularity. In a collaborative scenario, in particular, interaction with a human upper limb, the technology of manipulator route planning requires high accuracy. The advanced velocity potential field algorithm proposed in this paper allows for effective collision avoidance and reduces the problem of local oscillations of manipulators near obstacles. The implementation of this algorithm can improve the safety and feasibility of the human-robot collaboration process, making collaborative robots safer and smoother in the work environment. A common aspect between this study and the present one is the active use of robots and robotic solutions to improve manufacturing processes and production efficiency. Both studies discuss technological developments in robotics, addressing the challenges of improving manipulator motion control and developing intelligent systems for robot motion planning. The differences lie in specific aspects of the research, such as the use of neural networks to analyse manipulator movements in this paper and the improvement of velocity potential field algorithms to avoid collisions in human interaction with the other.

J. Yu *et al.* (2023) applied a neural network-based adaptive control strategy for a flexible robot manipulator to track areas in the presence of constraints in the zone. The developed strategy can be used to globally stabilise the robot manipulator and manage model uncertainties and external unknown constraints. However, unlike previous approaches, the use of sliding mode technology and singular perturbation theory in this strategy does not require high-order derivatives of the chain state, which facilitates its implementation and provides greater stability in real-world conditions. Both studies are aimed at developing strategies for controlling robotic manipulators using intelligent technologies such as neural networks. However, while the aforementioned study focuses on adaptive control using neural networks to track areas with zone constraints, this study focuses on developing ways to move robotic manipulators based on an intelligent system based on neural networks.

W. Quan *et al.* (2023) analysed high voltage lines, which are a key element for electricity transmission. They emphasised that the use of electric robots for transmission line maintenance is essential to improve efficiency and safety. They also presented a configuration of a two-armed robot for optimal coordination of movement in various maintenance tasks. It employs polynomial interpolation and matrix laboratory (MATLAB) trajectory simulation techniques, improving the robot's efficiency and performance compared to the one-arm mode. Thus, the common aspects of the research include the use of robots and their movement. At the same time, the main focus of the aforementioned research is on the physical aspects of robot maintenance and coordination. In contrast, this study defines the planning of manipulator movement using intelligent systems, in particular, neural networks.

Scholars M. Suguitan *et al.* (2023) used a method to personalise human-robot interaction by using emotional facial expressions to create affective robot movements. Motion is a key means of expressing the affective states of robots, and using autoencoders to compress motion data and emotional images allows new movements to be generated according to the input. The use of reproduction loss and triplet loss to equalise emotional embeddings allows for affective robot movements. The evaluation was carried out using a user survey, confirming that the generated movements can match the original emotional face images. Both studies employ neural networks, but the difference lies in the use of neural networks for motion planning and interaction for this study and for generating affective expressions in the robot in the other study.

K. Takahashi (2021) considered high-dimensional neural networks based on hypercomplex numbers, such as quaternions, co-quaternions, and others that form a four-dimensional algebra over real numbers. Such networks are investigated for their applicability in the control system of a robotic manipulator. The control system uses the output of a high-dimensional neural network to control the movement of the robot's end-effector in three dimensions. Computational experiments on a long-lasting robotic arm show that the quaternion neural network performs better in learning and control than other networks. Both studies explore the use of neural networks in robotics. The aforementioned study focuses on high-dimensional neural networks based on hypercomplex numbers for controlling a robotic manipulator. This study focuses on an intelligent motion planning system for robotic manipulators using neural networks.

In general, innovative approaches such as the use of high-dimensional neural networks and intelligent motion planning systems play a key role in improving the efficiency and accuracy of robotic manipulator control. All of the above studies, including this one, contribute to the further development of robotic technologies and their implementation in various industries.

CONCLUSIONS

As a result of the study, an approach to planning the movement of manipulative robots using an intelligent system and neural networks was developed. To achieve this goal, analysis methods were used, as well as a special approach that included design methods, machine learning, integration strategies, and optimisation methods. Analysis methods were used to summarise and systematise existing data and approaches in the field of traffic planning. The design aims to create adaptive integrated systems that can effectively interact with the environment. Machine learning was used to train neural networks to ensure their ability to self-regulate and adapt to new conditions. Integration strategies and optimisation methods were applied to improve the efficiency and accuracy of robot motion planning in various scenarios. In other words, this integrated approach allowed us to achieve high autonomy and flexibility in manipulative robot control.

The evaluation of existing methods for planning the motion of manipulators and the analysis of intelligent control systems included the results of a comparative review of geometric path planning, dynamic programming, inverse kinematics, random positions, and optimisation. This review highlighted their characteristics, advantages, and limitations. The developed robot trajectory methods reflected a variety of approaches, such as hierarchical trajectory planning, the use of neural networks for adaptive control, dynamic prediction for obstacle avoidance, and genetic algorithms for trajectory optimisation. The process of training a neural network for optimal route planning has shown the advantages of using networks and architectures such as CNN, RNN, DNN, autoencoders and LSTM, as well as a network diagram to determine the controlled influences. As for the implementation of the developed methods in a real production environment, the use of the Unity3D tool was demonstrated, and static and dynamic interference was considered. An example of the correct trajectory of the SCARA robot is shown and the YOLOv7 structure is presented. The analysis and optimisation of the developed approaches determined the relative errors of the trained model, the average errors of the execution time of real movement, the extreme values of possible robot speeds, as well as the universal table of trajectory execution times, which was conducted using YOLOv7 and RRT.

In general, the developed approach to planning the motion of manipulative robots offers a promising way to achieve high efficiency and flexibility in their use in various production conditions. For further development in the field of motion planning for manipulative robots, it is recommended to study methods for optimising the system's operating parameters, improving machine learning algorithms, and expanding the application of the technology in the field of variable production and robotic systems for various tasks.

ACKNOWLEDGEMENTS

None.

CONFLICT OF INTEREST

None.

REFERENCES

[1] Bogdanovsky, M.V. (2020). Analysis of the main errors and assessment of the accuracy of industrial robots. *Technical Engineering*, 2(86), 67-72. doi: 10.26642/ten-2020-2(86)-67-72.

[2] Cui, J., Cui, L., & Jiang, H. (2021). Archive access robot for smart archive repositories. *Industrial Robot*, 49(4), 745-759. doi: 10.1108/IR-08-2021-0171.

[3] Galvan-Perez, D., Yañez-Badillo, H., Beltran-Carbajal, F., Rivas-Cambero, I., Favela-Contreras, A., & Tapia-Olvera, R. (2022). Neural adaptive robust motion-tracking control for robotic manipulator systems. *Actuators*, 11(9), article number 255. doi: 10.3390/act11090255.

[4] Kalani, H., Akbarzadeh, A., Moghimi, S., & Khoshraftar, N. (2017). Forward kinematics solution of stewart-gough using improved hybrid strategy (neural network and 3rd-order Newton-Raphson). *Journal of Computational Methods in Engineering*, 35(2), 113-129. doi: 10.18869/acadpub.jcme.35.2.113.

[5] Khotsyanivskyi, V., & Sineglazov, V. (2023). Machine learning in the task of auto-calibration of moving elements of robotic systems on the example of stepper motor control. In *International scientific and technical conference "AVIA"* (pp. 9.37-9.41). Kyiv: National Aviation University.

[6] Koruniak, P., Nishchenko, I., & Sheremeta, P. (2023). Vibration mobile devices in robotic systems. *Bulletin of Lviv National Environmental University. Series Agroengineering Research*, 26, 22-29. doi: 10.31734/agroengineering2022.26.022.

[7] Kumhar, H.S., & Kukshal, V. (2022). Inverse kinematic solution for 6-r industrial robot manipulator using convolution neural network. In *Select proceedings of IPDIMS 2021 "Recent trends in product design and intelligent manufacturing systems"* (pp. 923-930). Singapore: Springer. doi: 10.1007/978-981-19-4606-6_84.

[8] Latorre, W.F., Castro, F.C., Caviativa, Y.P., Amaya, J.C., & Sanz, F.A. (2023). Implementation of a reinforced learning algorithm in a simulation environment for path planning of a robot manipulator with 3 degrees of freedom. In *Proceedings of the 10th workshop on engineering applications "Applied computer sciences in engineering"* (pp. 151-162). Cham: Springer. doi: 10.1007/978-3-031-46739-4_14.

[9] Lazar, D. (2021). *Creating a simple RNN from scratch with TensorFlow*. Retrieved from https://medium.com/nabla-squared/creating-a-simple-rnn-from-scratch-with-tensorflow-8995a03c976d.

[10] Litvin, O., & Pankov, S. (2021). Robotic manipulators special purpose. *Technical Sciences and Technology*, 1(19), 81-88. doi: 10.25140/2411-5363-2020-1(19)-81-88.

[11] Mężyk, J. (2016). A concept for intelligent tool exchange system for industrial manipulators. *Solid State Phenomena*, 251, 158-163. doi: 10.4028/www.scientific.net/SSP.251.158.

[12] Nalobina, O., Holotiuk, M., Bundza, O., Shymko, A., & Mikhailov, A. (2022). The task of an agricultural robot during the passing of turns. *Advances in Mechanical Engineering and Transport*, 2(19), 141-147. doi: 10.36910/automash.v2i19.912.

[13] Quan, W., Zou, D., Xi, C., Qiao, M., Liu, L., & Jiang, W. (2023). Simulation research on trajectory planning of double-arm cooperative live working robot for transmission lines. *Journal of Physics Conference Series*, 2433, article number 012013. doi: 10.1088/1742-6596/2433/1/012013.

[14] Rakhimov, T., Erkinov, S., & Takhirova, G. (2023). Positional-velocity control of the manipulator built on the basis of an intelligent mechatron module. *E3S Web of Conferences*, 452, article number 03011. doi: 10.1051/e3sconf/202345203011.

[15] Si, W., Wang, N., & Yang, C. (2021). Composite dynamic movement primitives based on neural networks for human-robot skill transfer. *Neural Computing and Applications*, 35(32), 23283-23293. doi: 10.1007/s00521-021-05747-8.

[16] Suguitan, M., DePalma, N., Hoffman, G., & Hodgins, J. (2023). Face2Gesture: Translating facial expressions into robot movements through shared latent space neural networks. *ACM Transactions on Human-Robot Interaction*. doi: 10.1145/3623386.

[17] Takahashi, K. (2021). Comparison of high-dimensional neural networks using hypercomplex numbers in a robot manipulator control. *Artificial Life and Robotics*, 26(3), 367-377. doi: 10.1007/s10015-021-00687-x.

[18] Wang, X., Wu, Q., Wang, T., & Cui, Y. (2023). A path-planning method to significantly reduce local oscillation of manipulators based on velocity potential field. *Sensors (Basel, Switzerland)*, 23(23), article number 9617. doi: 10.3390/s23239617.

[19] Yu, J., Wu, M., Ji, J., & Yang, W. (2023). Neural network-based region tracking control for a flexible-joint robot manipulator. *Journal of Computational and Nonlinear Dynamics*, 19(2), article number 021003. doi: 10.1115/1.4064201.

[20] Zalypka, V. (2023). Simulation of the stress-deformed state of the elements of the multifunctional manipulator of multipurpose robotic platforms. *Advances in Mechanical Engineering and Transport*, 2(21), 101-109. doi: 10.36910/automash.v2i21.1214.

[21] Zhang, Z., He, H., & Deng, X. (2023). An FPGA-implemented antinoise fuzzy recurrent neural network for motion planning of redundant robot manipulators. In *IEEE transactions on neural networks and learning systems* (pp. 1-13). Piscataway: IEEE. doi: 10.1109/TNNLS.2023.3253801.

[22] Zhu, W., Wang, Q., Luo, L., Zhang, Y., Lu, Q., Yeh, W.-C., & Liang, J. (2022). CPAM: Cross patch attention module for complex texture tile block defect detection. *Applied Sciences*, 12(23), article number 11959. doi: 10.3390/app122311959.

[23] Zulqarnain, M., Khalaf Zager Alsaedi, A., Ghazali, R., Ghouse, M.G., Sharif, W., & Aida Husaini, N. (2021). A comparative analysis on question classification task based on deep learning approaches. *PeerJ Computer Science*, 7, article number e570. doi: 10.7717/peerj-cs.570.

Володимир Петрович Хоцянівський
Аспірант
Національний авіаційний університет
03058, просп. Любомира Гузара, 1, м. Київ, Україна
https://orcid.org/0000-0003-0415-777X

Віктор Михайлович Синєглазов
Доктор технічних наук, професор
Національний авіаційний університет
03058, просп. Любомира Гузара, 1, м. Київ, Україна
https://orcid.org/0000-0002-3297-9060

Розробка методу планування руху роботів маніпуляторів з використанням інтелектуальної системи заснованої на нейронних мережах

Анотація. Актуальність досліджуваної проблеми випливає з постійного розвитку промисловості та використання роботів маніпуляторів у виробничих процесах. Метою дослідження є розробка підходу до планування траєкторії робота маніпулятора за допомогою інтелектуальної системи на основі нейронних мереж. Для досягнення поставленої мети використано метод аналізу, а також спеціальні методи, такі як проектування, машинне навчання, інтеграційні стратегії та оптимізаційні методи. Основні результати дослідження охоплюють широкий спектр досягнень у розвитку методів планування руху роботів маніпуляторів та їхньої інтеграції в реальні виробничі умови. Аналіз існуючих методів планування руху роботів маніпуляторів та огляд інтелектуальних систем управління надали вичерпну картину сучасного стану цієї проблематики. Розроблені методи траєкторії робота маніпулятора визначили ефективні стратегії управління, які враховують як динамічні, так і статичні сценарії. Навчання нейронної мережі для планування оптимального шляху переміщення зробило можливим виявлення, відстеження та уникнення перешкод в реальному часі. Для способів інтеграції розроблених методів в реальне виробниче середовище використано ієрархічне планування траєкторії, адаптивне керування нейронною мережею, генетичні алгоритми для оптимізації траєкторії та динамічне прогнозування для уникнення перешкод. Оптимізація та вдосконалення створених підходів показали позитивні результати у покращенні безпеки та продуктивності роботів маніпуляторів, зниженні ризику зіткнень та уникненні пошкоджень роботів. Крім того, реалізація ієрархічного планування траєкторії та адаптивного керування нейронною мережею сприяла значному підвищенню точності та стабільності рухів маніпуляторів в різних сценаріях виробничого процесу. Практичне значення дослідження полягає у розробці інтелектуальної системи управління та методи планування руху роботів маніпуляторів, що сприяє підвищенню ефективності та безпеки їхньої роботи в реальних виробничих умовах

Ключові слова: траєкторія пересування; промислова автоматизація; мехатронічні структури; розумні технології; моделі глибокого навчання

ТЕХНІКА ТА ЕНЕРГЕТИКА

Науковий журнал

Том 14, № 3. 2023

Заснований у 2010 р. Виходить чотири рази на рік

Оригінал-макет видання виготовлено у відділі науково-технічної інформації
Національного університету біоресурсів і природокористування України

Відповідальний редактор:
Г. Івченко

Редагування англомовних текстів:
С. Воровський, К. Касьянов

Комп'ютерна верстка:
О. Глінченко

Підписано до друку 11 серпня 2023 р. Формат 60*84/8
Умов. друк. арк. 17,1
Наклад 50 прим.

Адреса видавництва:
Національний університет біоресурсів і природокористування України
03041, вул. Героїв Оборони, 15, м. Київ, Україна
E-mail: info@technicalscience.com.ua
www: https://technicalscience.com.ua/uk

MACHINERY & ENERGETICS

Scientific Journal

Volume 14, No. 3. 2023

Founded in 2010. Published four times per year

The original layout of the publication is made in the Department of Scientific and Technical Information of National University of Life and Environmental Sciences of Ukraine

Managing editor:
H. Ivchenko

Editing English-language texts:
S. Vorovsky, K. Kasianov

Desktop publishing:
O. Glinchenko

Signed for print of August 11, 2023. Format 60*84/8
Conventional printed pages 17.1
Circulation 50 copies

Editors Office Address:
National University of Life and Environmental Sciences of Ukraine
03041, 15 Heroiv Oborony Str., Kyiv, Ukraine
E-mail: info@technicalscience.com.ua
www: https://technicalscience.com.ua/en